Using a spatial model of geodiversity to guide conservation within mountains at the pan-tropical-scale.

Parks, Kate

Awarding institution:
King's College London

Title: Using a spatial model of geodiversity to guide conservation within mountains at the pan-tropical-scale.

Author: Kate Parks

USING A SPATIAL MODEL OF GEODIVERSITY TO GUIDE CONSERVATION WITHIN MOUNTAINS AT THE PAN-TROPICAL-SCALE.

KATHERINE ELISABETH PARKS

A THESIS SUBMITTED TO THE UNIVERSITY OF LONDON FOR THE DEGREE OF DOCTOR OF PHILOSOPHY

KING'S COLLEGE LONDON
DEPARTMENT OF GEOGRAPHY

2012

Abstract

Literature review and past empirical work suggests that a resource based model of geodiversity may be a useful proxy for biodiversity within tropical mountains and could provide a valuable conservation planning tool. Here, geodiversity is defined as variation in overall resource availability, along with spatial and temporal (seasonal) variation in resource availability. Using freely available pan-tropical datasets at a 1 km resolution, a spatial model of geodiversity that is informed by an understanding of ecological processes was developed and tested before being used to address three research questions:

1. Is there a quantifiable relationship between geodiversity and biodiversity?
2. Do areas included in multiple conservation prioritisation schemes include a higher proportion of geodiversity than would be expected by chance?
3. What are the likely impacts of climate change on the spatial distribution of current geodiversity classes and what might be the implications of this with respect to the suitability of current protected area configuration in tropical mountains to protect geodiversity and thus biodiversity into the future?

Some support for a relationship between geodiversity and biodiversity was found across a range of spatial aggregations and a variety of taxa, however a full validation of this relationship was not possible due to a lack of suitable validation data. It was found that areas rated as valuable on a greater number of conservation prioritisation schemes do not conserve a greater proportion of geodiversity or biodiversity than would be expected by coverage alone or from a random selection. The impacts of climate change on geodiversity were evaluated in terms of change from current conditions under three SRES scenarios and based on projected temperature and precipitation as a mean of five GCM. It was found that there will be significant changes to the current state of geodiversity by the period 2040-2060 and 2080-2100, with the most severe changes occurring by the 2040-2060 period. The implications of these findings are considered in detail for protected areas within Colombia and suggestions for climate change stable conservation strategies are made. It is concluded that the model of geodiversity proposed in this thesis has potential to become a useful conservation tool when considering the effectiveness of current protected areas, and changes in geodiversity due to climate change.

Acknowledgements

I started this journey inspired by the beauty of the world's "crinkly bits", and completion of this thesis represents the end of one of the most challenging, but ultimately enjoyable, periods of my life. I would like to extend my gratitude to Mark Mulligan for guiding me through the last four years and for going "above and beyond the call of duty" in developing my skills and experience outside the PhD process; something which has undoubtedly enabled me to progress my career thus far.

Most people have an inspirational teacher at some stage in their lives; I would like to thank Mr Waters for teaching me to structure and write coherent essays – I didn't enjoy it at the time but I hope it has paid off! Similar thanks are owed to Bruce Malamud for his input in my MSc, and to Dave Moore for his technical and moral support through my PhD.

Away from the academic and intellectual support, emotional support has come from so many friends they are too numerous to mention individually – if you have helped over the last four years, from a cup of tea to proof-reading to unofficial IT support, thank you. To my four-legged friends – thank you for providing light relief from the trials and tribulations of writing up through laughter and enforced walks.

My family have always, without fail, supported me. You have helped me with spelling (Mum), maths (Dad), design (Mike) and have endowed me with perseverance (Nana), logic (Grandad), curiosity (Nanny) and the occasional grump (Dumpy). Thanks to each of you – whether you are here or not.

Last, and the antithesis of least, thanks go to Andy for doing significantly more than 50% of the cooking, cleaning and dog walking for far too long, and particularly for your patience through the last few months of this process – I couldn't have done it without you.

Contents

List of Figures

List of Tables

Chapter 1. Aims, Objectives and Strategy.

1.1. Research Problem.

Climate and land use change are two of the greatest global threats to the world's ecosystems (e.g. Araujo and Rahbek, 2006, Thomas *et al.*, 2004, Jetz *et al.*, 2007). Global climate change is likely to cause range shifts among species, both towards the poles and upwards in elevation at rates of 6.1 m per decade (Parmesan and Yohe, 2003, Root *et al.*, 2003), meaning that ecosystems and species at the top of mountains may not be able to retreat upwards to avoid temperature increases (Korner and Spehn, 2002, Parmesan, 2006). Given that deforestation is more pronounced in the tropics (FAO, 2010), and that deforestation tends to lead to additional regional climate change through impacts on water and energy balances (Feddema *et al.*, 2005), tropical mountains are one of the most vulnerable global ecosystems (Pressey *et al.*, 2007, Sarkar *et al.*, 2006, Thomas *et al.*, 2004).

Mountains provide provisioning, regulating, cultural and supporting services (Millenium Assessment, 2005), directly supporting 22% of the world's population according to (UNEP-WCMC, 2002) and with an indirect effect on over 50% (Korner and Spehn, 2002). Mountains provide fresh water by capture of precipitation and fog interception, and storage in lakes (artificial or natural). Most tropical rivers originate in mountains, and so mountains provide the lowlands with freshwater; this is particularly important given that montane rainfall tends to be higher than that in the lowlands, especially during the dry season, and because evapo-transpiration tends to be suppressed in tropical mountains (Bruijnzeel *et al.*, 2011). Floodplains also rely on seasonal flow from mountains for fertilisation, increasing the agricultural productivity of lowland valleys (UNEP-WCMC, 2002). Naturally vegetated mountain ecosystems provide protection from landslides and erosion as the roots can bind the soil preventing it from washing away. Moreover, a biodiverse montane ecosystem is more effective as the plants will have a variety of root structures, thus increasing the overall binding effect (Korner, 2002).

Mountains tend to be highly biodiverse when compared with a lowland region of the same extent because of the presence of many climatic zones in close proximity, leading to higher habitat heterogeneity and more niche space (Korner, 2002) and the presence of strong resource gradients leading to high levels of biodiversity (Stevens *et al.*, 2007). Biodiversity in the tropics tends to be higher than that in temperate regions, however there is no consensus on the cause of this (Ding *et al.*, 2006). As a result of these two factors tropical mountains

tend to be more biodiverse than their temperate counterparts and, when corrected for area, more biodiverse than their adjacent lowlands (Hamilton, 2002). Distinguishing between the generation and maintenance of biodiversity can be challenging, as the same mechanisms that generate biodiversity (e.g. spatial heterogeneity leading to allopatric speciation) can also maintain biodiversity (e.g. spatial heterogeneity maintaining separate populations of the same species thus providing a buffer against total extinction) (Begon *et al.*, 1996). In addition, the disturbance regimes of tropical mountains result in communities from many different successional stages, with a high proportion of diverse young and mid-successional communities leading to high overall biodiversity (Korner, 2002). Given the complex topography of mountains (leading to spatial heterogeneity), combined with the high energy availability in the tropics, it is fair to state that tropical mountains are a highly important ecosystem in terms of biodiversity.

However, mountains are also considered one of the most threatened ecosystems, with Mountain Watch (UNEP-WCMC, 2002) suggesting the threats to mountains fall into five categories (in no particular order):

1. Technological
2. Demographic
3. Economic
4. Global biophysical
5. Socio political

These can be grouped into the two major threats of land use change and climate change, with feedbacks occurring between the categories. Demographic change, in terms of both numbers, spatial distribution of populations, increasing globalisation and per-capita consumption, causes land use change as more rural populations move to urban areas seeking work. This has a double-edged impact; urban populations tend to be less self-sufficient and so food production is less sustainable and local knowledge of traditional land management techniques are lost (Millenium Assessment, 2005). Mountain Watch (UNEP-WCMC, 2002) argue that technological change could enable more intensive farming, allowing conversion of land previously too infertile for agriculture (such as many mountainous areas), which has the potentially to impact on the regulation of climate; as tropical forests are cleared for farming, carbon storage and water regulation services may be lost.

Protected areas are used as one of a suite of techniques aimed at conserving important ecosystems and biodiversity. The location of these areas tends to be based on territorial and political constraints but are advised by current understanding of the distribution of

conservation priority areas through field inventory and our understanding of species distribution for key taxa, which are then used to generate prioritisation schemes, such as the Biodiversity Hotspots proposed by Myers *et al.* (2000). However these assessment are often based on sparse species distribution data, particularly in under-sampled regions such as the tropics, and so complex algorithms are required to help overcome the lack of data and results remain limited by the data so whilst they may be appropriate for large-scale regional schemes such as the biodiversity hotspots, they are much less relevant for the designation of most protected areas which are much more localised in extent. Since there is often no detailed local data important conservation policy decisions can be based on models and datasets with high levels of uncertainty (Phillips and Dudik, 2008).

Within tropical mountains, the increasing pressures arising from climate combined with the frequent lack of detailed biological data results in the need for a conservation strategy which is locally relevant even for areas with a paucity of biological data and is able to consider the impact of climate change. In order to protect tropical mountains under these circumstances, a robust conservation strategy is required. Hamilton (2002) suggests that although protected areas in mountains seem to offer good "value for money" for conservation due to their high habitat heterogeneity, they still need to be of sufficient size to protect a viable population of naturally occurring species. Many large mountainous mammals have adapted to take advantage of the closely packed climatic zones, Hamilton cites the example of the spectacled bear (*Tremarctos ornatus*) will migrate up and down the mountain in response to changes in available food or weather patterns. The resulting large range sizes mean many mountain protected areas, which tend to focus on mountain peaks, are too small to support a viable population. Hamilton goes on to argue that many mountain protected areas are effectively "sky islands" and are too fragmented to provide a useful network.

In order to improve protected areas within mountains, three dimensions must be considered:

1. Horizontally along mountain ranges
2. Elevation
3. Across international and national political an administrative borders

Hamilton (2002) suggested that the opportunity of designating land in IUCN categories I - IV has passed as there is little appetite for further designation of protected areas, and instead the focus should move to the use of stewardship schemes to provide suitable connecting land between existing protected areas. However, statistics from the IUCN and UNEP-WCMC (2012) demonstrate that designation of both nationally and internationally recognised protected areas has continued to increase in terms of extent and number of parks. Indeed, the growth in

number of parks over the period 2002 to 2011 was higher for internationally designated protected areas (61.9%) than nationally designated areas (22.4%).

Given the lack of locally specific data coverage for species occurrences, and the importance of conserving disappearing ecosystems, an alternative approach to protected area planning appears necessary. Freely available datasets with global coverage and local relevance are available for abiotic environmental data, and empirical research has shown species richness to be related to aspects of the abiotic environment which provide resources (e.g. Gorelick, 2008, Aubry *et al.*, 2005, Moser *et al.*, 2005) and influence biotic interactions (for example, dispersal barriers, e.g. Dufour *et al.*, 2006). Using these relationships between the biotic and abiotic environment, Parks and Mulligan (2010) and Mulligan (2000) proposed a model of geodiversity (diversity of resource availability within the abiotic environment) which combines measures of total resource availability, spatial variation in resources and temporal variation in resource availability. Individually, these components of geodiversity have been used to investigate patterns of evolution and biodiversity using different terms, such as niche space, spatial or environmental heterogeneity and environmental diversity. The key development in the model of geodiversity proposed and tested in this thesis is the combination of each of these individual components into a single metric aimed at capturing the key spatial patterns in biodiversity.

Geodiversity could then be used as a solid foundation for protected area planning, as it is very much locally specific (rather than being based on highly interpolated species distributions). Furthermore, if the theoretical links between geodiversity and species richness prove to be valid, geodiversity assessment could provide a measure of potential species richness in a pristine environment. By basing the model on physical environmental data, it is also possible to apply scenarios for climate and land use change to the model and thus investigate the potential impact of global change on geodiversity, thus allowing temporal, as well as spatial, planning. This is particularly important for understanding likely responses to climate and land use change in the world's hyper-diverse but highly pressures tropical mountains.

1.2. Research questions.

One of the earliest formal definitions of geodiversity comes from Gray (2004, p.8): *"the natural range (diversity) of geological (rocks, minerals, fossils), geomorphological (land form, processes) and soil features".* Gray's most recent publication draws parallels between ecosystem services and geosystem services, highlighting the regulating, provisioning,

supporting, knowledge and cultural services provided by abiotic nature (Gray, 2011). However, despite this emphasis on the wide range of abiotic nature encompassed within geodiversity, the majority of current research focuses on mapping and inventorying geologically diverse and / or rare features at the regional to national scale; a Web of Knowledge search (February 2012) for research with the word "geodiversity" in the title returned 26 papers, whilst a search with "geodiversity" as a key word returned 66. Of those with geodiversity in the title, the overwhelming majority (18) were geologically focussed - given the broader scope of the original definition of geodiversity, there is clearly a need for research which explores the wider context of the geodiversity paradigm. Furthermore, figure 1.1, part a, shows that whilst the topic of geodiversity is a growing research concern, there is little published research on the links between geodiversity and biodiversity (part b). There has been a high volume of published research on the three individual components of the geodiversity model used in this thesis (figure 1.1, parts c, d, e and f), yet there have only been 34 published articles (of which only 11 are from the last 20 years) which fulfil the Web of Knowledge search term

Topic=("temporal variability" OR seasonality) AND Topic=(resources) AND Topic=("environmental heterogeneity" OR "environmental variability" OR "spatial heterogeneity" OR "spatial variability") AND Topic=(biodiversity)

and can thus be considered as using the broader definition of geodiversity used in this thesis.

The aims of this PhD are to map and model components of this wider definition of geodiversity in tropical mountains, and then investigate the relationships between these components and various measures of biodiversity. It is hoped that, by answering the following three questions, these results can be used to inform policy decisions regarding protected area planning.

Question one: Is there a quantifiable relationship between geodiversity, as modelled using Parks and Mulligan (2010), and biodiversity as measured by overlay of the available species distributions for key taxonomic groups?

Question two: Do areas that are consistently prioritised by multiple conservation schemes offer protection to a higher proportion of geodiversity than would be expected by chance alone?

Question three: What are the likely impacts of climate change on the spatial distribution of current geodiversity and what are the implications of this in terms of the suitability of current

protected area configuration in tropical mountains to protect geodiversity and thus biodiversity into the future?

a. Geodiversity

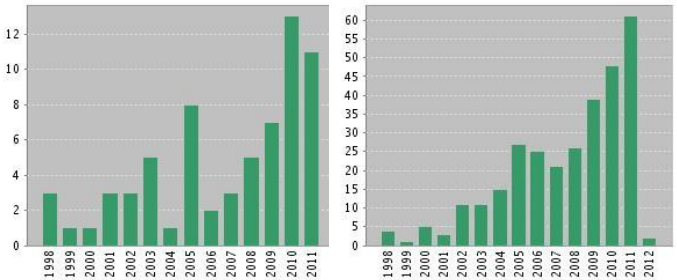

b. Geodiversity AND resources AND biodiversity

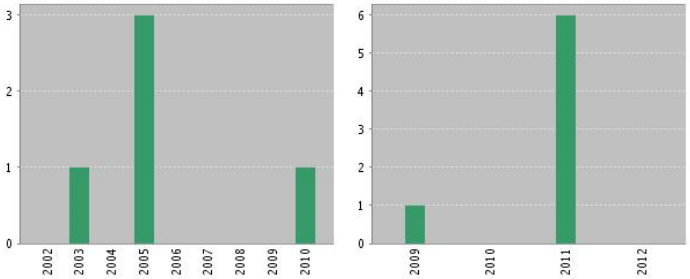

c. "Environmental heterogeneity" OR "environmental variability" AND resources AND biodiversity:

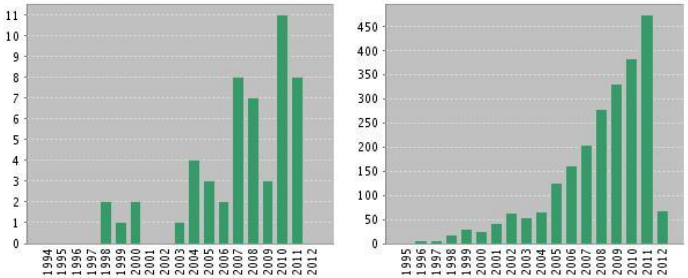

d. "Spatial heterogeneity" OR "spatial variability" AND resources AND biodiversity:

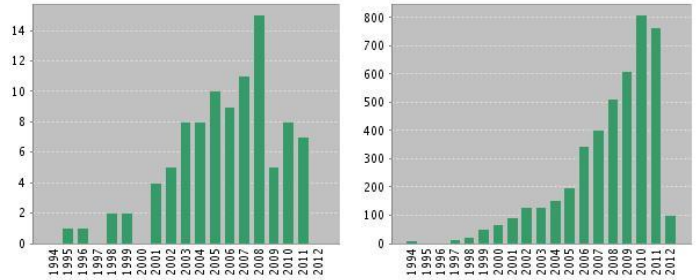

e. "Niche space" AND resources AND biodiversity:

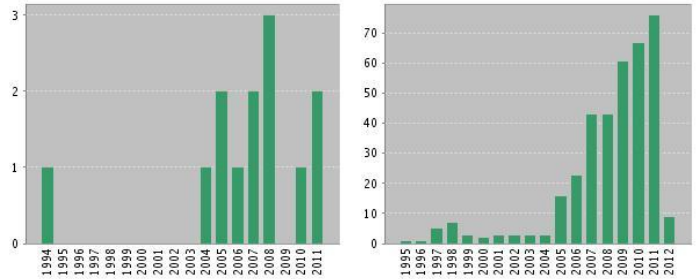

f. "Temporal variability" OR seasonality AND resources AND biodiversity

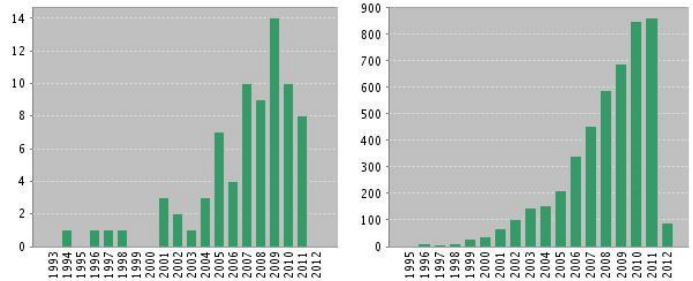

Figure 1.1. Web of Science citation reports (February 2012) based on the number of returns for the search criteria given. The left hand panel of each pair shows the number of papers published each year, whilst the right hand panel gives the number of citations each year.

1.3. Research strategy.

In order to achieve the aims and answer the questions set out in the previous section, the following objectives will need to be fulfilled:

1. Carry out a comprehensive review of the literature on bio- and geo-diversity, as well as spatial modelling and conservation prioritisation techniques.
2. Recode and further develop the Mulligan (2000) and Parks and Mulligan (2010) theoretical model of geodiversity into an executable script for the Python programming language and carry out initial testing on a 10 x 10 degree tile.
3. Run the geodiversity model to cover all tropical mountains (based on a standard definition of mountains)
4. Carry out sensitivity analyses to understand the impacts of spatial resolution and uncertainty in input datasets.
5. Compare the distribution of geodiversity with various measures of biodiversity and its distribution.
6. Within various selected study sites, compare the levels of geodiversity and biodiversity within areas of varying conservation priority
7. Evaluate the results in terms of the coverage of current conservation actions for protecting the geodiversity and biodiversity of tropical mountains.
8. Within the model test site, implement scenarios for climate change and analyse their potential impacts on geodiversity and its coverage in the existing protected areas system.

The methodological strategy taken for the PhD will reflect the three research questions. First, a map of modelled geodiversity for all tropical mountains will be produced. Model testing and sensitivity analyses for this map will be carried out on a smaller study area. Second, the differences between geodiversity scores within areas of different conservation priority will be investigated. Finally, the model will be run under IPCC climate change scenarios to investigate the potential future distribution of geodiversity and its implications.

The significance of geodiversity in terms of its relevance for global ecology and economics (see chapter 2.1.4 for details) means it is important to map its spatial distribution. In order to produce this map, the geodiversity model developed for this thesis will be run for all tropical mountains at a 1km resolution and for a smaller study area over the tropical Andes at a 90m resolution, thus enabling investigation into the effect of spatial resolution on geodiversity. The model will be validated against measures of biodiversity based on expert opinion, thus

avoiding the issues of circularity and uncertainty associated with testing the model using species distributions that are essentially modelled on the basis of climate and terrain.

When the map of current geodiversity has been produced and thoroughly tested, levels of geodiversity and biodiversity within areas of high conservation priority will be compared with those of lower conservation priority to test whether conservation priority schemes are efficiently conserving geodiversity and biodiversity. To evaluate the impact of climate change on conservation of geodiversity, geodiversity within protected areas will be characterised under current climate conditions. This analysis will then be re-run based on future projected geodiversity scenarios modelled under a range of climate change scenarios, in order to test whether current protected areas will continue to protect current levels of geodiversity. Finally an attempt will be made to suggest extensions to the existing protected area network that would conserve geodiversity through into the climatic future. Clearly these extensions may not be possible on the ground for issues of land tenure, policy, politics and cost but nevertheless such knowledge could provide a useful guide for conservation planning.

1.4. Thesis Structure.

The second chapter in this thesis is a literature review covering the history and background of geodiversity as a term, and its applications within conservation. General definitions and patterns of biodiversity are then be discussed, before the theoretical links between bio- and geo-diversity are reviewed. Finally, the status and threats of both bio- and geo-diversity are considered, along with methods of valuation and importance ranking for biodiversity for the natural world and options for conservation.

Chapter three outlines the study sites and includes an introduction to the geography and ecology of tropical mountains, along with their importance in terms of ecosystem services and current threats arising from climate and land-use change. Chapter four details the technical model development, testing and sensitivity analyses of the thesis.

Chapters five, six and seven cover the empirical work carried out for this PhD and relate to the three research questions respectively. Each chapter gives an introduction to the respective question, along with methods, results and a discussion of the implications of the finding. Chapter eight draws the results of the three previous chapters together and discusses common themes, before drawing the overall conclusions.

By answering the three research questions, this thesis presents innovative, new research. For the first time, a map of the theoretical model of geodiversity proposed by (Parks and Mulligan, (2010) and Mulligan (2008) is presented, which plots geodiversity across all tropical mountains - a larger study region than any previous geodiversity mapping efforts. A novel method for assessing the efficiency of protected areas is developed and applied in three case study sites, and finally an assessment of the impact of climate change on protected areas in Colombia is presented.

Chapter 2. Literature Review.

Although the term geodiversity is becoming more wide-spread, for example Natural England are producing Local Geodiversity Action Plans (LGAPs) as parallels to Biodiversity Action Plans (BAPs, Natural England, 2009), a solid peer reviewed literature of the concept does not exist. The first section of this chapter will outline the definition of geodiversity used in the thesis, before giving an overview of the ecological basis for each component of geodiversity as conceived of here (in terms of their processes and their interactions with each other, as well as how they contribute to overall geodiversity) and the potential application of geodiversity as a tool for use within conservation of biodiversity.

2.1. Introduction to geodiversity.

2.1.1. Defining geodiversity.

Within this thesis the term geodiversity is used as a measure of resource availability. Resources are considered as the energy, water, space and nutrients necessary to support plant and animal life and are derived from climate, topography, soils and geology. It is important to differentiate this use of geodiversity from the geomorphological definition of the term as the diversity of rocks and minerals in a landscape (as per Gray, 2004, and Gray, 2008). When the three elements of geodiversity considered here (overall resource availability, temporal variability of resources and wider spatial context of resources, figure 2.1) are combined, they provide a measure of the availability of abiotic resources and their complexity. Geodiversity exists regardless of life (although there is sometimes close interplay between the two, for example through plant control of edaphic processes). This non-living complexity (geodiversity) is hypothesised to lead to complexity within the living world (biodiversity) (Gray, 2008, Barthlott *et al.*, 1999).

Although the theoretical foundations of geodiversity have been developed over the past 100 years, the term itself is relatively new, first appearing in the literature in 1993 (Gray, 2008) in the geological sense before being adopted for use in the resource sense by Mulligan (2000) and Parks and Mulligan (2010). Geodiversity encompasses a wide range of disciplines within the geographic community from pure landscape diversity through to the diversity of environmental properties over space (Gray, 2004) and can be considered as the diversity within components of the non-living world (i.e. diversity within the geosphere, as opposed to the biosphere). The definition used here focuses on overall resource potential, temporal

variation in resource availability and wider variation of resources over space (the three elements of geodiversity, figure 2.1). Resources are defined as those properties of relevance to the development and evolution of ecosystems, specifically energy (temperature and solar radiation), water, nutrients and the space that these occupy.

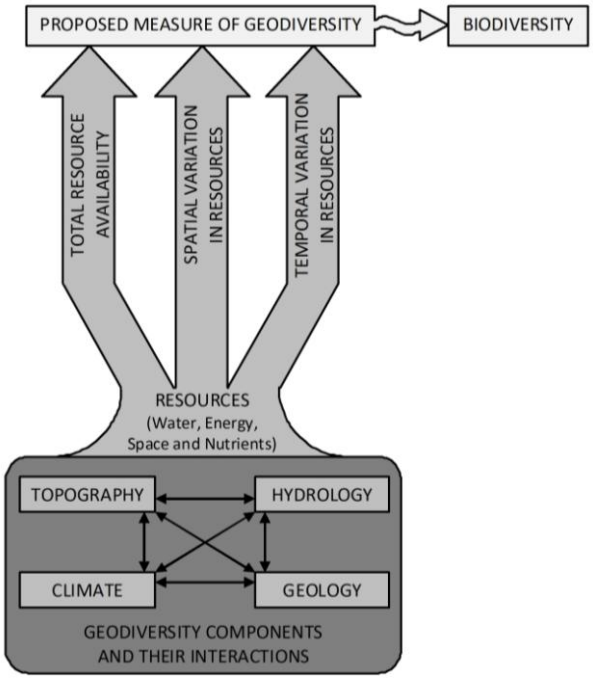

Figure 2.1. Relationships between the fundamental components of geodiversity and the measure of geodiversity used in this thesis. The theoretical relationship between geodiversity and levels of biodiversity is indicated by the wavy arrow. Total resource availability is considered in terms of a point measure of energy, water and nutrients and the space that they occupy. Temporal variation is considered in terms of a point based measure of long term trends in resource availability, seasonality of resources and stochastic events which might impact upon resources. Spatial variation is considered in terms of the wider spatial context of resource distribution. When considering biodiversity patterns, the explanatory power of each element of geodiversity may vary across ecosystems, and may be different when considering the generation versus the maintenance of biodiversity.

2.1.2. Components of Geodiversity

The four prime controls on geodiversity are topography, hydrology, climate and geology (figure 2.1, Parks and Mulligan, 2010). Soils and structural vegetation can also be considered as components of bio-geodiversity, as they contribute to the resource potential of an area,

however due to their intrinsic relationship with the biotic environment and biodiversity levels they are, for the purpose of this thesis, considered separately to the four prime controls.

The interactions between these controlling factors of geodiversity lead to the production of resources (water, energy and nutrients and the space that they occupy) which are here considered to form the three components of geodiversity (total resource availability, spatial resource context and temporal (seasonal) variation in those resources). These components of geodiversity have been shown in the literature to act as controls on biodiversity, as discussed further in chapter 2.4. Given the multi-disciplinary nature of this thesis, the next few paragraphs will outline the fundamental processes which act as controls of the geodiversity model used in this thesis (topography, hydrology and climate) increases overall geodiversity levels. Unless otherwise referenced, all information in section 2.1.2 is based on Strahler and Strahler (2005)

Topography, or the terrain of an area, varies in many ways, the most commonly applied measures being elevation, slope and aspect. Many other indices exist to cover elements such as topographic exposure and landscape form. Generally, steep slopes at a high elevations (mountain peaks) have a higher topographic exposure than gentle slopes at a lower elevation (valley floors). Topography has varying effects on other components of geodiversity; elevation influences temperature and rainfall through the adiabatic lapse rate and orographic effects (Whittaker and Niering, 1975); slope gradient affects water flow, soil erosion and geomorphological processes; slope aspect affects radiation receipt and its timing as well as exposure to dominant winds. A complex terrain will lead to a spatially structured environment with well defined and different niche spaces.

Climate influences geodiversity in terms of resource provision, via insolation and precipitation, and landscape shaping through geomorphological processes. Insolation is the ultimate source of almost all energy on the Earth's surface, with the amount and intensity of insolation at any one time being controlled by latitude, the time of day, time of year, aspect, slope and shading (from vegetation or other structures, as well as cloud cover and atmospheric transmissivity). It is possible to model insolation using these factors (e.g. Iqbal, 1983); once this has been modelled, the output can be corrected for cloud cover to give the amount of insolation reaching the surface layer. This will show the amount of insolation reaching tree canopies, rather than reaching the ground.

Precipitation provides water - necessary for all life on Earth, but also an essential component of geodiversity in terms of hydrological processes. Precipitation can reach the Earth's surface in a liquid state (rain / fog / dew) or solid state (snow / hail / frost). In the tropics, liquid precipitation is the predominant form. It tends to be measured in mm, however measuring precipitation can be difficult for two reasons. First, the patchy nature of rainfall means that although there could be a high level at one rain station, there is no measurement of actual volume of water fallen because the rain-gauges simply give a point measurement and no indication as to the area over which the precipitation fell. For example, a highly localised rain storm will release a lower volume of water than a wide-spread rain storm, however if both passed over the same rain gauge they could deposit the same amount of water in it. Second, some precipitation may not make it into the rain gauge; for example, wind driven precipitation may be blown over the mouth of the rain gauge - an important consideration within tropical mountains where a substantial amount of precipitation is wind-driven (Hijmans *et al.*, 2005). Moreover, precipitation with very fine droplets could get stuck to the side of the gauge and evaporate before reaching the measuring cylinder.

The movement of water can be divided into terrestrial and underground flows. In a non-human influenced system, terrestrial flows consist of interception of the precipitation either directly onto the surface or via vegetation. The precipitation then either infiltrates the soil to become part of the underground flow, or runs off into streams / rivers which can be classified using the Strahler system (figure 2.2). Streams of different orders have differing characteristics and therefore differing influences on the surrounding environment. In terms of geodiversity, the main impacts of hydrology are on the supply of resources and the evolution of the topography of the landscape; fluvial processes are one of the predominant driving forces which shape the "raw" geology into the variety of landscapes present across the globe by erosion, transportation and deposition.

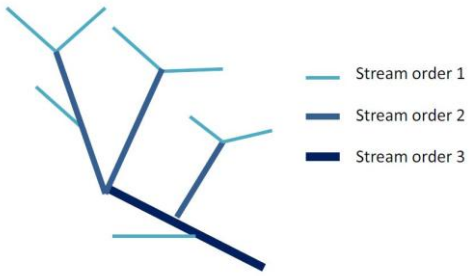

Figure 2.2. Strahler (1952) stream classification; when two first order streams join, they become a second order stream. When two second order streams join, they

become a third order stream. The order value only increases when two streams of the same order come together.

Once underground, the water becomes soil-water before either resurfacing and flowing to the sea, or becoming ground water. Water then re-enters the atmosphere via evaporation from surface water or transpiration of ground water by vegetation, collectively known as evapotranspiration. There is a distinction between actual evapotranspiration and potential evapotranspiration; actual being the volume of water physically returned to the atmosphere, whilst potential is the amount of water that would be returned to the atmosphere given an unlimited water supply. Actual evapotranspiration is difficult to model (and measure), however various models of potential evapotranspiration have become widely accepted (see chapter 4.2.3.3.7 for further details of the Latent Heat, Thornthwaite and Penman models).

Stochastic events change geodiversity by disturbing the existing, established niche patterns. For example, a volcanic eruption can disrupt all other elements of geodiversity. Examples of stochastic events include treefall, landslides, volcanoes, earthquakes, fires and floods. The main characteristics of these events, in terms of geodiversity, are that they occur at unpredictable / irregular intervals and that they cause a disturbance to the existing geodiversity thus generating space under a different resource regime for new individuals or species. Some stochastic events may display a degree of seasonality (for example, flooding), however they often do not follow a strict, regular rhythm. Stochastic events occur across a range of scales from point (e.g. treefall) to global (e.g. impacts of volcanic eruptions). High levels of disturbance would lead to high levels of geodiversity (under the model considered in this thesis); when considering the links between biodiversity and geodiversity, consideration of the intermediate disturbance hypothesis suggests that regions with mid-level disturbance may be the most diverse (Connell, 1978).

Although it is not possible to model exactly when or where stochastic events are going to occur, it is often possible to create statistical distributions of their frequency and magnitude (for example, Malamud *et al.*, 2004, Corral *et al.*, 2008). This is a practice used frequently in flood risk management, for example a flood may be classified as a ten year event, meaning that, although an event of that magnitude is statistically likely to occur once every ten years, the event does not have a regular ten year periodicity and it may occur twice in two years or not at all in 20 years.

2.1.3. Geodiversity - a resource based approach

Regions with a high level of overall resource availability are those with higher temperatures (as a measure of energy) and high levels of available water, for example tropical rainforests - a constant supply of water with high temperatures indicating high energy levels. By contrast cold, dry regions, such as tundra, have a low level of overall resource availability because of little available water or energy. Intermediate levels of resource availability could come from either intermediate levels of both water and energy, or could arise when one factor becomes limiting and thus act according to Liebig's Law of the Minimum (Sprengel, 1828, Liebig, 1855). For example, tropical dry forests have lower overall water availability than rainforests so despite the similar energy regimes the overall resource availability in tropical dry forests would be lower than those for rainforests.

The availability of resources at a single point is not independent of the wider resource context; invoking Tobler's first rule of geography (Tobler, 1970), it becomes apparent that the wider spatial context of resources also influences the resource regime at a given point. The second component of geodiversity, spatial context of resources, considers this. Areas with a low local resource availability, in a regional context of low available resources, would have a lower geodiversity score than a locality with a similarly low local resource availability in a regional context of higher resource availability. Consideration of this wider resource context enables maintenance of a fine model resolution, whilst also considering processes that occur at a more coarse grain. Biologically, this is equivalent to the "species richness by small grid cells, including neighbouring grid cells" approach to measuring biodiversity illustrated in figure 1g of Kier and Barthlott (2001) and discussed in further detail in section 2.2.5 below.

Temporal variability (seasonality) is also an important component of geodiversity. In terms of energy availability, seasonality is predominantly dependent on latitude, with lower (tropical) latitudes having lower seasonal variability in day length and insolation. However, seasonality in rainfall does exist in the tropics with some regions experiencing distinct rainy seasons, whilst others have more constant conditions. The level of seasonality provides a temporal structure to the environment in a similar way to the spatial structure provided by spatial variation, thus leading to a more complex system.

When the three elements are combined to give a measure of overall geodiversity, regions that have a high overall level of available resource and are seasonally structured will have a high geodiversity score whereas regions that have few resources and / or are unseasonal will exhibit a low geodiversity score. Not all controls (terrain, climate etc.) contribute to all

components of geodiversity, for example not all controls exhibit seasonality. Furthermore, the influence of each individual component of geodiversity may vary from region to region; in some regions it may be the temporal variation that determines the biological characteristics of the region whereas in others it could be the overall resource availability that is most significant.

2.1.4. Potential applications of geodiversity

The value humans put on nature is evident from the policies designed to protect it (for example the Convention on Biodiversity, CBD, 1992) and the amount of money donated to conservation charities (for example, between June 2007 and June 2008, the Nature Conservancy received $113 387 000 in unconditional pledges, combined with $81 139 000 in conditional pledges, giving a total of almost $200 million. In total their assets were over $5.6 billion (Nature Conservancy, 2008). What is more open to debate is the motivation behind this commitment to conservation, and what it is that is being conserved. This section will discuss different methods of valuing nature before considering how geodiversity can be used as a tool to guide conservation decisions.

Species specific conservation is a dominant source of conservation funding, however donations and funding are not evenly distributed among taxa. Lorimer (2006) gives an example from the UK; the Royal Society for the Protection of Birds raised over £60 million in 2004, as opposed to the £80 000 raised by the Dragon Fly Society. He argues for an axis of anthropomorphism with "wild, unruly" species at one end and "cuddly, doe-eyed mammals" at the other. Both ends of the spectrum have non-human charisma for differing groups of naturalists, who are often diametrically opposed to the conservation fund raising methods of the other group. The Global Biodiversity Assessment (UNEP, 1995) suggests that the focus of research and conservation resources needs to be targeted to keystone, indicator, threatened, umbrella, flagship, agricultural, medical or commercially valuable species.

Even if there was a general consensus over which species we ought to conserve, there are several researchers who debate whether species conservation in itself is the most efficient technique for conservation. Mace (2004) argues that, as species classification can be arbitrary, we lack a valid taxonomy on which to base species conservation; if we don't know what a species is, how can we conserve it? Even using the established taxonomic system we have classified under 2 million species (IUCN, 2010a), whilst estimates of total numbers of species suggest there are in total approximately 8.7 million (± 1.3 million, Mora *et al.*, 2011). In

addition, our knowledge of the geographic range of the vast majority of species is limited (Pimm *et al.*, 1995). These problems are summed up by Whittaker *et al.*, (2005) who define two shortfalls in our taxonomic knowledge; we don't know what species exist (the Linnaean Shortfall) and, of the species we know of, we don't reliably know where they are found (the Wallacean Shortfall).

Furthermore, if we could reliably define a species, and knew their precise geographic ranges, the species may not be the most stable unit on which to base conservation decisions as different species will react differently to climate change (e.g. Harris *et al.*, 2006). An alternative would be to conserve phenotypic diversity, i.e. diversity within species, as not all species represent the evolutionary diversity necessary to generate phylogenic diversity (Owens and Bennett, 2000). Conserving areas high in phylogenic diversity would conserve existing diversity, however an alternative approach is to conserve areas of low phylogenic diversity as these have potential for sudden evolution (Spathelf and Waite, 2007). Parallels can be drawn between this and the debate over reactive and proactive conservation (section 2.6.3).

An alternative way of selecting which species to conserve is to value those with a high level of endemism. Endemic species have long been valued as conservation targets because they tend to be unique species (i.e. have few close relatives) and are often found in exotic locations; some NGOs have focussed on endemism as a major conservation strategy, for example Birdlife International's Endemic Bird Areas (Brooks *et al.*, 2006). Endemics are also targeted for conservation efforts because they are most at risk of extinction due to their vulnerability to climate change (Malcolm *et al.*, 2006) and their inability to re-colonise (Pimm *et al.*, 1995). However, endemics are not intrinsically at risk of extinction; for example healthy communities of highly endemic species persisted on the Galapagos Islands until the arrival of humans (Whittaker *et al.*, 2005).

It is often assumed that endemism, total species richness and number of threatened species are correlated however, for birds, endemism can be used as a surrogate for total and threatened species richness but this is a one way relationship (i.e. species richness and number of threatened species do not act as a surrogate for endemism) (Orme *et al.*, 2005). Further research reports that endemism is a good surrogate for the threat level to all terrestrial vertebrates (Lamoreux *et al.*, 2006). In terms of prioritising areas for conservation, hotspots of narrow endemism and hotspots of complementary species richness conserve more species than random selections, whilst hotspots of species richness performed no better than a

random selection (Williams *et al.*, 2000). However, when defining an endemic area it is vital to take sampling effort into account, as the two can be correlated (Whittaker *et al.*, 2005).

It is important to remember that current biodiversity is merely a snap-shot in evolutionary history; an alternative to placing inherent value on existing species is to value the process that led to the existence of those species. The Orlog Model for conservation (Bowen and Roman, 2005) argues that the three disciplines of phylogeny, ecology and evolution are inherently important for conservation (figure 2.3).

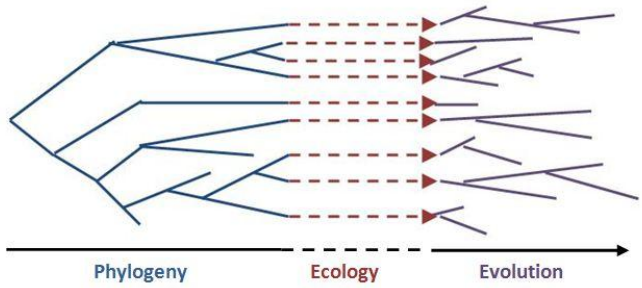

Figure 2.3. The Orlog Model (after Bowen and Roman, 2005). Today's ecology (red dashed lines) is the product of evolutionary history (phylogeny, blue lines), and provides the foundation for future evolutionary diversity (purple lines). Time is represented by the black arrow, and is stretched at the present time to represent ecology as a snapshot in an evolutionary continuum.

Given the limited resources of conservation efforts, Diniz (2004) asks the legitimate question, should we conserve evolutionary novelty (phylogenic divergence) or evolutionary potential (genetic divergence)? Mace and Purvis (2008) argue that it is impossible to take evolutionary processes into account as conservation schemes often last, at the most, for decades whereas (in most cases) evolutionary processes are much slower. They suggest that rather than conserving specific processes, the species branch length ought to be considered as this provides a measure of their evolutionary distinctness and is a surrogate for the pattern and character of the species diversity. They conclude that, unfortunately, it is only the Cape Floristic province that has genetic data detailed enough to be able to make these kinds of decisions.

An alternative to valuing and conserving biological diversity *per se* is to place an economic value on the services provided by nature. Fully functioning ecosystems provide humans with a number of services, without which we could not survive. These include food, fibres, potable water, shelter and medicine (Diaz *et al.*, 2006). The Millennium Ecosystem Assessment

categorises ecosystem services into supporting, provisioning, regulating and cultural, with the concept of biodiversity underpinning all four (figure 2.4). It is virtually impossible to place a monetary value on these services and estimates of global ecosystem services vary enormously from $33 trillion in 1997 (Costanza *et al.*, 1997) to $973 trillion in 2007 (Hsiung and Sunstein, 2007). Even taking inflation into account, this illustrates the huge discrepancy in estimates and has led to such estimates being highly controversial (Hoekstra *et al.*, 2005).

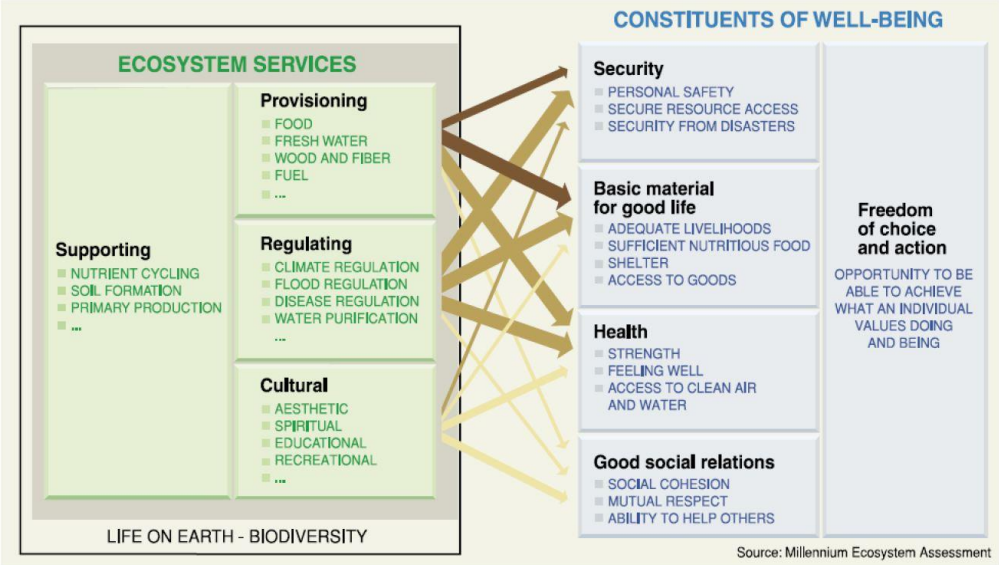

Figure 2.4. Classification of ecosystem services and the links to human well-being by the Millennium Ecosystem Assessment (Millenium Assessment, 2005)

In order for continued provision of these services, ecosystems need to be fully functioning. However, defining the functional role of a species within an ecosystem is not an easy task. For example, Jax (2005) outlines four meanings of the word "function" in biology (figure 2.5). It can be argued that, in order for the ecosystem to be functional, each functional role needs to be filled to allow for the functional processes between organisms to continue and thus provide the function that humans use the ecosystem for. Diaz *et al.* (2006) consider this functional diversity (of functional roles, processes and services) the most important component of biodiversity.

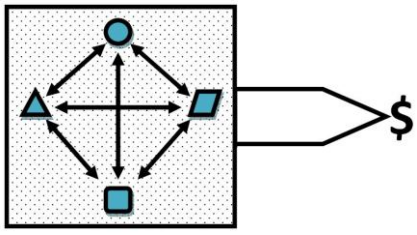

Figure 2.5. Illustration of four definitions for the use of the word "function" in biology (Jax, 2005). Functional interactions between species are represented by arrows, the

functional role of different species are represented by the various small shapes, the functioning ecosystem is illustrated by the spotted background, whilst the ecosystem service function is represented by the $.

The relationship between species richness and ecosystem function is debated; Scherer-Lorenzen *et al.* (2007) cite examples of increases in productivity and nutrient cycling in diverse sites compared to mono-cultures (Stanley and Montagnini, 1999), whilst Zhang and Zhang (2007) found that communities with high species richness tend to be more productive (however, this was based on micro-experiments using algae and so scaling results up to ecosystem level is not a trivial issue, especially given the co linearity of climate with both productivity and biodiversity). Tilman (1999) reports modelled and empirical evidence to suggest that increased plant richness leads to increased primary production, primarily due to niche specialisation. On the other hand, Kareiva and Marvier (2003) report that ecosystems that provide important services are often found in locations that are considered "cold-spots" in terms of species richness. They cite the example of tidal salt marshes which, although very low in terms of species diversity (20 - 30 species), provide approximately $10 000 per hectare per year in terms of flood protection and fishery production.

Conservation of functional diversity avoids the size-ism of species based conservation, however it can be difficult to fully audit the functional traits within an ecosystem as these can include broad, trophic level traits (such as carnivory), narrow traits (such as eating specific sizes of prey) and also facilitation traits (such as symbiotic relationships) (Petchey and Gaston, 2006). Furthermore, functional diversity can be controversial as it could potentially involve introducing alien species to fulfil a certain functional role (Harris *et al.*, 2006). In addition, it is very difficult to measure and map.

Geodiversity can be considered the bedrock of biodiversity (Gray, 2011), and can be linked to all the values of nature outlined above; to species-based conservation measures through its provision of habitat and niche space in which organisms exist and evolve, and to ecosystem-service based conservation measures through its provisioning of the raw resources necessary for many of the vital services provided by nature. Gray (2004) cites the example of fresh water provisioning which cannot happen without the necessary climatological, topographical and hydrological conditions. He also points out that, historically, geodiversity has been valued over biodiversity; the world's first protected area (Yellowstone National Park) was designated due to its geological features. Many protected areas in mountains are still designated primarily for their geological and topographic uniqueness, rather than their biodiversity (Hamilton, 2002).

Geodiversity could be a useful conservation tool for two reasons. First, data availability, accuracy, detail and monitoring potential is much greater than for biodiversity. Remotely sensed global datasets are available for the majority of geodiversity elements, allowing like-for- like comparisons of global geodiversity. Second, if geodiversity proves to be a reliable predictor of biodiversity, there is potential to use measures of geodiversity to guide protected area planning. Ensuring a full range of geodiversity is protected may increase representation of unknown species within the protected area network, whilst also allowing for the evolution of new species (Bonn and Gaston, 2005).

2.2. Defining biodiversity.

Although the word "biodiversity" was first used by E.O. Wilson in 1987 (Nobis and Wohlgemuth, 2004), the majority of journal articles referring to biodiversity do not offer an explicit definition and assume the reader understands the meanings and implications of the term (Redford *et al.*, 2003). This potentially results in a multitude of differing definitions, each with different underlying assumptions regarding, for example, species-richness (number of species within a given area), species evenness (the evenness of the number of individuals / total biomass of each species within an area, a measure of whether the area is dominated by a few species) and degree of endemism (how common the species are outside the study area). Some authors deliberately do not offer a definition "we will speak throughout of 'biodiversity' without dwelling too much on its definition" (Pearce, 2007, p. 315). Others acknowledge the difficulties of giving a specific definition, due to the complexity of measuring all components of biodiversity, and thus conclude it is not possible to fully define biodiversity (Sarkar *et al.*, 2006). It is also common for conservation groups to define biodiversity in such a way to promote the conservation of their particular target organism or system (Redford *et al.*, 2003). However, due to public "bio-philia" (Wilson, 1984, Thompson and Starzomski, 2007) and the need to achieve the conservation goals set out in international policies (e.g. the Convention on Biodiversity, CBD, 1992), it is important to have a degree of consensus on a definition of biodiversity (Botkin *et al.*, 2007). Drawing on different fields of expertise, three types of definition for biodiversity are outlined below, before methods for measuring and modelling biodiversity at various spatial scales are discussed.

2.2.1. Ecologically derived definitions

Ecology customarily divides diversity within and among ecosystems into three measures: α, β and γ. Thompson and Starzomski (2007) define these as:

α - The number of species at a given location; species richness

β - The variability of species between localities

γ - The potential number of species at a location

Buckland *et al.* (2005) also refer to three aspects of biodiversity; number of species, species evenness and overall abundance (or biomass if species vary considerably in size). These can be considered as approximately equivalent to α, β and γ.

Buckland *et al.* (2005) go on to argue that, although the three aspects of biodiversity are theoretically easy to quantify (based on a count of all species), biological surveys tend to be biased towards large, easily-detected species and therefore in reality α, β and γ are not useful working definitions. They also point out that methodological inconsistencies and variations in survey extent mean results from different surveys are often incomparable, even if the same geographical region is surveyed.

Thompson and Starzomski (2007) state that the problems with α, β and γ as working definitions of biodiversity remain even if full species inventories from methodologically consistent surveys are available, as information on abundance or temporal variation is not provided. They go on to point out that it is possible for α to increase, whilst β and γ are declining. For example, local diversity (α) may increase due to an invasive species, whilst overall global diversity (γ) is decreasing.

2.2.2. Policy derived definitions

There is a general consensus among policy makers that conservation of biodiversity is important; currently 193 Nations are listed as ratified Parties to the International Convention on Biodiversity (CBD, 2010). However, what is lacking is an agreed definition of exactly which aspect of biodiversity polices are aiming to conserve. One of the earliest international policies aiming to conserve the variation of life on earth was the United Nations Educational Scientific and Cultural Organisation's Man and Biosphere programme (UNESCO-MAB). Founded in the 1970s, the MAB work focused on interdisciplinary research and capacity building to support a growing network of biosphere reserves (areas which protect a range of ecosystems) (UNESCO-MAB, 2008).

Today the three aims are:

1. To minimise biodiversity loss through the use of science in policy making.

2. To promote environmental sustainability through the World Network of Biosphere Reserves.
3. To enhance links between cultural diversity and biodiversity.

MAB focuses on conserving the uses of biodiversity for humanity, using a broad definition of biodiversity; "biodiversity encompasses the wide variety of genetic resources and species as well as ecosystems and landscapes" (UNESCO-MAB, 2008). This wide scope has led to the MAB programme being involved in many globally important conventions ranging from the World Heritage Convention to the Convention on Biodiversity.

The Convention on International Trade in Endangered Species (CITES) came into force in 1975 and, whilst not specifically addressing the issue of biodiversity loss, it aims to protect endangered species, implying that species richness is the most important aspect of biodiversity (CITES, 2008).

In 1992 the United Nations Conference on Environment and Development (UNCED) took place in Rio de Janeiro, Brazil. The 2 week conference brought together 172 governments with the intention of moving global environmental policies forward from the 1972 Stockholm UN Conference on the Human Environment (UN, 1997). The Convention on Biodiversity, outlining targets and conservation strategies for conservation of global biodiversity, was one of five documents resulting from the Rio conference. The convention text (CBD, 2006, article 2) defines biological diversity as

> *"the variability among living organisms from all sources including, inter alia, terrestrial, marine and other aquatic ecosystems and the ecological complexes of which they are part; this includes diversity within species, between species and of ecosystems".*

This definition is very broad and therefore all facets of biodiversity are covered by the convention. However, the convention fails to become more specific with terms when setting targets. For example, the targets set by the convention (Appendix 1) aim to conserve "areas of particular importance" (Target 1.2, CBD, 2009), but do not specify which aspect of biodiversity is under consideration. Areas of importance for genetic diversity (the only target specifying genetic diversity, Target 3.1, refers specifically to crops and harvested species) are likely to differ significantly from areas of importance for ecosystem conservation. Furthermore, by defining genetic diversity as diversity within crops, the convention does not provide protection for within-species genetic diversity; a vital component of diversity which allows populations of species at the edge of their range to adapt to sub-optimal environmental conditions (Mace and Purvis, 2008).

One of the major realisations at the CBD was the lack of knowledge regarding the world's biodiversity. In an attempt to remedy this, the United Nations Environment Programme (UNEP) undertook a Global Biodiversity Assessment, GBA (UNEP, 1995). This 1140 page document aimed to document the state of scientific knowledge; highlighting areas where consensus had been reached as well as where further research was necessary. Biodiversity was defined as "the total variety of life on earth " (UNEP, 1995, p. 5) and was considered to consist of:

- Taxonomy - species and organisms
- Ecology - the links between species and organisms
- Ecological diversity - the number of species in a given area, the function of these species in terms of ecosystem dynamics and how this changes in different areas
- Genetic diversity - the amount of variability within crop plants
- The human dimension - human interactions with all aspects of biodiversity

The GBA raises an interesting point with regards to the usage of the word biodiversity; it is used as both a noun and adjective. The scientific community tend to use it as an adjective, for example describing a property of an ecosystem, whereas policy makers tend to use it as a noun, for example policies listing the biodiversity present within an ecosystem. This highlights the potential confusion that can arise when discussing a concept, such as biodiversity, which has a wide range of meanings and usages. This thesis will use the word as to describe species richness.

2.2.3. Mathematical indices of biodiversity

Depending on their purpose, mathematical indices have used varying combinations of α, β and γ to produce alternative measures of biodiversity. The simplest measure is *S*, species richness (equivalent to α). However, this takes no account of the evenness of species abundance or overall dominance of a single species within the community (β).

Species richness indices (measuring α) can be divided into two classes; those that measure the numerical species richness and those that measure the species density (species per sample area) (Magurran, 2004). Two examples, taken from Magurran (2004), are the Margalef index

$$D = \frac{(S-1)}{\ln N} \qquad 1$$

and Menhinick's index

$$D = \frac{S}{\sqrt{N}} \qquad 2$$

where *S* is the number of species recorded, *N* is the total number of individuals recorded (from all species). However, she points out that although these are simple to calculate, they do not show relative abundance and also generate values which are dependent on sample size.

The two earliest attempts to give an indication of relative species dominance (β), which are still recommended for use (Hubalek, 2000), come from Shannon (1948) and Simpson (1949).

Shannon's (1948) diversity index

$$H = -\sum_{i=1}^{S} P_i \ln P_i \qquad 3$$

where *S* is the total number of species in the community and P_i is the proportion of species *i* within community *H* (in terms of biomass or individuals), is used to calculate the proportional contribution of each species within the community. A problem with this index arises if sampling does not cover all species in a community; however the impact on the index score decreases with decreasing actual abundance of the species omitted (Magurran, 2004).

An alternative to the Shannon index is Simpson's (1949) diversity index

$$D = \frac{1}{\sum_{i=1}^{S} P_i^2} \qquad 4$$

although this is less sensitive to rare species within the community as it is dependent on the underlying species abundance distribution (Magurran, 2004). Sherwin *et al.* (2006) suggested that the two measures ought to be used in combination to reveal details within the species composition of communities. They give the hypothetical example of two communities with identical *D* but different *H* values; this suggests that although the two had similar overall diversity values, there are key differences in the composition of the rare species. Countless alternative diversity indices have been proposed; Buckland *et al.* (2005) give a comprehensive review of these.

Faiths *et al.* (2008) have criticised traditional biodiversity indices for being too concerned with characterising diversity, rather than measuring the "quality of biodiversity", measured as the intactness of an ecosystem. They propose using the Biodiversity Intactness Index (Scholes and Biggs, 2005) as a measure of the quality of biodiversity. However, it is of questionable benefit to attempt to assess the quality of something we have not yet been able to fully quantify.

D and *H* are widely used in small scale biodiversity studies; they are not appropriate for use at a larger scale due to lack of consistency between survey methods for different locations and

taxa (Buckland *et al.*, 2005). As a result, at the continental scale, mapping schemes based on expert knowledge rather than empirical data, such as the Myers *et al.* (2000) hotspots scheme, tend to be favoured as the data required for calculation of indices is seldom available (Whittaker *et al.*, 2005). The next two sections consider techniques for measuring or modelling biodiversity at these larger scales, whilst section 2.7.3 discusses conservation prioritisation.

2.2.4. The taxon versus the inventory approach

Carrying out a complete inventory of biodiversity everywhere on Earth is clearly an impossible task and as a result surrogate measurements are necessary (Callicott *et al.*, 2007). Sarkar *et al.* (2006) report that pre-1980s, species area curves were combined with general ecological principles and used to determine which areas were likely to have high biodiversity. In the 1980s geo-distributional data was included, and more recently (1990s onwards) socio-economic data has also been included, requiring the use of ever more complex algorithms and high levels of computing power. Most of these approaches are based on the assumption of adequate species distribution data being available, however this is often not the case and so surrogates based on species distribution models are often used instead (Rodrigues and Brooks, 2007, Elith *et al.*, 2006).

Currently a wide range of surrogates is used; the selection of an appropriate one is often a bewildering choice with at least 14 in regular use in the USA (Andelman and Fagan, 2000). However, Ferrier and Watson (1997) have classified all types of surrogates into three classes:

1. Mapped land classes, based on land attributes (e.g. bio-regions, Thackway and Cresswell, 1995, and other references in Ferrier and Watson, 1997)
2. Classifications based on primary environmental data (e.g. environmental domain analysis, Belbin, 1993, and other references in Ferrier and Watson, 1997). The use of geodiversity as a surrogate for biodiversity would fall into this class.
3. Species distribution models (e.g. use of taxonomic surrogates, Rodrigues and Brooks, 2007)

They argue that the use of surrogates is valid when they are used to fill an information gap, either in terms of taxonomic knowledge or geographical (distributional) knowledge.

A common type of taxonomic surrogate used by conservation NGOs is the "*Flagship Species*". An example of the use of a charismatic species for fundraising purposes is the panda logo of the World Wildlife Fund (WWF). Initially it was hoped that by conserving the panda other species would also benefit. However, work based on the African "Big 5" (*Loxodonta africana*

(elephant), *Ceratotherium simum* and *Diceros bicornis* (white and black rhino), *Syncerus caffer* (buffalo), *Panthera leo* (lion) and *Panthera pardus* (leopard)) has been shown that, after controlling for the effect of area, protecting the habitat of a different assemblage of randomly selected species could protect approximately 20% more mammals and birds than protection of the Big 5 (Williams *et al.*, 2000).

A further issue with using Flagship Species as surrogates is that the distribution of the surrogate species may not be fully known; usually the distributions are based on model outputs. Often these are modelled on the basis of environmental factors (as discussed in section 2.2.5), leading arguments that it is increasingly possible to use environmental data alone as a biodiversity surrogate (e.g. Sarkar *et al.*, 2006). By using species distribution models as surrogates, conservationists risk "one set of predictions ... being used to evaluate another set of predictions" (Ferrier *et al.*, 2002, p.350), however there is too little detailed species distribution data to eliminate the need for modelled distributions (Elith *et al.*, 2006).

In this thesis, the potential of the model of geodiversity proposed to act as a proxy for biodiversity will be explored; thus being more closely aligned with the taxon rather than inventory approach. However, it is important to note that at no point are the outputs of the geodiversity model meant to represent distributions of particular species or taxonomic groups.

2.2.5. Modelling Biodiversity.

Species modelling algorithms can generally be classed into three groups: those that require just presence data for the target species, those that require presence and absence data and those that require presence data and background environmental data from which "pseudo-absence" data can be determined (Elith *et al.*, 2006). The aim of the models is to describe a species distribution in terms of its niche space, which is then projected into geographic space (Phillips *et al.*, 2006).

More recently, models that take into account species assemblages have been developed - these community models use data on other species' presence to predict the presence of the target species (for example, MARS-COMM, Elith *et al.*, 2006). Due to the lack of extensive, good quality presence absence data, many studies use presence only and pseudo absence data; particularly those working in under-sampled regions such as the tropics (Phillips *et al.*, 2006). In a review of 16 modelling techniques, Elith *et al* (2006) found that MaxEnt was one of a group of four models which performed consistently well across different regions and species.

This chapter will discuss MaxEnt, along with another commonly used model - BIOCLIM, and compare these approaches with modelling of overall trends in biodiversity and with the approach taken in this thesis.

Based on point occurrence data and up to 35 climatic variables, BIOCLIM calculates a rectilinear niche envelope that will include 90% of the recorded occurrences. This envelope can then be projected onto geographical space and the system will map areas where the climatic conditions meet those of the accessions within the test dataset (Beaumont *et al.*, 2005). Envelope models are criticised because they are highly sensitive to their initial occurrence dataset and can therefore over-fit the model to the occurrence data (Whittaker *et al.*, 2005). They also fail to take biological processes into account, for example competitive release and local adaptations (Hampe, 2004). However, they have been found to be useful for predicting general patterns in distributions at continental / global scales (Pearson and Dawson, 2003).

MaxEnt is a modelling algorithm based on the second law of thermodynamics that, without constraints, a system will increase in entropy over time (Phillips and Dudik, 2008). The model uses presence and background environmental data to estimate an unknown probability distribution for species occurrence over the modelled area; the distribution is constrained only by known occurrences of the target species (presence data) and the output is the distribution which satisfies those constraints and maximises entropy (Phillips *et al.*, 2006). In order to test the model, pseudo-absence points are generated from the background data; this is done in such a way to reduce the risk of accidental inclusion of unrecorded occurrence points in the pseudo-absence points (Phillips and Dudik, 2008).

Another method of mapping biodiversity is to generate distributions for individual species and then sum these to create maps of species richness. Depending on the extent of the study area, this can be a highly computer intensive methodological strategy. An alternative is to model species richness directly, rather than creating distribution maps for individual species and then overlaying these. Kier and Barthlott (2001) outline three approaches to this (figure 2.6):

1. Species richness by region, for example mapping vascular plant species richness by ecoregion (Kier *et al.*, 2005).
2. Species richness by standardised grid cell (large or small), for example mapping diversity of sphingid moths in Malesia (Beck and Kitching, 2007).
3. Species richness by small grid cells, including neighbouring grid cells, for example use of indicator species presence to predict overall species richness in butterflies in Nevada, USA (Mac Nally and Fleishman, 2002).

All of these methods are, to varying degrees, vulnerable to the ecological fallacy - depending on the size of the grid cell or region. When a single value is assigned to a region, the spatial variation within that region is not represented and the assigned value may be unrepresentative of large portions of the region. However, when there is limited distribution data or computing power, these approaches are valuable when appropriately applied.

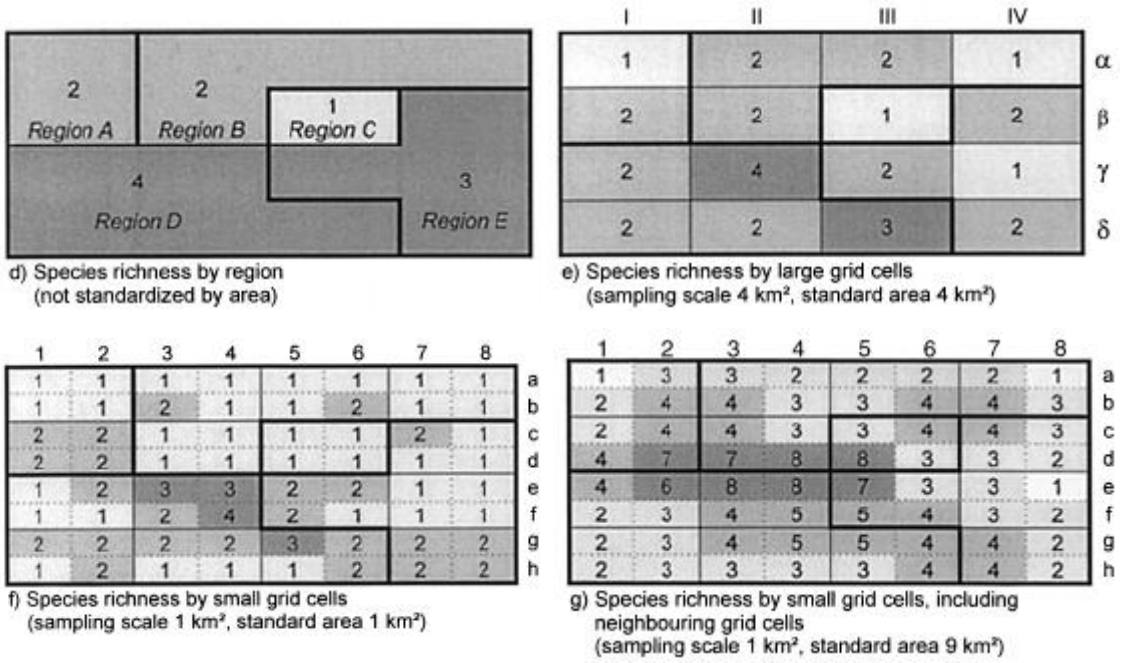

Figure 2.6. Species richness measures illustrated in figure 1 from Kier and Barthlott (2001)

2.3. Patterns of biodiversity.

Biodiversity is not randomly or evenly distributed over the Earth; it shows distinct geographical patterns - a reflection of the nature of biodiversity and not, as some authors consider, a data problem requiring correction (Hawkins and Diniz, 2004). There are many gradients in these patterns; the most universally accepted being the species-area relationship, that the number of species increases with the extent of the sampling area (Begon *et al.*, 1996). The latitudinal gradient, which has been found to exist since before 65 mybp (Mittelbach *et al.*, 2007) and today exists across a wide range of marine and terrestrial taxa (Gaston, 2000), and gradients in species distributions across altitudinal bands (Romdal and Grytnes, 2007) are also recognised phenomena. All these broad-scale patterns in biodiversity need to be considered in conjunction with each other, because gradients taken individually do not give a complete description of a spatial pattern that has at least two dimensions (Hawkins and Diniz, 2004). It is worth noting that the species is the unit generally used for biodiversity studies, so little is known of diversity patterns at alternative phylogenic levels (Gaston, 2000).

2.3.1. The latitudinal gradient

The latitudinal gradient has been recognised for 230 years (Hawkins and Diniz, 2004) and refers to a general pattern of high biodiversity in the tropics which declines non-linearly towards the poles (Gorelick, 2008). This general pattern may be interrupted by other factors, such as topography, and does show some deviation from the generally accepted pattern in that the peak may not occur at the equator and the decline may not be symmetrical in both hemispheres (figure 2.7, from Gaston, 2000). However, this pattern is not found globally, for example in Australia there is a stronger longitudinal gradient (Hawkins and Diniz, 2004). Furthermore, it is important to remember that latitude is not, in itself, an explanatory variable; it is a surrogate for other environmental variables which vary with latitude and in turn control the distribution of species (Gaston, 2000). The model of geodiversity used in this thesis does not include a direct measurement of latitude, but does include climatic variables which co-vary with latitude (e.g. insolation).

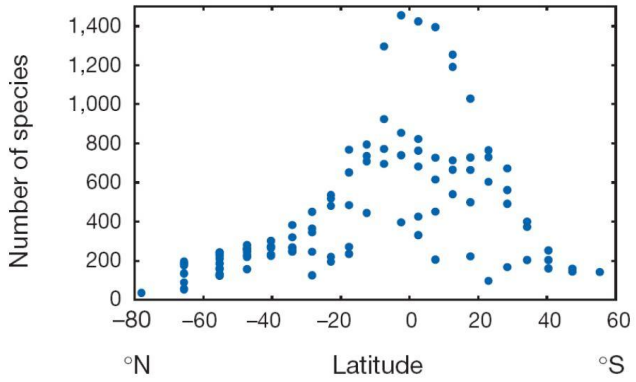

Figure 2.7. From Gaston (2000). The species-latitude gradient in bird species across North and South America.

2.3.2. The altitudinal gradient

The altitudinal gradient is not as clearly defined as the latitudinal gradient; some authors have reported a monotonic decline in richness with increasing altitude (e.g. Patterson *et al.*, 1998), whilst others have found a hump-shaped curve with a mid-elevational increase in diversity (e.g. Kessler, 2001, Aubry *et al.*, 2005). In a review of 71 studies, a general pattern was not found (Romdal and Grytnes, 2007), although Levin *et al.*, (2007) assert that a sinusoidal curve is the most common, with a peak in mid-elevations. Studies with small areas tend to exhibit a monotonic decline, whereas those with larger study areas tend to show a sinusoidal curve (Nogues-Bravo *et al.*, 2008). It is possible that small study areas only detect the declining section of the sinusoidal curve. Alternatively, it could be that those studies finding a

monotonic decline did not consider the decline in area with altitude; when this is corrected for, studies which had previously shown a monotonic decline revealed a mid-elevational peak in diversity (Rahbek, 1997). Most studies do show an overall decline in diversity between low and high elevations, whether this is monotonic or displays a hump-shape (Rahbek, 1995). As with the latitudinal gradient, the model of geodiversity used in this thesis does not include a direct measure of elevation but instead includes variables that follow the elevational gradient (e.g. temperature).

2.3.3. The species-area relationship

The species area relationship (SAR) - that the number of species recorded increases with the area sampled - is a recognised major ecological pattern (Storch *et al.*, 2003) and one of the few geographical / ecological generalizations (Triantis *et al.*, 2008). The SAR is generally accepted as non-asymptotic (Williamson *et al.*, 2001), however some authors dispute this (Lomolino and Weiser, 2001). It can be characterized as

$$\log S = \log C + z \log A \qquad 5$$

where *S* is species richness, *A* is area, *C* is a constant giving the number of species when *A* = 1, and *z* is the slope of the line (Begon *et al.*, 1996).

Measurement of the SAR is not a trivial matter; Fattorini (2007) reports that previous studies tended to use planar areas for SAR calculations. She found that this does not accurately represent the actual surface area for topographically diverse areas such as mountains, and that the fit of the SAR was improved by modelling the surface area of the peak as a cone. However, it has also been shown that increased accuracy in area calculation does not impact on the SAR (Triantis *et al.*, 2008).

Factors such as available energy, sampling effort and habitat diversity can be explanatory variables for species richness (Storch *et al.*, 2003, Storch *et al.*, 2005). As these tend to co-vary with area, it is difficult to distinguish between the impacts of each different co-variant. Baldi (2008) managed to differentiate between habitat heterogeneity and area. They looked at arthropod species richness in Hungarian nature reserves; large reserves had been predominantly established in homogenous habitats, meaning that habitat heterogeneity was not correlated with area. They found that the SAR did not hold, suggesting that habitat heterogeneity could be an important factor in determining species richness.

2.4. Geodiversity and biodiversity; theoretical links.

There is evidence from the literature that the components of geodiversity outlined in section 2.1.2 are linked with the mechanisms that create and maintain biodiversity. These links will be discussed in the context of the geodiversity model developed and tested as the basis of this thesis.

2.4.1. Total resource availability

Energy, water, nutrients and the space that they occupy are four key resources necessary for life to exist. The availability of these resources enable species to co-exist through niche-partitioning (Hutchinson, 1957, Schoener, 1974). Energy, water and nutrients tend to co-vary over space, making it difficult to distinguish between the impacts of each different covariant (Storch *et al.*, 2003, Storch *et al.*, 2005) and it is possible that area is a surrogate measure for total energy receipt, thus providing an explanation for the SAR (Wright, 1983, Rosenzweig and Rosenzweig, 1995). Many studies have focused on energy availability as it is a driver of total resource availability (Triantis *et al.*, 2008), and it has been shown that, at the continental scale, there is a positive monotonic relationship between energy and species richness (Ding *et al.*, 2006, Benton, 2009). Indeed, vascular plant species richness in temperate mountains can be explained primarily by energy based processes (Moser *et al.*, 2005).

Nine potential explanations for the positive association between resource availability (in terms of energy) and biodiversity were evaluated by (Evans *et al.*, 2005). Not all were mechanistic explanations, for example the sampling hypothesis (Hairston *et al.*, 1960, Turner *et al.*, 1988) states that increased energy increases the number of *individuals* the area can support. Sampling from a large population increases the chance of sampling rare species, thereby increasing the number of species sampled irrespective of any mechanistic relationship operating on biodiversity *per se*. When the sample size is corrected for, the relationship is no longer apparent (Honkanen *et al.*, 2010).

Higher energy levels increase the amount of biomass in each trophic level of the community, potentially generating and maintaining higher levels of biodiversity in three ways. First, higher energy levels could allow for more trophic levels and therefore additional complexity and niches to be occupied, thus generating increased biodiversity (Oksanen *et al.*, 1981, Fretwell, 1987, Schoener, 1989, Kaunzinger and Morin, 1998). Second, competition between species at the same trophic level could decrease due to increased energy from the level below, reducing competitive exclusion and allowing for maintenance of existing biodiversity (Paine, 1966,

Janzen, 1970, Abrams, 1983, Abrams, 1995). Third, competition between species at the same trophic level could decrease due to increased predation from the level above, which would also reduce competitive exclusion and help maintain biodiversity (Evans *et al.*, 2005). Increased biomass will also tend to provide more structural substrate for life, thus effectively increasing the available space per unit area of ground (for example, through increased leaf area index).

Energy is not the only resource to contribute to biodiversity; space, or area, is also important. Most work on the SAR has replicated the early results of Arrhenius (1921) and Preston (1948), revealing a log-log relationship between area sampled and species richness. Although subsequent studies have found variations in the shape of the relationship (e.g. Gleason, 1922, He and Legendre, 1996, Lennon *et al.*, 2001), they all report the general trend that the number of species recorded increases with the area sampled, leading to the SAR being recognised as one of the few geographical and ecological generalizations that can be made (Triantis *et al.*, 2008). At the regional scale, topographically sloping areas have a larger surface area per unit of Cartesian space than topographically flat areas. The majority of studies tend to use planimetric (Cartesian) measures of area for SAR calculations. This does not accurately represent the actual surface area for mountainous regions, which for very steep slopes can be up to 30% greater. For example, calculations of true surface area on the $90m^2$ SRTM DEM in the Colombian Andes from the surface area ratio dataset of SimTerra show that the ratio of true surface area to Cartesian surface area for a 10^o tile with the upper left corner at -80^o, 10^o, is on average 1.09 over the entire tile, 1.12 when focussing on areas above 300 m and increases to a maximum of 3.4 for some individual very steep cells (Parks and Mulligan, 2010).

Although support for the general pattern of species richness declining with elevation has been found in a range of studies using plot-based sampling along an elevational gradient (e.g. Kessler, 2001, Aubry *et al.*, 2005, Levin *et al.*, 2007), it is likely that this relationship is also influenced by the SAR. When working at the scale of an individual mountain chain, surface area generally decreases with elevational gradient; when same-sized plots are used along the elevational gradient, the sample is drawn from a greater proportion of the species pool at higher altitudes, and the results are thus impacted by the SAR (Romdal and Grytnes, 2007). This effect is likely to be enhanced in a spatially heterogeneous environment, as different elevational bands are likely to have very different species assemblages.

At a finer spatial scale, gap dynamics also play an important role in generating new space for occupation in otherwise highly ecologically competitive environments. Without gap

formation, it would be impossible for colonists to establish themselves. The establishment of new communities in gaps helps generate diversity, and it has been shown that areas with intermediate levels of gap formation tend to have higher species richness than those with little disturbance (Horn, 1975, Connell, 1978, Shea *et al.*, 2004). Plant species richness in forest plots is better explained by disturbance regime than by current environmental conditions, supporting the notion that the disturbance regime is an important explanatory factor of diversity (Takafumi and Hiura, 2009).

2.4.2. Temporal variability

Temporal variability can be considered in terms of two key types; short term seasonal variation occurring over the course of a year, and longer term variation through climatic cycles and stochastic events. The impact of spatially varying seasonality on biodiversity is a poorly researched area compared with long-term change and stochastic events, which are considered a major element of environmental heterogeneity (Dufour *et al.*, 2006).

The "Time Theory" (Pianka, 1966) argues that communities which have had a longer uninterrupted climatological history (such as parts of the tropics, which avoided the Pleistocene glaciations) will be more speciose for both ecological and evolutionary reasons. Ecologically, more species will have had time to populate the area, whilst evolutionarily more species will have had time to evolve from existing populations. Stable conditions will have led to the generation of complex, highly specialised species interactions, generating many species at low populations and leading to high diversity if these can be maintained in co-existence. There are higher speciation and lower extinction rates in the climatically stable tropics, lending support for this theory (Mittelbach *et al.*, 2007). In addition, the shorter generation times typical of tropical species (often with many generations per year as a result of low seasonality) affords natural selection more opportunities to act (Rohde, 1992). The importance of uninterrupted evolutionary time in driving latitudinal patterns of biodiversity may have been underestimated because it is co-linear with many other variables, such as continental area which increases along the same gradient (Field *et al.*, 2009).

Theoretically, short term temporal variability of resources (seasonality) can create multiple niches within the same physical space by creating temporal niches occupied by different species at different times including nocturnal species, hibernating species and migrants (Chesson, 2000, Araujo *et al.*, 2004). Previous work has also suggested that the seasonality of resources may in itself be considered a resource (Levins, 1979, Brown, 1989). For example,

modelling studies have shown that seasonality in rainfall can influence productivity of semi-arid vegetation independently of changes in the total rainfall volume. Working with a vegetation model for arid environments developed by HilleRisLambers *et al.* (2001) and Rietkerk *et al.* (2002), Guttal and Jayaprakash (2007) added seasonality to the rainfall parameter (replacing an assumed constant rainfall throughout the year). When the total annual rainfall was uniform between model runs, but with varying seasonal patterns, different levels of productivity were simulated. Given that, as outlined in the previous section, more productive regions tend to exhibit higher biodiversity, it is fair to suggest that seasonality can influence species richness.

Empirically, work by Beck *et al.* (2006) on sphingid moths in Southeast Asia has found seasonality, along with bio-geographical region, to be a highly significant predictive parameter of species richness for all subfamilies at all range-size classes. In this study, seasonality was based on classification of habitat as evergreen or semi-evergreen, rather than measuring seasonality in resources. Research from the agricultural literature has found that seasonality impacts on productivity; for example, seasonality in precipitation (measured as standard error of mean monthly precipitation) has been shown to significantly affect crop yield of *Jatropha* (Trabucco *et al.*, 2010).

Conversely, it has also been shown that high levels of seasonality can reduce levels of biodiversity due to the resource "bottle-neck" created by the season when resources are at their lowest levels (e.g. dry seasons, cold seasons) (Williams and Middleton, 2008). This negative relationship between seasonality and biodiversity could help explain the higher levels of diversity in the seasonally stable tropics compared with the increasingly seasonally variable temperate and polar regions. It is possible that seasonality in resources influences species richness by different mechanisms depending on the strength of the seasonal signal (Jin, 2008), so adaptations to seasonality, such as seasonal growth and reproduction that occur in mid - high latitude species, are effective in reducing competition at these latitudes but become less so as the resource bottleneck becomes tighter at high latitudes. In the context of this thesis, with the focus on tropical regions, the assumption is that this bottle-neck effect will not be severe enough to limit productivity and will instead add structure and thus increase niche space (and hence species richness).

2.4.3. Spatial context of resources

Environmental and habitat heterogeneity, leading to spatial variation in resources, is an important factor in the generation and maintenance of biodiversity (Menge and Sutherland, 1976, Tilman, 1994, Aubry *et al.*, 2005, Moser *et al.*, 2005). However, quantifying spatial structure of resources has proved a difficult task as the spatial distribution of resources tends to be patchy, meaning the law of distance decay commonly applied in geostatistical interpolation does not apply (Palmer, 1992). Furthermore, the nature of resource patchiness tends to co-vary with spatial scale (Mac Nally and Watson, 1997) and so differentiating between habitat heterogeneity effects and the species area effect is difficult, as outlined in section 2.3.3.

Species composition has been shown to respond to various components of geodiversity (Jones *et al.*, 2008). Geodiversity can operate at the species level and upwards to change entire ecosystems over space. For example, spatial structure in topographically-controlled wetness has been found to have control over the presence of woody species in the Serengeti (Reed *et al.*, 2009) and tree species richness in boreal forests (Zinko *et al.*, 2005). Dufour *et al.* (2006) quantified spatial structure as environmental "roughness" (*G*), which increases with decreasing spatial aggregation (i.e. at high levels of spatial auto-correlation, *G* is low). They argue that *G* can influence the rates of processes such as immigration, emigration, death and competitive exclusion in a way that can delay extinction and thus increase overall biodiversity. For example the spatial structure introduced by increasing *G* increases the likelihood of meta-populations surviving stochastic events. However, they go on to state that there is likely to be an optimum level for *G* as, although it creates additional niches, excess spatial variability will cause habitat fragmentation, isolation, low populations and greater potential for local extinction thus causing species diversity to decline.

The measure of geodiversity used here does not specifically quantify heterogeneity of resources, instead the wider spatial resource context is examined. This provides a measure of the broader-scale structure in resources and so, when looking beyond a pixel-based measure of geodiversity, provides an indication of the influence of the regional resource regime for the location in question. Since the seed and pollen source for many plant species, and the home range for motile species, extends well beyond the location in which they occur, and because regional factors will affect the pool of competitors as well as the local resource base, it is important to consider the wider resource context. By examining the wider spatial context, the research presented in this thesis moves on from work by Luoto *et al.* (2002) and Luoto *et al.*

(2004) which examined the relationship between topograhic and soil moisture characteristics and plant species richness using only in-pixel measurements.

2.4.4. Interactions between the elements of geodiversity

One common theme running through the research reviewed is that the three elements of geodiversity (resources, their temporal variation and wider spatial context) do not act in isolation. For example, in highly seasonal environments (such as at high latitudes), the total amount of available resource will be greatly reduced due to the low-resource availability in winter. Given that regions with lower levels of available energy support less biomass, it follows that higher latitudes will have fewer species than less-seasonal regions but for reasons of higher total available energy level rather than seasonality (Gaston, 2000).

Species richness may be different at sites with similar levels of seasonality due to differences in resource magnitude or regional variation in resources at those sites. Species may respond differently to resource availability variation at different life stages (Lundholm, 2009), or under different resource magnitudes (Marini *et al.*, 2008). The interplay between the elements of geodiversity and their relationship with biodiversity may also be hierarchical with resource availability proving to be more of a control than the wider spatial context or temporal variation. On the other hand, the main control could vary from system to system. The majority of articles reviewed here support the notion of total resource availability being the strongest controlling factor over species richness, though this is also the area in which most research has taken place.

2.4.5. Current geodiversity

The tropics exhibit a varied topography (figure 2.8), with some of the highest peaks of the world (outside of the Himalaya). In terms of hydrology, the high levels of solar radiation in the tropics result in an active hydrological cycle (Balek, 1983). In terms of climate, the tropics contain both the warmest and wettest regions on earth (figure 2.9 - 2.10). The climates vary from hot and dry, for example the Sahara, to hot and wet, for example the Amazon. Whilst the central tropics have little seasonality in terms of temperature, regions at slightly lower latitudes (e.g. the Sahara and the Australian deserts) do exhibit variation. In terms of precipitation, there are distinct rainy seasons for Chile, the Sahara through the Gulf region and across to India, southern / eastern Africa and northern Australia (figure 2.10). These themes will be expanded in chapter 3.

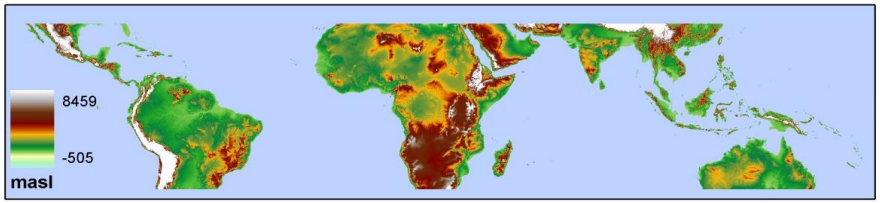

Figure 2.8. 1km DEM of the tropics. (CGIAR-CSI, 2004

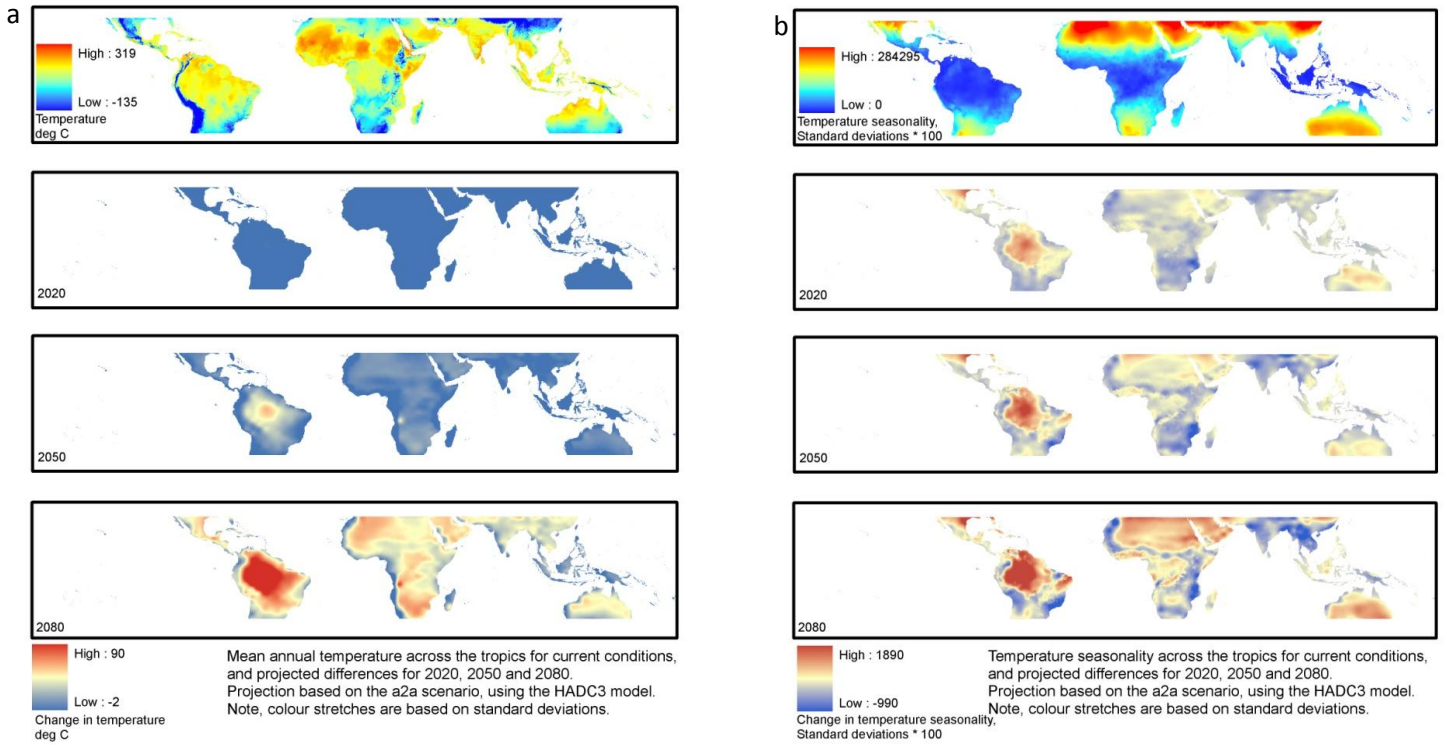

Figure 2.9. Current and future mean annual temperature (a) and temperature seasonality (b) across the tropics. (Hijmans *et al.*, 2005).

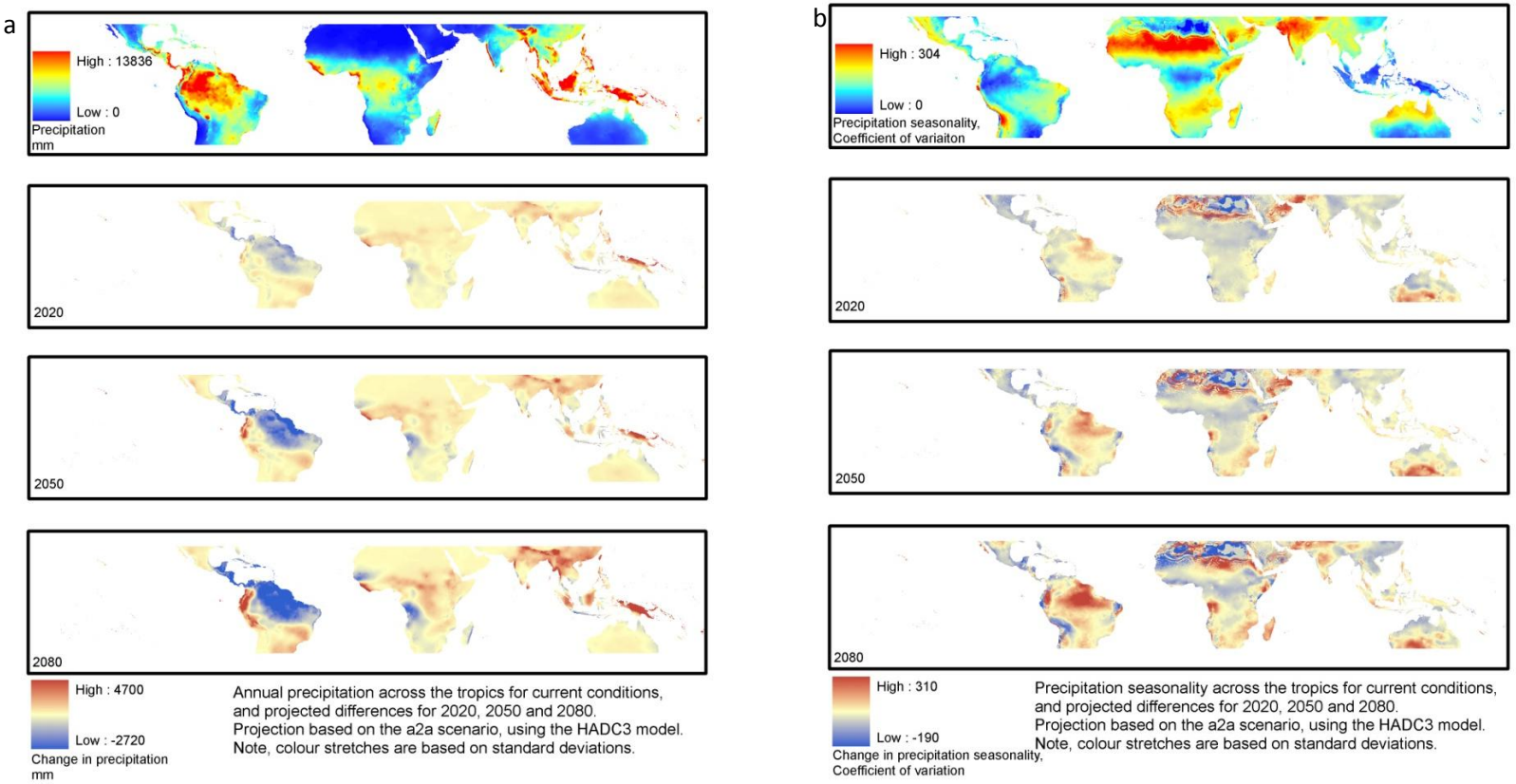

Figure 2.10. Current and future mean annual precipitation and precipitation seasonality across the tropics. (Hijmans *et al.*, 2005).

2.5. Threats to geodiversity and biodiversity.

The Fourth Report of the International Panel on Climate Change (IPCC) declares that "warming of the climate system is unequivocal" (IPCC, 2007, p.30). The report also clearly states the link between human activities and the increase in atmospheric CO_2, and that there is "a very high confidence" that human activity has led to the overall warming of the atmosphere (IPCC, 2007, p.37). Harris *et al.* (2006) list the major impacts of climate change as:

- Changes in weather patterns
- An increase in mean temperature
- Changes in patterns of precipitation
- An increase in the number of extreme climate events
- An increase in mean sea levels

A further threat to both geodiversity and biodiversity comes from land-use change; perhaps a less well known but equally complex partner to climate change (Dolman *et al.*, 2003). The primary distinction that needs to be drawn is between land-use change and land-cover change; land-use change (i.e. change to the human use of the land) often leads to changes in the land-cover (Lambin, 2005). For example, increasing agriculture (a change in land-use) can lead to deforestation (a change in land-cover). The key drivers of land-use change, according to Lambin (2005), can be classified as:

- Population and affluence
- Technology
- Political economy
- Political structure, attitudes and values
- Accessibility

These drivers interact with each other, creating a spatially and temporally complex pressure on current land-uses which manifests itself most strongly in the tropics.

2.5.1. The impact of climate change on geodiversity

Given that many of the resources used in the geodiversity model used here arise from the climate system, current patterns of geodiversity are highly likely to be affected by climate change. Figures 2.9 - 2.10 show the distribution of current rainfall and temperature, with the seasonality of each, alongside maps showing the differences between current conditions and the SRES A2A scenario (an increasingly industrialised world), as modelled using the HADCM3 GCM (Hijmans *et al.*, 2005). A2a describes "a highly heterogeneous future world with

regionally oriented economies. The main driving forces are a high rate of population growth, increased energy use, land-use changes and slow technological change" (IPCC, 2000).

Under the A2A scenario, the Amazon is likely to experience the most dramatic changes in temperature and precipitation regimes in the tropics both in terms of changes to annual totals and to seasonality. Precipitation is likely to decrease, whilst seasonality of precipitation increases resulting in a change in precipitation regime from a constantly wet environment to a seasonally dry environment. This will be compounded by increases in temperature in the region. By contrast, the Andes will become wetter and, in parts, less seasonal.

In Africa, there are less dramatic changes in precipitation and temperature, although the general trend is for a warmer, wetter environment. In terms of seasonality, sub-Saharan regions show a general increase in precipitation seasonality, whilst the Sahara itself exhibits a complex spatial pattern in precipitation seasonality. The temperature in Africa generally increases, although with a distinctly cooler band along the western coast. Temperature seasonality is likely to increase over the Sahara and Congo, with a mosaic of increased and decreased seasonality over the rest of the sub-Saharan regions.

Asia sees a general increase in precipitation, with Papua New Guinea and the Himalaya seeing the greatest increases. Precipitation seasonality will remain similar across Asia. Temperatures are forecast to rise, but not as dramatically as in the Amazon or Africa, whilst the seasonality will remain constant. Australia follows a similar trend to Asia, although there are alterations in seasonality with both temperature and rainfall becoming more seasonal.

2.5.2. The impact of land use change on geodiversity

It is important to note that the model developed in this thesis gives an indication of levels of geodiversity in a pristine environment; effects of existing human land-use will not be reflected by the model. The predominant impact of land-use change on geodiversity will be through the interruption of the hydrological and atmospheric cycles the ensure the continued flow of resources through the environment. This is not discussed in detail, as the focus of the research has been the impact of climate change on geodiversity.

2.5.3. The impact of climate change on biodiversity

Since the early 1700s, a correlation between species distribution and climatic gradients has been noted (Guisan and Zimmermann, 2000) and the relationship between climate and species

distribution forms the foundation for the discipline of biogeography (Pearson and Dawson, 2003), and for the model of geodiversity adopted here. Given the link between species distributions and climate, it is inevitable that climate change will have an impact on species distributions and therefore on global biodiversity (Malcolm *et al.*, 2006), directional changes in the environment are likely to cause a directional selection pressure on biodiversity of the type that can trigger a mass extinction event (Skelly *et al.*, 2007). Currently, the five predominant pressures on global biodiversity are habitat loss, invasive alien species, over exploitation of resources, pollution and climate change (WWF, 2008). Of these, climate change has the strongest direct impact in many regions (Thomas *et al.*, 2004) and is often further compounded by habitat change and fragmentation which can prevent species migrating to avoid the effect of climate change (Mace and Purvis, 2008). Despite these threats, many biodiversity conservation prioritisation schemes do not include climate change or habitat loss in their algorithms for assessing priority (Brooks *et al.*, 2006).

In terms of direct impacts on biodiversity, some species respond to climate change with behavioural adaptations (Buchholz, 2007), although some species such as herptiles (amphibians and reptiles) and plants are less able to do so, placing them more at risk of climate change (Araujo and Pearson, 2005). A general pole-ward movement of approximately 6.1 km per decade in species distributions has been documented, along with a change in life history traits such as migration timings and breeding dates (Hsiung and Sunstein, 2007). Observed responses to the historic 0.6^{o}C change have already been reported; it is therefore not unreasonable to expect much more widely occurring responses if temperatures increase by (potentially) 6^{o}C or (more likely) 1.5 ^{o}C - 3.5 ^{o}C (Beaumont *et al.*, 2005). In mountains, the impacts of temperature increases are more dramatic due to the compounding effect of altitude; a 6^{o}C temperature change is the equivalent of a 1000 m elevational change (UNEP-WCMC, 2002).

Evolutionary changes are also found, as the pressure of climate change can dramatically increase the rate of natural selection (Mace and Purvis, 2008). Examples of this include an increase in temperature tolerance in a frog species (Skelly *et al.*, 2007), evolved resistance to cane toad toxin (an alien species) in an Australian snake (Kinnison and Hairston, 2007) and earlier maturation in North Atlantic cod due to overfishing (Mace and Purvis, 2008). However, species with long generation times cannot evolve as quickly and are thus unable to adapt to the change climate (Araujo and Pearson, 2005).

In relation to conservation, it is worth noting that communities that existed in the past often have no modern day equivalent community (Whittaker *et al.*, 2005) and that, whether climate change is reversible or not, it may not be possible to restore ecosystems that are lost over the next few decades (Harris *et al.*, 2006).

2.5.4. The impact of land use change on biodiversity

Climate change tends to reduce available habitat and therefore alter biodiversity patterns. This effect is likely to be increased by land-use change, so the impacts of land-use change can be considered as concentrating the effects of climate change into specific areas (Pressey *et al.*, 2007). This has led to some authors labelling land-use change the "single greatest threat to biodiversity" (Sanderson *et al.*, 2002, p.893). Generally, the tropics have a higher land-use change rate due to increasing population in rural areas and large scale agricultural development (which occurred earlier throughout the developed world), therefore the effect of climate change is amplified (Sarkar *et al.*, 2006). This then sets up a vicious cycle whereby an increased land-use change increases the impact of climate change, which in turn drives further land-use change (Hsiung and Sunstein, 2007).

2.6. Options for conservation.

Conservation strategies can be divided into two broad categories, *in-situ* and *ex-situ*, both of which tend to be aimed at conserving biodiversity, rather than geodiversity. Ex-situ conservation focuses on maintaining a captive sample of threatened species, acting as an insurance policy if the species was to go extinct in the wild, whilst in-situ techniques focus on conserving existing ecosystems. This literature review will only consider *in-situ* conservation options, as these are relevant to this thesis, and will focus on stewardship schemes whereby local stakeholders are given responsibility for environmental conservation of their local region, and protected area designation.

Stewardship schemes encourage stakeholders to engage with the sustainable use of an ecosystem / natural resource. For example, the Marine Stewardship Council (MSC, 2009) takes livelihoods into account and sets out to ensure that fishing and fisheries are as sustainable as possible. Involving the stakeholders in designing the certification schemes helps ensure the schemes are as feasible and desirable as possible for all involved. However, given the diametrically opposed needs and goals of conservationists and stakeholders who rely on the natural environment, some authors have concluded that stewardship schemes alone are not enough to guarantee effective conservation (Gulbrandsen, 2009).

The most widespread in-situ conservation technique is to designate an area as protected with the aim of preventing damage to the ecosystem from land-use change and overexploitation. Once an area has been designated as a protected area (PA), it is classified by the World Commission on Protected Areas (WCPA), the world's authority on protected areas which is administrated by the World Conservation Union (IUCN). PAs are classified into the following categories (IUCN, 1994):

1. Strict Nature Reserves / Wilderness Areas (area for scientific research / wilderness protection)
2. National Park (for ecosystem protection / recreation)
3. Natural Monument (conservation of specific natural features)
4. Habitat / Species Management Area (conservation through habitat intervention)
5. Protected Landscape / Seascape (landscape / seascape protection and recreation)
6. Managed Resource Protected Area (sustainable use of a natural ecosystem)

Of these, categories 1 - 4 are generally considered adequate protection in terms of conservation needs (Hoekstra *et al.*, 2005, Mittermeier *et al.*, 2003).

Many techniques have been devised for selecting protected areas, outlined in section 2.6.1. However, regardless of the prioritisation technique used the eventual success of the protected area will be dependent of the physical design of the area and level of enforcement. In terms of a protected area's spatial configuration, the first issue to be addressed is whether one single large area or several small areas will offer the best option (the SLOSS debate). The argument that a single large PA will conserve more species is based on the assumption that the species in the population are "nested", i.e. that a smaller area will always contain lower species richness. When metapopulation dynamics and patchy species distributions are taken into account, this is not a valid assumption and several small PAs may prove the most effective design strategy. The exact size and number of protected areas in the optimum design is likely to be determined by a combination of local immigration / extinction rates and the spatial homogeneity of habitat types (Ovaskainen, 2002).

A second consideration with regards to spatial design of PAs is the overall shape of the park. Edges of protected areas are generally less favourable in terms of habitat - and prone to access and degradation by land use change - and thus have lower species richness than would otherwise be expected; the result of this is that protected areas with a small perimeter are preferable to those with a long perimeter. A review of studies on the impact of area and edge on populations found more consistent support for an edge effect, rather than an area effect,

suggesting the shape of a protected area could be more important than its area (Fletcher *et al.*, 2007).

2.6.1. Protected area selection techniques

The aim for many conservation NGOs is to ensure available funds are spent effectively by conserving as many species as possible (Myers *et al.*, 2000). In order to do this, a global strategic monitoring and prioritisation plan is needed (Faiths *et al.*, 2008). Whittaker *et al.* (2005) argue that it is the role of scientists to propose different prioritisation schemes, and the role of the NGOs to select and act upon a well-researched scheme that will meet their mission statements. This occurs to some degree, although often NGOs commission their own research to develop schemes tailored to their mission (e.g. WWF and the Global 200, Olson and Dinerstein, 1998).

Brooks *et al.*, 2006) classified prioritisation schemes as proactive (e.g. High Biodiversity Wilderness Areas (HBWA, Mittermeier *et al.*, 2003), Frontier Forests (FF, Bryant *et al.*, 1997), Last of the Wild (LW, Sanderson *et al.*, 2002)) or reactive (e.g. Biodiversity Hotspots (BH, Myers *et al.*, 2000), Crisis Ecoregions (CE, Hoekstra *et al.*, 2005)). This classification was based on the positioning of the scheme on a framework comparing the valuation of irreplaceability and vulnerability; some schemes did not have a measure of vulnerability and were therefore neither pro- nor reactive (e.g. Endemic Bird Areas (EBA, Stattersfield *et al.*, 1998), Centres of Plant Diversity (CPD, WWF-IUCN, 1994 - 1997), Megadiverse Countries (MC, Mittermeier *et al.*, 1997), Global 200 (G200, Olson and Dinerstein, 1998)). Figure 2.11 shows the distribution of the prioritisation areas for each scheme.

Of the reactive schemes, BH has been adopted by Conservation International. A hotspot is defined as an area with at least 1500 species of vascular plants as endemic; equivalent to over 0.5% of the world's total number of plant species. Potential hotspots must also have lost at least 70% of their original habitat over the last 500 years in order to be classified. The boundaries are defined to correspond with WWF eco-regions as CI believes this will enable a higher degree of cooperation between the two NGOs.

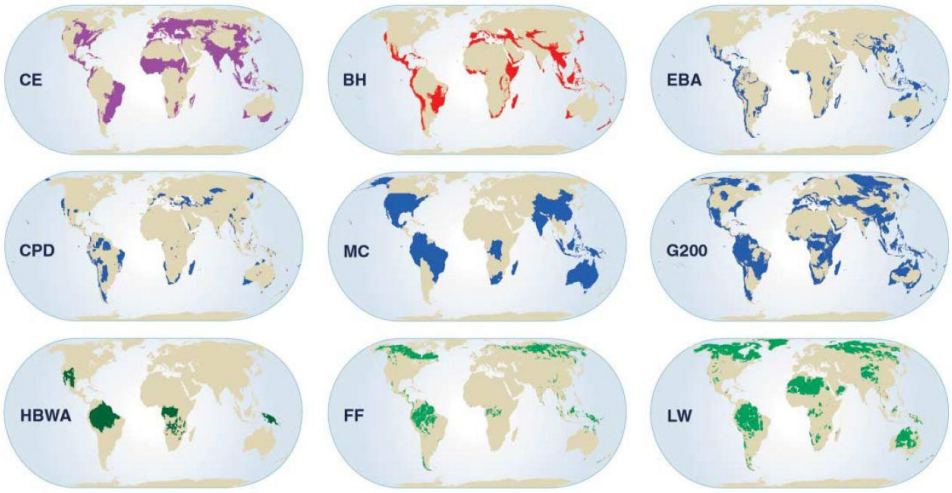

Figure 2.11. From Brooks *et al.*(2006). Nine different prioritisation schemes for selecting conservation areas. CE (Crisis Ecoregions) and BH (Biodiversity Hotspots) are reactive; EBA (Endemic Bird Areas), CPD (Centres of Plant Diversity), MC (Megadiverse countries) and G200 (Global 200 Ecoregions) are neither re- or proactive; HBWA (High Biodiversity Wilderness Areas), FF (Frontier Forests) and LW (Last of the Wild) are proactive. See text for further details.

WWF commissioned the research leading to the development of the G200 scheme. Having defined the ecoregions of the world (an ecoregion being an area with characteristic species, habitats and ecosystems, Olson and Dinerstein, 1998) it was decided to prioritise these in order to ensure conservation planning covered an example of each ecoregion that was distinct in terms of endemism, taxonomic uniqueness, unusual ecological / evolutionary phenomena and global rarity of the major habitat type; the G200 are the 200 ecoregions most highly prioritised. This work is different to that of the reactive schemes because it acknowledges that, although hotspots conserve a large amount of species in a small area, biodiversity found outside the hotspots is also important (Olson and Dinerstein, 1998). WWF are working in a selection of the G200; they would like other NGOs to prioritise the remaining ecoregions (WWF, 2009).

Another charity that has commissioned a prioritisation scheme tailored to its own needs is Birdlife International. They identify the highest priority areas for conservation efforts as Endemic Bird Areas (EBAs) or Important Bird Areas (IBAs). EBAs are areas of overlap between two or more species with a range of less than 50 000 km^2 (BirdLife, 2009a). So far 218 have been identified. IBAs either hold one or more globally threatened species, or are home to bird

species with small home ranges, or are important migratory / congregation points for birds (BirdLife, 2009b). These schemes, like the G200, have no measure of vulnerability.

2.6.2. Effectiveness of the current protected area network within the tropics

The CBD set the target of protecting at least 10% of the world's terrestrial area and areas high in biodiversity (Targets 1.1 and 1.2, CBD, 2009). As of 2010, 12.7% of the world's terrestrial area (excluding Antarctica) is deemed protected, however there is a high degree of variation between geographic regions (from a minimum of 3% coverage in Caucasus and Central Asia to a maximum of 20.4% in Latin America) and between economic regions (10.2% of the Least Developed Countries being protected, whilst 11.6% of developed regions are protected) (WDPA, 2011). In addition to this disparity in terms of extent of coverage, ecosystems and physical characteristics are often not equally represented (Tuvi *et al.*, 2011, Soutullo and Gudynas, 2006, Barnard *et al.*, 1998, Catullo *et al.*, 2008). Furthermore, coverage of a given fraction of land surface is not a guarantee of species coverage; as the number of target species increases, so does the extent of protected area required to ensure representation of all target species (Rodrigues and Gaston, 2001).

Various attempts at assessing the robustness of the existing protected area network have been made, predominantly based on a gap analysis approach whereby the degree to which different classes of physical or biological parameters are represented within the protected area network is assessed - various examples of this are outlined below. The gap analysis approach considers the effectiveness of all protected areas within the study region as a collective, forming a network, rather than considering the merits of individual protected areas. In order to carry out an effective gap analysis, it is necessary to consider a variety of parameters, for example ecoregions, ecosystems and biodiversity hotspots (Tuvi *et al.*, 2011).

There are examples from all three tropical continents illustrating cases where the 10% coverage target has been made, but where further gap analysis reveals short-falls in terms of coverage of key ecoregions or habitat types. The protected area network of the MERCOSUR countries (Argentina, Brazil, Paraguay and Uruguay) represents 14% of the land-mass and yet fewer than half the ecoregions are represented at the 10% level (Soutullo and Gudynas, 2006). In Thailand, the protected area network represents 18.2% of the terrestrial surface, however the majority of protected area are found at high elevations, whilst high biodiversity levels tend to be found at lower elevations (Trisurat, 2007). This pattern of greater protection of high elevations is found across south east Asia, where the median elevation in protected areas is 438 m, compared with 190 m in non-protected areas (Catullo *et al.*, 2008). In Namibia the

protected area network covers 13.8% of the land, but massively over-represents the Namib Desert (69% of the protected area network) and under-represents the Karoo (1.6% of the protected area network) (Barnard *et al.*, 1998).

Nelson and Chomitz (2011) state that the global protected area network covers 25% of all tropical forest, however there has been some doubt over the level of protection actually afforded by the different types of protected area. They analysed the effectiveness of different types of protected area at preventing land-use change (monitored in terms of levels of fire within strictly protected areas and those protected by stewardship schemes allowing local use of the natural resources). They found that areas protected by stewardship schemes were less likely to be subject to wildfire than strictly protected areas. However, it can be argued that this is not necessarily the best measure of land-use-change as wild-fire can form part of the natural disturbance regime of tropical forests. It would be interesting to re-run these analyses using a more direct measure of deforestation.

The current protected area network has been designed based on the assumption of a static climate (Willis *et al.*, 2009). In terms of the ability of the existing protected area network to provide protection against climate change, literature suggests different impacts are projected for temperate and tropical zones. Results from work on Canadian butterflies found that the existing protected area network offered little protection for future ranges projected using MaxEnt (Kharouba and Kerr, 2010). Similarly, research into the impact of changes in extent of bird species distributions found that whilst in a temperate country (Finland) ranges are likely to contract and species become less well represented in the protected area network, whereas in a tropical region (Africa) bird ranges are likely to increase in extent and become more represented in the current protected area network (Kujala *et al.*, 2011).

Further work on the impact of climate change on the robustness of the sub-Saharan African Important Bird Area network found that the impacts of climate change vary regionally, however across the entire network suitable climate is maintained for approximately 90% of priority species (Hole *et al.*, 2009). Whilst these results appear to suggest that the current protected area network offers mitigation against climate change, it is important to remember that birds are motile species and are more easily able to migrate to suitable climate than sessile organisms such as plants. There is a need for a network that provides a combination of both core protected areas alongside corridors of semi-natural habitat that provides connectivity between core habitats (Hannah, 2001).

2.7. Moving forward

This chapter has set out the history of the term geodiversity and reviewed evidence and previous research underpinning the resource based model of geodiversity developed and implemented in this thesis. Given that the key applications of the model in this thesis are concerned with its use as a proxy of overall biodiversity, methods of mapping biodiversity were discussed and key patterns of biodiversity across the globe were outlined in the context of key environmental gradients found in the geodiversity model. Finally, threats to both geo- and bio-diversity were summarised, along with potential strategies for conservation and their efficacy in the face of land-use and climate change were discussed. The remainder of the thesis will first present the development of a spatial implementation of the model of geodiversity, resulting in 1 km resolution maps of geodiversity across all tropical mountains. Using 10 degree case study regions, this model will then be applied to answer the three research questions.

Chapter 3. Introduction to study areas.

This chapter will give an overview of the geography and ecology of tropical mountains, focusing on the three major chains of the Andes, the Eastern Arc Rift Mountains of Africa and the peaks of South East Asia, before considering threats to and conservation efforts within tropical mountains. The chapter concludes with a more detailed overview of the topography and climate within the model testing site, a 10 x 10 degree tile over the northern Andes.

3.1. Tropical mountains - working definitions

The Oxford English Dictionary defines a mountain as "A large natural elevation of the earth's surface, especially one high and steep in form (larger and higher than a hill) and with a summit of relatively small area" (OED, 2010). Whilst the majority of people will be able to conjure up an image of a mountain based on this definition, in terms of providing a quantified, scientific basis for classifying land-forms it is somewhat lacking - a reflection of the lack of consensus among the scientific community as to what constitutes a mountain. Two approaches, ecological and topographical, are outlined below.

The Mountain Biodiversity Global Assessment (Korner and Spehn, 2002) follow an ecological definition based on climatic zones and the location of the climatic treeline. They include the alpine zone (located above the climatic treeline), the treeline ecotone itself and the uppermost montane forests within their definition of a mountain. Following an ecological definition means that there is no lower altitudinal cut off as the elevation of the climatic zones varies with temperature and latitude, generally being higher in the tropics. Using this definition, mountains constitute 5% of the earth's land surface, with the treeless alpine zone covering 3%.

UNEP-WCMC's Mountain Watch (UNEP-WCMC, 2005) use definitions based firmly on terrain characteristics. They argue that the importance of slope and elevation on the microclimates within mountains justifies this choice. Seven classes are defined, with the first three being based purely on elevation whilst the following three also take into account surrounding terrain. The seventh class allows small basins that are highly influenced by surrounding mountains to be included within the classification system. The seven classes defined are:

1. Elevation greater than 4500 m
2. Elevation between 3500 m - 4500 m
3. Elevation between 2500 m - 3500 m
4. Elevation between 1500 m - 1500 m and slope greater than 2^{o}

5. Elevation between 1000 m - 1500 m and slope greater than 5°, or a local elevational range (within a 7 km window) greater than 300 m
6. Elevation between 300 m - 1000 m and local elevational range (within a 7 km window) greater than 300 m
7. Isolated inner basins and plateaus of less than 25 km^2 that are surrounded by mountains of classes 1 - 6.

Three chains of tropical mountains have peaks consistently higher than 1000 m; the Andes in South America, the mountains of the Albertine Rift Valley in Africa, and the peaks forming the islands of South East Asia. Mountain chains below 1000 m are found in south-east Brazil, the West African coast and across tropical India (figure 3.1).

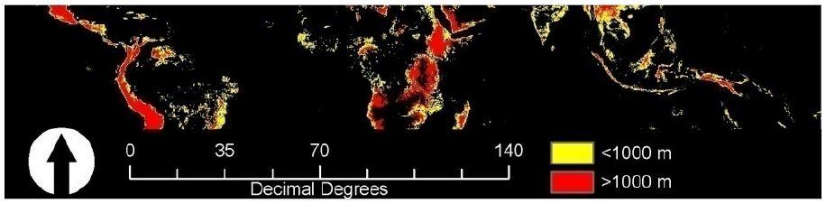

Figure 3.1. Location of the world's tropical mountains, according to the Mountain Watch definition (UNEP-WCMC, 2005).

3.2. Geography of tropical mountains

The geography of mountains is complex and structured; in many respects, due to the elevational gradients of temperature and influences of the terrain on rain and wind, mountains effectively represent a compressed version of latitudinal gradients as a tropical mountain of 5000 m will represent almost all global climatic zones (Korner and Spehn, 2002, figure 3.2). However, as outlined in section 2.3.2, the relationship between elevation and climate is more complex than that between latitude and climate meaning figure 3.2 represents a greatly simplified picture. This section will consider the physical geography of each of the three major tropical mountain chains.

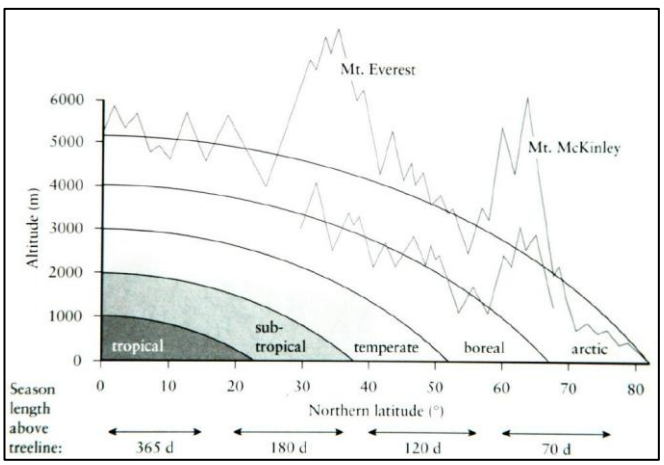

Figure 3.2. From Korner and Spehn (2002). Relationship between altitude, latitude and climate zones.

The Andes, which contain the highest peaks of the tropical mountains, are a young mountain range formed above the subduction zone of the Pacific and South American tectonic plates. Along most of its 6400 km length, the Andes fall into two major chains, the Occidental (western) and Oriental (eastern) cordillera. The Occidental Cordillera are predominantly volcanic, whilst the Oriental Cordillera are predominantly folded and faulted mountains. The northern Andes, in Colombia and Ecuador, have a third, Central Cordillera. Between the Eastern and Western Cordillera lie high plateaus. The highest of these, the Altiplano, covers parts of Chile, Argentina, Bolivia and Peru. The plateaus are characterised by large saline lakes, Titicaca and Poopo being the largest. The headwaters of the Amazon, Orinoco and Parana rivers are found in the Andes (Fothergill, 2006).

The peaks of the African Rift system are formed by the tectonic activity of three plates; the newly forming Somalian plate is moving eastward, away from the African Nubian plate and Arabian plate. The thinner crust between the plates has formed into two larval bulges, the Ethiopian and Kenyan domes. These have then cracked to form trapezoidal horst and graben type peaks (Wood and Guth, 2010). At the northern end of the Rift System, the Ethiopian Simien Mountains are the tallest mountain range (Ras Dasehn, 4620 m, is the highest peak in the range); the terrain is rugged with sheer cliffs and canyons. Moving further south, the Rwenzori mountains of South-West Uganda are formed from uplifted crystaline rocks and, along with Kilimanjaro (Tanzania) and Mount Kenya, they have permanently snow-capped peaks (UNEP-WCMC, 2006).

South East Asia can be divided into the mainland and the island chains, both of which have arisen from geographic activity. The mainland was formed when the Indian and European tectonic plates collided, whilst the islands are predominantly volcanic; Krakatoa, Tambora and Pinatubo being notable examples. The mainland consists of two main chains running north-south on either side of the Thai lowlands. The eastern chain ends in south Vietnam, whilst the western chain continues from the Thai peninsula, into mainland Malaysia (Gupta, 2005).

3.3. Ecology of tropical mountains.

This section will briefly outline the key ecological features of the Andes, the East African Rift System and South East Asia, focussing on the biomes, as defined by WWF (WWF, 2009) and illustrated in figure 3.3.

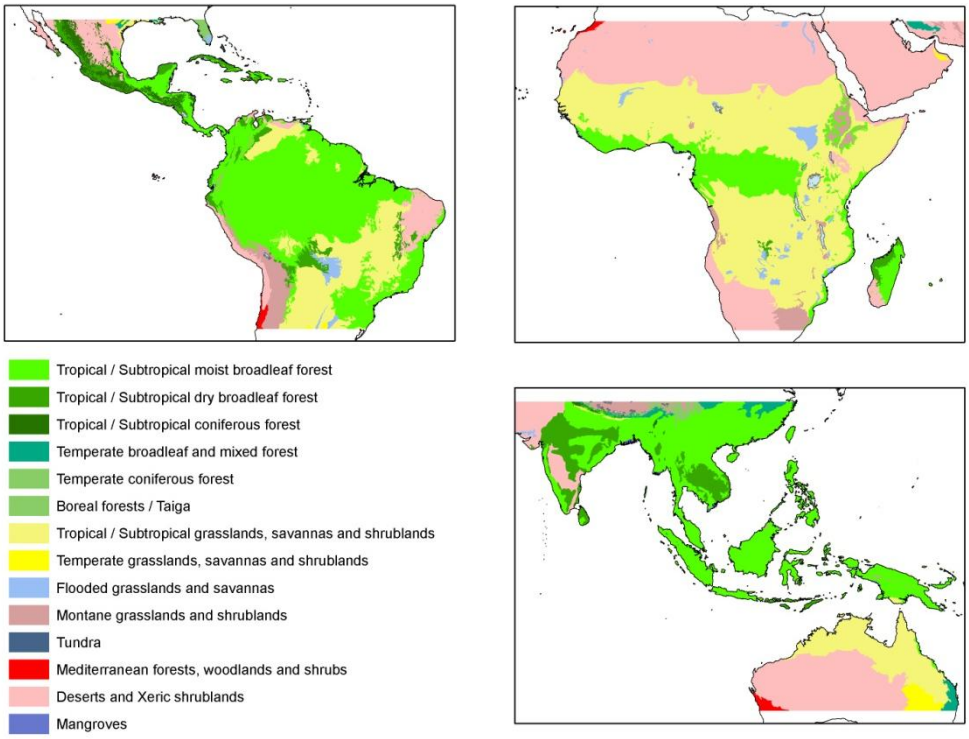

Figure 3.3. Biomes of the tropics (WWF, 2009).

The tropical Americas are dominated by tropical moist and dry broadleaf forests, stretching from northwest Mexico, through central America and into south America. In the tropical Andes, vegetation patterns respond to geodiversity gradients, with different types of forest forming distinct altitudinal bands before giving way to grass, scrub and paramo at the highest altitudes and at the southern tip of the mountain range (Conservation International, 2007). The Chilean coastline is predominantly desert, whilst to the north, Baja California and northeastern Mexico are also desert ecosystems (WWF, 2009).

Although the tropics generally have a higher species richness than the temperate zones, Africa is notably less speciose than tropical Americas and southeast Asia. Whilst the tropical Americas and southeast Asia are predominantly forested, eastern Africa is predominantly a savanna ecosystem, with grassland and shrublands covering much of the surface. The slopes of the Ethiopian highlands are forested, however the higher elevations (above approximately 1800 m) are covered in mountainous grassland and shrubland. Further south through the Rift System the grassland is broken with pockets of dry forest, occurring on mountain slopes, and desert (WWF, 2009).

Southeast Asia is, like the tropical Americas, dominated by forest. The mainland contains patches of both moist and dry broadleaf forest, however the islands are predominantly moist broadleaf. Papua New Guinea and Borneo contain some mountainous grasslands and shrublands at high altitudes, and there is some lowland grassland to the south of Papua New Guinea, which also dominates tropical Australia. An interesting ecological feature of Southeast Asia is the Wallace Line, which is an ecological reflection of the tectonic boundary between Indonesia and Australia; Australian species tend to be found to the southeast, whilst Asian species exist to the northwest of the line (WWF, 2009).

Figure 3.2 shows the general climatic zones found within mountain ecosystems. Elevation does not have a direct, mechanistic effect on the distribution of these climatic zones, rather there is an indirect effect on the distribution of these climatic zones through the creation of resource gradients in terms of rainfall and temperature (Gaston and Spicer, 2004).

3.4. Model test site

3.4.1. Colombian Andes

This test site (figure 3.4) is a 10^{o} x 10^{o} tile over the northern Andes (predominantly Colombia), with the upper left corner at -80^{o}, -10^{o}. This tile was selected because it represents a wide range of topographic and climatic conditions, thereby allowing the geodiversity model to be developed and tested across a broad range of environments. It was used for initial model testing (chapter 4), quantifying the relationship between geodiversity and biodiversity (chapter 5), characterising geodiversity within areas prioritised by the international conservation community (chapter 6) and as a pilot area for developing climate change stable conservation strategies (chapter 7). Earlier work on the model of geodiversity developed in this thesis was carried out on plot level studies in this region (Jarvis, 2005).

The topography of the test tile is varied, from lowland plains in the east to peaks reaching over 5500 masl (figure 3.4). Over half the tile is below 500 masl, resulting in an extreme positive skew to the frequency distribution, which is also found in the slope frequency distribution. With regards to aspect, there are more easterly - south-easterly slopes than any other direction, with a smaller corresponding peak in northerly - north-westerly slopes. This reflects the orientation of the peaks; the more gently-sloping easterly slopes having a greater surface area than the steeper westerly slopes. The mountains are primarily a continuation of the Cordillera Central, running south-west to north-east. The Cordillera Oriental splits from the Cordillera Central just above the centre of the tile, forming the Magdalena Valley. The

Cordillera Oriental itself splits south of the Lago de Maracaibo, with two subsidiary chains flanking the bay.

In terms of rainfall, the tile contains one of the wettest regions on the planet, receiving in excess of 11200 mm per year on the western side of the Andes (figure 3.5). By contrast, some of the drier regions in the test tile receive as little as 450 mm per year, whilst the majority of the tile receives between 2000 - 3000 mm per year (figure 3.5). Temperature varies from an annual mean of -6 ^{o}C in the mountain peaks, some of which are permanently snow covered, to 33 ^{o}C on the northern coastal regions and in the Magdalena valley, although the majority of the tile has an average temperature of 25 - 30 ^{o}C. This is not a reflection of solar radiation, which is at its highest in the eastern lowlands, reaching over 1245 W/m^2 in places. Cloud cover is, perhaps unsurprisingly, highest in the wettest region of the west coast and along the mountain slopes, with very little cloud occurring along the northern coast. In terms of potential evapotranspiration, the highest potential is in the peaks (Mulligan, 1999).

The climatic variables are all influenced by topography, however only temperature shows a clear relationship with elevation (figure 3.6). Whilst there appears to be no overall relationship between rainfall and elevation, maximum rainfall appears to decline with elevation in a non-linear fashion. Solar radiation bears no relationship with elevation, cloud cover seems to decline slightly with elevation, whilst potential evapotranspiration seems to increase slightly with elevation.

Previous work in this region has found a good relationship between individual tree species (*Palicourea angustifolia* and *Palicourea guianensi*) and environmental gradients (Armenteras and Mulligan, 2010), as well as for a wide range of bird species (Verhelst, 2011). Both these studies have found working with data at a 1 km resolution captures sufficient detail in environmental gradients when working at the national scale and above.

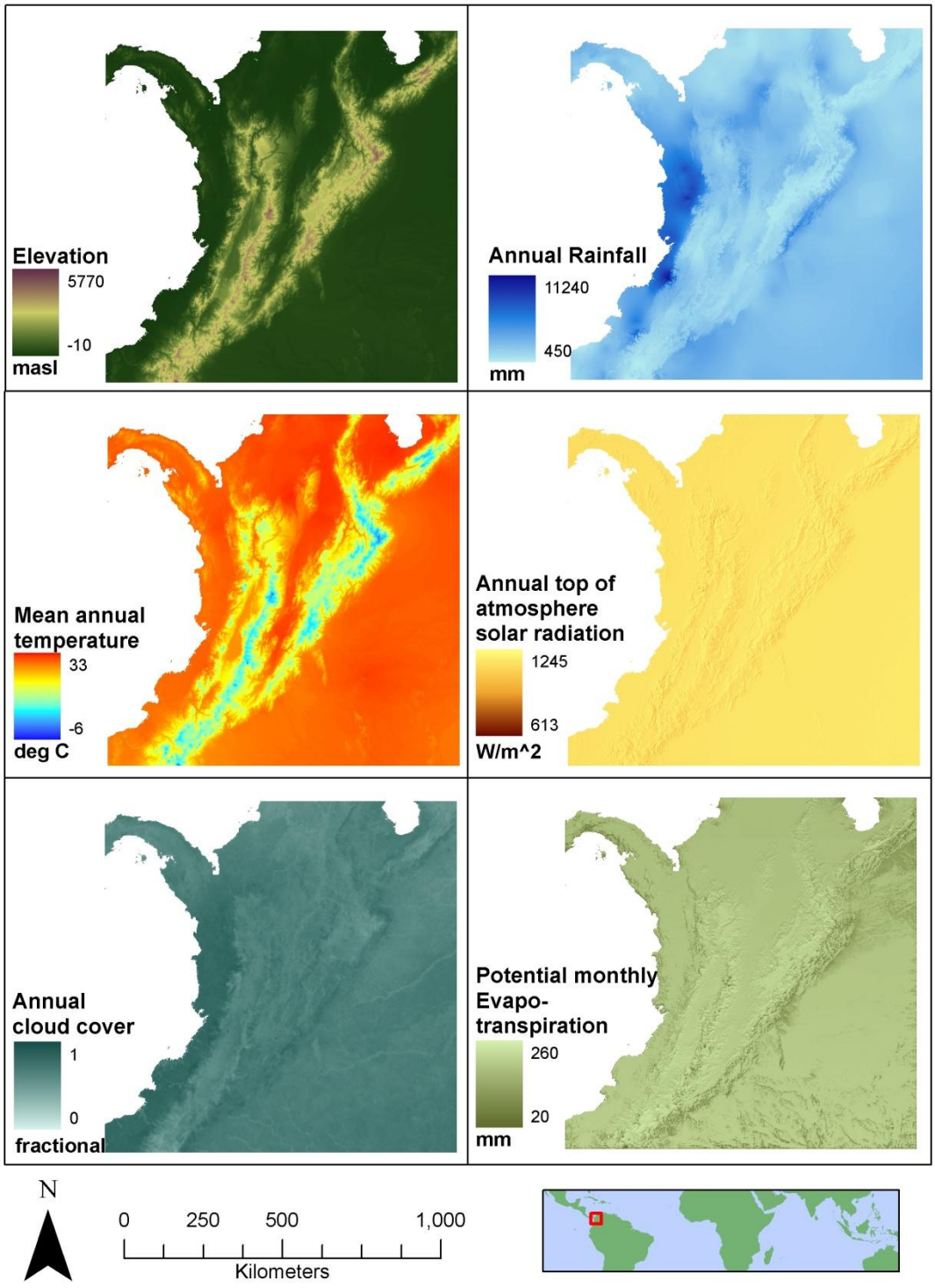

Figure 3.4. Topography and climate variables for the model test site. (DEM: CGIAR-CSI (2004), rainfall and temperature: Hijmans *et al.* (2005), solar radiation: calculated using Iqbal (1983), cloud cover: Mulligan (2006a), Evapotranspiration: calculated using Mulligan, (1999)).

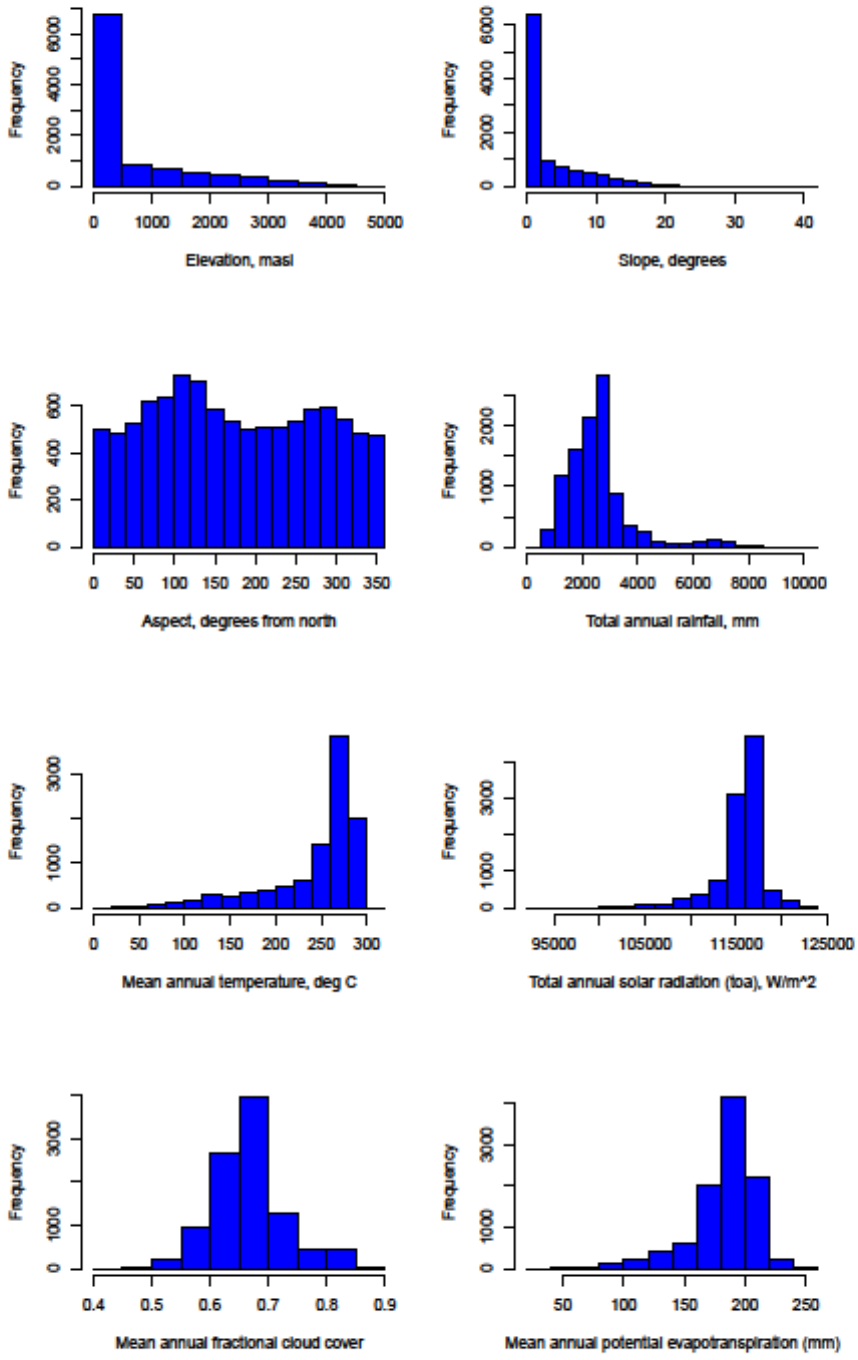

Figure 3.5. Frequency-density plots for the climatic and topographic variables of the test site.

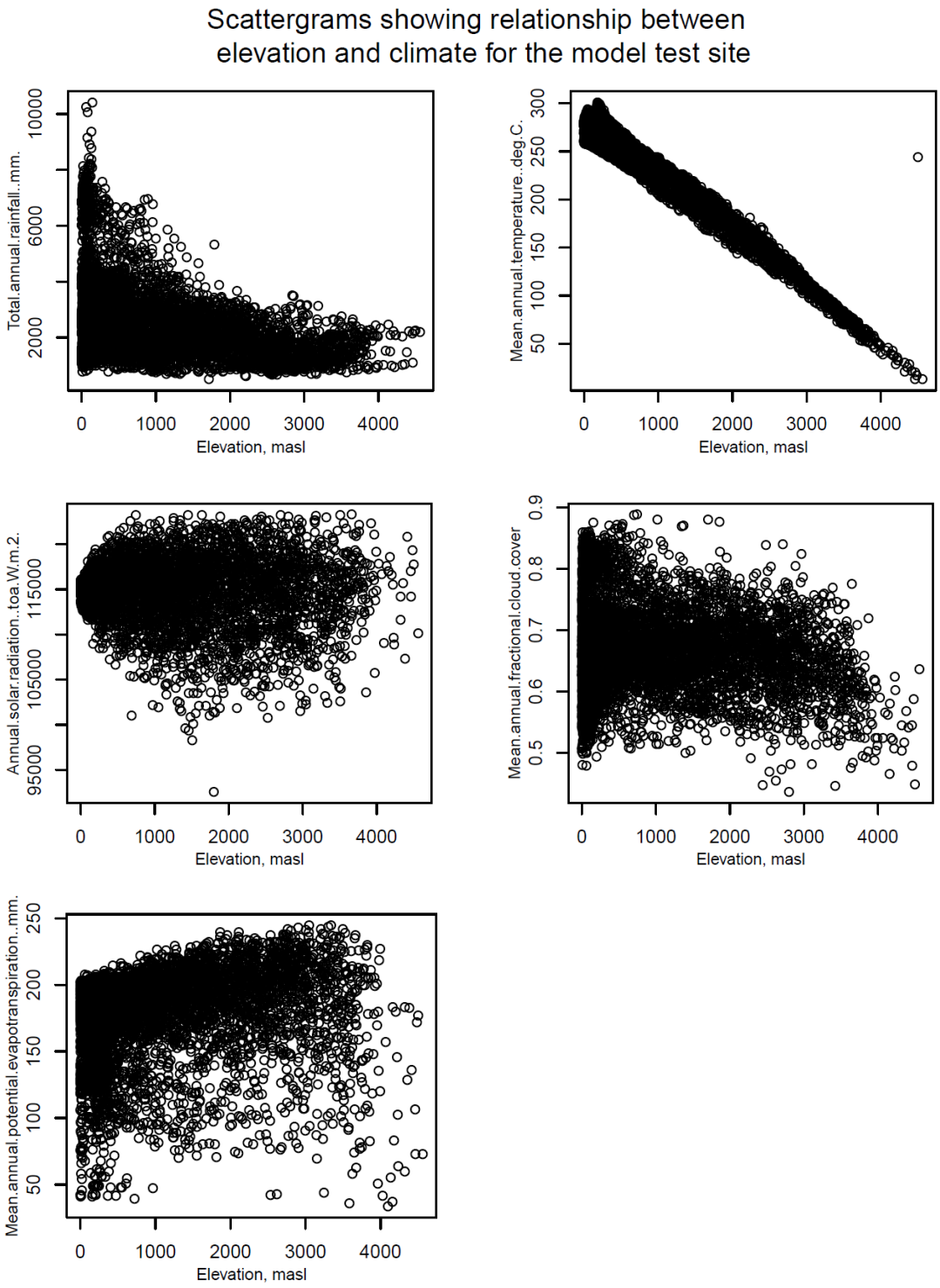

Figure 3.6. Relationship between elevation and climate for the main model test site.

3.4.2. Albertine Rift Mountains

A tile covering the Kenyan rift valley was selected as the African testing tile (figure 3.7). This tile was selected as it contains a large proportion of mountainous terrain, with high topographic variation in order to cover a wide range of conditions. The upper left corner of the 10° tile is located at 24.557°, 1.587°; the tile is a composite of parts of 4 SimTerra tiles (as

outlined in chapter 2), which were mosaiced and then clipped in order to maximise the mountainous terrain within the study region. In some datasets the edges of the original SimTerra tiles are apparent due to the nature of the calculations (for example topex calculations cannot take into account terrain in a neighbouring SimTerra tile).

The study area covers the borders of Rwanda, Burundi and the Democratic Republic of Congo, with elevations reaching 4900 masl in places . The mountains in the area are divided by lake Tanganyika towards the south, however there is a reasonably extensive mountainous region following a north-south orientation (as in the Colombian Andes). When compared to the South American and south-east Asian study areas, there are more escarpments than peaks. In terms of temperature there is little variation, with a maximum difference in mean annual temperature of 3 ^{o}C within the tile (temperatures varying from 25 ^{o}C to 28 ^{o}C according to Hijmans *et al.*, 2005). Solar radiation follows a latitudinal gradient with higher values occurring closer to the equator (modelled according to Iqbal, 1983). There is some impact on solar radiation from the topography, however this is not as apparent as in the Colombian tiles (figure 3.4). There appears to be a south-west to north-east gradient in both rainfall (Hijmans *et al.*, 2005) and cloud cover (Mulligan, 2006a), with the south-eastern corner of the tile receiving much lower annual rainfall and lower mean annual cloud cover. In terms of ecoregions, the mountainous area of the tile is dominated by the Albertine Rift Montane Forests and the Central Zambezian Miobmo Woodlands (WWF, 2009).

The African test tile is used in chapters 5 (quantifying the relationship between geo- and biodiversity) and 6 (conservation priority and geodiversity).

3.4.3. Papua New Guinea

The tile used to represent South-East Asia covers Papua New Guinea, with the upper left corner located at 140^{o}, 0^{o} (a complete SimTerra tile, figure 3.8). This tile was chosen because Papua New Guinea represents the largest continuous mountainous land-mass in South-East Asia - other tiles contain many islands as opposed to a single mountainous range.

The elevations in the tile cover a similar range to those found in the African and South American tile (reaching approximately 4700 masl, CGIAR-CSI, 2004), however a key difference is the south-east to north-west orientation of the main mountain range as opposed to the north-south orientation of the ranges in the other test sites. In terms of temperature, the region is more similar to the Colombian tile with temperatures ranging from 3 ^{o}C to 28 ^{o}C

(Hijmans *et al.*, 2005). Solar radiation is higher in the north-west of the region, with a strong topographic influence (calculated using Iqbal, 1983). The southern side of the mountain range appears to be wetter with both higher annual rainfall (Hijmans *et al.*, 2005) and cloud cover (Mulligan, 2006a). The dominant ecoregions in this tile are the Central Range montane rainforests and the Southeastern Papuan rainforests (WWF, 2009).

This tile was used in chapter 6, looking at geodiversity levels within areas prioritised for conservation.

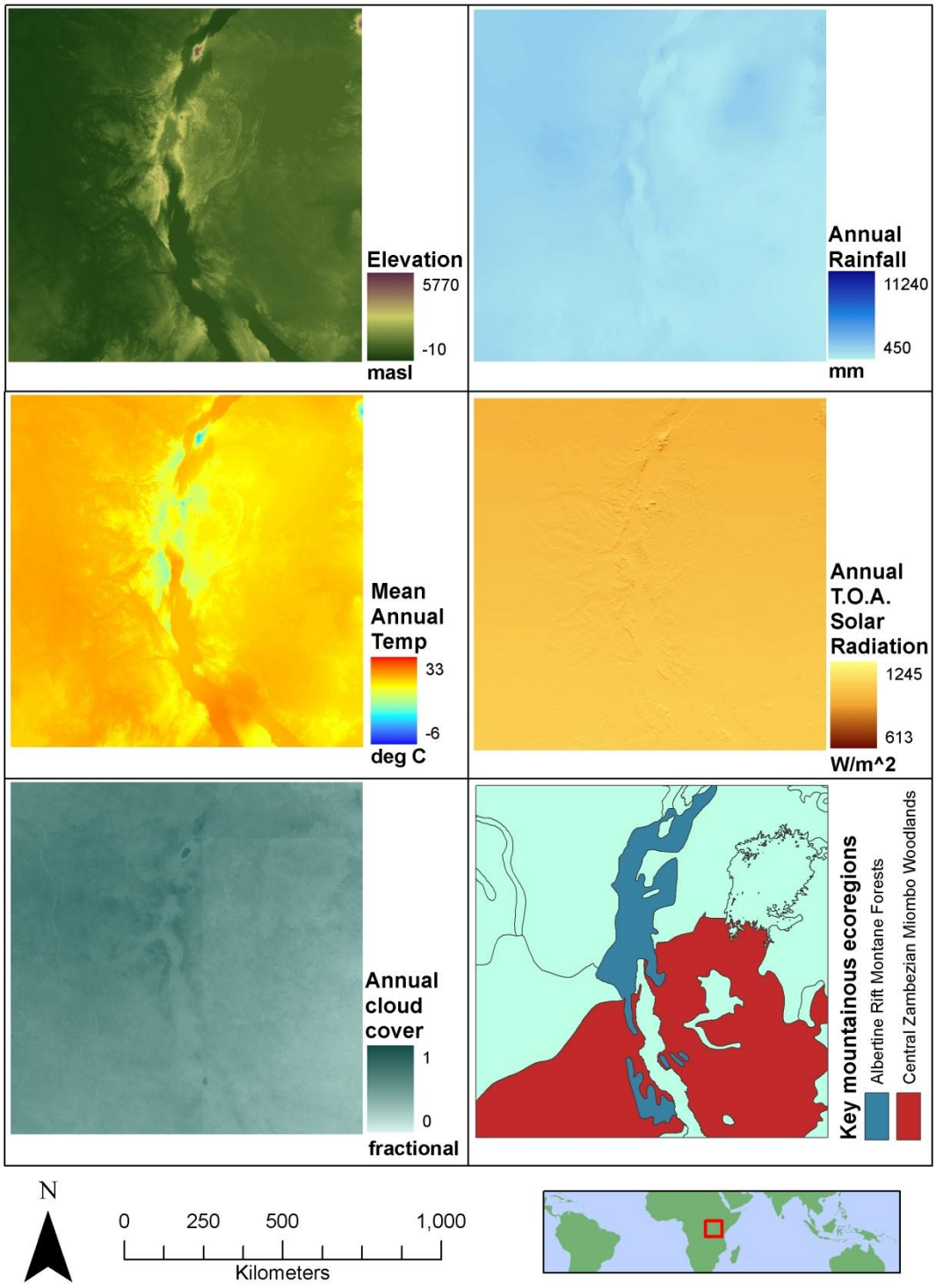

Figure 3.7. Climate and key ecoregions containing mountainous terrain of the African study area used for analysis in this chapter. (DEM: CGIAR-CSI, (2004), rainfall and temperature: Hijmans *et al.* (2005), solar radiation: calculated using Iqbal, (1983), cloud cover: Mulligan, (2006a), ecoregions: WWF, (2009)).

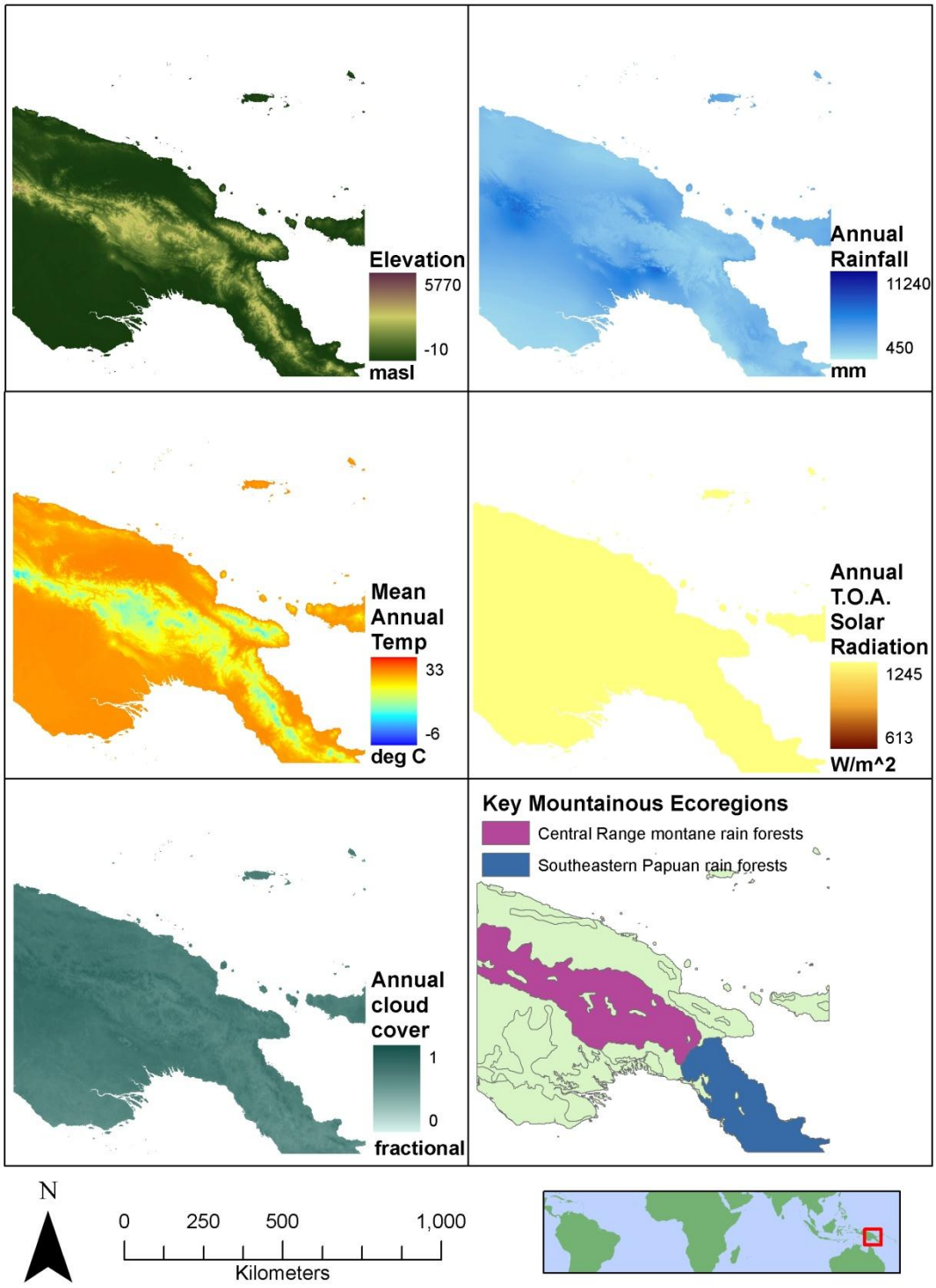

Figure 3.8. Climate and key ecoregions containing mountainous terrain of the South East Asian study area used for analysis in this chapter. (DEM: CGIAR-CSI (2004), rainfall and temperature: Hijmans *et al.* (2005), solar radiation: calculated using Iqbal (1983), cloud cover: Mulligan (2006a), ecoregions: WWF (2009))

To summarise, three 10 x 10 degree study regions were selected to represent mountainous terrain on each of the three tropical continents. The Colombian tile was selected as it covers a

wide range of topographic and climatic conditions, and the original test plots used in the geodiversity model development were also located within this region. The tiles representing Africa and South East Asia were both selected as they included high proportions of contiguous mountainous terrain and represented wide ranges of topographic and climatic conditions. The key differences between the study sites are: the orientation of the mountain chains (with the Colombian Andes and African Rift Valley running north-south, whilst the Papua New Guinea mountains are oriented east-west); the seasonal variation in temperature (lower variation in the African Rift Valley); maximum rainfall (approximately a five-fold difference between the Colombian site (wettest) and African Rift Valley (driest)).

The Colombian test site was used for the model development (chapter 4), and all subsequent analyses. To investigate the relationship between geo- and bio-diversity both the Colombian and African Rift Valley sites were used (chapter 5), whilst all three test sites were used to examine the prioritisation of biodiversity and geodiversity for conservation (chapter 6). The Colombian test site is the only tile used in Chapter 7, which investigates the potential impact of climate change on geodiversity.

Chapter 4. Quantifying geodiversity: model implementation and testing.

4.1. Introduction

This chapter details the process of creating an executable model based on the theoretical model outlined in chapter 2, Mulligan (2000) and Parks and Mulligan (2010). The first section of the chapter will detail the methodological strategy, the data used and describe the technical implementation of *GDiv*. The model testing, sensitivity analysis and validation attempts are then outlined, before the results of initial runs are presented. Although *GDiv* is an expression of a theoretical model, it was hoped to frame the results in a more applied context and so the results are discussed within a conservation framework.

As outlined in chapter 2, there is a growing need for locally relevant and well-tested models on which conservation decisions can be based. The major aim of this chapter is therefore to develop a well-tested and robust model.

4.2. Methods

4.2.1. Methodological strategy

The significance of geodiversity in terms of global ecology and economics (as outlined in chapter 2) means it is important to map the spatial distribution of geodiversity. In order to produce this map, the theoretical model of geodiversity discussed was developed into a spatial model implemented across all tropical mountains. Initially the model was implemented over a small study region in order to be able to carry out the necessary sensitivity analyses, verification and calibration thoroughly without the long processing times that would be incurred when running the model over the whole tropics. The initial test region, the 10^{o} x 10^{o} tile situated over northern Colombia (chapter 3.4.1) had highly diverse topographic and climatic conditions. This meant the model covered a wide range of environments, thus enabling simulations over the entire tropics to remain within the tested environmental boundaries of the model. The model was implemented using the PCRaster-Python framework, as this enabled the native functionality of PCRaster to be combined with the flow-controls and manipulations of Python. When the model had been thoroughly tested, it was run for all tropical mountains and was validated using two further 10^{o} x 10^{o} tiles, one in Africa and one in South East Asia.

4.2.2. Data

One of the key benefits of using geodiversity as a conservation prioritisation tool is the availability of detailed spatial environmental data necessary for a calculation of spatio-temporal variation in availability of resources; this section will outline the datasets that were used in the implementation and testing of the geodiversity model. The geodiversity model implemented here requires mean monthly temperature, mean monthly rainfall, a digital elevation model (DEM), mean monthly fractional cloud cover, topographic exposure (topex), mean monthly wind speed and wind direction as data inputs; all other inputs are calculated from these. The SimTerra (Mulligan, 2009)[1] compiles existing and new global climatic datasets into a standard tiled grid and file format (ARCASCII and PCRaster files) with square cells of 1 km resolution (actual cell size 8.3×10^{-3} decimal degrees at the equator) and 90 m resolution where available (actual cell size 8.3×10^{-4} decimal degrees at the equator). The data are in unprojected geographic coordinates using the WGS84 datum. All maps shown in this thesis are in GCS, WGS84 unless otherwise stated. The 1 km data was used for pan-tropical model runs, as well as for initial model testing. The 90 m data was used to investigate the impact of data resolution on model output within the initial testing tile.

For four of the seven data inputs (DEM, temperature, rainfall and cloud cover), SimTerra contains two alternative datasets. A sensitivity analysis of the model to the input dataset was conducted and, combined with a literature review of the reported accuracy levels of each dataset, a decision was made with regards to which dataset to use in final analyses.

4.2.2.1. DEM

SimTerra contains two DEMs covering the tropics; NASA's Shuttle Radar Topography Mission (SRTM, NASA, 2009), and the USGS's Hydro1k (USGS, 2009a). The SRTM data was collected during a 10 day NASA mission using the Endeavour Shuttle in February 2000. The shuttle was fitted with a radar transmitter and receiver in the main body, as well as a radar receiver at the end of a 60 m side-mast which extended when in orbit. The shuttle-based transmitter sent radar signals to the surface below. The two return signals were received at both the shuttle body and at the end of the side-mast. These were used to calculate an interferogram showing the differences between the two return signals. As the two receivers were a known and consistent distance apart, any differences between the two return signals were due to the topography below and so calculation of the surface topography was possible. It is important

[1] www.policysupport.org/simterra

to note that the elevation given by the SRTM data is surface data, i.e. it represents canopy height rather than ground height (USGS, 2009b).

The SRTM (version 4.1) raw data consists of 90 m DEMs with a vertical accuracy level greater that 16 m; this data was processed by the National Geospatial-Intelligence Agency (NGA) to correct for spikes and wells greater than 100 m different from the surrounding area, and to fill small areas of no-data. Areas larger than the cut off of 16 adjacent posts were left as no-data holes in the finished SRTM dataset (USGS, 2009b). The data held in SimTerra has been hole-filled by the Consultative Group on International Agricultural Research - Consortium for Spatial Information (CGIAR-CSI) to provide continuous elevation surfaces in metres through interpolation over the data holes and infilling with other datasets (CGIAR-CSI, 2004).

The hydro1k dataset is a set of hydrologically corrected variables, including elevation. The elevation data is derived largely from the USGS's GTOPO-30 DEM, a 30 arc-second resolution DEM based on a range of raster and vector sources. In the initial test site, northern Colombia, the GTOPO30 was based predominantly on the Digital Chart of the World, with some data from the Digital Terrain Elevation dataset. Elsewhere in the tropics these two sources were supplemented by Army Map Services, the International Map of the World and the Peru Map. In order to create a unified DEM, these source maps were first projected to Lambert Azimuthal Equal Area, closed basins were then identified and protected during subsequent processing by inserting an artificial "drainage hole" at the lowest point (a no-data cell through which flows would drain) and, once true closed basins had been protected, artificial closed-basins were removed iteratively, and the DEM was verified for correct flow lines and basins (USGS, 2009a).

4.2.2.2. Rainfall data

Two sets of rainfall data are available from SimTerra; WorldClim (Hijmans *et al.*, 2005) and the 2b31 rainfall climatology produced by Mulligan (2006b) from NASA's Tropical Rainfall Measuring Mission 2b31 product (TRMM, NASA, 2008). The TRMM's precipitation radar measures the 3d structure of rain events; the 2b31 product uses the data from the precipitation radar and the microwave imager to provide an estimate of total rainfall in mm month^{-1} for each pass of the sensor. This is calculated using a Bayesian approach whereby the parameters describing the shape of all potential raindrop size distributions are used to estimate the range of potential signal returns. The actual return signal is then compared to all the potential return signals, and the closest matching raindrop size distribution is selected. Although measuring the 3d structure of individual rain events has the potential for high levels of accuracy, there are complications. The algorithms do not differentiate between ice and

raindrops; the high return signal from ice particles in the atmosphere mean over-estimation of rainfall is probable (NASA, 2008). The climatology covers the period 1998 - 2006and provides mean monthly and annual rainfall pan-tropically. The instrument has a return period of 10-14 days so the climatology is made of approximately 240+ swaths at each site (Mulligan, 2006b).

The WorldClim rainfall surfaces (Hijmans *et al.*, 2005) are based on interpolation of 47,554 rain stations across the globe (figure 4.1). The mean rainfall values were based on rain stations with a minimum of 10 years continuous data, between 1950 and 2000. The input data quality was initially checked by verifying that each datapoint (i.e. each weather station) was located in the recorded country and at the correct elevation (based on the hole-filled SRTM DEM). After the first interpolation run, data points with large residual values were checked and, where appropriate, typing and geo-referencing errors were corrected before the interpolation was re-run. The interpolation was carried out using thin plate smoothing splines in the ANUSPLIN 4.3 package with latitude, longitude and elevation used as second order, independent variables. The resulting continuous surfaces are at a 1km resolution and of a global extent (Hijmans *et al.*, 2005).

4.2.2.3. Temperature data

Both the temperature datasets listed on SimTerra (WorldClim, Hijmans *et al.*, 2005 and HadCRUT3, New *et al.*, 2002) are based on interpolation of measurements from weather stations (figures 4.1 and 4.2). The WorldClim mean temperature surfaces, based on interpolation of 12,783 stations, were calculated using the method outlined in the previous section and were stored as ^{o}C×10 to reduce file size (Hijmans *et al.*, 2005). The HadCrut3 dataset was based on mean temperatures calculated from 12,783 stations. If possible, the mean was derived from the minimum and maximum temperature, however if this was not possible (for example if the station did not record minimum / maximum temperature) the given mean was used even if the derivation was not known. In order to qualify for inclusion, the monitoring stations had to have at least 15 years worth of data from the period 1961 - 1990. After quality checking (removing duplicate stations and outliers greater than 5δ from the local mean), the datapoints were interpolated using thin plate smoothing in the ANUSPLIN package however elevation, latitude and longitude were used as co-variants (rather than as independent variables as in the Hijmans *et al.* (2005) interpolations) (New *et al.*, 2002).

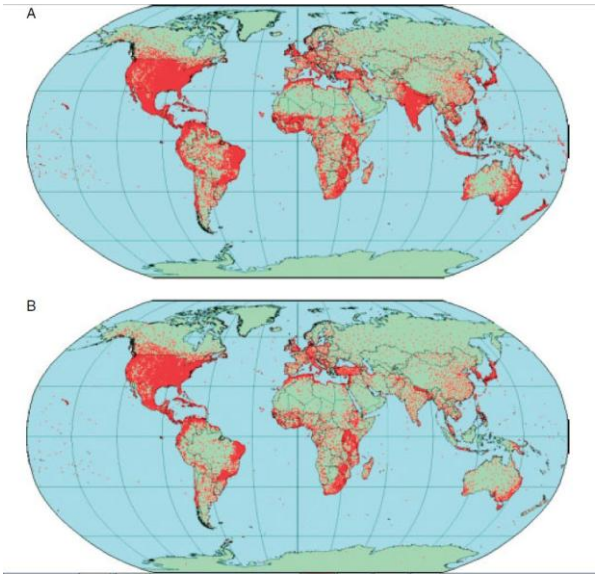

Figure 4.1. From Hijmans *et al.* (2005). Distribution of the 47,554 rainfall monitoring stations (A) and 24,542 temperature monitoring stations (B) used in the interpolation of the WorldClim mean precipitation and temperature interpolated surfaces.

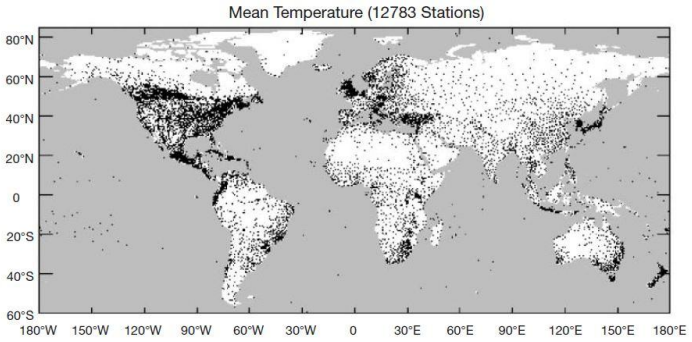

Figure 4.2. From New *et al.* (2002). Distribution of the temperature monitoring stations used in the interpolation of the HadCRUT temperature surface.

4.2.2.4. Cloud cover data

There are two cloud datasets available from SimTerra. The Moderate Resolution Imaging Spectroradiometer (MODIS) MOD-35 daily cloud mask product from 2001 - 2006 was used to calculate a five year climatology of fractional cloud frequency, giving a 1 km or 250 m resolution raster surface representing monthly, seasonal and annual mean cloud cover as a decimal fraction (Mulligan, 2006a). The MODIS instruments have a daily temporal resolution, and a high spatial resolution. The MOD-35 product, a daily cloud mask, is produced by first using the visible spectrum to assign field-of-views as high confidence clear, probably clear, undecided or cloudy. For field of views with an uncertain classification, spatio-temporal tests based on spectral frequency signals from alternative MODIS instruments are combined with land / water masks, a DEM, ecosystem classifications, a snow / ice map, temperature, wind-speed and precipitable water data in order to classify as either cloudy or clear (MODIS, 2009).

The second available dataset is the HIRS cloud climatology, based on cloud frequencies calculated using CO_2 slicing which is more accurate than temperature based methods (Wylie *et al.*, 1994).

4.2.2.5. Wind speed data

The wind-speed dataset in SimTerra is collated from New *et al.* (2002) and is interpolated following a similar method to that used for the HadCRUT3 temperature dataset, as outlined in section 4.2.2.2. A total of 3952 monitoring stations were included in the interpolation. The measuring height varied between 2 and 20 m, although the majority of stations were monitoring at approximately 10 m and so this is the assumed height for the dataset. The dataset gives monthly values for wind-speed in m s^{-1}. The distribution of monitoring stations is shown in figure 4.3. Both the CRU datasets were interpolated from the original resolution to 1 km resolution using bilinear interpolation for inclusion in SimTerra (Mulligan, 2009)

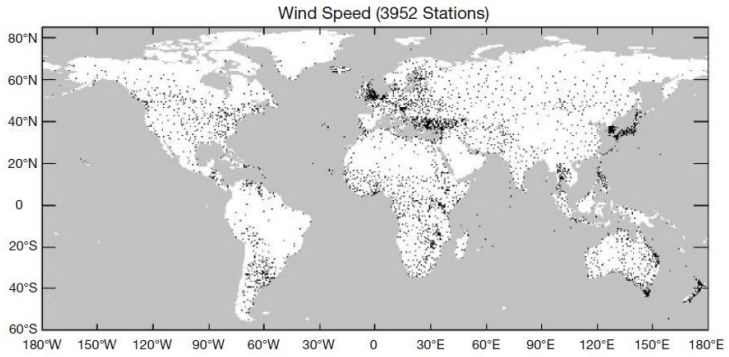

Figure 4.3. From New *et al.* (2002). Distribution of the 3952 wind monitoring stations used to create an interpolated surface of mean wind-speed at an assumed height of 10 m.

4.2.2.6. Wind direction data

Directional wind data was also obtained from SimTerra. It was calculated using the methodology outlined in Mulligan and Burke (2005) and gives the geostrophic wind based on a global mean sea level pressure climatology from the BADC that is also in the Simterra (British Atmospheric Data Centre, 2000).

4.2.2.7. Topographic exposure (Topex) data

Topographic Exposure (Topex) data was also downloaded from SimTerra. The raster surfaces were calculated by running the WaterWorld model (Mulligan and Burke, 2005, Bruijnzeel *et al.*, 2011) for the tiles used. WaterWorld[2] calculates topographic exposure using a topex algorithm based on the DEM (Ruel *et al.*, 2002). It represents exposure at the surface to wind from each of 8 compass directions. In *GDiv* this data was then combined with the wind direction data to

[2] www.policysupport.org/waterworld

give a measure of overall exposure for each pixel in the study area, as outlined in section 4.3.2.3.4.

4.2.2.8. Solar Radiation data

Solar radiation was calculated prior to the main model run due to the lengthy processing time. The output maps were then saved and used as input for *GDiv*, the spatial geodiversity model, as outlined below. It was modelled using latitude, longitude, Julian day, hour, slope and aspect using standard equations (Iqbal, 1983, Mulligan, 1999) again as part of a WaterWorld simulation. The slope and aspect were derived from the SRTM 1 km DEM, and the output was a raster coverage in W m^{-2}, giving total potential radiation at the top of the atmosphere. This was later corrected for cloud cover in *GDiv*, as outlined in section 4.2.3.2.

4.2.2.8. Species richness data

Initially, two sets of species richness data were to be used for verification and validation of the geodiversity model; 1 km resolution overlay maps of distributions of IUCN Redlist species for amphibians, birds and mammals as well as accession data for tree species taken from the Global Biodiversity Information Facility (GBIF).

The raw data from the IUCN consisted of individual shapefiles showing the distribution, based on expert opinion, of each threatened species within the broader taxonomic groups (IUCN *et al.*, 2008a, IUCN *et al.*, 2008b, BirdLife, 2009b, BirdLife, 2009a). These shapefiles were then converted to Boolean maps (with a value of 1 in the species range), which were then summed within the taxonomic group to give a measure of overall species richness (Mulligan, 2009).

For the tree distribution data, all species occurrence records for 135 genera were downloaded from GBIF in April 2010 (GBIF, 2009). Records not based on a sampled specimen, live specimen or direct observation (i.e. fossil or arboretum records etc.), and those with no geo-reference were excluded, resulting in an initial dataset of 752 829 accessions globally. Although the GBIF data was not used in final analyses, due to the low number of records of a suitable quality, a description of the methods used to clean the data and discussion of potential future use of GBIF data is included in section 5.2.1.

4.2.3. Model implementation

The model outlined in Parks and Mulligan (2010) was initially proposed and developed as a PCRaster spatial model by combining measures of resource availability, temporal variability (seasonality) and wider spatial resource context by Mulligan (2000) and was applied at the

regional scale within two locations in Colombia. The model proposed in Parks and Mulligan (2010) seeks to use freely available datasets to model geodiversity at a cell resolution anywhere between 25 m and 1 km. Each of these three components of the model (resources, wider spatial resource context, temporal variability) is based on combinations of varying measures of raw geodiversity inputs derived from the topographic, temperature, precipitation and solar radiation data outlined in chapter 2.1. The final output of the model is a raster coverage scaled 0 - 1, with high scoring areas showing high levels of geodiversity. Aspects of the model presented here have been previously tested on fine (25 m resolution) data for small plots in Colombia, where the distribution of tree diversity and mid-elevational peak in diversity predicted by the model was found (Jarvis, 2005). However, the current thesis is the first broad scale assessment of geodiversity patterns with this model.

The model script was coded here using the PCRaster Python framework. PCRaster is a free, raster-based GIS programme with high levels of built in functionality for environmental modelling purposes. Available for Windows since 1991, a beta-release of the Python framework was made available in January 2010 which allowed integration of the high level PCRaster functionality with the flexibility of Python syntax and control statements. This software combination was selected as the SimTerra database was already available in PCRaster's native .map format, and the tiled nature of the data required the ability to implement "for" loops to process each tile iteratively.

The three key steps in the model implementation were to process the raw data, derive the raw geodiversity inputs, and finally to calculate the three components of geodiversity (*RES*, *Sc* and *Tv*), along with overall geodiversity. All metrics were calculated on a per-pixel basis for the study region, with the resulting maps being written to file as PCRaster .map files. The user controled model parameterisation through a series of on-screen prompts. The three stages of model implementation are represented graphically in figure 4.4, whilst the model code is provided in Appendix 2. Sections 4.2.3.1 and 4.2.3.2 give further detail on the model calculations, working in reverse chronological order (i.e. beginning with the equations for overall geodiversity and the three components, before presenting the calculations for each of the raw geodiversity inputs), whilst section 4.2.3.3 outlines the raw-data processing necessary to run G*Div* and section 4.2.3.4 describes the user control of the model set up.

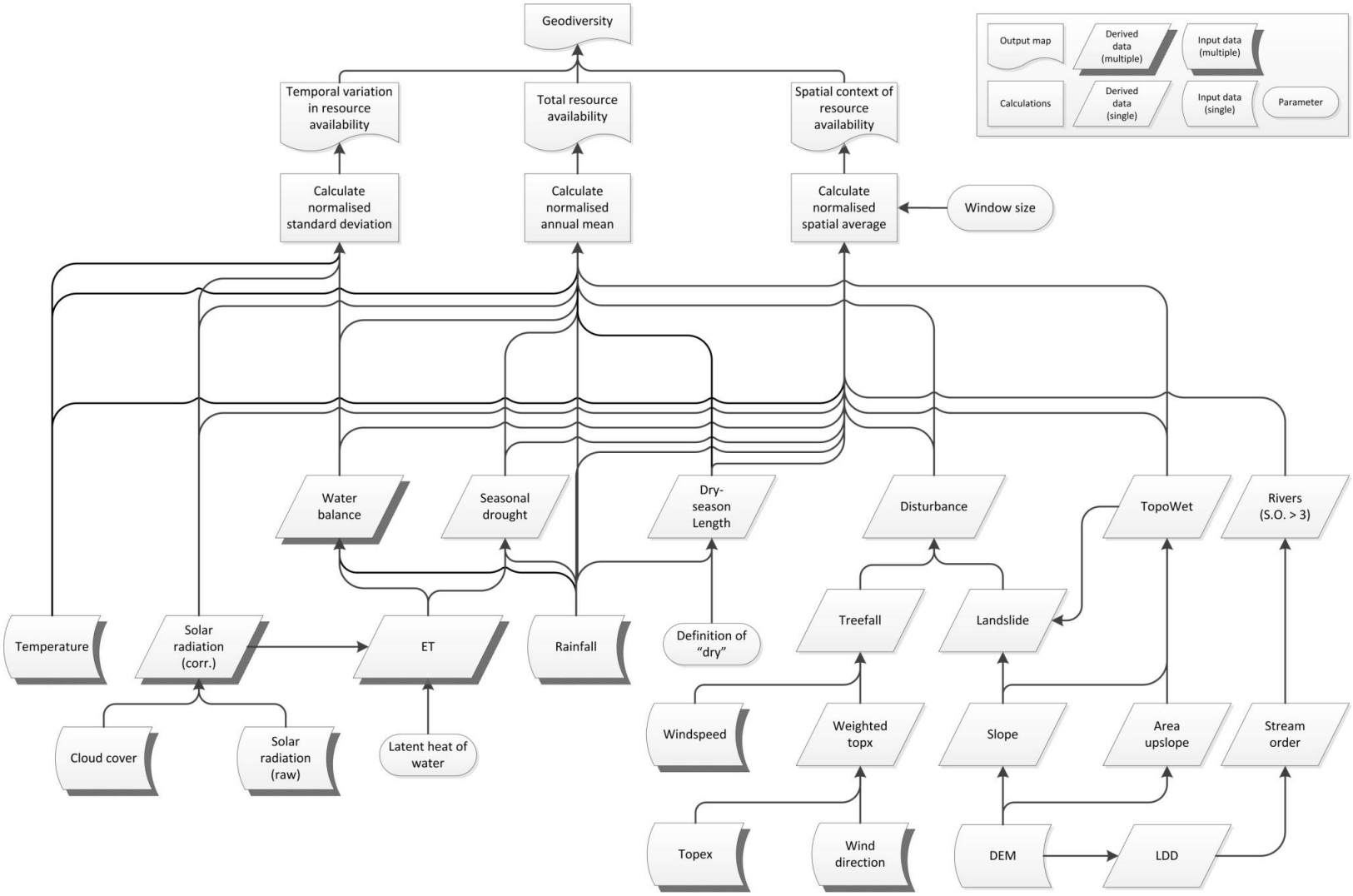

Figure 4.4. Flow diagram of *GDiv* implementation.

4.2.3.1. Model implementation - calculation of geodiversity and components.

Overall geodiversity is calculated as

$$GD = \frac{RES+SV+TV}{3} \quad 6$$

where

$$RES = \frac{\sum_{i=1}^{n} I_{TOT}}{n} \quad 7$$

$$Sc = \frac{\sum_{i=1}^{n} I_{AV}}{n} \quad 8$$

$$Tv = \frac{\sum_{i=1}^{n} I_{SE}}{n} \quad 9$$

and *RES* is a measure of total resources at the pixel level based on the summed values of the inputs (I_{TOT}), *Sc* is a measure of the wider spatial context or resource availability and is based on a moving average across the annual mean of the inputs (I_{AV}) and *Tv* is a measure of seasonality, based on the standard error of the monthly input values (I_{SE}). *n* is the number of inputs included in the respective component calculation, as outlined in table 4.1. I_{TOT}, I_{AV} and I_{SE} are defined fully below.

Each of the components of geodiversity is based on a different aspect of the raw inputs. The standard model configuration calculates the components based on the input environmental phenomena shown in table 4.1, however a sensitivity analysis was carried out whereby the impact of removing each input was investigated (section 4.2.4.3). Dividing the summed component scores by *n*, the theoretical maximum score, maintains the 0 - 1 scaling across the whole study region. In these initial calculations all inputs and components were given an equal weighting in the final calculations as there was no evidence for doing anything other. The impact of varying these weightings is investigated further in chapter 5.

Table 4.1. Environmental phenomena included in *GDiv*, and their inclusion in the three components of geodiversity.

Variable	*RES*	*Sc*	*Tv*
Temperature	Yes	Yes	Yes
Solar Radiation	Yes	Yes	Yes
Water Balance	Yes	Yes	Yes
Rainfall	Yes	Yes	No
Topographical Wetness	Yes	Yes	No
Disturbance	Yes	Yes	No
Seasonal Drought	Yes	Yes	No
Drought Length	Yes	Yes	No

Rivers	No	Yes	No
Evapotranspiration*	No	No	No

* Evapotranspiration was used in the calculation of monthly water-balances, rather than being included as a direct input itself.

4.2.3.2. Model implementation - input calculations.

As each of the three geodiversity components is concerned with a different element of the geodiversity inputs, it was necessary to calculate the annual total, annual mean (for resources) and, where applicable, the standard error based on 12 monthly values (for temporal variation in resources). These maps were scaled 0 - 1, based on division by the maximum observed value across the entire study area, in order to produce a series of unitless relative input measures which were given equal initial weightings for combination into a geodiversity metric.

Annual totals for each input were calculated using

$$I_{TOT} = \left(\frac{\sum_{i=1}^{n} I_i}{\max\left(\sum_{i=1}^{n} I_i\right)} \right) \quad 10$$

where I_{TOT} is the annual total of the input *I*, and *i* represents the monthly value of all *n* months. I_{TOT} is used for calculating the total resource availability. The bottom term normalises the I_{TOT} map from 0 - 1 and is based on the maximum *I* value across all tiles in the study area.

In order to calculate the wider spatial context of input resource values (for the *Sc* term of the model), a kernel based spatial moving average is taken; the score for each cell is the mean value of the scores of those cells falling in the window (or fraction thereof if a section of the cell falls outside the window). For each input it was calculated with a square window using

$$I_{AV} = \left(\frac{\left(\frac{\sum_{a=1}^{n} fa \times I}{\sum_{a=1}^{n} fa} \right)}{\max\left(\frac{\sum_{a=1}^{n} fa \times I}{\sum_{a=1}^{n} fa} \right)} \right) \quad 11$$

where I_{AV} is the moving spatial mean of the annual mean of the input *I*, based on a user defined window size. *f* is the fraction of the cell falling within the window and *n* is the number of cells falling partially or totally within the window. The window length is defined by the user; a sensitivity analysis of *GDiv* to window length was carried out (section 4.2.4.2) which resulted in the default length being set to 30 km. Again, the bottom term normalises the map on a 0 - 1 scale and is calculated across the entire study area.

Seasonal variation in resource availability is calculated based on the standard error of monthly measurements (as a measure of temporal variability) using

$$I_{SE} = \left(\frac{\sqrt{\frac{\sum_{i=1}^{n} (\bar{I} - I_i)^2}{n-1}}}{\max\left(\sqrt{\frac{\sum_{i=1}^{n} (\bar{I} - I_i)^2}{n-1}} \right)} \right) \quad 12$$

where I_{SE} is the standard error of the input, *I* and *i* represents the monthly value of each *n* month. The bottom term normalises the map on a 0 - 1 scale and is calculated across the entire study area.

In order to calculate I_{TOT}, I_{AV} and I_{SE} raw data was processed in order to derive the various environmental inputs necessary for calculation of the three components of geodiversity. Table 4.1 gives an overview of all the environmental variables used in *GDiv*, as well as the components of geodiversity to which they contributed, whilst the specific equations are outlined below.

4.2.3.2.1. Water balances

Previously the water balance in the geodiversity model was an annual water balance, and the water balance was only used in *RES* and *Sc* (Mulligan, 2008). *GDiv* modifies this to calculate monthly water balances, meaning water balance can be used in the *Tv* component. Water balances were calculated using

$$WB_i = P_i - ET_i \quad 13$$

where P_i and ET_i are monthly precipitation and evapotranspiration for month *i* respectively.

4.2.3.2.2. Topographic wetness

The topographic wetness index was used to give an indication of the potential topographically controlled substrate wetness at a site. It was calculated using

$$WET = \ln\left(\frac{A}{\tan(m)}\right) \quad 14$$

where *A* is the area upslope and *m* is the slope in degrees. An artificial slope value of 10^{-12} for areas with an actual slope of zero was applied to avoid numerical overflow due to division by zero.

4.2.3.2.3. Disturbance

Gap dynamics and disturbance regimes are modelled based on the relative likelihood of landslides and treefall in order to give a measure of space as a resource; these were calculated as a phenomenological model designed to describe patterns, rather than as physically based equations. In terms of modelling treefall dynamics, topography plays a key role with slopes (as opposed to ridges and valleys) being associated with larger gaps, and soil depth and wind also

playing a key role in treefall related gaps of 46 - 85 m^2 (Ferreira de Lima and de Moura, 2008). Although this suggests that tree gap dynamics may be working at a smaller scale than the 1 km^2 data used in the preliminary analyses, other studies have found treefall regime to be a predictor of species richness and community composition at a 1 km^2 scale (Grau, 2002), suggesting that treefall should be included in the disturbance regime.

Landslide likelihood was modelled based on the slope and topographic wetness. Although it has been found that this measure could be improved with inclusion of potential seismic activity (Restrepo and Alvarez, 2006) and also soil / geology properties, it was decided to use a more parsimonious model. The inclusion of treefall dynamics in the disturbance regime is a novel modification to the original Mulligan (2000) geodiversity model that has been previously tested only with the landslide component.

$DIST_{landslide}$, the potential for landslides per pixel, was calculated as

$$DIST_{landslide} = WET \times m \quad (15)$$

where *WET* is the topographic wetness index and *m* is the slope in degrees. Treefall likelihood was calculated per pixel as

$$DIST_{tree} = w \times Tw \quad (16)$$

where *w* is the surface windspeed (measured in m sec^{-1}) and *Tw* is a measure of topex, weighted by the predominant wind direction and normalised.

Overall disturbance (*DIST*) was then calculated giving an equal weighting to landslide and treefall using

$$DIST = \frac{DIST_{land} + DIST_{tree}}{2} \quad (17)$$

4.2.3.2.4. Seasonal Drought

Seasonal drought is a measure of how water-stressed an area is during its most stressed month. It was calculated using

$$WS = max_{i=1}^{12}(P_i - ET_i) \quad (18)$$

where P_i and ET_i are monthly precipitation and evapotranspiration respectively (i.e. *WS* is the month with the largest difference between *P* and *ET*).

4.2.3.2.5. Length of dry season

The original Mulligan (2000) model measured drought using the *WS* measure outlined in the previous section. However, another important factor influencing tree distributions in tropical forests is the length of the dry season (Condit, 1998). Therefore, it was decided inclusion of a measure of length of dry season, in conjunction with *WS*, in the *RES* component would be beneficial.

The Normalised Difference Vegetation Index (NDVI) uses the spectral reflectances of visible red and near infrared by canopy leaves to measure the amount of green biomass. Whilst the lack of climatic seasonality means tropical forests do not have a wholesale seasonal leaf-shed and the NDVI therefore does not show such dramatic seasonal fluctuations, meaning "greenness" can be used as a proxy for water stress (Whitmore, 1998), it was decided that use of the NDVI would not be appropriate in this case as it can be influenced by land-use. As *GDiv* is intended to measure "raw" geodiversity, without considering the impact of humans on the environment, a direct hydrological measure that was not influenced by land-cover / land-use was chosen.

The potential water stress factor (*DL)* was defined as any month with rainfall less than one standard deviation below the mean, and potential water stress duration was calculated by summing the number of days in all months falling below this threshold.

4.2.3.2.6. Rivers

The presence of large rivers has been found to lead to greater diversity levels through the structuring of the landscape (Bates *et al.*, 2004, Khomo and Rogers, 2009). The presence of rivers (*RIV*) was determined by deriving the stream orders (Strahler, 1952) from a map showing local drainage direction (the LDD) on a per pixel basis. The LDD was derived from the DEM with the flow direction being to the steepest downhill neighbour; the LDD was then converted to a map showing streams with an order of 4 or greater, as per the original implementation of the model (Mulligan, 2000). The ordinal map was then converted to scalar to allow for use in further modelling.

4.2.3.2.7. Evapotranspiration

During preliminary analyses several methods for calculating potential evapotranspiration were considered. The FAO (2009a) recommends using the Penman-Monteith equation. This method is based on a combination of mass transfer of water and an energy balance approach and required net radiation, soil heat flux, vapour pressure deficit of the air, mean air density, specific heat of the air, saturation vapour pressure temperature relationship and surface and

aerodynamic resistances. Although calculations for situations where some of these data are missing are given by the FAO, it is recommended that the data based on daily measurements of climatic variables. Given that the datasets available in SimTerra do not meet these minimum data requirements and such data are not globally available elsewhere, it was decided use of the Penman-Monteith method would be inappropriate.

Recognising that hourly / daily meteorological data will not necessarily be available, the FAO (2009b) also recommend the use of the Blaney-Criddle method for areas where use of a locally parameterised method is not possible. This technique uses temperature data combined with number of daytime hours to estimate monthly evapotranspiration. However the technique is known to be inaccurate in climatically extreme regions; overestimating in windy, dry and sunny regions by up to 60% or underestimating in calm, humid or cloudy areas by up to 40% (FAO, 2009b). This is of particular relevance to a pan-tropical study where climatic conditions are likely to exhibit high levels of variation, so the Blaney-Criddle technique was also deemed inappropriate.

Two methods of calculating potential evapotranspiration which do not require complex parameterisation are the Thornthwaite and Latent Heat methods. The Latent Heat method works on the assumption that all net radiation (i.e. insolation) is used for evapotranspiration; this is a reasonable assumption in a wet environment where surface water and leaf area mean few restrictions on water availability (Mulligan, 2007) but under drier conditions would need to be considered alongside a Bowen ratio or other approach for estimating the partitioning between latent and sensible heat. Monthly evapotranspiration from the latent heat method (ET_{LH}) was calculated using

$$ET_{LH} = \frac{SR_i}{2260} \qquad 19$$

where SR_i is monthly solar radiation in W m^{-1} and 2260 is the latent heat of the vaporisation of water in kJ kg^{-1}. Whist the solar radiation is usually corrected to give net radiation, in this instance the relative differences in evapotranspiration across the study area are required (as opposed to the absolute values) so this additional calculation was not deemed necessary.

Thornthwaite's method is an empirical method, based on a correlation between temperature and evapotranspiration (Thornthwaite, 1948). Monthly evapotranspiration using the Thornthwaite method (ET_{Thorn}) was calculated using

$$ET_{Thorn_i} = 1.6d\left(\frac{10T_i}{I}\right)^a \qquad 20$$

where *d* is monthly daylight hours / 360, assuming year round 12 hour daylight as the study area is tropical, and T_i is the temperature for month *i* and

$$I = \sum_{i=1}^{12} T_i^{1.514} \quad 21$$

and

$$a = (6.75 \times 10^{-7})I^3 - (7.71 \times 10^{-5})I^2 + (1.79 \times 10^{-2})I + 0.49 \quad 22$$

where the parameter values for *a* were taken from Pereira and Pruitt (2004). *I* and *a* are based on an empirical measure of the local climatic temperature regime; although the values are based on Thornthwaite's (1948) work in the USA, this study is interested in the relative differences in evapotranspiration across the study area (not the absolute magnitudes of ET) so it was assumed these parameter values were acceptable.

When these two methods were tested, it was found that they showed very little correlation (R^2 = 0.002), as shown in figure 4.5. Although this lack of correlation between two models for the same environmental phenomena is at first surprising, it can be explained when the known strengths and weaknesses of each of the models are considered. It is documented that Thornthwaite tends to underestimate in locations with high cloud / fog cover, as this has a higher impact on the insolation than the temperature thereby changing the nature of the correlation between temperature and insolation on which the model is dependent (Mulligan and Burke, 2005). On the other hand, the latent heat model tends to underestimate in drier regions (due to the violation of the assumption that all net radiation is used to evaporate available water). Furthermore, because the solar radiation data used in these initial tests was not corrected for cloud cover, the latent heat method would over estimate in cloudy regions. The combinations of these factors means that, in wet (i.e. cloudy / foggy) regions, Thornthwaite will underestimate and, whilst the latent heat technique would generally be more accurate, it would tend to over-estimate when uncorrected for cloud cover (as in this instance). In drier regions (with less cloud cover), the latent heat method tends to underestimate, whilst the Thornthwaite tends to be more accurate. As a result, in a region of high climatic variability (such as the study region used in these analyses) there is likely to be a lack of linear correlation between the two models (figure 4.6)

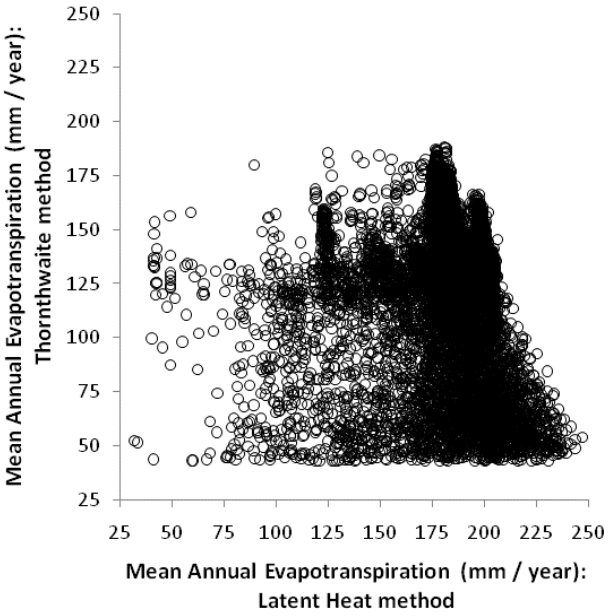

Figure 4.5. Estimation pairs for the two evapotranspiration models tested: The Latent Heat method and the Thornthwaite method.

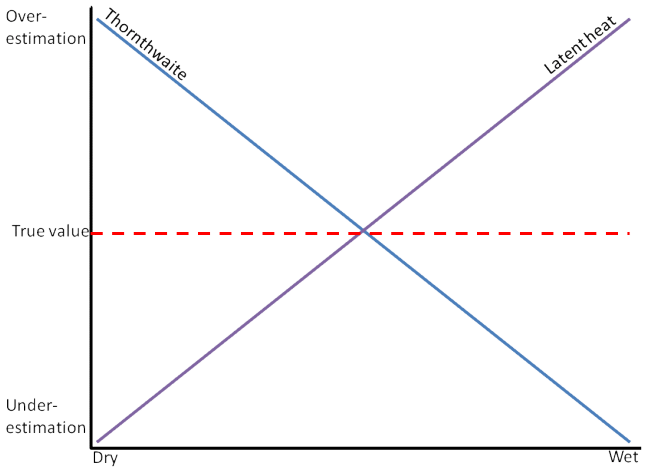

Figure 4.6. Theoretical reason for lack of correlation between the Latent Heat and Thornthwaite method for modelling evapotranspiration.

Whilst there is no empirical evidence to differentiate between the two models of evapotranspiration in terms of accuracy, it was decided to use the latent heat method for calculating the potential evapotranspiration input to *GDiv* as this is the more parsimonious model and the model used in previous implementations of the geodiversity model used in this thesis (e.g. Jarvis, 2005). Were *GDiv* to be used at a more local scale, where evapotranspiration validation data is available, a more thorough evaluation of the two potential models would be possible. Through the remainder of this thesis, the latent heat method was used for calculating the potential evapotranspiration, with solar radiation data

that had been corrected for cloud cover (though the method is designed for net radiation the simplification of using solar radiation affects only the absolute magnitude and not the relative magnitude of the results).

4.2.3.3. Model implementation - pre-processing of raw data

Some of the raw datasets required pre-processing prior to use as inputs in *GDiv*. Depending on the user-defined set-up (which was recorded in the run-record) the following pre-processing was carried out as necessary:

- Rainfall data: the TRMM dataset has a couple of large outliers in the Colombian tile used for model testing. These were corrected by removing values greater than 3 standard deviations from the mean value across the map and replacing them with a local spatial mean.
- Temperature data: WorldClim temperature data is stored as ^{o}C * 10 in order to minimise the file size; these were converted as required in the model runs.
- Solar Radiation: Initially calculated as Top of Atmosphere (ToA) radiation, the data was corrected for cloud cover using either a MODIS cloud frequency climatology (Mulligan, 2006a) or the HIRS cloud statistics (Wylie *et al.*, 1994) outlined in section 4.2.2.4 combined with transmissivity parameters taken from (Burridge and Gadd, 1977)

  $$tk = (0.4 \times C_{low})(0.7 \times C_{mid})\left(0.4 \times C_{high}\right) \quad 23$$

  where C is the fractional cloud cover of low, mid and high clouds. As the cloud cover maps were for all cloud, an even split between low, mid and high clouds was assumed so equation 10 was modified to give

  $$tk = \left(0.4 \times \frac{1}{3}C\right)\left(0.7 \times \frac{1}{3}C\right)\left(0.4 \times \frac{1}{3}C\right) \quad 24$$

  The ToA radiation values were then multiplied by the *tk* factor to give cloud corrected solar radiation

  $$SR_{corr} = SR_{toa} \times tk \quad 25$$

4.2.3.4. Model implementation - user control of model set up.

In the initial section, the user is asked to set the model parameters of the size of the square window used for the calculation of *Sc* (using a spatial kernel mean based on this size), define any necessary data conversions (e.g. convert between units for input data), input the text for the run-record log and to define the model set up (which components and inputs are to be

included in the model run, and to define how the input values are to be varied - used to control sensitivity analysis runs).

4.2.4. Sensitivity and uncertainty analyses and model testing

A range of sensitivity analyses were carried out with the aim of testing *GDiv's* response to varying input datasets, initial parameters and model setup. Further tests also investigated co-variation between model inputs, as well as an investigation into the impacts on the model outputs of systematically co-varying of altitude and topographic variation using an artificially calculated DEM.

4.2.4.1. One-at-a-time variation of model inputs

In order to systematically investigate the impact of the initial datasets on the results, and to check that the model was responding in the expected manner, the first sensitivity analysis consisted of varying the values of each of the input datasets, whilst keeping the remainder fixed. Each input dataset was varied in the range -100% to +100% in intervals of 10, on a per pixel basis. From each run, 10 000 samples were taken at random locations from across the results maps (*GD, RES, Sc* and *Tv*) and these values were used to calculate the mean and standard deviation for each of the components and the overall geodiversity.

4.2.4.2. Sensitivity to kernel size

There is a trade-off between the size of the kernel used to calculate *Sc* and processing time: the larger the window, the longer the model run-time. In order to optimize model performance, it was necessary to find a window size that generated a stable mean geodiversity score (based on 10 000 samples from across the map, as outlined in the previous section) but took the shortest processing time. To achieve this, the model was run with increasing window sizes until the mean geodiversity score stabilised.

4.2.4.3. Sensitivity to model components

In order to establish which of the model components had most influence over the model results, *GDiv* was run with the standard model configuration (Appendix 3) but removing each of the inputs from the calculation in turn. The mean and standard deviation of the resulting *GD*, *RES, Sc* and *Tv* maps were then calculated as outlined previously.

4.2.4.4. Sensitivity to initial data resolution

In order to investigate the sensitivity of *GDiv*'s results to the spatial resolution of the initial datasets, the model was re-run using the standard set-up, but with a 90 m DEM. The remaining datasets were downscaled from their initial 1 km resolution to match the 90 m

resolution by simple nearest neighbour re-sampling. The relevant 90 m 1 degree tile used for Colombia was selected to represent a high elevational range; the location is shown in figure 4.24 (in section 4.3.4).

4.2.4.5. Sensitivity to initial datasets

The two major sources of uncertainty within *GDiv* arise from the components of geodiversity that are included within *GDiv* (the model specification) and the uncertainty in the input datasets used. In order to assess the second type of uncertainty, the model was run using alternative sets of data (where available). All possible combinations of the datasets outlined in section 4.2.2 were implemented.

4.2.4.6. Controlled variation of topographic variation

GDiv was designed to be run in mountainous environments - many of the inputs are highly dependent on topographic variation. In order to systematically pick apart the relationship between geodiversity and characteristics of topographic variation an artificial DEM was generated whereby mean elevation varied along the y axis and the standard deviation of the elevation varied along the x axis. This is conceptualised in figure 4.7 and was calculated as an array of values in Python (Appendix 4). Initially, an empty array was created which was then filled iteratively, on a cell by cell basis, using random numbers drawn from a Gaussian distribution. The mean value of the distribution from which the random numbers were drawn increased along the y axis, representing increasing elevation, whilst the standard deviation of the distribution increased along the x axis, representing increasing topographic variation. To ensure the relationships between topographic variation and elevation were within realistic bounds, the slope frequency distribution within the model test site were derived. The artificial DEM was then smoothed to obtain a similar distribution.

In order to run *GDiv* using the artificial DEM it was necessary to calculate, where possible, input datasets based on the artificial DEM and the empirical relationship between the elevation and the input in question. This was straightforward for slope and stream order. For the remaining datasets, if linear regression did not provide a good explanatory power, the dataset was kept constant across the "study area" to reduce complexity. For the purpose of this sensitivity analysis, *GDiv* was run without the *Tv* component, as there is no seasonal variation in elevation or topography.

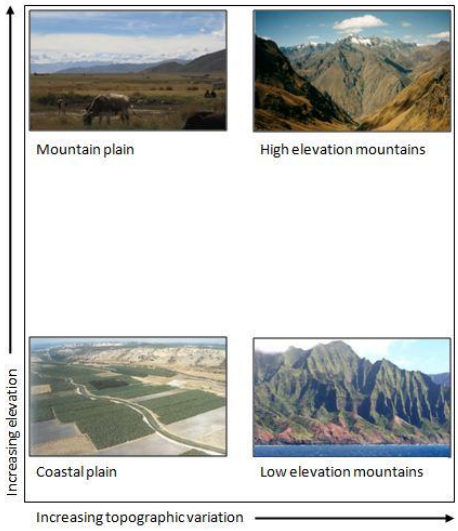

Figure 4.7. Conceptualisation of the artificial DEM created for the sensitivity analysis.

4.2.4.7. Co-variation between model inputs and outputs

For each of the model input maps, and *GDiv's* output maps, 10 000 random sample points were used to generate datasets. From these a cross-correlation matrix was derived in order to assess the internal correlations and possible redundancies within *GDiv*.

4.3. Results

The baseline results of *GDiv* are shown in figures 4.6 – 4.8 for all tropical mountains and the initial test sites (the Colombian Andes, the Albertine Rift and Papua New Guinea). Figures 4.9 – 4.11 show the input maps that went into calculating each of the three components of geodiversity across the tropics. The results across all tropical mountains are scaled across all mountains, whereas the test site results are scaled within the individual tiles hence the results from the test sites are not directly comparable with each other.

Across the tropics, the region with the lowest per-pixel geodiversity score is the tropical Andes, whilst the highest scoring pixel is the Vietnam / Laos border. In general, South East Asia and Africa show a stronger latitudinal gradient in their geodiversity scores than South America. Lower scores on both continents are located towards the equator, reflecting the lower seasonality. In the tropical Americas the altitudinal gradient in geodiversity score is far more apparent, reflecting the clear difference in topography between South and Central America. The lower elevations in Central America have higher scores than the higher elevations of the Andes. Whilst the Tropical Andes has the lowest scoring pixels, and a large extent of low geodiversity, there are also slopes of a smaller extent on the mid-elevations with high geodiversity scores.

Whilst the latitudinal gradient is clear in Africa and South East Asia for all three components, the high altitudes of the Andes blur this in the Americas and a strong altitudinal gradient emerges. This is particularly evident in the *RES* and *Sc* scores, with the Andes being the lowest scoring region for both these components. *Tv* scores follow a more consistent latitudinal gradient across all three continents, although the Americas do not score as highly as either Africa or South East Asia.

The results for the Colombian Andes test site show a clear altitudinal gradient, with the peaks having far lower geodiversity than mid-elevations. There is a clear hotspot in geodiversity on the eastern flanks of the Cordillera Oriental; when *GDiv* was run for the lowlands as well as the mountains, it was found that, whilst the high levels of geodiversity extended into the eastern grasslands of Colombia, there was a distinct mid-elevational peak in geodiversity. When the individual components of geodiversity are mapped, it becomes apparent that the mid-elevational hotspot is due to high levels of all three components, whereas the high level of geodiversity in the lowland grasslands is due to the increased seasonal variation only (figure 4.10).

The general latitudinal gradient in geodiversity is evident in the African test site; the tile straddles the equator, with approximately one quarter in the northern hemisphere. The altitudinal gradient is not as distinct in this tile. Towards the south of the tile, the latitudinal gradient becomes less apparent with eastern regions scoring more highly. In terms of the component scores, the high scores towards the south of the tile are more apparent in the *RES* and *Sc* scores, whilst the *Tv* score follows a clear latitudinal gradient. Both *RES* and *Sc* have high scores around the mid elevations of the mountains surrounding Lake Tanganyika.

The latitudinal gradient is also apparent in the Papua New Guinea test site. It is more difficult to distinguish the altitudinal gradient, as the mountains are oriented east - west, however mid-elevational peaks similar to that found in Colombia seem to occur on the north and south flanks of the central mountain range on the island. A further distinctive pattern in geodiversity on Papua New Guinea are the high scoring southern mountains. When the components are considered, these high overall scores in the southern mountains are due to increased *RES* and *Sc*, combined with increasing *Tv* scores from north to south. The highest scoring *RES* and *Sc* regions, the southern flanks of the central mountains, do not score as highly for overall geodiversity as the *Tv* is low.

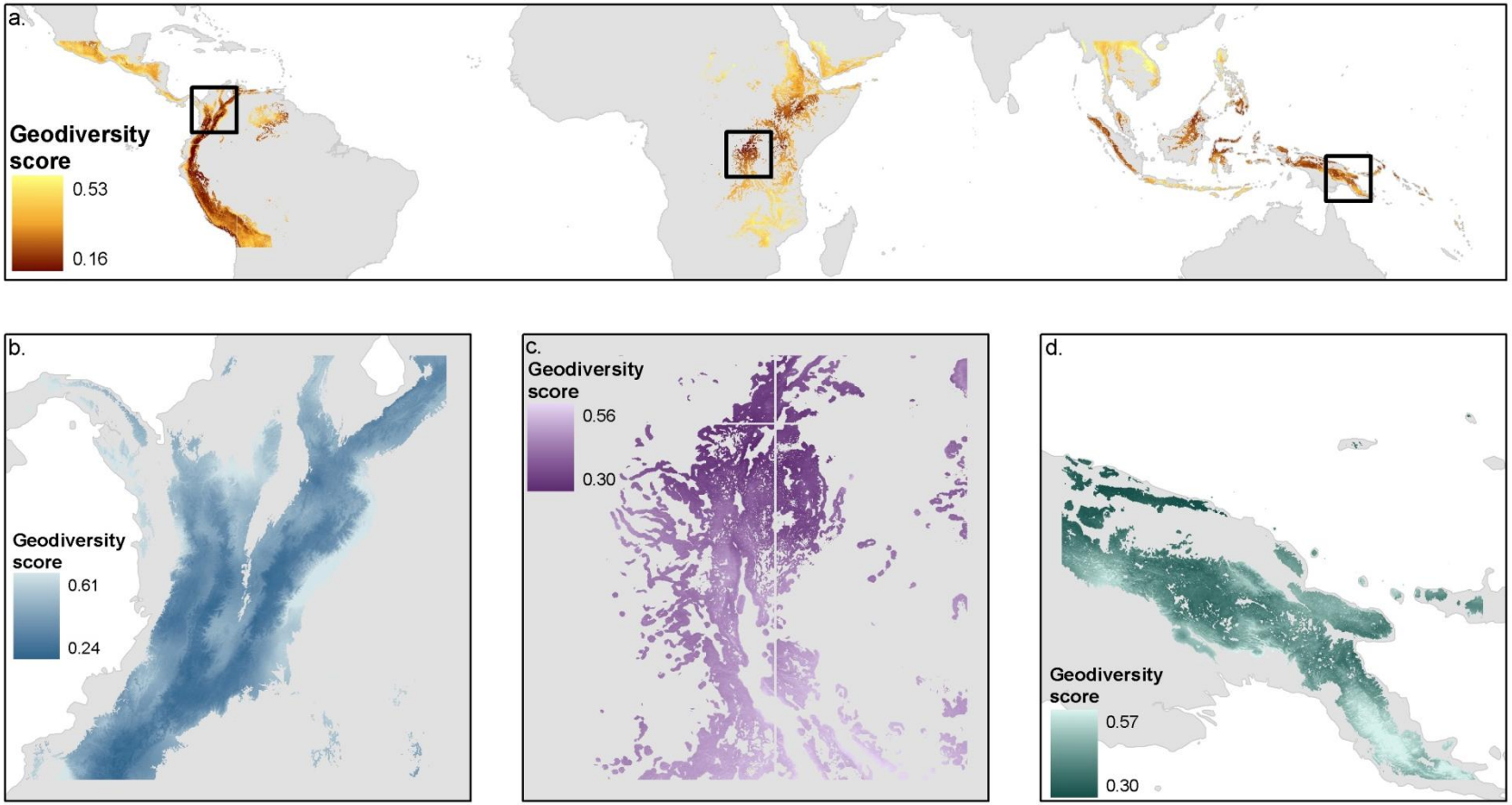

Figure 4.8. Raw geodiversity scores for all tropical mountains, and the three study sites used for further testing and analysis. Part a shows the results of a simulation across the entire tropical mountain study region; the scaling is pan-tropical. Each of the study site maps (parts b to d) present the result of a *GDiv* simulation with a single 10 x 10 degree study area, and so the scaling is different for each site (i.e. it is relative within the site, and not comparible between sites or with the pan-tropical simulation).

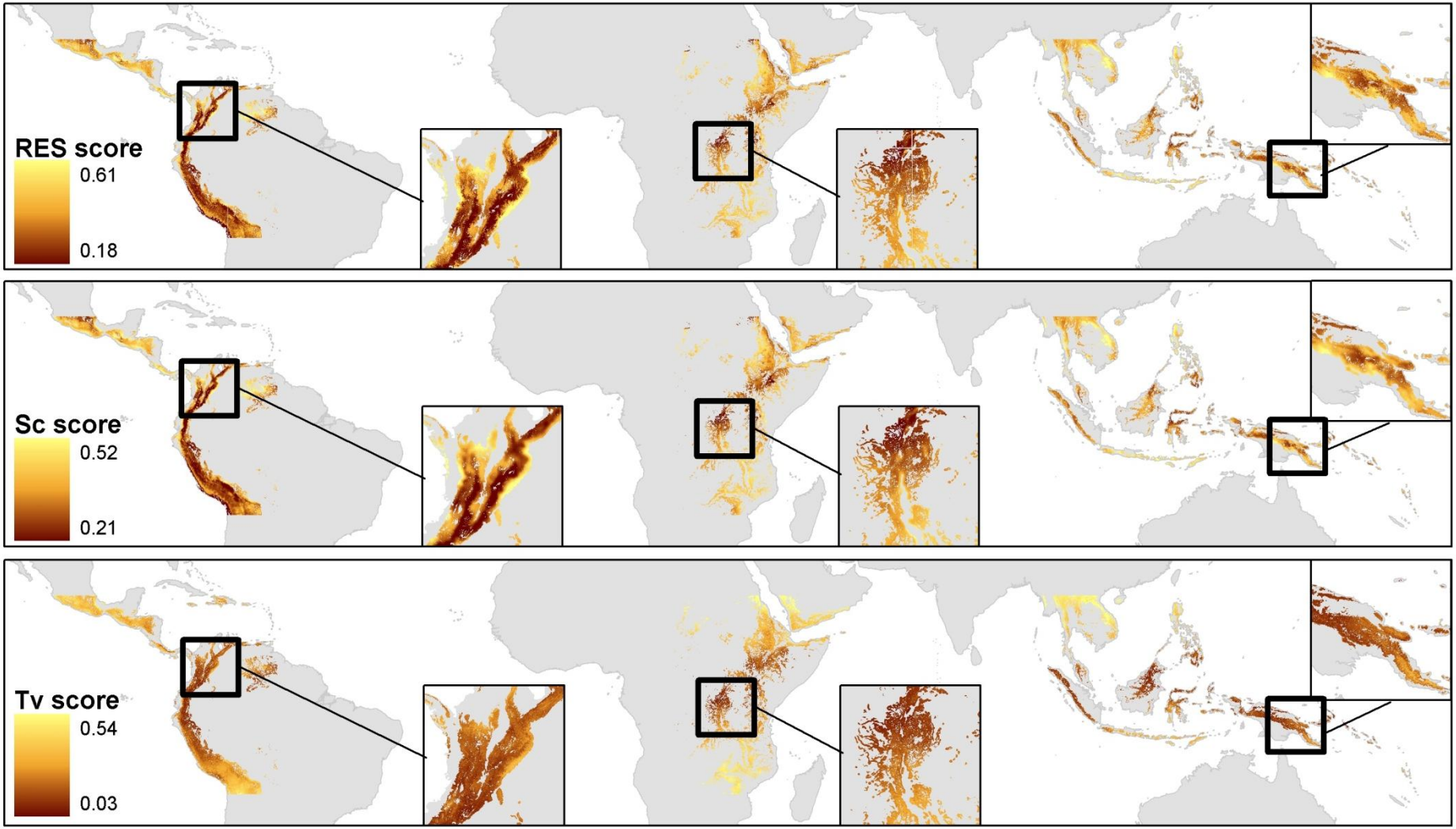

Figure 4.9. The three components of geodiversity across the world's tropical mountains and within the study regions.

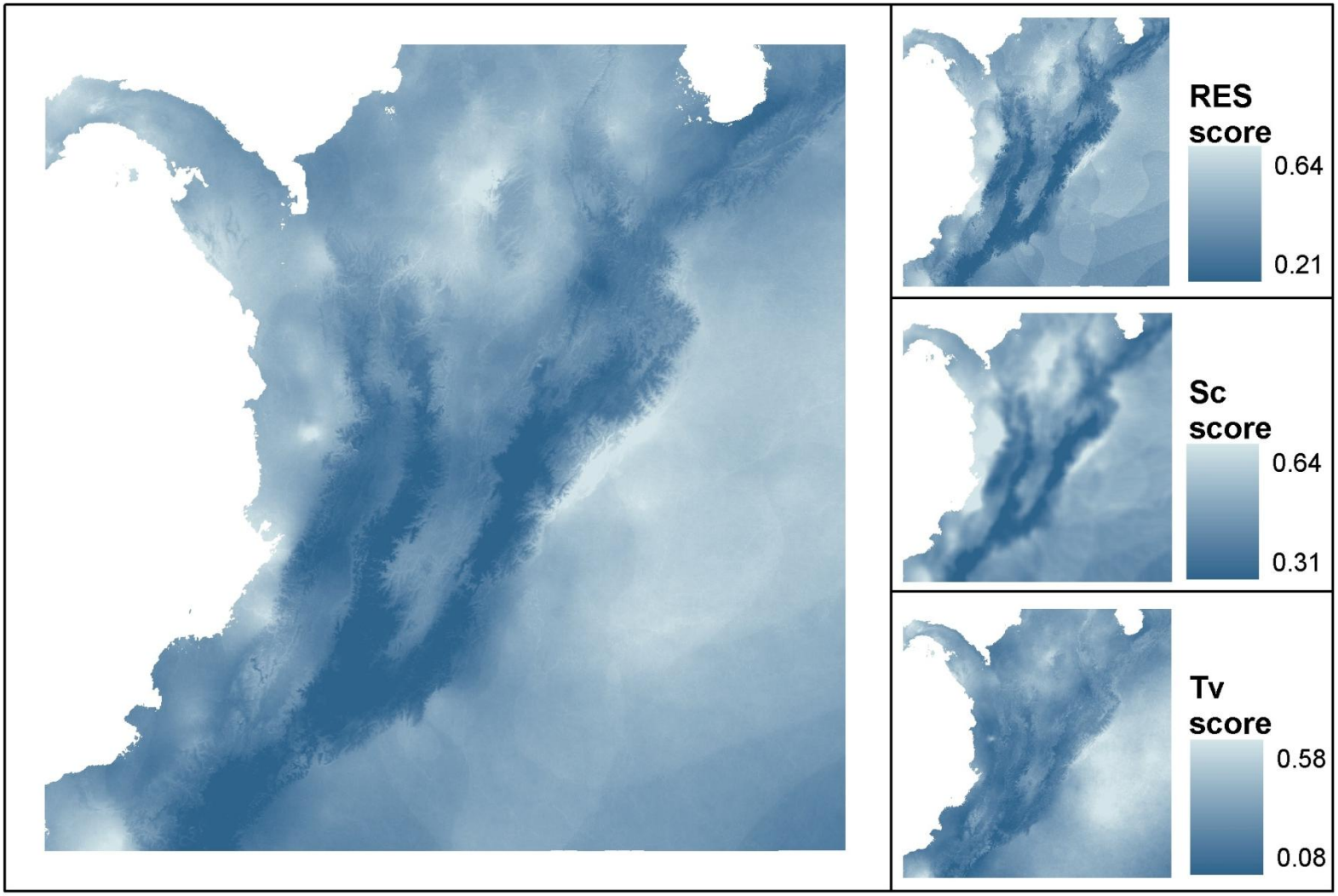

Figure 4.10. Results of *GDiv* across all altitudes in the Colombian test tile.

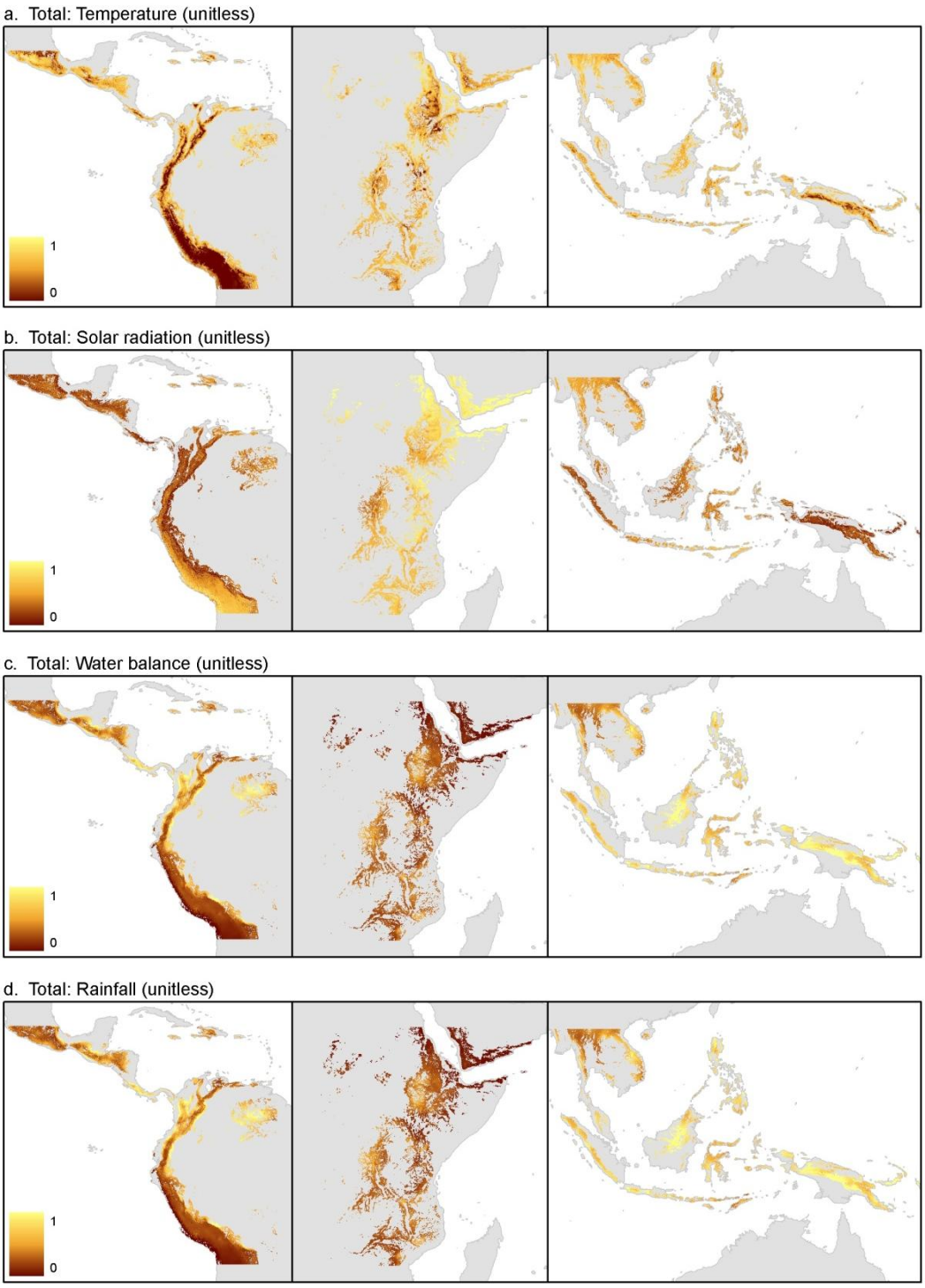

Figure 4.11 part 1: Pan tropical annual totals (scaled 0 - 1) for variables from which *RES* was calculated

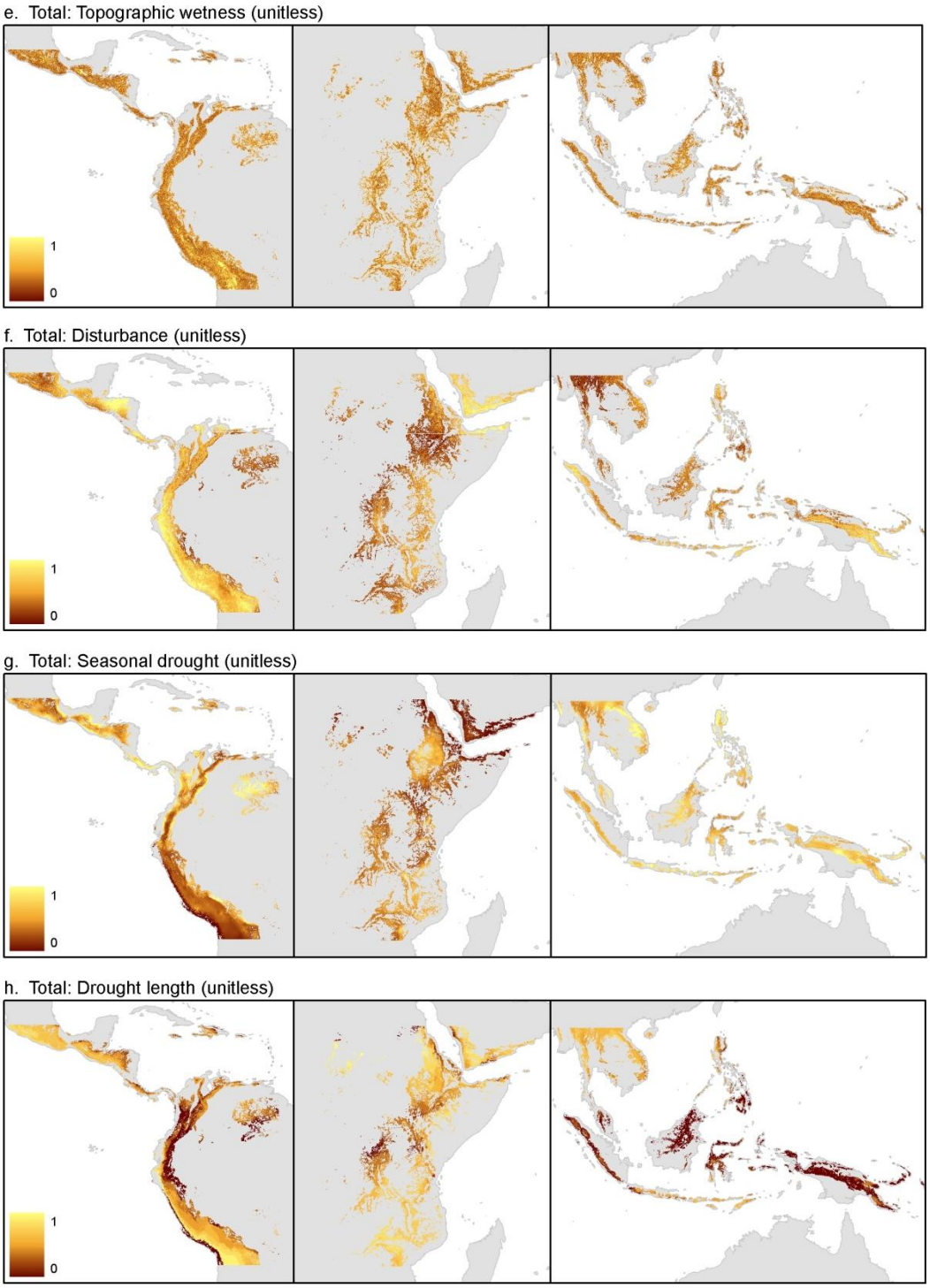

Figure 4.11 part 2: Pan tropical annual totals (scaled 0 - 1) for variables from which *RES* was calculated

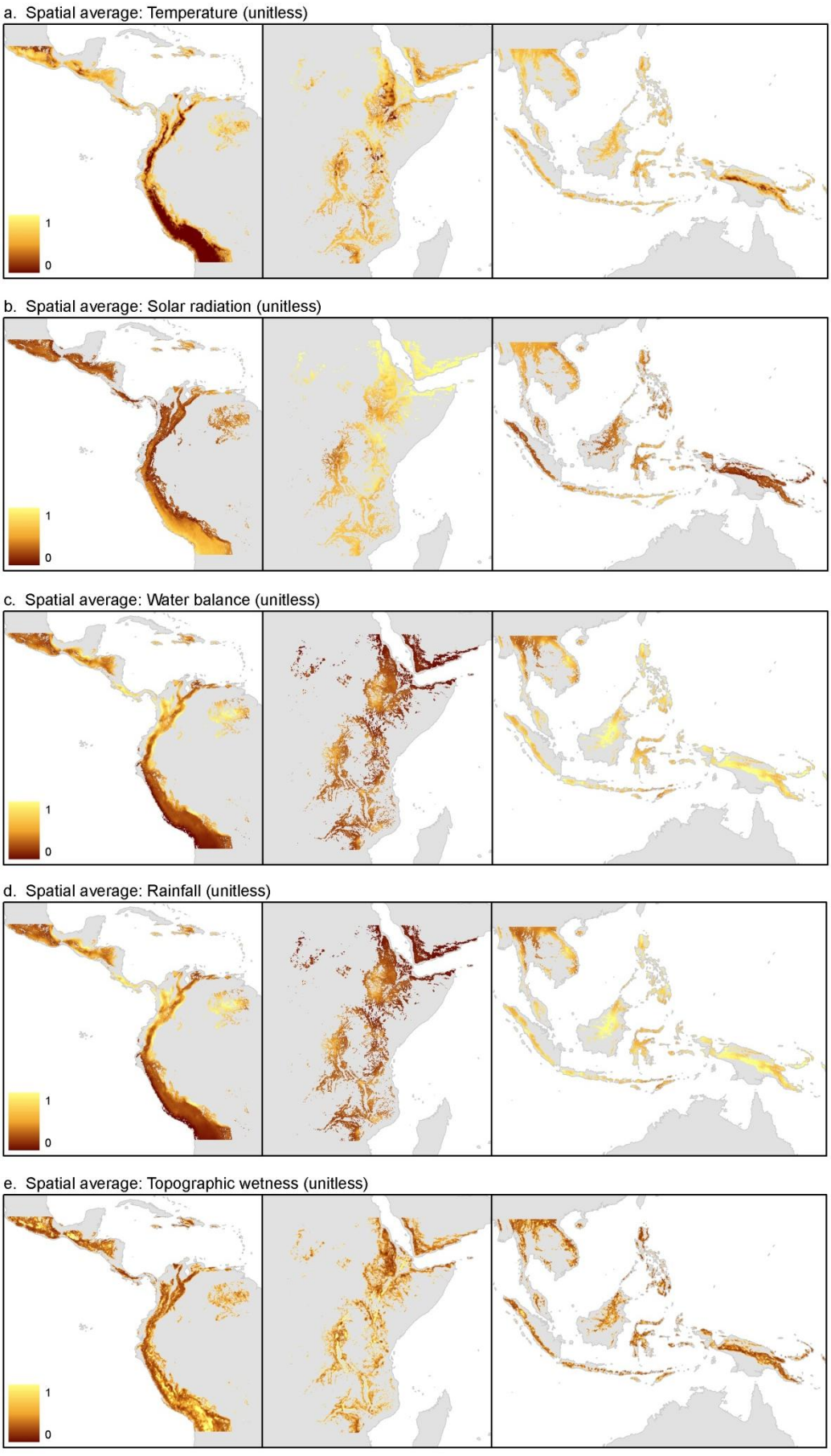

Figure 4.12 part 1. Spatial average (scaled 0 - 1) for variables from which *Sc* was calculated.

f. Spatial average: Disturbance (unitless)

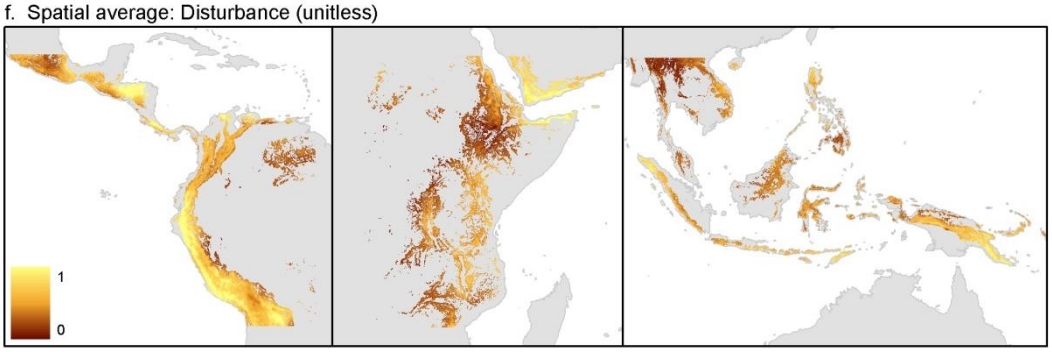

g. Spatial average: Seasonal drought (unitless)

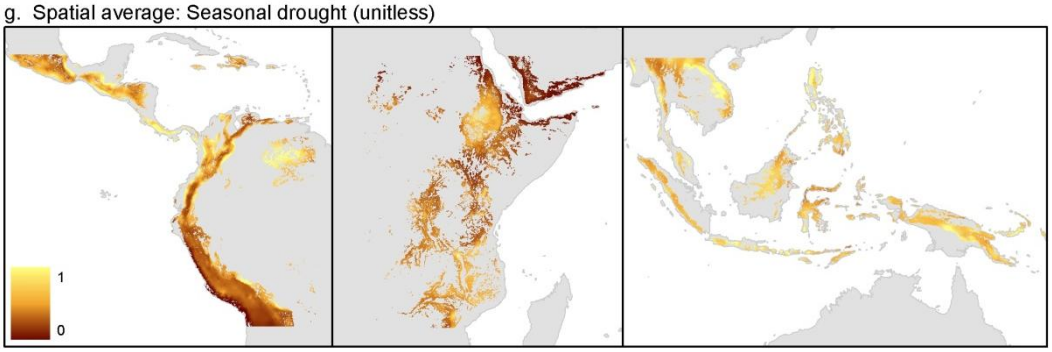

h. Spatial average: Drought length (unitless)

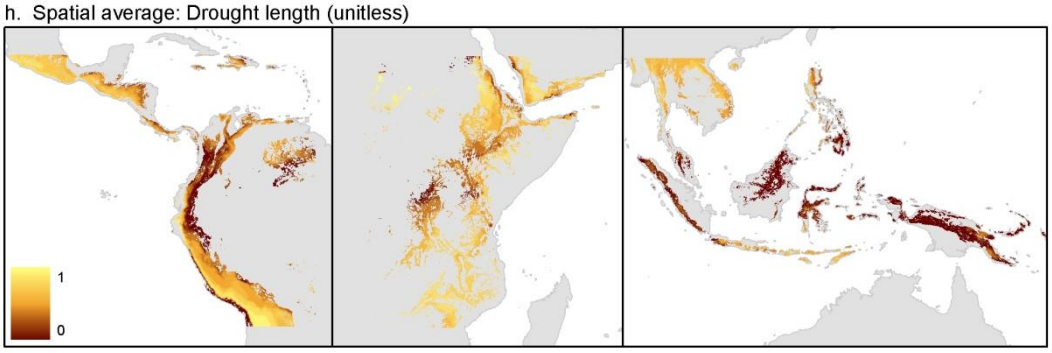

i. Spatial average: Rivers (unitless)

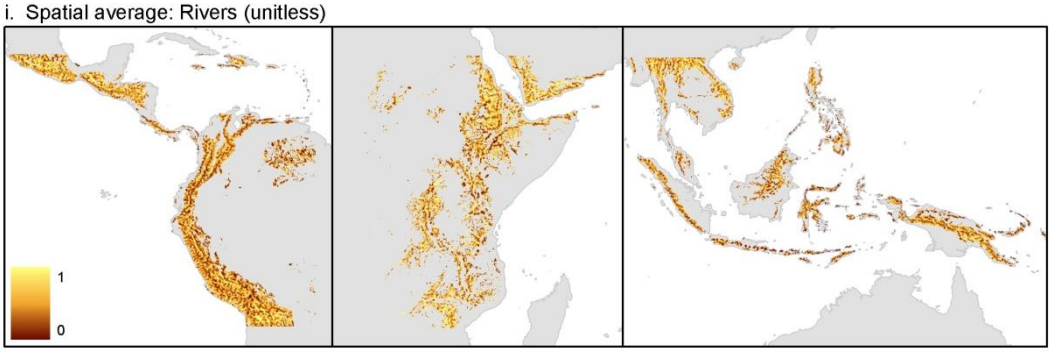

Figure 4.12 part 2. Spatial average (scaled 0 - 1) for variables from which *Sc* was calculated.

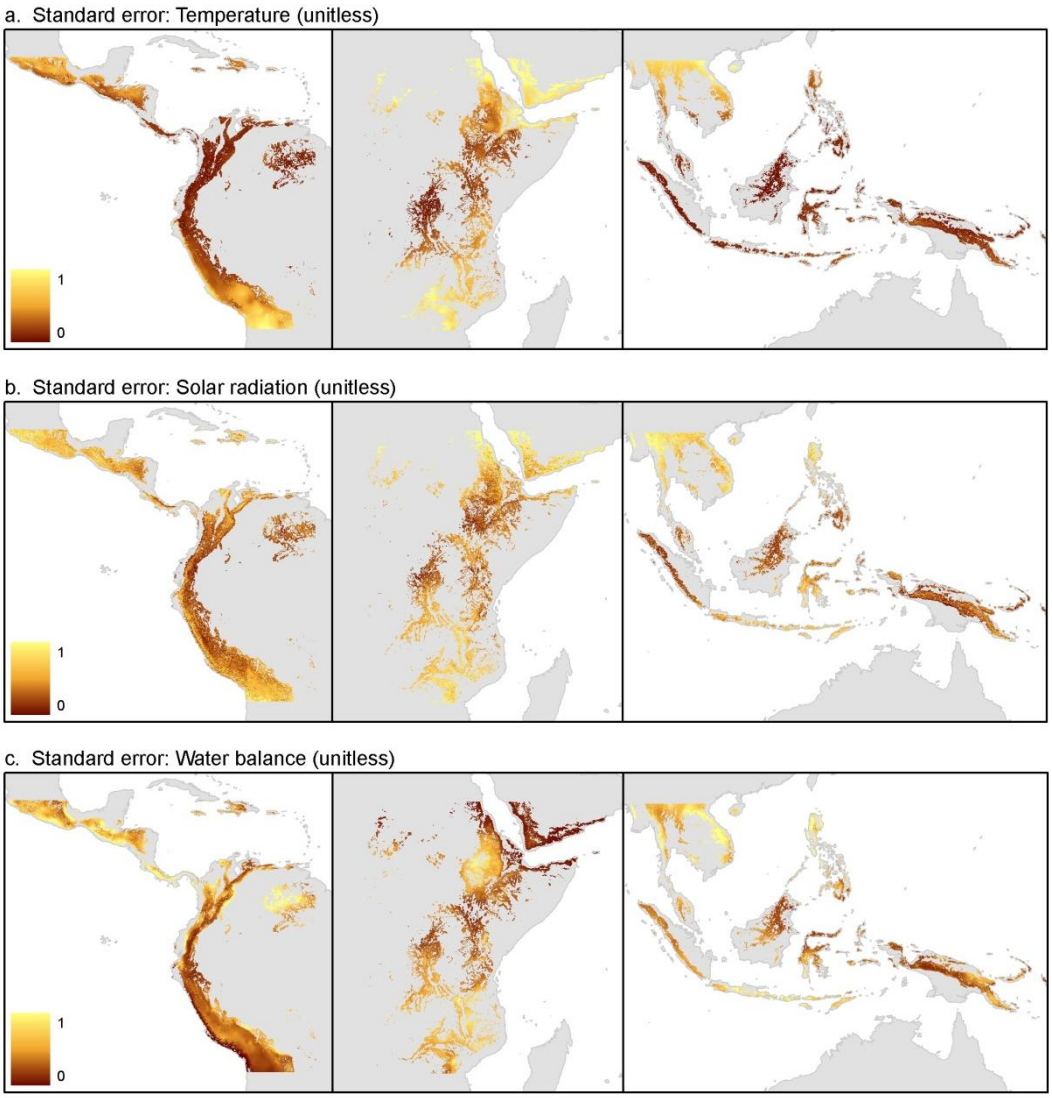

Figure 4.13. Pan tropical standard error (scaled 0 - 1) for all variables from which *Tv* was calculated.

4.3.1. One-at-a-time variation of model inputs

Figures 4.14 – 4.19 show the mean and distributions (as box-plots) for *GDiv* output maps when the model inputs were varied using the one-at-a-time method. Generally, for the DEM, rainfall, temperature and wind speed the model seemed to be most sensitive to a 100% reduction in the input value, with the response decreasing as the level of reduction to the input variable decreased. With regards to cloud cover and solar radiation, there was no discernible response.

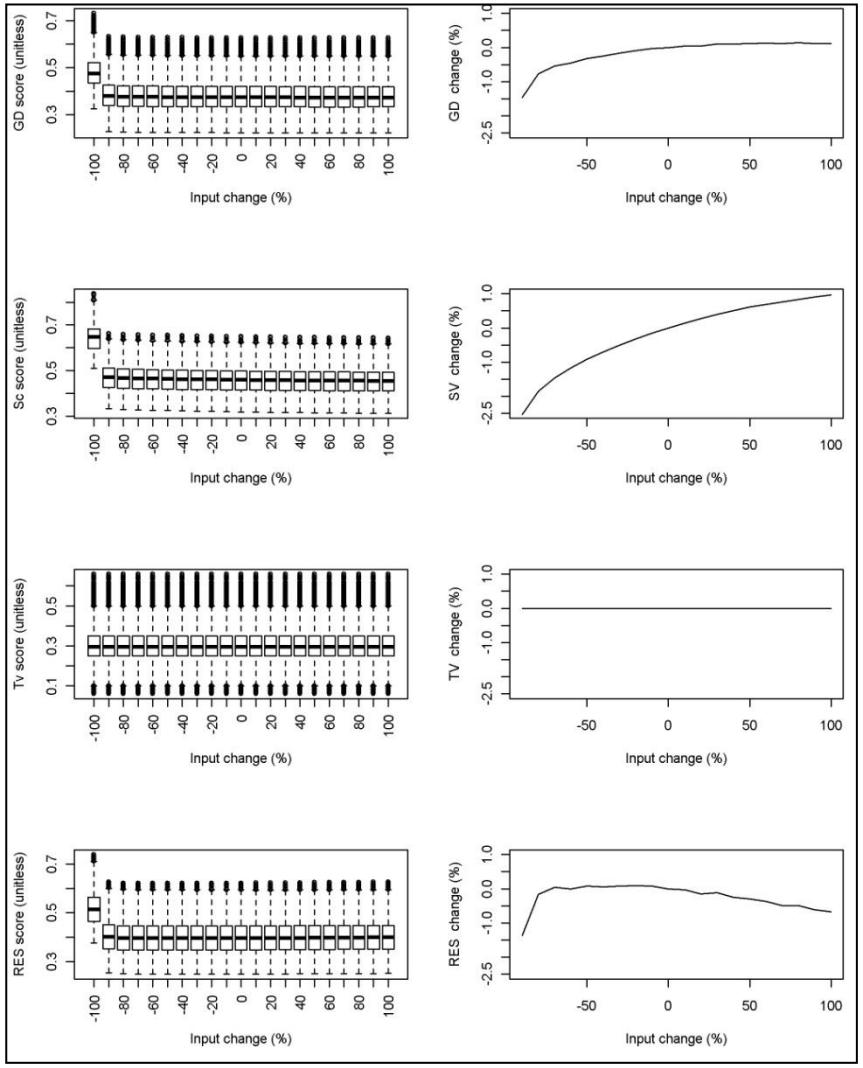

Figure 4.14. Response of *GDiv* to systematic variation of the DEM elevation

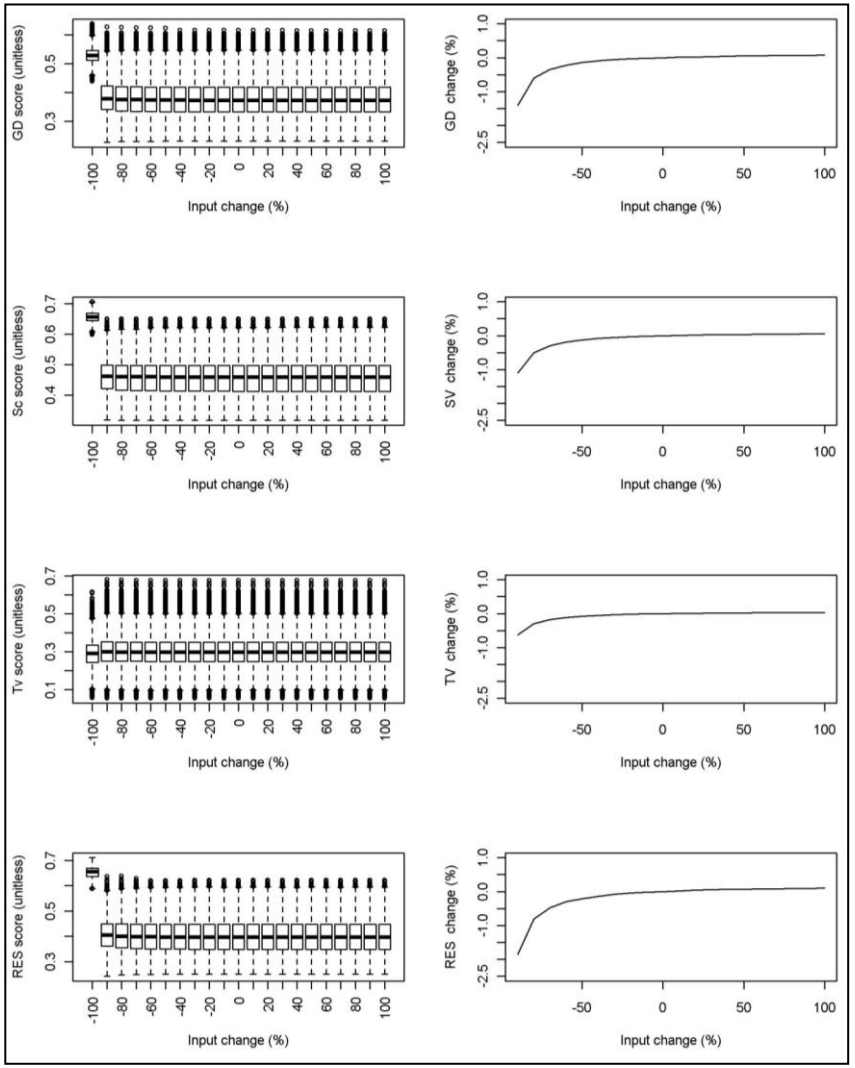

Figure 4.15. Response of *GDiv* to systematic variation of rainfall

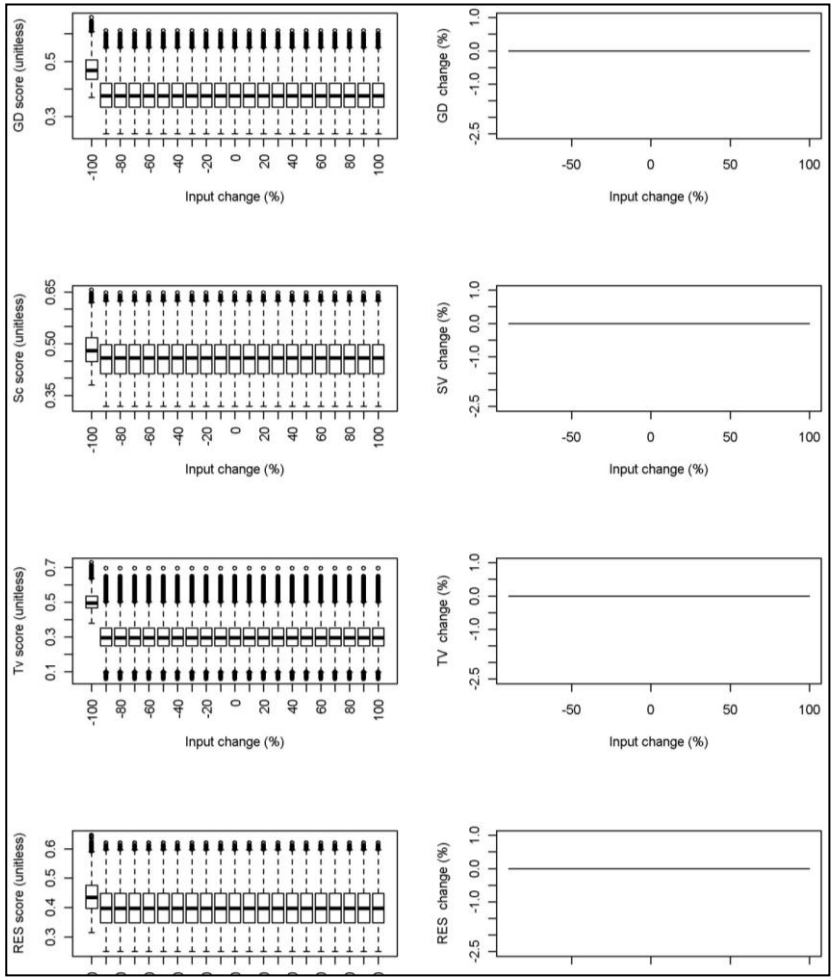

Figure 4.16. Response of *GDiv* to systematic variation of temperature.

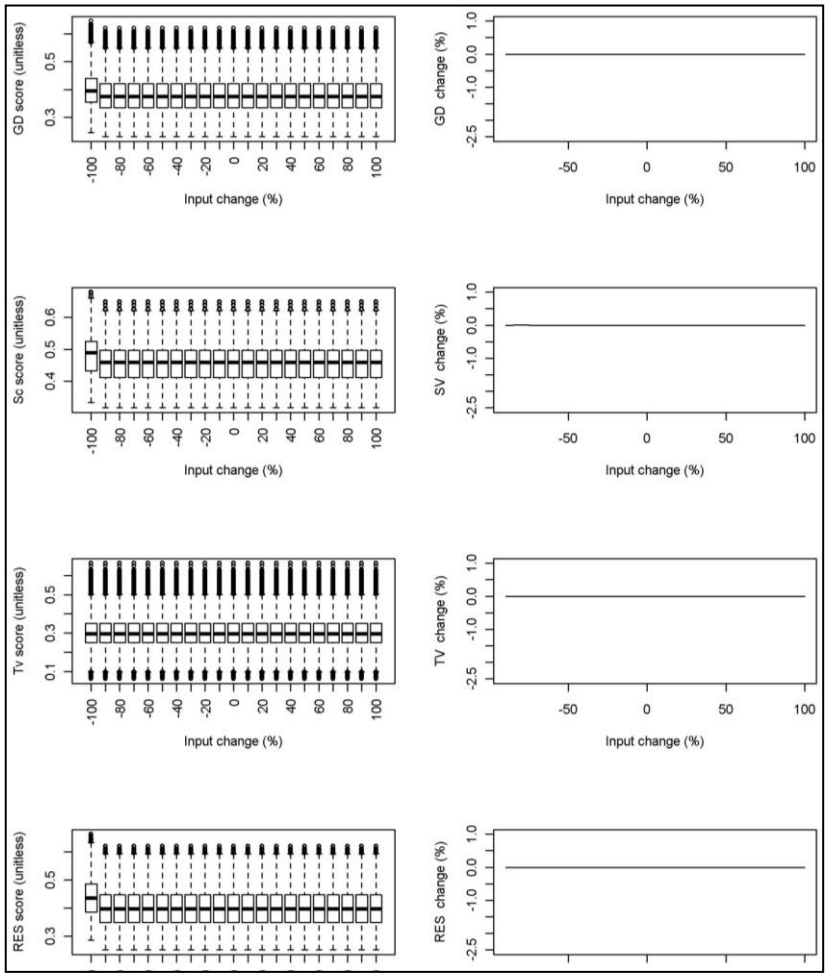

Figure 4.17. Response of *GDiv* to systematic variation of wind speed.

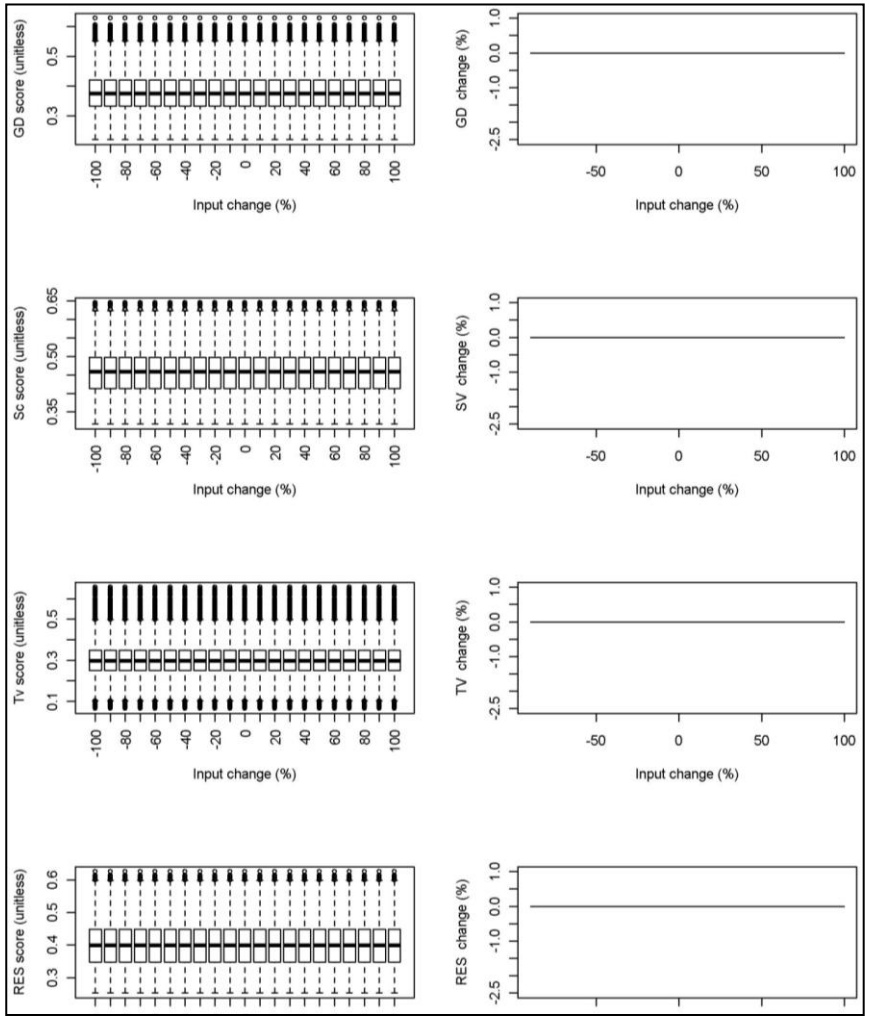

Figure 4.18. Response of *GDiv* to systematic variation of solar radiation.

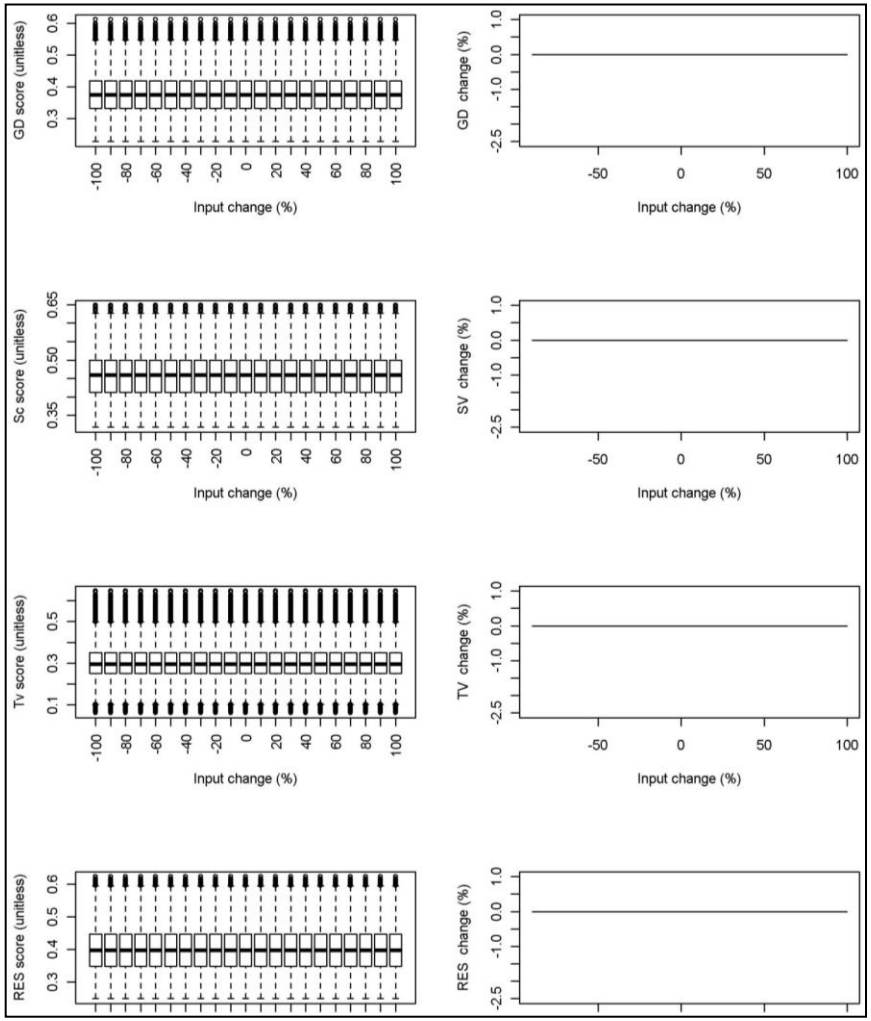

Figure 4.19. Response of *GDiv* to systematic variation of cloud cover.

4.3.2. Sensitivity to kernel size

Figure 4.20 shows the response of *GDiv* to variation of the kernel size for calculating *Sc*. As expected, *RES* and *Tv* showed no response (since a kernel is not used in their calculation . The only response was seen in the *Sc* component, with a slightly diluted response seen in the overall geodiversity score. As the mean geodiversity score reached a plateau in its response at a window size of 30 000 m, it was decided to use this as the standard kernel size for future runs in order to generate stable results in the quickest model run time.

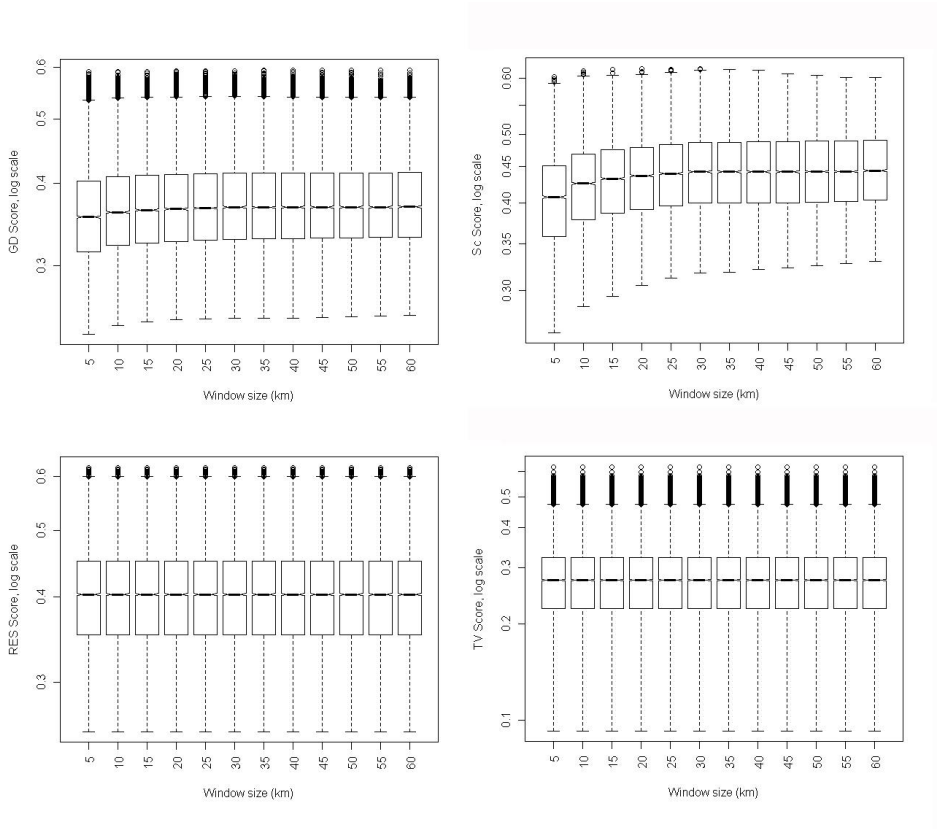

Figure 4.20. Response of the *GDiv* outputs to systematic variation of the *Sc* kernel size.

4.3.3. Sensitivity to model components

Figure 4.21 shows the response in terms of the geodiversity score when the *Sc*, *Tv* and *RES* are separately removed from the calculation. It appears that the *Tv* has the weakest impact on the overall geodiversity score as, when this component is not included in the final geodiversity score, the mean score increases. With regards to the impact of removing individual model inputs on the overall geodiversity score, it seems that temperature and solar radiation have the greatest effect; when they are removed geodiversity decreases suggesting that, when included, they are increasing the geodiversity score.

Figure 4.22 shows the impact of removing model inputs on the three components of geodiversity, as well as overall geodiversity. Overall resource availability is most strongly

suppressed by the disturbance input, and solar radiation is responsible for the greatest increase. The level of *Sc* is most strongly suppressed by the *RIV* input, with solar radiation being responsible for the largest increase. Unsurprisingly, *Tv* responds most strongly to temperature and solar radiation, and shows no response to non-temporal inputs. *Tv* is increased by increased temperature and decreased by a rise in solar radiation.

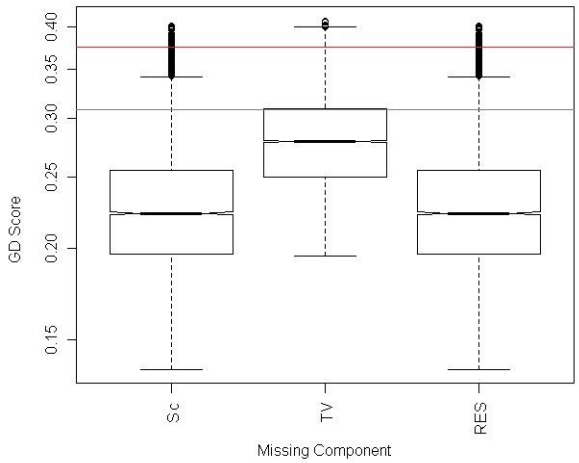

Figure 4.21. Response of *GDiv* to systematic removal of components. The red line represents the baseline mean geodiversity score, whilst the grey line shows 1 standard deviation.

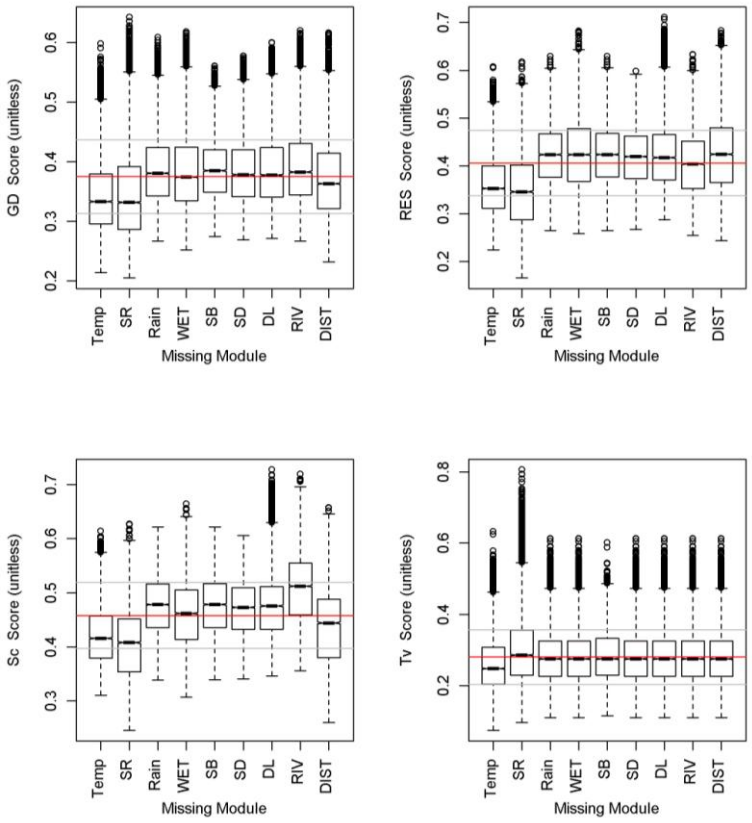

Figure 4.22. Response of *GDiv* to systematic removal of input modules. The red and grey lines shows baseline mean scores ± 1 standard deviation.

4.3.4. Sensitivity to initial data resolution

Figure 4.23 shows the absolute differences between the 90 m DEM And the 1 km DEM. The differences in the lowland regions are generally closer to 0 than those in the mountainous regions. In the mountainous regions the differences vary from -380 m to +221 m between the two DEMs, however there is no clear spatial patterning to the differences; there does not appear to be any consistent biases of over / under estimation by the 1 km DEM when compared to the 90 m DEM. The mean difference between the two DEMs is 0.488 m, with a standard deviation of 45 m.

With regards to the impact on the absolute values of Geodiversity, the 90 m DEM generally results in a higher level of overall *GD* (figure 4.24), with this effect being more pronounced in the low - mid slopes. Figure 4.24 shows difference maps (calculated as 1 km results - 90 m results), alongside changes in frequency distribution for each of the *GDiv* outputs. The lower difference between the 90 m and 1 km results is again apparent in the mountainous regions. The distributions show that the 90 m DEM tends to increase the mean score for all *GDiv* outputs, as well as increasing the range of scores; a pattern discussed further in section 4.4.4.

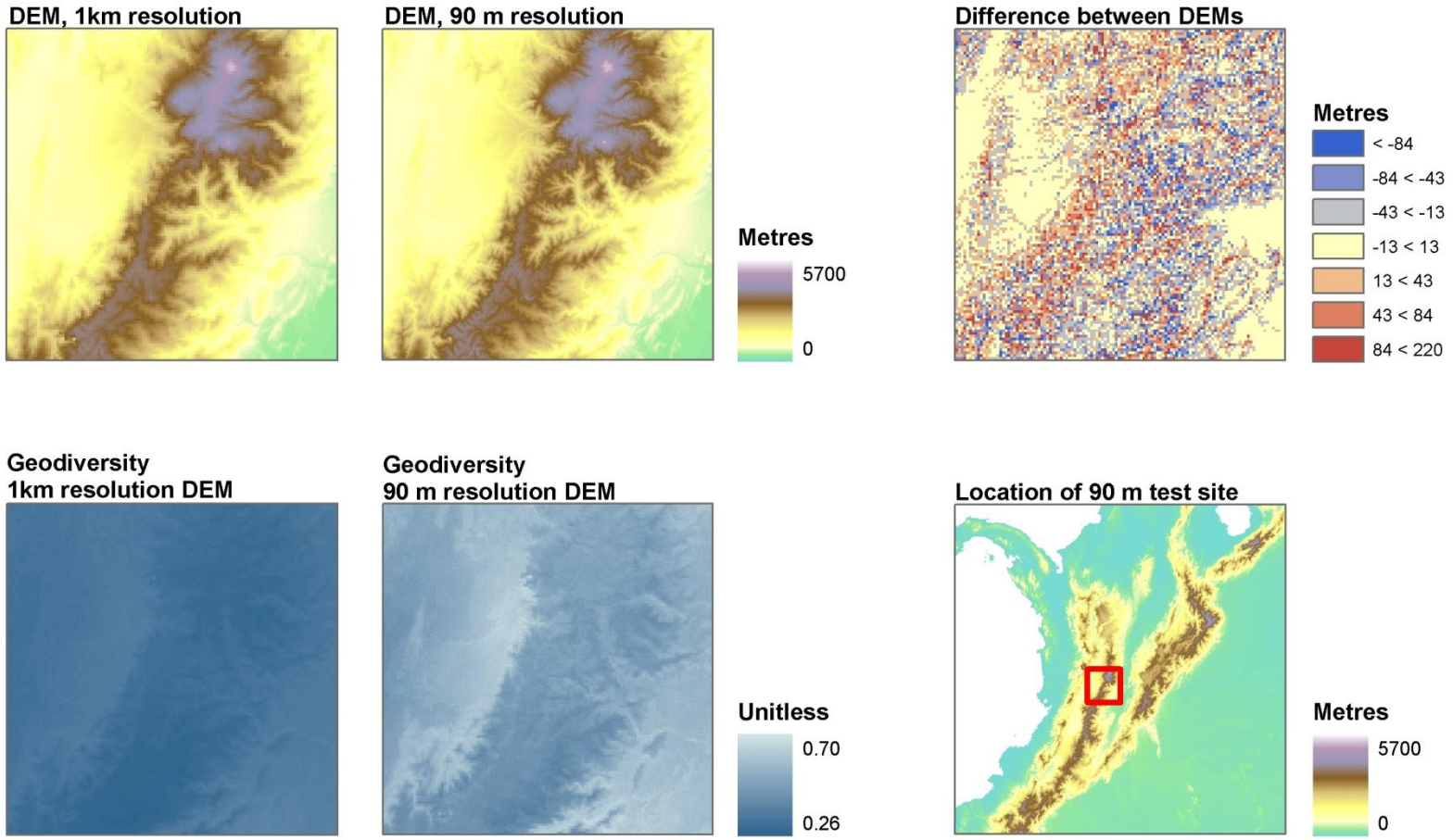

Figure 4.23. Differences between the 1 km DEM and 90 m DEM, and geodiversity as calculated using each DEM. The location of the 90 m DEM is also shown.

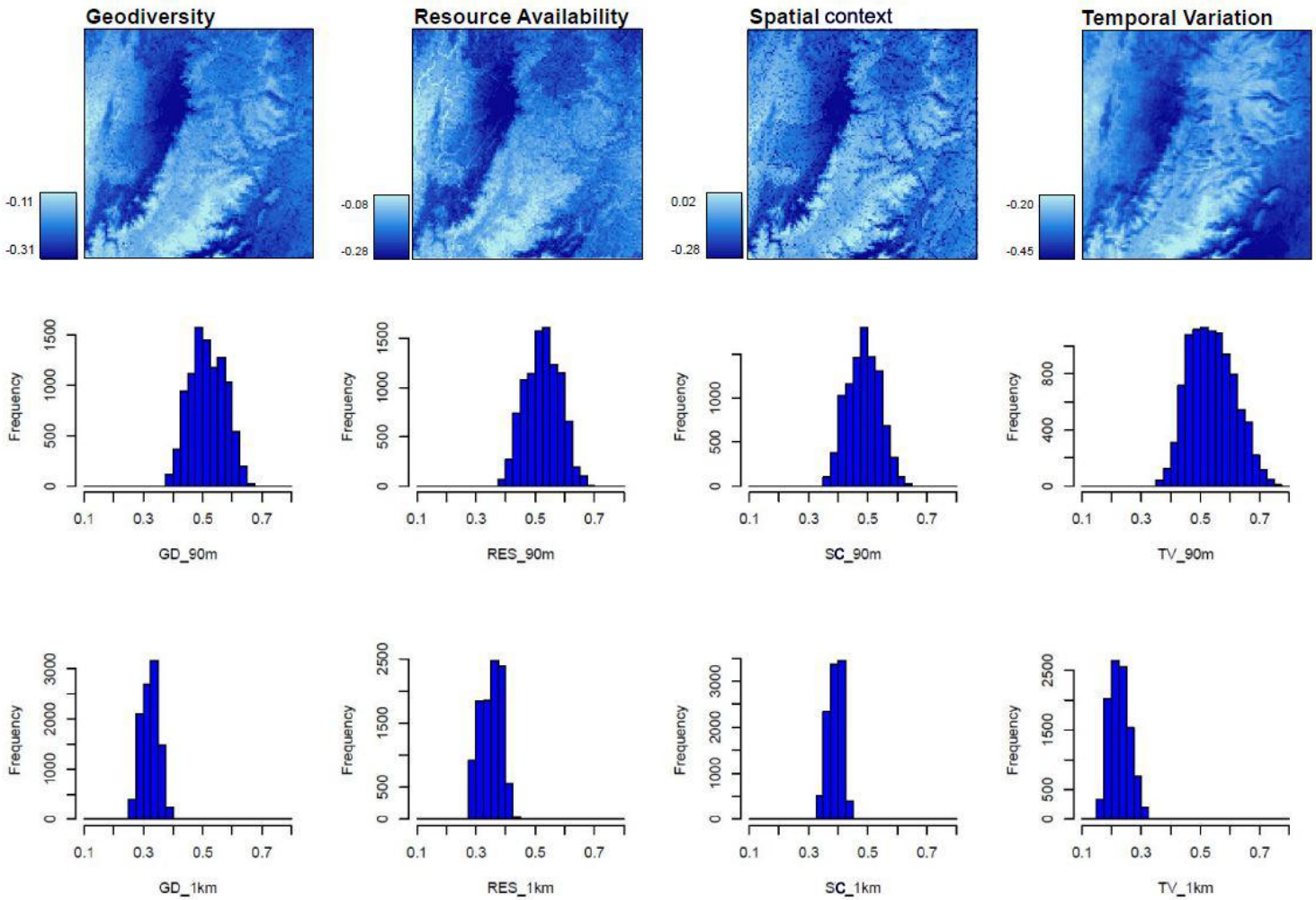

Figure 4.24. Differences in *GDiv* outputs when calculated on a 1 km DEM and a 90 m DEM.

4.3.5. Sensitivity to initial datasets

The overall geodiversity score seems to reduce when there is a combination of the TRMM rainfall dataset, and the MODIS cloud dataset (figure 4.25). The same is true for the *RES* and *Tv* scores. *Sc* does not show this response, in fact it does not seem sensitive (in terms of mean score) to the initial dataset. However the range of *Sc* scores is much larger when the WorldClim rainfall dataset and the MODIS cloud dataset are used. With regards to *Tv*, there is an increased range when the UEA temperature and the HIRS cloud datasets are used. The implications and potential reasons for these patterns is discussed in section 4.4.5.

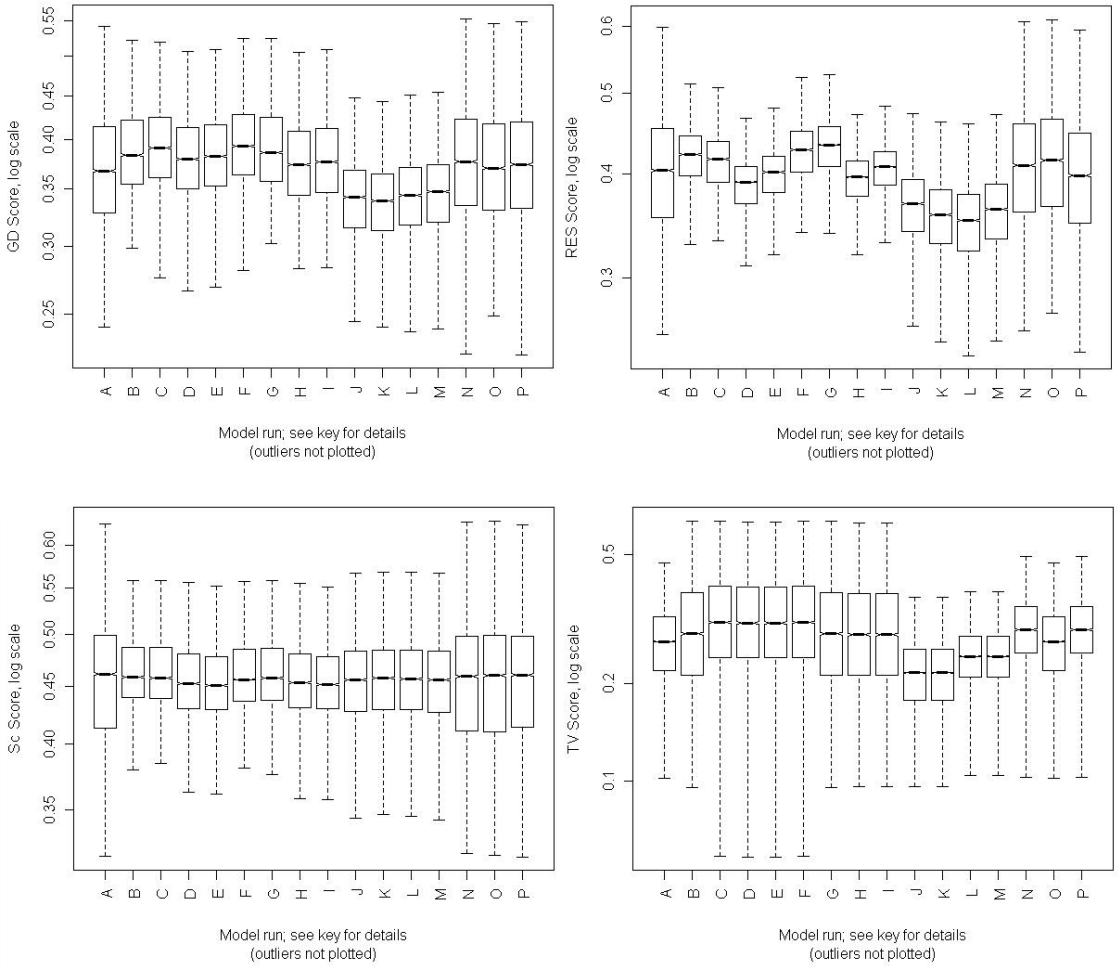

Figure 4.25. Response of *GDiv* to alternative input datasets. Key to datasets used for each simulation shown overleaf (Table 4.2)

Table 4.2. Key to figure 4.23, showing which datasets were used in each simulation.

Label	DEM	Rain	Temp	Cloud
A	SRTM	WCRain	WCTemp	MODIS
B	SRTM	WCRain	WCTemp	hCloud
C	SRTM	WCRain	UEATemp	hCloud
D	SRTM	TRMM	UEATemp	hCloud
E	Hydro1k	TRMM	UEATemp	hCloud
F	Hydro1k	WCRain	UEATemp	hCloud
G	Hydro1k	WCRain	WCTemp	hCloud
H	SRTM	TRMM	WCTemp	hCloud
I	Hydro1k	TRMM	WCTemp	hCloud
J	Hydro1k	TRMM	WCTemp	MODIS
K	SRTM	TRMM	WCTemp	MODIS
L	SRTM	TRMM	UEATemp	MODIS
M	Hydro1k	TRMM	UEATemp	MODIS
N	Hydro1k	WCRain	UEATemp	MODIS
O	Hydro1k	WCRain	WCTemp	MODIS
P	SRTM	WCRain	UEATemp	MODIS

4.3.6. Controlled variation of topographic variation

Figure 4.26 shows histograms for slopes in the Colombian test region, as well as the histograms generated from artificial DEMs that had been smoothed using various kernel sizes. The artificial DEM that had been smoothed using a kernel size of 7.5 times the cell size was selected as having a slope distribution that most closely matched that of the empirical (Hydro1K) distribution. Figure 4.27 shows this DEM, alongside maps of *RES* and *Sc* with the topographic dependent input variables calculated using the ArtDEM. It appears that *RES* and *Sc* both increase with topographic variation (left to right along the figure), and decreases with elevation (bottom to top), although there is a combined effect: as topographic variation increases, *RES* and *Sc* levels are increased most significantly at lower altitudes. Topographic wetness and disturbance both increase with topographic variation, whilst slope decreases with topographic variation. Temperature, as outlined in section 4.3.7, decreases with elevation.

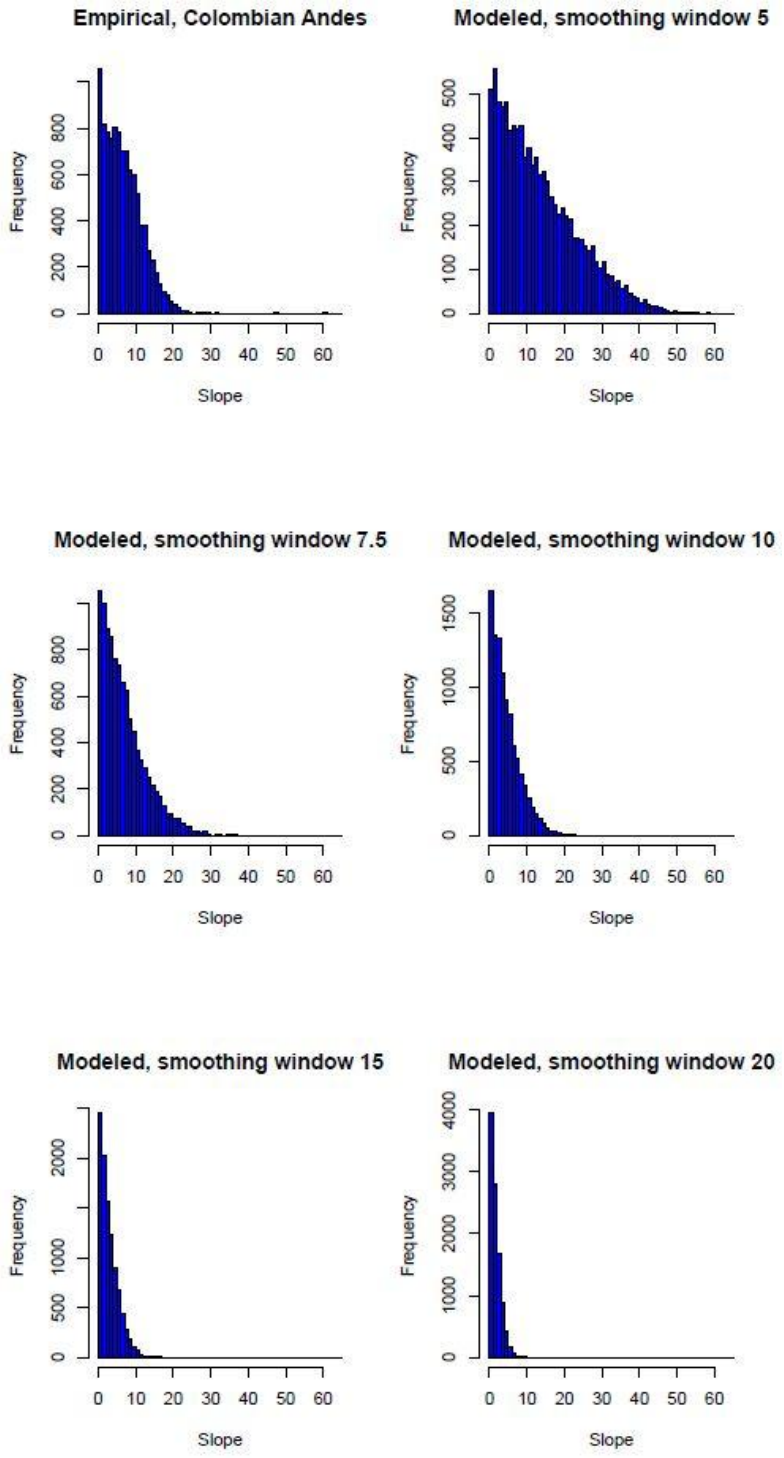

Figure 4.26. Empirical slope distribution for the Colombian Andes test-site, and for artificial DEMs smoothed using a kernel size of varying sizes. The window sizes are given in terms of cell length and slope is expressed in degrees.

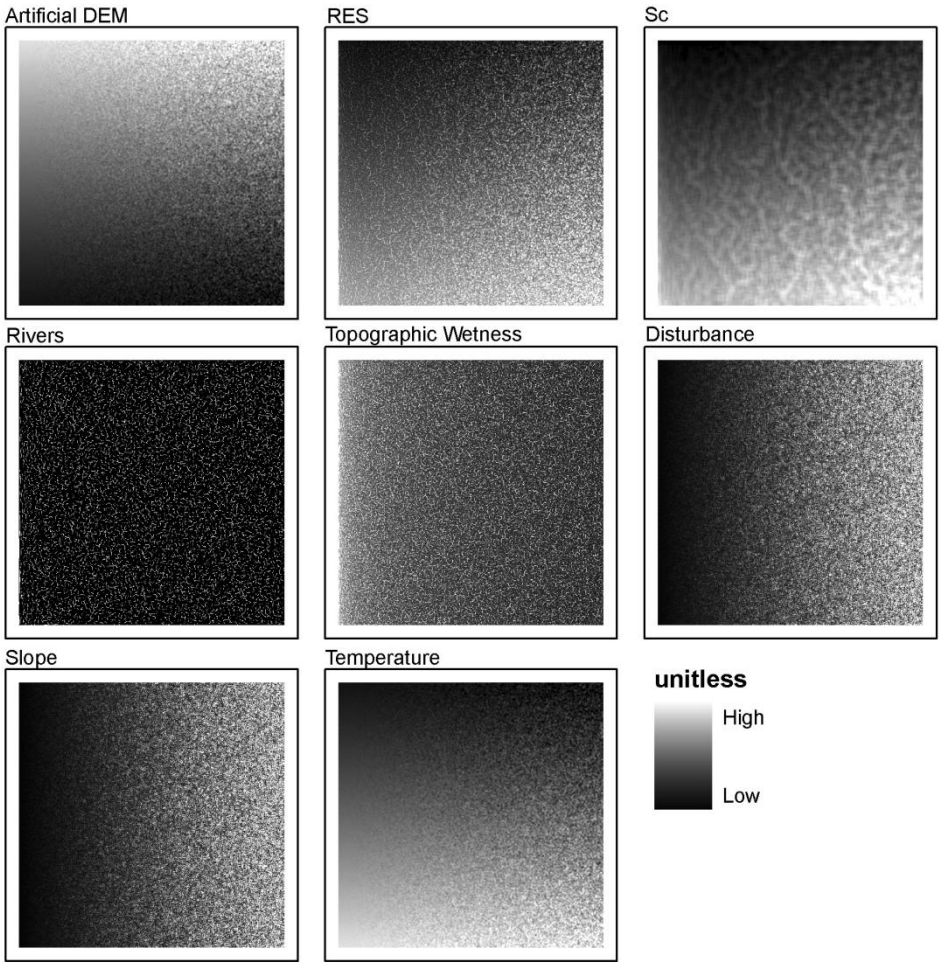

Figure 4.27. The artificial DEM (top left) used to investigate the impact of topographic variables on geodiversity inputs and components. The resulting maps of *RES* and *Sc*, and inputs derived from the DEM, are shown; areas at a low elevation and that are topographically diverse have the greatest potential *RES* and *Sc*.

4.3.7. Co-variation between model inputs and outputs

Figure 4.28 shows the cross-correlation matrix generated from the *GDiv* outputs and raw inputs. Among the model inputs (indicated with a blue box on figure 4.28), the strongest correlation is found between temperature and elevation (r=0.99). Aspect and solar radiation have an r value of 0.6, however the relationship is clearly non-linear. None of the other model inputs are strongly correlated, with the next highest r value being 0.46 found between elevation and rainfall. Within *GDiv's* outputs (indicated with a red box on figure 4.28), geodiversity is more strongly correlated with *RES* and *Sc* (r= 0.95) than *Tv* (r = 0.89), reflecting the strong correlation between *RES* and *Sc* (r = 0.95); not an unexpected result given that *Sc* is calculated based on the annual means of the same inputs used to calculate *RES*. With regards to correlations between *GDiv*'s inputs and outputs (indicated with green boxes on figure 4.28),

the strongest relationships are found between *Sc* and rainfall and *RES* and rainfall (r = 0.77 and r = 0.79 respectively), explaining why the strongest correlation between geodiversity and any input is found with rainfall (r = 0.68). Note that these results reflect co-variation between the default datasets (table 4.3) and *GDiv* outputs.

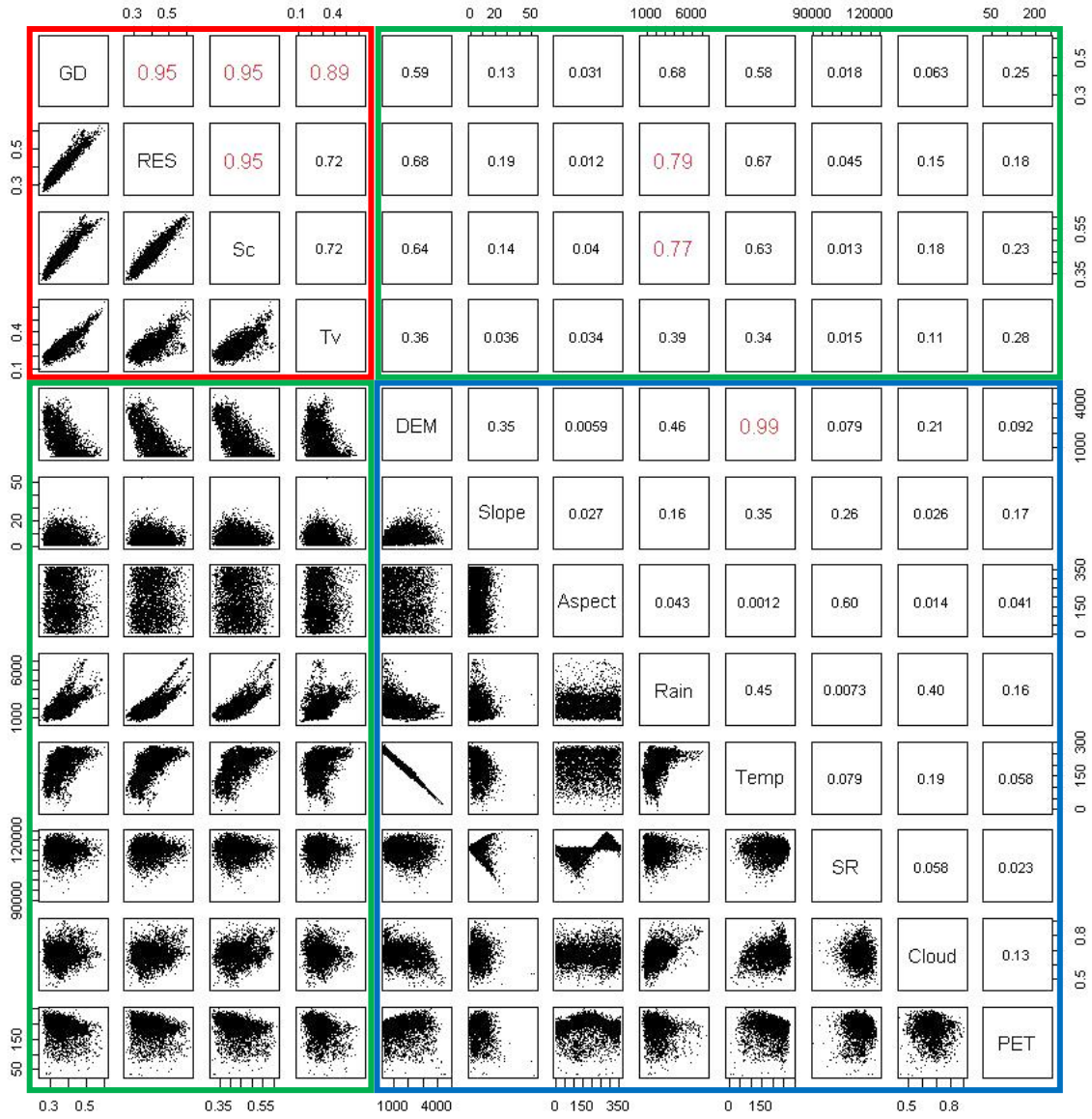

Figure 4.28. Correlation matrix for *GDiv*'s outputs and inputs. Correlations between the model inputs are highlighted with a blue box, between the model outputs with a red box and between the inputs and outputs with green boxes. Strong correlations (r value of over 0.75) are shown in red.

4.4. Discussion

The patterns of geodiversity across the tropics follow the broadscale patterns expected based on theory - lower *Tv* at the equator in conjunction with lower resource availability at higher elevations resulting in a complex pattern of geodiversity. The high elevations of the Andes

confound the more simple pattern found in South East Asia and Africa, with the Andes scoring far lower than other regions and also not exhibiting the strong latitudinal gradient; this suggests there could be a threshold at which altitude becomes more important than latitude in determining the geodiversity of a region (given the reduction in resources at altitude).

When these results are interpreted in terms of the physical environment, the mountains of northern Vietnam / eastern Laos emerge as the hottest, wettest and most spatially complex region in the world's tropical mountains, whilst the Andes appear to be the coldest, least spatially structured region (at least at the scale of this analysis). Whilst this lack of spatial structure in the Andes may seem counter intuitive, given the high topographic variation of the region, it is important to remember that the *Sc* component measures spatial trends in overall resource availability. If a region has a low level of total resource availability, the spatial trends in those resources will also be low. Both these regions are prioritised in major prioritisation schemes such as biodiversity hotspots (Myers *et al.*, 2000).

GDiv simulations are scaled by the highest scoring pixel in the study region. In the case of the whole tropics it may be more appropriate to scale results by continent as, under the current settings, one high scoring pixel in Vietnam impacts the final scores across the whole tropics. On the other hand, scaling to the 90th percentile across the whole tropics doesn't reveal any major changes in the patterns of modelled geodiversity. Furthermore, given the model simulations for the remainder of the thesis focus within individual 10 degree tiles the impact of scaling across the whole tropics will not be relevant.

GDiv, as it has been developed thus far, does not take into account human impact; the results presented here a measure of geodiversity in a pristine environment, or as a measure of potential geodiversity. If the model is run in regions known to have a high level of development this will need to be taken into account.

The model runs included in this chapter are all based on an un-weighted combination of *RES*, *Sc* and *Tv*. This can be considered as the simplest expression of the theoretical model. In reality, it could be that the importance of each of these components in determining biodiversity varies from region to region. This is a concept that will be explored more fully in the next chapter.

4.4.1. One-at-a-time variation of model inputs

Whilst varying the individual *GDiv* inputs on a "one at a time" basis does not allow investigation of complex interactions among the inputs, it does allow for systematic trialling of the model's response to changes in key variables thus the model's internal working to be checked and verified. The results show that the *Tv* output did not respond to changes in non-temporal inputs (e.g. DEM).

The systematic response of *GDiv* to changes in DEM and rainfall suggests that, in the Colombian Andes, altitude and rainfall are the key drivers of the geodiversity metric levels at the pixel scale. The very small responses found when temperature, windspeed, solar radiation and cloud cover were varied suggests that these are less important in determining the characteristic geodiversity of the region. Those variables with a non-systematic response were left in the model as they may prove important outside the model testing boundaries. When the DEM is varied, *Sc* and *RES* both show a systematic reaction, however whilst *Sc* increases as the DEM varies from -100 to +100 % of its true value (because the application of the percentage changes at the pixel level led to increased variability of elevation as well as increased mean), *RES* shows a sharp initial increase followed by a slower decline (Figure 4.14), representing the majority of land reaching the current situation and mid-elevational resource peak and then declining in resources thereafter.

When these results are placed in the context of the real world, the current geodiversity index for the Colombian Andes appears to be highly susceptible to changes in both the spatial and temporal patterns of rainfall, as well as the overall amount of rainfall. The results suggest that increases in total rainfall, as well as increased spatial and temporal structuring of that rainfall, will lead to a slight increase in geodiversity levels (as these are processes built into the model). Conversely, decreases in these will cause a decline in geodiversity, with a threshold at approximately -50% of current levels causing a distinct drop in geodiversity levels (of the order of 1% of current values).

4.4.2. Kernel size

The kernel size, used in calculation of the *Sc* index, was a trade-off between capturing broader scale variation in resource availability and increasing model processing time. The aim of this sensitivity analysis was to determine a window size at which a stable mean for *Sc* was calculated; the resulting 30 km window was found to be stable in the Colombian Andes. It was felt that it was appropriate to apply this window size to the larger study region of all tropical

mountains, as well as in the two additional study sites, as the test tile covered such a high range of topographic and climatic variation. Furthermore, the necessity for consistency of calculations between sites meant a choice had to be made.

One potential issue with using the largest possible kernel size is that processes operating at a smaller scale may be masked. When working at the tropical / continental scale, this is unlikely however future work investigating the relationship between raw data resolution and stable *Sc* kernel size may be of value.

4.4.3. Model components and modules

The increase in geodiversity score when *Tv* is not included in the final calculation suggests that final geodiversity levels are suppressed by the *Tv* score (which tends to be lower than the other two). The removal of *Sc* and *RES* have similar impacts on the geodiversity score as these two components are strongly related. This suggests that in the un-weighted simulations presented here, the final results are more dependent on overall amount of resource and its spatial structuring than they are on any temporal structuring of the resources. The next chapter will investigate the impact of weighting the components for *GDiv*.

The removal of the temperature and solar radiation modules has the greatest impact on overall geodiversity, however the mean score always remains within one standard deviation of the baseline *GDiv* simulation (figure 4.22), suggesting that the final geodiversity score is a robust and well balanced representation of all input modules with no one module having a disproportionate impact on geodiversity.

4.4.4. Initial data resolution

Figure 4.23 shows that the impact of an increase in data resolution for the DEM was less apparent in lowland regions than in mountainous regions; this is as expected – the smaller cell size allowed a more detailed representation of the complex topographic terrain, whereas in the lowland regions it simply introduced an element of data redundancy. The difference map highlights this, with relatively little difference in the lowland regions but a more “noisy” result in the mountains. The mean difference between the two maps was close to 0, suggesting that the differences between the two were not biased - i.e. the lower resolution DEM was not consistently over or under estimating elevation.

With regards to increasing the resolution for other input datasets, further work on more complex statistical downscaling of these variables would be interesting. Figure 4.28 suggests that some relationship between the DEM and rainfall and the DEM and PET may exist, and this is supported by the literature where examples of statistical downscaling exist (e.g. Lambert and Chitrakar, 1989, Daly *et al.*, 1994). By applying downscaled or higher resolution datasets for all the input variables, a more complete picture of the effect of increasing data resolution on geodiversity levels could be obtained.

The results of running *GDiv* using the higher resolution DEM (and downscaled temperature dataset) show an increase in mean and spread of geodiversity scores when the 90 m data is used. These increases can be attributed to the increasing complexity of the input dataset. The implication of these results is that the resolution of the coarser DEM (i.e. 1 km) suppresses geodiversity scores, reducing both the range and mean of the results. Investigation into whether the suppression occurs in a similar fashion across different study regions and terrains would be of use. The development of a robust down-scaling relationship between geodiversity calculated at 1 km resolution with that calculated using 90 m input data would be beneficial in mountainous regions, given the potentially large difference in elevation between two points situated within the same 1km grid cell.

4.4.5. Initial dataset variation

The low level of consistency in effect across *RES*, *Sc* and *Tv* suggested that varying the datasets did not impact on overall geodiversity scores in a systematic manner. The TRMM rainfall dataset, when combined with the MODIS cloud dataset seems to reduce overall levels of geodiversity (figure 4.25); this could be attributed to the fact that both the TRMM and MODIS datasets are more spatially detailed but less elevationally controlled than the HIRS or WorldClim alternatives. In terms of changes in the range of results, using the WorldClim rainfall dataset in conjunction with the MODIS cloud cover dataset causes a large increase in the range of both *Sc* and *RES* scores; this is also noticeable in the overall geodiversity scores. The most noticeable changes in the mean and range of results are both associated with the MODIS cloud dataset, rather than the HIRS Cloud dataset (which is highly smoothed in comparison). The HIRS Cloud dataset generally has a much higher fractional cloud cover than MODIS and, although they both show similar general spatial trends, the HIRS Cloud datasets shows larger areas of high cloud cover. It was decided to use MODIS cloud data for future model runs as the data are more spatially detailed.

The most important datasets, in terms of uncertainty propagation through *GDiv*, are the DEM and rainfall: these have been demonstrated to have the greatest impact on final *GD* results (figure 4.25). In terms of uncertainty associated with precipitation dataset choice, Imbach *et al.* (2010) investigated uncertainty in a range of precipitation datasets used in a hydrological model across meso-America and found that, of the two precipitation datasets used in this study, WorldClim has a lower level of associated uncertainty when compared with TRMM (using the relationship between measured and modelled runoff as an estimate of the real rainfall). When validated with run-off ground-truth data, a runoff model using WorldClim tends to underestimate by approximately 750 mm and has a correlation coefficient of approximately 0.9 whilst TRMM tends to underestimate by a similar amount but has a lower correlation coefficient (approximately 0.82) between the levels of precipitation and run-off. On one level, this may suggest that the choice of WorldClim as the rainfall dataset could reduce uncertainty within *GDiv*, although the use of run-off models as validation of rainfall can be seen as flawed as they tend to be aggregated over large catchments and so do not verify the spatial detail in the precipitation dataset; it is this spatial detail that is important in determining the output geodiversity metric from *GDiv.* As it is not possible to determine which rainfall dataset is "best", it was decided to use the WorldClim dataset as the standard option, as the projected climate scenarios used in chapter 7 are based on current WorldClim data. Whilst this could introduce co-linearity with the DEM (as elevation is a driving variable in the interpolation between the WorldClim data stations), this is not apparent from figure 4.28.

With regards to uncertainty associated with the DEM dataset choice, whilst the raw SRTM tends to have a lower level of vertical inaccuracy the Hydro1k has been corrected to produce hydrologically correct parameters (USGS, 2009a, USGS, 2009b). The GTOPO30, from which Hydro1k is derived, has been found to have a lower level of uncertainty than the SRTM when used to delimit drainage networks in an Ecuadorian river basin (Seyler *et al.*, 2009). However, a hydrologically correct DEM has been derived from the SRTM, which is also available in SimTerra (hydrosheds1k). Given that the primary use of the DEM in *GDiv* is to derive hydrologically relevant parameters, such as slope and drainage direction, rather than as a direct measure of elevation, it was decided that the use of either hydrologically correct DEM would reduce uncertainty associated with input dataset choice; as a result the Hydro1k was selected. The default datasets used in subsequent *GDiv* runs presented in this thesis is shown in table 4.3.

Table 4.3. Datasets used in subsequent *GDiv* simulations.

Variable	Dataset
Elevation	Hydro1k
Rainfall	WorldClim
Temperature	WorldClim
Cloud cover	MODIS

4.4.6. Controlled variation of topography

Running *GDiv* using the artificial DEM provided insight into the impacts of co-varying elevation and topographic complexity and the role of each in the topographic control of the model. Whilst the raw elevation does not feed directly into *GDiv*, except through its role in the interpolation of climate data (figure 4.4), the three derivatives of aspect, slope and drainage network are all used and changes to these, caused by the variation of elevation and topographic complexity, have impacts on geodiversity. Indirectly there will be an effect on the spatial structure of temperature across the test tile as this was modelled based on the linear relationship between the temperature and elevation. In reality there would also be an impact on rainfall due to orographic impacts, although these were not included in this analysis as no simple model between rainfall and elevation was found. The use of a smoothing function to maintain a realistic frequency distribution of slope values means that the results can be interpreted with reference to the physical world, although it is important to remember that all other inputs were held constant so the effects of co-variation of these with elevation or topographic complexity cannot be included in the interpretation.

Based on the artificial DEM, as elevation increases resource availability (both in terms of *RES* and *Sc*) decreases. That decline is more marked in areas with less complex topography, i.e. the rate of decline in geodiversity from coastal to high-elevation plane is greater than it is from coastal to high elevation mountains. This means that whilst complex terrain is more resource rich than flat terrain at an equivalent elevation, this increase in resources with topographic complexity does not at the same rate at all elevations. For example, there is a greater relative difference in geodiversity between flat and complex terrain at low elevations than at high elevations.

The decline in *RES* and *Sc* with increasing can be described with reference to real world conditions. High elevations tend to have low levels of resources, in terms of energy and water – i.e. they are cold, dry environments. This would therefore limit the maximum possible *RES* and *Sc* scores. Conversely, low elevations tend to be wetter and warmer and these regions will receive higher *RES* and *Sc* scores and the upper bound of both scores will therefore increase.

When interpreting these results in the context of ecology and biodiversity, it would seem that the most biodiverse ecosystem type should be coastal mountains, as these represent complex terrain at a low elevation.

It is important to remember that the *GDiv* implementation used in these runs did not include the seasonality index, *Tv*, as it was not possible to derive models accurately representing the spatial structure of *Tv* with elevation. Seasonal variation is spatially structured (figure 7.1, chapter 7) and, if related to topographic complexity and elevation, is likely to have an impact on the relationship between overall geodiversity and topographic complexity / elevation.

4.4.7. Model input and output co-variation

The bottom right segment of the scatterplot matrix of model input and output correlations (highlighted in blue in figure 4.28) shows there is little redundancy among the model inputs; the only strong correlation is found between the DEM and temperature. This is not a case of redundancy as the DEM is not used directly in *GDiv* calculations, rather the derived slope, aspect and LDD are used. Slope and aspect show no correlations with temperature and so cannot be considered redundant.

The correlations between the *GDiv* outputs and the model inputs show that rainfall has the strongest relationship with the final model outputs. When the model workflow is considered (figure 4.4), this is unsurprising as rainfall is used to calculate water balance, drought length and seasonal drought stress and these measures are included in several of the *GDiv* components. Each of these measures a different facet of water as a biologically important resource; water balance represents the amount of available water resource in the environment, drought length represents the duration of water stress whilst "seasonal drought" represents the severity of stress. The combination of these measures across the different components means that the rainfall dataset influences the final output in nine areas (*Sc*, *RES* and *Tv* of water balance, *Sc* and *RES* of raw rainfall, drought length and seasonal drought).

When considering geodiversity as the foundation for biodiversity, the significance of water cannot be understated – without water, life would not exist. It is therefore sensible that *GDiv*, as a model expressing the theory of where biodiversity should be greatest, should have a high reliance on water as an input.

4.5. Conclusions

The work presented in this chapter was carried out with the aim of developing a technically correct and robustly tested spatial implementation of the theoretical model of geodiversity outlined in chapter 2. The results of the sensitivity analysis and testing show that the model performs as expected, and so it is concluded that the implementation is running correctly and it is calculating geodiversity as set out in section 4.4.2.3.4. The baseline settings have been defined and the default datasets selected for future runs based on the sensitivity analyses in section 4.3.1 to 4.4.6. It is important to note that the results presented here are baseline runs and have not been validated or parameterised; such results are presented in the next chapter.

In terms of developing a robust model, it has been demonstrated that there is no redundancy among the model inputs (section 4.3.3 and figure 4.20). Furthermore, the use of 1 km resolution data has been justified as, although use of finer resolution data does impact the final distribution of geodiversity scores, it does so in a systematic manner with no apparent bias (section 4.3.4). Future technical development of the model should include further exploration of the possibility of statistical downscaling of inputs from 1 km data to a finer resolution.

The model runs presented as part of this chapter show that there is a complex relationship between model inputs and the four outputs. Geodiversity is most sensitive to the DEM and rainfall inputs (section 4.3.1), however all modules are important in the final calculations of geodiversity (section 4.3.3). Of the three model components, *Sc* and *RES* are the most influential in determining overall geodiversity, due to their close-knit relationship.

The final maps of geodiversity across the tropics show the clear latitudinal gradient, with lower scores around the equator (reflecting low seasonality and higher scores in the seasonal tropics). In high elevation mountain ranges, such as the Andes, the altitudinal gradient becomes more dominant with lower geodiversity at higher elevations. In the three study regions, there is some evidence for a mid-elevational peak in geodiversity (figure 4.8). Owing to the lower limitation of the study region (300 m) it is difficult to assess this for all test sites, however the model run for all elevations within the Colombian test tile does add further evidence to this. Further investigation of the results of *GDiv* when run at all elevations for a variety of sites would be necessary to verify whether this effect is unique to the Colombian site or is a general trend in geodiversity.

Chapter 5. Quantifying geodiversity: geodiversity and biodiversity

5.1. Introduction

Given that theoretically and (at the plot scale) empirically, elements of the proposed geodiversity metric have been shown to relate to biodiversity (chapter 2.4), the key aim of this chapter is to test *GDiv* against broad scale patterns of species richness, and thus provide an answer to the first research question "Is there a quantifiable relationship between geodiversity and biodiversity?"

In order to achieve this aim, the output maps were verified against the best available biodiversity data. Initially it was hoped to use the Global Biodiversity Information Facility's (GBIF, 2009) data point accessions to generate species richness surfaces for key taxonomic groups, however there was found to be an insufficient number of accurately geo-referenced accessions (the attempted use and testing of this data is outlined in the next section). As a result alternative datasets were used, namely species richness maps created by Mulligan, (2009) from the IUCN's RedList distribution maps for amphibians, birds and mammals (IUCN *et al.*, 2008a, IUCN *et al.*, 2008b, BirdLife, 2009a, BirdLife, 2009b), plant diversity aggregated to ecoregions (Kier *et al.*, 2005), and results showing broad scale trends in biodiversity established by literature review (Gaston, 2000).

It is important to note that a full validation of the model was not possible as there is no pan-tropical biodiversity dataset at the same fine spatial resolution. The animal richness data used (from the IUCN) is at a more coarse scale, created by IUCN using the "broad brush" approach of delimiting species presence / absence on maps (based on both observation, expert knowledge and associations with habitat). The mapped distributions for the thousands of species in each taxonomic group were then overlaid to create a surface of species richness and endemism richness (Mulligan, 2009). With regards to the plant richness dataset, the results from Kier *et al.* (2005) were joined to the ecoregion shapefile (WWF, 2009). At the time of writing, these were the best available species richness dataset available at the scale and extent required for model validation.

In order to investigate relationships between *GDiv*'s inputs (rainfall, temperature, elevation etc) and outputs (maps of *RES, Sc, Tv* and *GD*) and the species richness surface outlined in the

previous paragraph, the datasets were first aggregated to four different spatial classification systems; one based on ecological classification (ecoregions), one on a geographical classification (altitudinal - latitudinal bands) and two simple grid aggregations at 10 km and 0.5 decimal degree (approx 50km) grid squares. This aggregation was necessary in order to account for any "noise" in the data which would have the potential to mask any correlation effect based on a simple pixel level analysis. Using the mean value within each spatial class, for each aggregation, two analysis techniques were used to investigate the relationships between the *GDIv* inputs and outputs, and species richness. First, *GDiv's* inputs and outputs were tested for their association with the species richness metric using a simple correlation coefficient (*r*); this enabled a measure of the global associations between the mean value of *GDiv's* inputs and outputs with species richness at each of the four aggregations. Whilst this gave an overview of associations between the various datasets, it did not account for the spatial auto-correlation of the data. In order to formalise the relationships into a model, a technique for spatially non-stationary data was required. Geographically Weighted Regression (GWR) was chosen as the preferred modelling algorithm as it allows for spatial autocorrelation and therefore can be applied to spatially non-stationary data. Because the relationship between variables is permitted to vary over the study site, the non-stationarity of the data does not violate the assumptions of the technique and the relationship between the variables can be formalised into a mathematical model - a clear advantage over traditional regression techniques such as ordinary least squares. More detail on the GWR algorithm is given in section 5.3.3.

5.2. Data

5.2.1. GBIF Data

An attempt was made to utilise data from GBIF, however there was found to be insufficient GBIF data on which to base a validation attempt. This section outlines the efforts made to extract and quality control the GBIF data in preparation for use.

The aim was to create a surface of tree-diversity across tropical mountains as a potential validation of the geodiversity based model, following similar work on modelling tree diversity in Colombia by Armenteras and Mulligan (2010). The first problem encountered was the extraction of tree species from the GBIF database as trees represent a functional, rather than taxonomic, grouping. Downloading species data on an individual basis was impractical due to the high levels of tree species within the tropics and so it was therefore decided to work at the phylum level. 128 phyla were selected (Appendix 5), based on Barwick (2004). A check on the

number of individual species in these phyla suggested that the phylum list was comprehensive (approximately different 25 000 species were represented). All accessions for these phyla were downloaded from GBIF during April, 2010, and records with no geo-referencing were deleted. This resulted in 752 829 records, representing all geo-referenced accessions for the selected phyla across the entire world. For citations see Appendix 5.

In order to ensure that the final output represented pure tree-diversity, and was not biased towards collection effort, further data quality control was required. The dataset of 752 829 records was split into two groups; those records with the date of collection (used as a measure of sampling effort), latitude and longitude, and those records with the genus (used as a measure of tree diversity), latitude and longitude. Each of these datasets was stripped of duplicate records within grid cells (as the final output was not intended to include a measure of abundance), resulting in a global effort dataset of 196 339 accessions and a global tree diversity dataset of 345 890 accessions. Effort is measured as the number of separate sampling days evidence in the accessions data.

Two processing steps were then applied to each of these two datasets in order to check for geo-coding errors. First, accessions with latitude / longitude values of fewer than 3 decimal places were removed; this effectively removed accessions where the precision was less than 10 km. Second, samples with suspected false precision (i.e. accurate to exactly one quarter or one third of a degree) were extracted and a measure of altitudinal error was calculated by dividing potential error (i.e. the number of decimal places) by local slope derived from the DEM - effectively weighting the error more strongly if the sample is located on a steep slope (Verhelst and Mulligan, submitted). After these processing steps, 76 877 accessions within the sampling effort global dataset and 132 682 accessions within the tree diversity global dataset were available.

These two datasets were then imported into ArcMap (v. 9.3) and converted to a point shapefile. Using the Geospatial Modelling Environment (Beyer, 2010, R Development Core Team, 2010), a regular grid at 0.01^{o} (approx. 1km) that covered the study area (pan-tropical mountains) was constructed and the number of points falling within each grid-cell was calculated for both effort and diversity. In order to correct for sampling effort, the diversity score for each grid-cell was divided by the effort score, resulting in a measure of tree-phyla diversity per 0.01^{o} per sampling day (figure 5.1).

The resulting map was unusable for several reasons. First, the level of tree diversity suggested by the map is unrealistic - whilst the maximum number of phyla within any 0.01^{o} grid-cell was 17 the vast majority of the study region had an effort corrected phyla diversity score of 0, because there were more sampling days than species recorded, suggesting that no tree phyla were found across the majority of tropical mountains. Clearly this is not a valid suggestion. Second, despite the attempts at correcting the datasets for sampling effort, the results suggest that there is still an element of sampling effort reflected in the results, as seen in Costa Rica and the Ecuadorean and Peruvian Andes (figure 5.1), since there are large areas outside these regions with effectively no sampling effort. Third, the use of phyla as the taxonomic level at which diversity was measured resulted in non-tree species being included in the final data-set. For example including the *Solanum* phylum results in inclusion of all accessions for tomato, potato and aubergine species; as a result, of the approximate 55 000 *Solanum* records included in the analysis, only 289 were *Solanum wrightii* - the sole *Solanum* tree species listed in Barwick (2004).

The use of geostatistical interpolation was considered, however it was decided not to introduce further potential sources of error or circularity into this testing dataset; the error that is an inevitable component of interpolation and the circularity that would be introduced by using a co-kriging method based on elevation or climatic variables (both of which are inputs in *GDiv*). Due to the limitations of the GBIF data when applied in this context, and because an environmental model of geodiversity cannot be validated against modelled species distributions based on similar environmental data, it was decided that the IUCN datasets previously outlined represented the best possible (though not ideal) testing data for *GDiv*. The remainder of this section will outline the extraction and processing of this data.

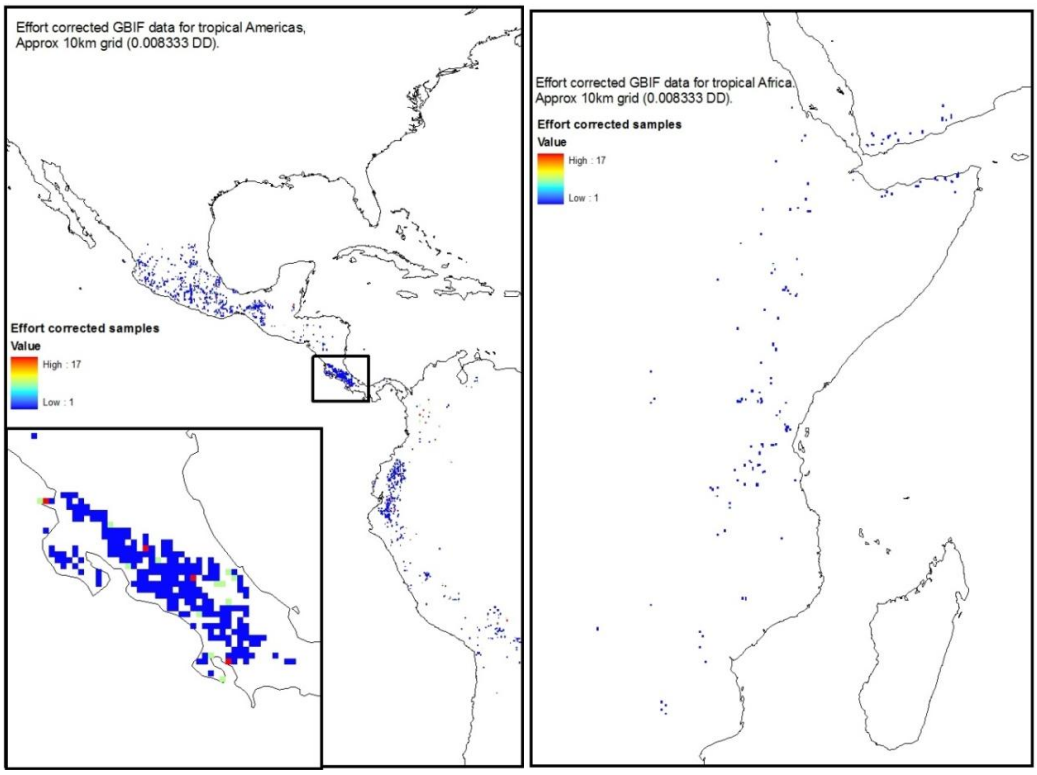

Figure 5.1. Effort corrected tree species richness, based on data from GBIF (GBIF, 2009) for mountainous regions in the tropical Americas and tropical Africa. Fewer points were found for South East Asia, so the results are not presented.

5.2.2. Species richness data used in validation attempts

General trends in biodiversity were taken from Gaston (2000) (figure 5.2), specifically figures 1b and 1d which show trends in species richness as a function of latitude (birds) and elevation (bats) respectively (figure 5.3). Gaston's figures 1a (area), 1c (regional number of species) and 1d (precipitation) were not used as they were based on studies in locations outside the study-region of this thesis.

For the distribution overlay data, use of species distribution models (such as those outlined in Elith *et al.*, 2006) was not considered appropriate as the majority of these are based on the same climatic variables used in the calculation of geodiversity and therefore circularity would be introduced. Instead, overlays based on heuristic maps giving the ranges for IUCN Redlist assessments for mammals, amphibians and birds (IUCN *et al.*, 2008a, IUCN *et al.*, 2008b, BirdLife, 2009a, BirdLife, 2009b) were created. These heuristic maps were generated by the IUCN based on expert knowledge, literature review and habitat association (IUCN, 2010b). Maps for each individual species were overlain to give an overall measure of diversity in terms of species richness.

Kier *et al* (2005)'s data (Figure 5.3) was used as a measure of phytodiversity. The authors estimated plant diversity based on literature review, ecological theory and taxon data to estimate plant richness within ecoregions. They assessed the quality of data, enabling users of the data to evaluate uncertainty levels.

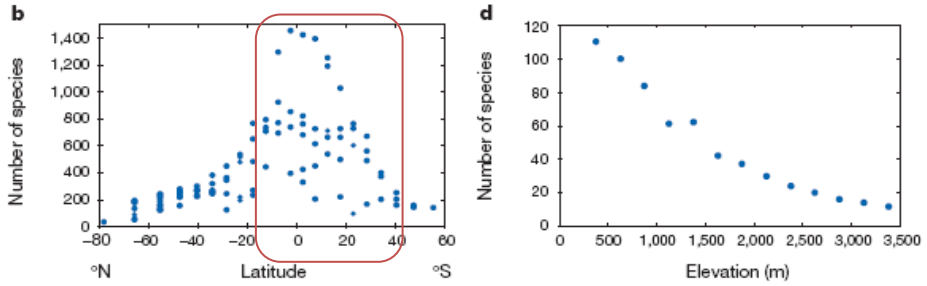

Figure 5.2. Figures 1b and 1d from (Gaston, 2000). Part b shows species richness of new-world birds as a function of latitude, with this study's region of interest (-30 - +30 latitude) highlighted. Part d shows species richness of bats in Manu National Park, Peru, as a function of elevation.

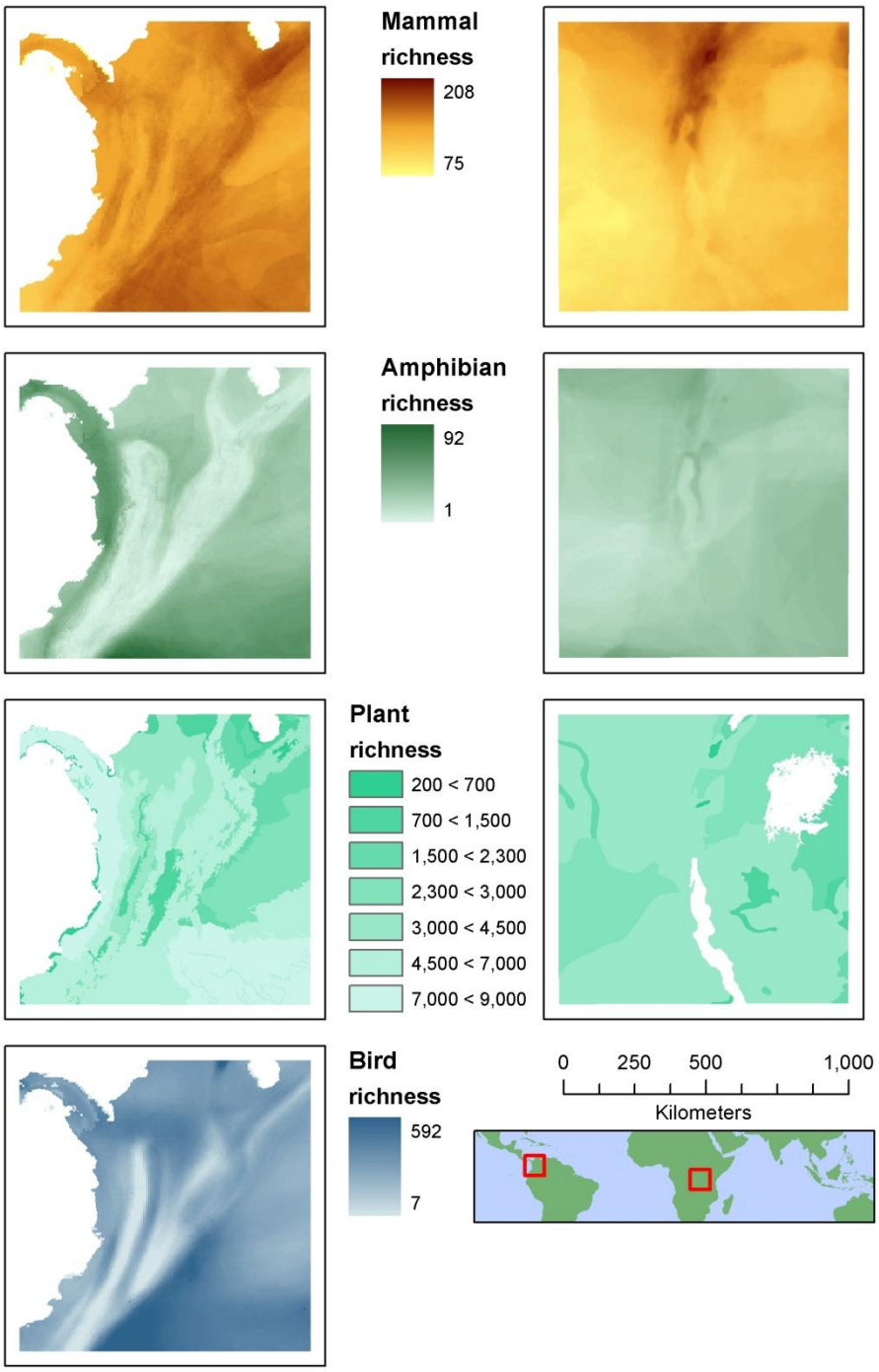

Figure 5.3. Species richness and endemism maps for mammals, amphibians and birds based on the IUCN Redlist assessments and plant species richness based on Kier *et al.* (2005), shown for the Colombian tile (left) used for model testing and the African tile used in the validation attempts (right). Note that, at the time of analysis, bird data was only available for the neo-tropics and is therefore not shown for the African tile.

5.3. Methods

5.3.1. Correlations between geodiversity and measures of biodiversity

In order to investigate any relationships between biodiversity and geodiversity, correlations between the two were assessed, as outlined below. The relationships were later formalised through regression models (as outlined in section 5.3.3) where the spatial non-stationarity (i.e. changes in the relationship between variables over space) of the data was accounted for, however it was felt that exploring the relationship between the biodiversity and geodiversity as a simple correlation within the initial study area was an important exploratory step.

Four sets of correlations were calculated; one based on aggregation of the species richness data to ecoregions, one on aggregation to altitudinal-latitudinal bands, and two aggregated to grids of approximately 50 km (half a degree) and 10 km squares respectively. In each instance the mean species richness within the area class (i.e. individual ecoregion, altitudinal-latitudinal band or grid-cell) was taken as representative of the biodiversity of the area class These aggregation areas were selected as representing an ecological and a geographical classification, as well as a stratified sampling technique at two scales. *GDiv* output maps were also aggregated by taking the mean geodiversity within these areas, thus allowing correlations to be calculated.

In addition to the correlations between the modelled *GDiv* outputs and biodiversity surfaces, variance partitioning was used to determine the independent contribution of each of the independent variables (i.e. the *GDiv* outputs and the raw *GDiv* inputs) to explaining the variation in the biodiversity surfaces. The "hier.part" package in r was utilised, which implements the Chevan and Sutherland (1991) hierarchical partitioning algorithm. R^2 was used as the measure of goodness of fit, and these analyses were carried out using the same method and spatial aggregations outlined above.

5.3.2. Comparison of general patterns of geodiversity with general patterns of biodiversity

In order to validate the *GDiv* results against global patterns of biodiversity, results from Gaston (2000) were used – specifically those showing trends in species richness with latitude and species richness with elevation. Samples of the *GDiv* outputs were taken across the length of the tropical Americas (between -30 and 30 degrees) and across all elevations. Data for the lowlands were included in order to replicate Gaston's study area. These were sorted into 500 m elevational bands examined separately in order to enable the investigation of latitude

alone without the confounding influence of elevation. The samples for the elevational validation were taken in the 10 degree tile over Manu National Park and Biosphere Reserve, Peru, from elevations between 300 and 3500 m in order to match the location and elevational range used in the example cited (Gaston, 2000).

5.3.3. Geographically Weighted Regression; introduction

The correlation measures outlined in section 5.3.1 provide a 'global' measure of the relationship between geodiversity and biodiversity, however the spatial structure of the relationship is not taken into account. This section will outline the use of a local regression method used to further investigate the geodiversity - biodiversity relationship. A range of local techniques will be discussed, before a more detailed overview of geographical weighted regression (GWR). Finally, the specific methods used in the analyses for this thesis are outlined.

Relationships between variables across space is often not consistent throughout a given study region, that is the relationship is non-stationary. Global regression techniques do not take this spatial structure in the data into account, and can produce misleading results owing to the Simpson's paradox whereby aggregation of data, spatially or otherwise, masks underlying relationships in the disaggregated data (Fotheringham *et al.*, 2002). Local regression techniques, whilst sometimes criticised for not providing a global model, do take into account the spatial structure of the underlying data and thus can allow greater understanding of the relationships between dependent and independent variables across the study region by allowing the relationship between those variables to vary with space and thus highlight detail missed by global models (Trivedi *et al.*, 2008).

Various local regression techniques, such as univariate methods including splining, LOWESS regression, kernel regression and variable parameter models, are outlined by Fotheringham *et al.* (2002) and references therein. These are designed for non-spatial problems, as they take account of local variation of data in terms of variable space rather than physical space. This becomes a problem when considering spatial data as spatial data varies in at least two dimensions. Given that these methods are not specifically designed for spatial problems, it was decided not to use them in determining the relationships between the geodiversity inputs and biodiversity.

Local multivariate methods outlined by Fotheringham *et al.* (2002) include spatial expansion, spatially adaptive filtering, multilevel modelling, random coefficient models and spatial regression models. The expansion method allows the regression coefficients to be placed in the context of their "neighbourhood", be that a spatial or parameter space neighbourhood. For example, the value of parameter *a* at location *i* is based on the observed value of *a* plus *n* values for surrounding locations. Whilst this does take non-stationarity into account, it is highly dependent on the choice of the neighbourhood of observation data points and so does not provide a robust model.

Adaptive filtering was developed for time-series analysis in order to correct parameter drift through time whereby the estimate for parameter *a* at time *t* is adjusted based on estimates for *a* at times directly before *t*. Whilst this has proved effective in time-series analysis, the unidirectional, linear characteristic of time-series analysis does not apply in spatial analysis where relationships operate in at least two dimensions and moreover the definition of unique neighbours is not trivial (Fotheringham *et al.*, 2002).

Multilevel modelling takes the form

$$y_{ij} = \alpha_j + \beta_j x_{ij} + \varepsilon_{ij} \qquad 30$$

where y_{ij} is the value of individual *i* at location *j*, x_{ij} is the *i*th observation of *x* at *j* and α_j and β_j are location specific parameters. In order to parameterise this model spatially, values for α_j and β_j have to be calculated for all *i* values; a highly complex procedure.

The random coefficient technique is founded in Bayes theory, whereby parameter estimates are drawn from a matrix of random weightings and then Bayes theory is applied to select which weighting is included in the final model. Whilst this technique can be successful, it does not explicitly take location into account meaning parameter estimates at close physical locations could have very different values - thus violating Tobler's first law of geography that features close together are more similar than those further apart.

Spatial regression techniques, such as Kriging and co-Kriging, have been developed to specifically cope with the issue of non-independence of spatial data, however the model is still formulated based on the entire dataset and so is not truly local.

By contrast to the above techniques, GWR is an explicitly local regression model that allows for variation in relationships over space (Fotheringham *et al.*, 2002). It is similar to a moving

window regression in that parameterisation occurs on a local scale within a moving kernel, however the kernel is not fixed and the influence of the regression points varies within the kernel according to a distance decay function from the centre of the kernel. If a global regression model takes the form

$$y_i = \beta_0 + \sum_1^k \beta_k x_{ik} + \varepsilon_i \quad 31$$

where *i* is the observation point location and *k* is the number of parameters, then GWR takes the form

$$y_i = \beta_{0(u_i v_i)} + \sum_1^k \beta_{k(u_i v_i)} x_{ik} + \varepsilon_i \quad 32$$

where $(u_i v_i)$ are the coordinates of point *i* thus making the parameter values location specific. Fotheringham *et al.* (2002) point out one potential problem with calibrating such a model is the fact that over the study region there will be far more unknown than known values, This can be overcome by using Tobler's first law of geography and assuming such unknown values are a deterministic function of distance from a known value, thus parameter values for each point *i* can be estimated based on a regional subset of observations.

5.3.4. Geographically Weighted Regression; implementation

GWR can be used to determine which, of a set of models, is the most useful. In the work presented here, univariate GWR was used to assess the value of a set of geodiversity maps in modelling trends in biodiversity; i.e. a series of different geodiversity maps were used as the independent variable, whilst the IUCN overlays were used as the dependent variable. This was carried out using both the Colombian and African test tiles.

The set of *GDiv* model outputs used in the GWR are shown in table 5.1. In summary, there were 42 simulations based on different parameterisations of *GDiv* whereby the contribution of *RES*, *Sc* and *Tv* each varied from 0 - 100% in 10% increments. The balance is described using a three digit RST value, where the first digit represents the proportional contribution of *RES* to the final geodiversity map used in the GWR, the second digit represents the proportional contribution of *Sc* whilst the third digit represents the *Tv* contribution. For example, an RST value of 721 represents a 70% contribution of *RES*, 20% contribution of *Sc* and 10% contribution of *Tv* to the overall *GD* score. The sum of the three RST digits will always be 10. The implementation of these calculations is described below. In addition to the parameterised geodiversity maps, a baseline *GDiv* run, where each component contributed 33% was included (labelled as *GD*), the three components of *GDiv* (*RES*, *Sc* and *Tv*) were included and, in order to assess the "added value" of *GDiv*, GWR models using raw elevation and rainfall data as

independent variables were also included (labelled as DEM and Rain respectively). This resulted in a set of 48 models being tested.

A set of weighted *GDiv* runs were calculated using the raw *RES*, *Sc* and *Tv* outputs for the Colombian and Africa baseline runs described in chapter 4. Equation 6 was modified to give

$$GD = (R \times RES) + (S \times Sc) + (T \times Tv) \quad 33$$

where R,S and T are the contributing fractional proportions of the three components, varying between 0 and 1 with a sum of 1 (table 5.1 gives the weightings for each model included in the analyses). This calculation was carried out using PCRaster Python on data at a 1km resolution.

After the raw data to be used as independent variables had been prepared, four different spatial aggregations were applied; ecoregions, altitudinal-latitudinal bands, a half-degree grids and a 10 km grid. These aggregations were selected to represent an ecological classification system, a physical classification system and two stratified classification systems at different scales. The Geospatial Modelling Environment (Beyer, 2010, R Development Core Team, 2010), run as an extension to ArcGIS 9.3, was used to carry out the aggregations, resulting in four shapefiles with 49 columns in the attribute table representing the 48 independent variables and 1 dependent variable. The number of rows in each of the attribute tables represented the number of observation points used in the GWR model runs (Table 5.2).

Prior to running GWR, each of the independent variables was confirmed as non-stationary meaning the use of GWR was appropriate. The GWR tool in ArcGIS uses a Gaussian kernel, the size of which can be fixed (based on either number of neighbours or a fixed distance) or varied (using the AIC or Cross Validation methods outlined by Fotheringham *et al* (2002). In order to allow a fair comparison between the different spatial aggregation systems used, a fixed-distance kernel was selected. After initial tests, a bandwidth of 200 km was used; this being the minimum distance necessary in order to use the ecoregions aggregation. 200 km represents approximately 16% of the overall width of the study region.

Table 5.1. The 48 simulations used in the GWR analysis, showing *RES*, *Sc* and *Tv* weightings where appropriate.

Model name	*RES* proportional contribution	*Sc* proportional contribution	*Tv* proportional contribution
GD	0.33	0.33	0.33
RES	1.00	0.00	0.00
SC	0.00	1.00	0.00
TV	0.00	0.00	1.00
Rain	-	-	-
DEM	-	-	-
181	0.10	0.80	0.10
271	0.20	0.70	0.10
361	0.30	0.60	0.10
631	0.60	0.30	0.10
541	0.50	0.40	0.10
451	0.40	0.50	0.10
172	0.10	0.70	0.20
721	0.70	0.20	0.10
811	0.80	0.10	0.10
262	0.20	0.60	0.20
532	0.50	0.30	0.20
442	0.40	0.40	0.20
352	0.30	0.50	0.20
622	0.60	0.20	0.20
712	0.70	0.10	0.20
163	0.10	0.60	0.30
253	0.20	0.50	0.30
343	0.30	0.40	0.30
433	0.40	0.30	0.30
523	0.50	0.20	0.30
613	0.60	0.10	0.30
154	0.10	0.50	0.40
244	0.20	0.40	0.40
334	0.30	0.30	0.40
424	0.40	0.20	0.40
514	0.50	0.10	0.40
145	0.10	0.40	0.50
235	0.20	0.30	0.50
415	0.40	0.10	0.50
325	0.30	0.20	0.50
136	0.10	0.30	0.60
226	0.20	0.20	0.60
316	0.30	0.10	0.60
127	0.10	0.20	0.70
217	0.20	0.10	0.70
118	0.10	0.10	0.80

Table 5.2. Number of observation points for each aggregation system within each study site.

Spatial aggregation system	Colombian Andes	African Rift Valley
Ecoregions	20	18
ALBs	154	57
50 km grid	203	400
10 km grid	4749	14161

The GWR was run using each of the 48 independent variables as a single explanatory variable for biodiversity. The usefulness of each of these GWR models was assessed using the corrected Akaike Information Criterion (AICc) in order to establish the best performing model within each of the eight sets (i.e. for each of the spatial aggregations at each of the study sites). The AIC is based on the Kullback-Leibler information difference, $I(f, g)$, the difference between the model distribution (*g*) and reality (*f*). The "best" model within a set, according to the AIC, is that which has the smallest K-L difference. It does not assume that *f* is included in the model set, rather it indicates which of those models included in the set has the lowest K-L difference and can therefore be deemed the most useful. The AIC is calculated based on the log-likelihood of the model parameters

$$AIC = -2\log(\mathcal{L}(\hat{\theta}|y) + 2K \quad 34$$

where $\log(\mathcal{L}(\hat{\theta}|y)$ is the log likelihood of the model parameters and *K* is the number of parameters in the model. The corrected version (AICc) is used for small sample sizes, but is also appropriate for larger sample sizes as it converges with AIC as the sample size increases (Burnham and Anderson, 2002) and will therefore be appropriate for comparing each of the different spatial aggregations given the varying number of regression points. It includes an additional penalty for models with a high number of parameters and is calculated as

$$AICc = AIC + \frac{2K(K+1)}{n-K-1} \quad 35$$

where n is the sample size. These AICc scores were then scaled to relative AICc scores, whereby the lowest AICc score was subtracted from each AICc score resulting in the most useful model having a relative AICc score of 0, and all others having higher scores.

Adjusted R^2 values, $\bar{R}^2$, were also calculated. Using the adjusted value accounts for the number of degrees of freedom associated with the model, and gives a measure of the amount of variance within the sample population that is explained by the model. These were calculated using

$$\bar{R}^2 = 1 - (1 - R^2)\frac{n-1}{n-K-1} \quad 36$$

where the unexplained variance, *1 - R^2,* is multiplied by a correction term based on the number of parameters within the model. In the case of GWR, *K* is dependent on the bandwidth, as well as the usual regression model parameters.

These two statistics (AICc and $\bar{R}^2$) were used in conjunction to infer different information regarding the models. The AICc statistic gives an indication of how close, out of the entire set, each model is to the expected "real" distribution (i.e. reality) - it is a comparative measure for models within the same set. Each of the models is compared to the expected distribution, without assuming the true distribution is contained within the model set. On the other hand, $\bar{R}^2$ gives an indication of the amount of variance within the sample data that is explained by each model but does not allow any inference beyond this. AICc was used to guide the selection of the best model from each set, whilst $\bar{R}^2$ was used to make inter-set comparisons among the selected models.

5.4. RESULTS

5.4.1. Correlations between geodiversity and measures of biodiversity

Table 5.3 gives correlation coefficients (*r*) between the various measures of species richness and the *GDiv* outputs as well as the raw input data, for all four spatial aggregations. These relationships are represented visually in figures 5.4 - 5.7. In terms of taxonomic groups, geodiversity has the strongest association with amphibian richness with r values of 0.6 or above in three of the four spatial aggregations. The weakest associations are found with overall plant species richness; note that this map was generated based on data already aggregated to ecoregions, rather than on a per-pixel overlay of distribution maps. The implications of this are discussed further below.

There is some evidence of non-linear relationships between amphibian richness and *GDiv* outputs at the 50 km aggregation (figure 5.6). However, this is not as pronounced with *Tv* and is not apparent at different spatial aggregations. Bird and total IUCN species richness appear to have an asymptotic relationship with *Tv* at the 10 km aggregation, however this is less apparent at alternative aggregations. There is clear evidence of data binning in the plant dataset at the 10 and 50 km aggregations.

With regard to the three components of geodiversity, *Tv* showed the highest average r value across all taxonomic groups and spatial aggregations (r = 0.31), followed by *Sc* and *RES* (both r = 0.24), suggesting that, overall, there is a stronger association between the various

measures of biodiversity and temporal variation of resources than the other components. The raw model inputs have varied r scores across the different taxonomic groups and spatial aggregations. The strongest correlation comes between elevation and amphibians (r = -0.70) at the 50 km grid, whilst the weakest association is between mammals and geodiversity at the 10 km aggregation (r = 0.00).

The relative performance of *GDiv* outputs at modelling broad-scale patterns in biodiversity compared with using the raw input variables is seen in table 5.4. In terms of mean variance explained over all spatial aggregations and taxonomic groups, *Tv* has the highest (18.62%), followed by *GD* (16.17%) and then Rainfall (16.05%). However, of the 6 individual explanatory contributions which explain over 30% , four are from Rainfall as the explanatory variable (Plants / 10 km, Plants / 50 km, Mammals / ALBs and Total IUCN / Ecoregions). This lack of consistency in explanatory power across the spatial aggregations and taxonomic groups is illustrated in the high standard deviation for Rainfall when compared with *GD* or *Tv* (10.35%, 5.24% and 8.73% respectively) and can be seen in the pattern on the heatmap (table 5.4). For example, whilst rainfall is found to explain high proportions of the variance in the biodiversity datasets, this is sensitive to the spatial aggregation and, within each spatial aggregation, to the taxonomic grouping. On the other hand, a more consistent pattern is seen in the *GDiv* outputs. For example, *Tv* is seen to explain high levels of variance across all spatial aggregations and, within those aggregations, performing better for Mammals, Birds and Total IUCN biodiversity datasets.

Table 5.3. Correlations (r values) between various measures of biodiversity and *GDiv* outputs aggregated to ecoregions, altitudinal-latitudinal bands (ALB), a half-degree square grid and a 10 km square grid. r values over 0.6 are highlighted.

Spatial aggregation	Taxonomic group	*GD*	*RES*	*Sc*	*Tv*	Temp	SR	Rain	DEM
Ecoregions	Amphibian	**0.60**	0.58	0.48	0.57	0.42	-0.12	0.54	-0.47
	Mammal	-0.17	-0.27	-0.18	-0.03	-0.28	0.19	-0.02	0.32
	Bird	0.37	0.32	0.31	0.39	0.25	0.33	0.36	-0.30
	Total IUCN	0.41	0.34	0.33	0.44	0.25	0.30	0.42	-0.27
	Plant	0.07	0.04	0.09	0.11	-0.03	-0.44	0.15	0.02
ALB	Amphibian	0.40	0.52	0.45	0.12	0.58	0.12	0.26	**-0.60**
	Mammal	0.42	0.19	0.24	**0.60**	0.01	0.07	-0.38	-0.02
	Bird	0.48	0.26	0.33	**0.61**	0.04	0.22	-0.23	-0.07
	Total IUCN	0.50	0.28	0.35	**0.64**	0.07	0.20	-0.26	-0.10
	Plant	0.17	0.39	0.41	-0.26	**0.65**	-0.01	0.35	**-0.66**
50 km	Amphibian	**0.64**	**0.64**	**0.63**	0.54	**0.65**	0.03	0.54	**-0.70**
	Mammal	-0.05	-0.15	-0.17	0.11	-0.10	0.19	-0.18	0.10
	Bird	0.46	0.37	0.36	0.52	0.41	0.04	0.20	-0.44

	Total IUCN	0.51	0.42	0.41	0.55	0.45	0.07	0.25	-0.49
	Plant	0.27	0.2	0.32	0.15	0.27	0.01	0.44	-0.34
10 km	Amphibian	**0.60**	0.59	**0.60**	0.50	0.52	0.02	0.52	-0.57
	Mammal	0.00	-0.08	-0.10	0.14	-0.13	0.06	-0.12	0.11
	Bird	0.41	0.34	0.34	0.47	0.18	0.01	0.25	-0.23
	Total IUCN	0.45	0.37	0.37	0.50	0.22	0.02	0.28	-0.27
	Plant	0.15	0.20	0.20	0.05	0.05	-0.09	0.35	-0.10

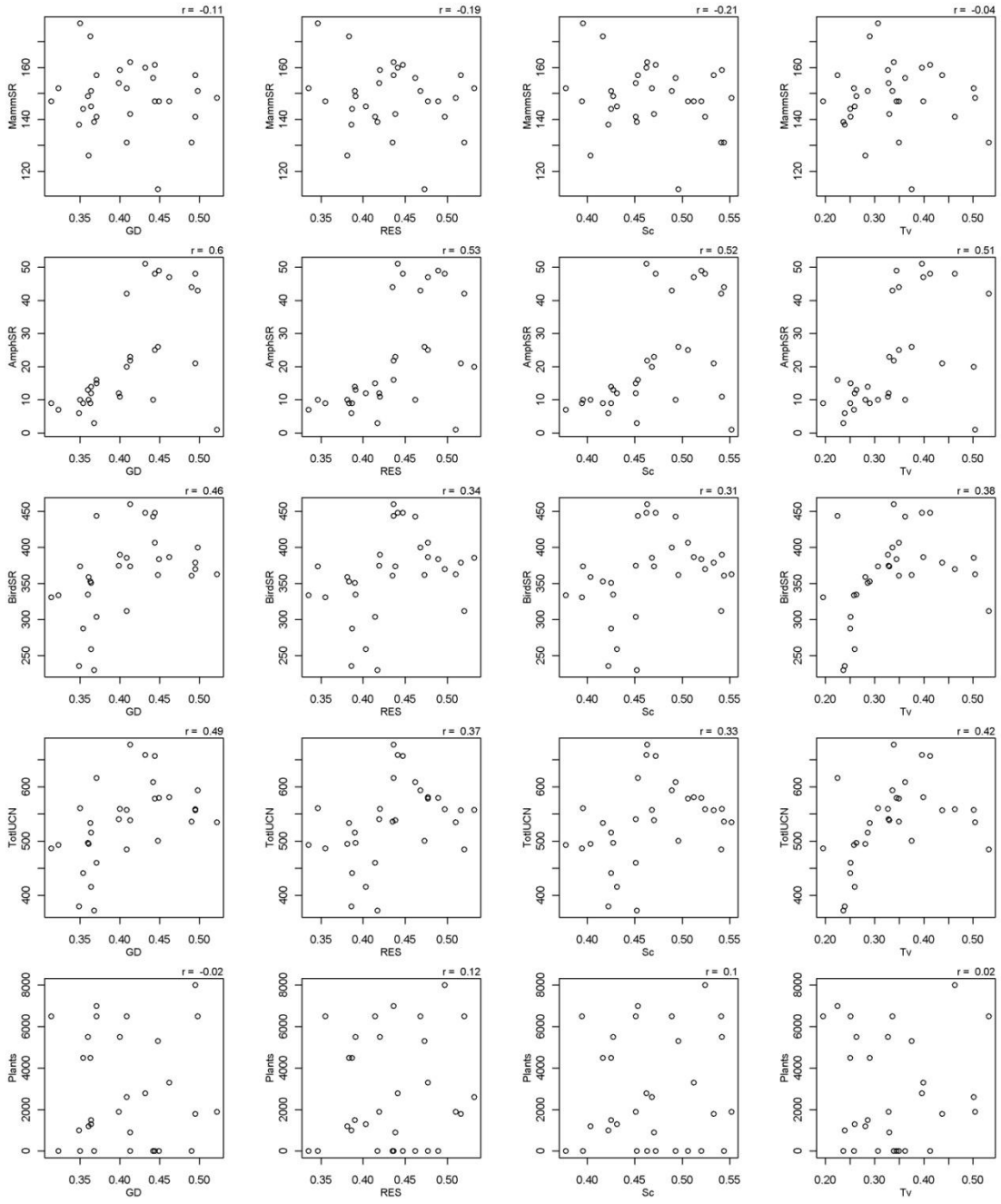

Figure 5.4. Relationship between species richness and *GDiv* outputs, aggregated to ecoregions within the Colombian Andes. Mammals, Amphibians, Birds and TotalIUCN data based on overlays of the IUCN distribution maps (IUCN *et al.,* 2008a, IUCN *et al.,* 2008b, BirdLife, 2009a and BirdLife 2009b), whilst the Plant data is from Kier *et al.* (2005).

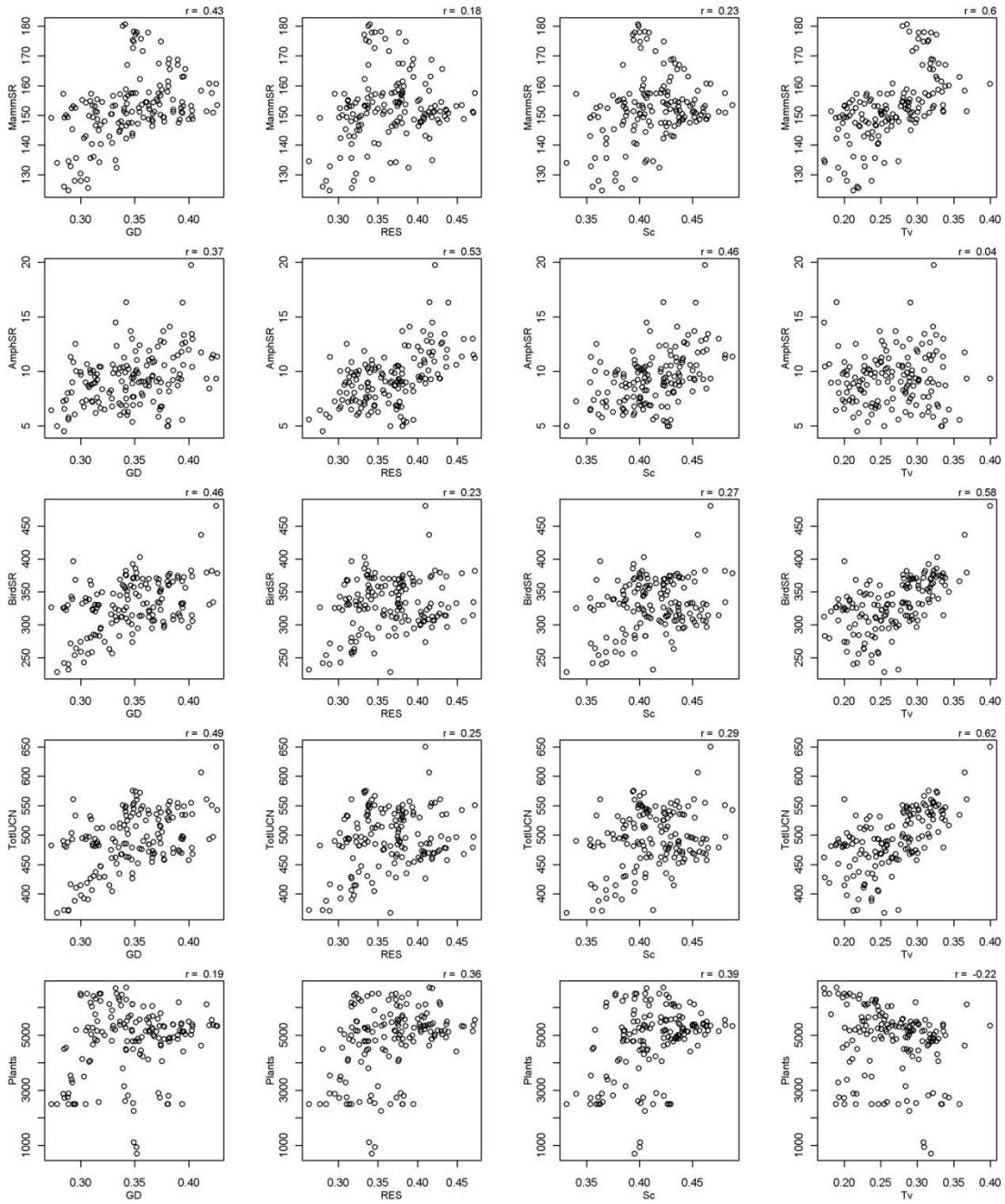

Figure 5.5. Relationship between species richness and *GDiv* outputs, aggregated to altitudinal-latitudinal bands within the Colombian Andes. Mammals, Amphibians, Birds and TotalIUCN data based on overlays of the IUCN distribution maps (IUCN *et al.,* 2008a, IUCN *et al.,* 2008b, BirdLife, 2009a and BirdLife 2009b), whilst the Plant data is from Kier *et al.* (2005).

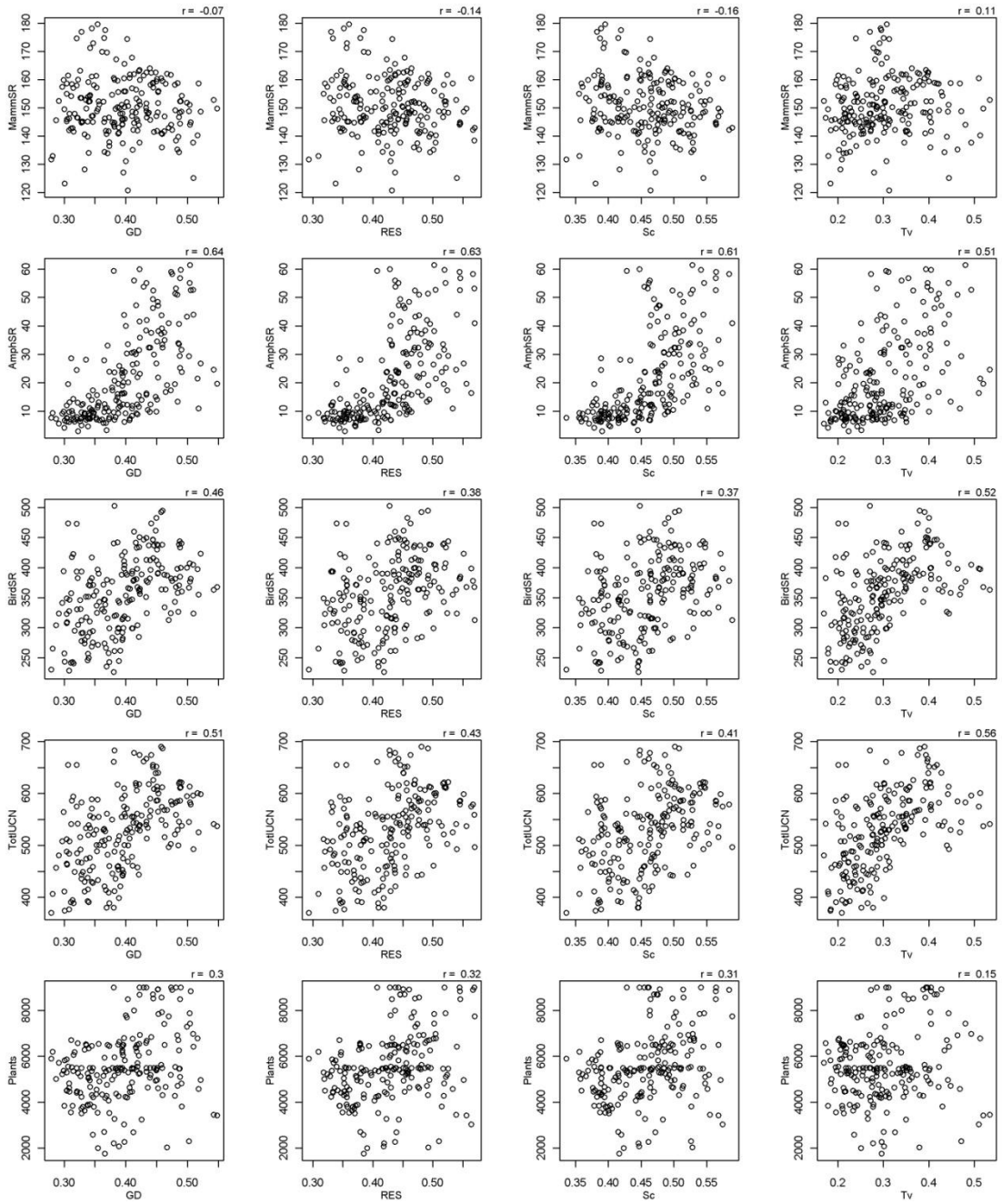

Figure 5.6. Relationship between species richness and *GDiv* outputs, aggregated to a 50 km grid within the Colombian Andes. Mammals, Amphibians, Birds and TotalIUCN data based on overlays of the IUCN distribution maps (IUCN *et al.,* 2008a, IUCN *et al.,* 2008b, BirdLife, 2009a and BirdLife 2009b), whilst the Plant data is from Kier *et al.* (2005).

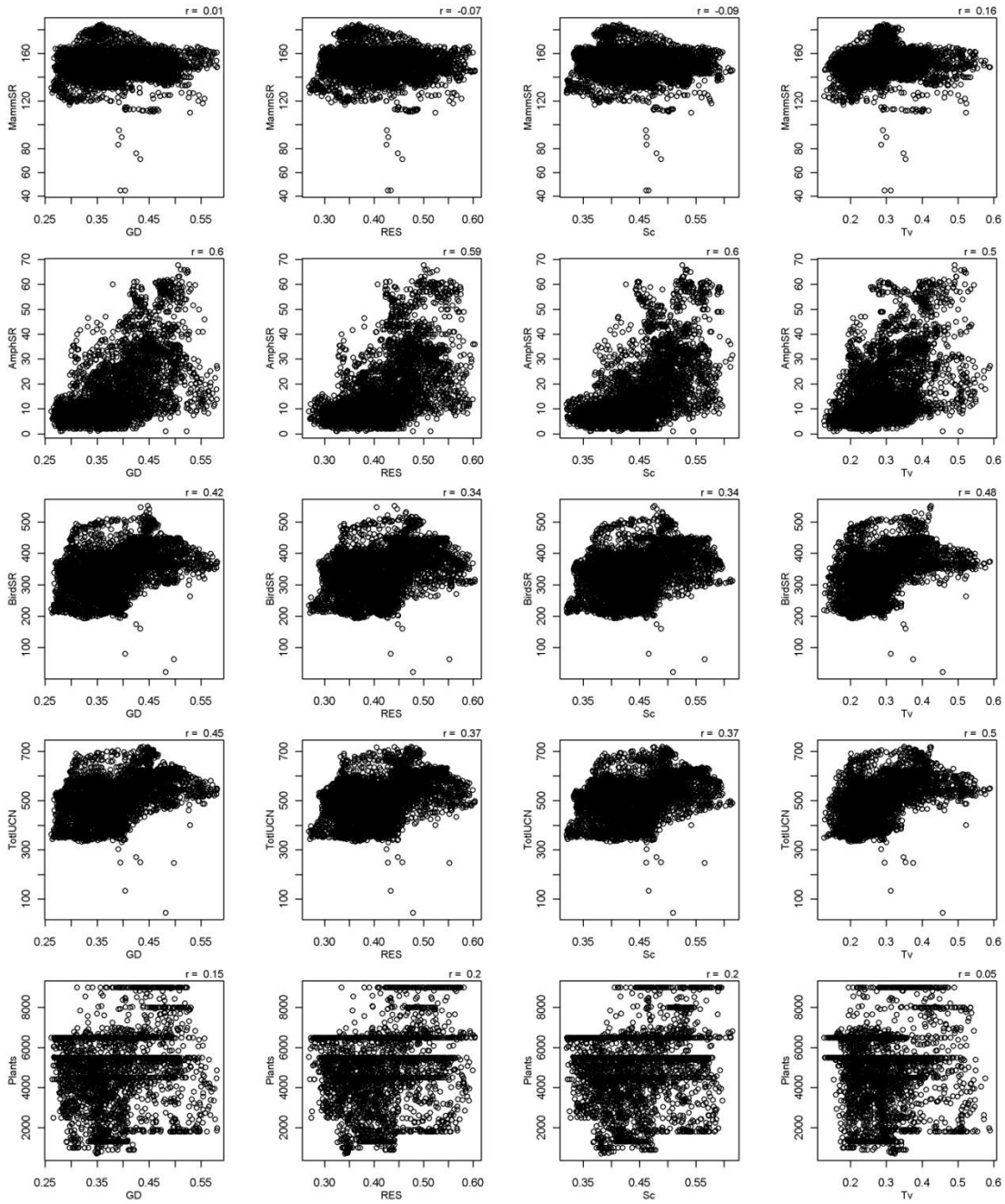

Figure 5.7. Relationship between species richness and *GDiv* outputs, aggregated to a 10 km grid within the Colombian Andes. Mammals, Amphibians, Birds and TotalIUCN data based on overlays of the IUCN distribution maps (IUCN *et al.,* 2008a, IUCN *et al.,* 2008b, BirdLife, 2009a and BirdLife 2009b), whilst the Plant data is from Kier *et al.* (2005).

Table 5.4. Percentage of explained variation in the biodiversity datasets under each spatial aggregation contributed by each of the raw input datasets and the *GDiv* outputs. Darker shades of orange represent a higher explanatory power.

Spatial aggregation	Taxonomic group	Temperature	Solar Radiation	Rainfall	DEM	GD	RES	Sc	Ty
Ecoregions	Amphibian	9.37	0.71	25.93	12.21	14.97	12.48	8.27	16.06
	Mammal	5.03	0.65	14.68	6.31	23.50	21.09	8.96	19.79
	Bird	8.51	6.28	26.15	10.14	15.66	14.09	2.47	16.70
	Total IUCN	5.17	2.92	30.62	6.35	17.38	15.60	3.10	18.85
	Plant	1.92	33.63	14.62	2.65	14.16	11.64	2.43	18.95
ALB	Amphibian	22.32	1.11	3.73	24.86	11.88	17.10	12.93	6.08
	Mammal	2.60	0.84	31.23	2.73	19.81	7.18	7.08	28.53
	Bird	11.60	6.38	12.31	10.44	18.91	6.66	8.05	25.63
	Total IUCN	8.38	5.21	15.52	7.61	20.35	7.25	8.42	27.26
	Plant	22.81	0.73	6.78	25.15	10.03	9.97	12.45	12.08
50 km	Amphibian	18.57	0.48	13.88	25.98	11.83	10.28	9.89	9.10
	Mammal	1.83	14.54	8.13	2.00	19.45	13.65	15.57	24.84
	Bird	13.30	0.52	5.54	18.41	19.85	8.76	8.66	24.95
	Total IUCN	13.90	0.80	6.79	19.36	18.74	8.69	8.56	23.16
	Plant	19.56	0.37	31.37	27.23	5.38	6.50	6.33	3.26
10 km	Amphibian	16.49	0.13	14.05	22.42	13.14	11.93	12.10	9.75
	Mammal	6.73	2.93	6.43	5.31	21.90	9.24	16.63	30.84
	Bird	11.59	0.29	8.06	13.67	20.93	9.46	8.83	27.17
	Total IUCN	11.89	0.37	8.58	14.64	20.28	9.40	8.84	26.01
	Plant	20.16	2.38	36.61	19.15	5.27	6.43	6.62	3.38
	Mean	11.59	4.06	16.05	13.83	16.17	10.87	8.81	18.62
	Standard deviation	6.73	7.77	10.35	8.49	5.24	3.90	3.82	8.73

5.4.2. Comparison of general patterns of geodiversity with general patterns of biodiversity

When plotted against latitude, the variables 'total resource availability' *RES* and 'spatial context of resources' *Sc* both follow a similar pattern (figure 5.8), with a peak at approximately 10°N, and a notable increase in the effect of elevation at the equator (i.e. a larger difference in scores at low elevations and high elevations at the same latitude, with lower elevations generally showing higher scores at the equator for both *RES* and SV) [note that in the figure from Gaston (2000), figure 5.3, latitude is plotted from north to south along the X axis, whereas in figure 5.8 it is plotted from south to north].

Interestingly mid-elevations (approximately 2300 - 3800 masl) show higher scores in *RES* and *Sc* at lower / higher latitudes, but have the lowest scores at the equator; i.e. further north / south from the equator, mid-elevations have relatively higher levels of *RES* and *Sc*, whereas at the equator the mid-elevations have the lowest levels of these two components when compared with the foothills and peaks. Temporal variation decreases towards the equator, with less of an elevational effect, although there is still an increase in difference between scores at low and high elevations at the equator and in the most northerly latitudinal band (25^{o} - 30^{o} N). Overall geodiversity for the tropical Americas (between 30^{o} N and 30^{o} S) appears to be higher in the northern hemisphere, with a slight decrease at the equator. Again, the differences with elevation are greater at the equator and in the northern hemisphere.

With regards to variation with elevation, the mean value of *GD*, *RES*, *Sc* and *Tv* remains relatively consistent (figure 5.9). In terms of range of scores, *GD*, *RES* and *Sc* show a marked decrease in range of scores with elevation, with a sharp decline at around 1550 masl for both *GD* and *Sc*. *RES* shows a sharp increase in length of the lower tail of the distribution at approximately 2300 masl; there is no corresponding change in the upper tail of the distribution. This suggests that above 2300 masl there is an increase in low *RES* scores, but no increase in high *RES* scores.

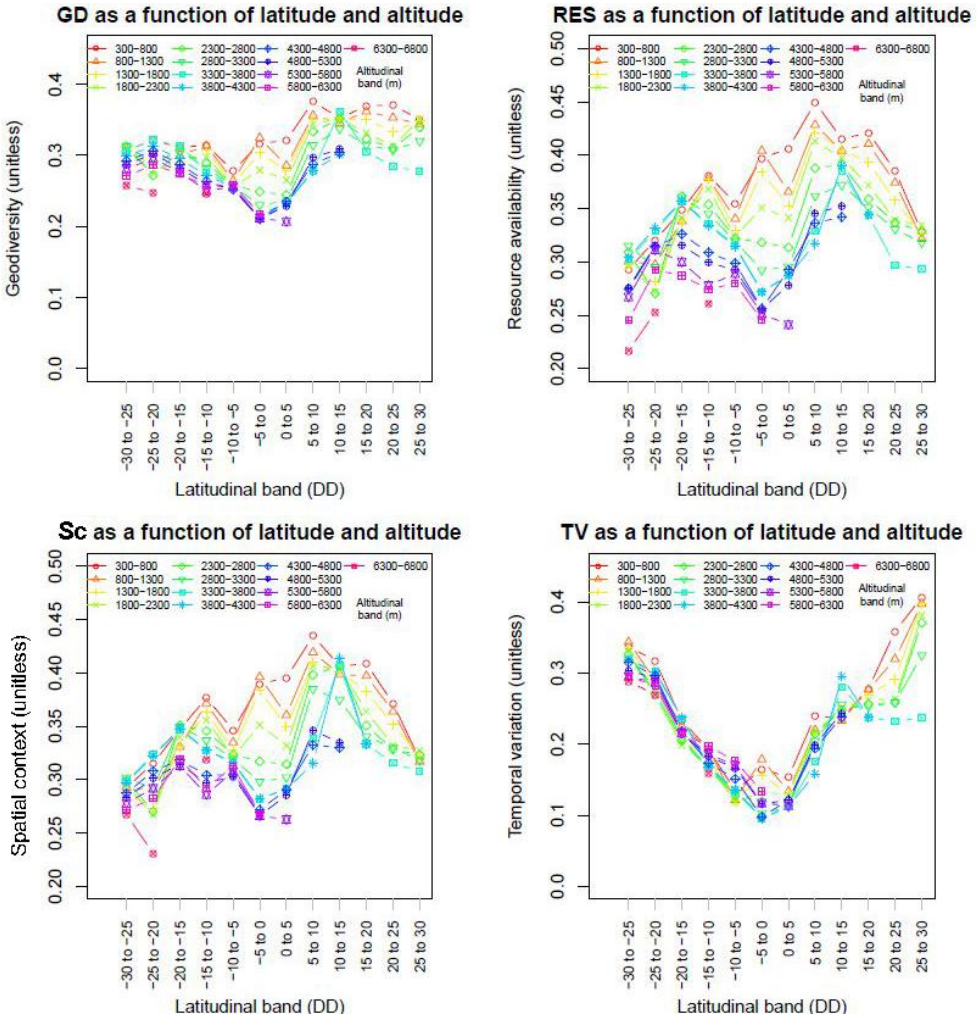

Figure 5.8. Geodiversity and its components plotted as a function of latitude, and split into 500 m elevational bands, for the tropical Americas.

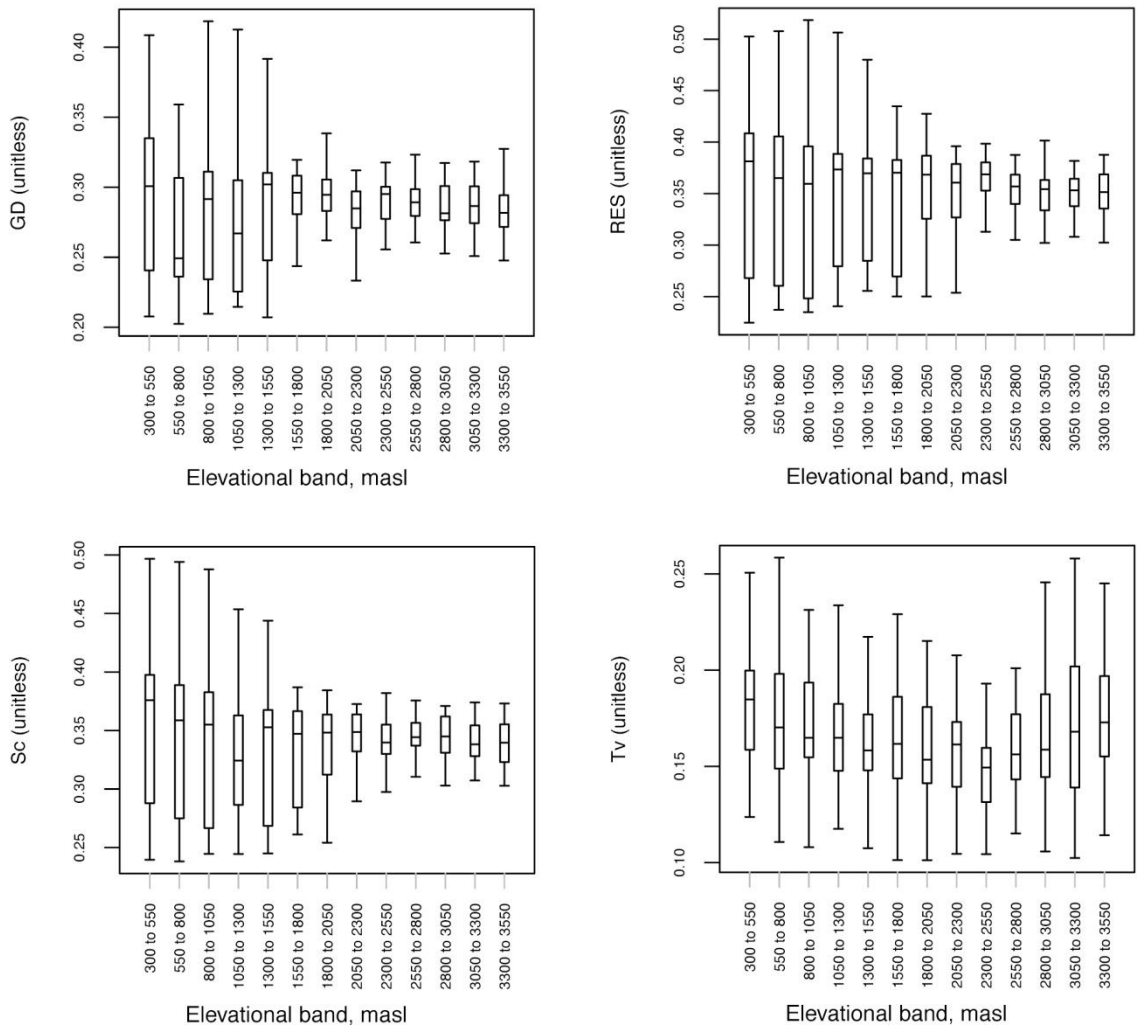

Figure 5.9. Variation in geodiversity and its components with elevation. Mean score is represented with the central black line, 1 standard deviation by the box and 2 standard deviations by the vertical bars.

5.4.3. Geographical Weighted Regression

Generally *Sc* proved to be the best model of biodiversity within the model sets, with the African Ecoregions and Colombian ALBs being the only exceptions (figures 5.6 and 5.7). The $\bar{R}^2$ results suggest that *GDiv* is better at modelling biodiversity in the African test site than the Colombian test site (table 5.5).

Within the Colombian tile, the AICc scores for the ALB spatial aggregation are the only results which do not suggest SC is the most useful model of the set. A parameterisation of *GDiv* with an RST value of 163 performed the best, with the second best performing model being the RST 154 model. RST 154 had an AICc score 35.62 (unitless) higher than the RST 163 model. Given that Fotheringham *et al.* (2002) suggest that a relative difference in AICc scores of 3 is the minimum required to consider the models "different", RST 163 can be considered the single most useful model of this set under the ALB aggregation. The remaining spatial aggregations

within the Colombian test site all suggest that *Sc* is the most useful model of the set, with RST 181 being second most useful at the 10 km and half-degree grid aggregations and RST 163 being second most useful at the ecoregion aggregation (relative increases of AICc of 299.39, 70.91 and 15.04 respectively – all unitless values).

The AICc scores from the African test site suggest *Sc* is the most useful model of the set under three spatial aggregations (ALB and both grid aggregations). The second most useful model in all three cases was RST 181, with a relative AICc score of 11.15 unitless under ALB aggregation, 39.45 unitless under the 50 km grid and 139.52 unitless under the 10 km grid. Under the Ecoregion aggregation no single model was clearly the most useful, with RST 145, 235, 325 and 415 all falling within a relative AICc of 1 unitless. As such, it was not possible to select a single model as the "best" from this set based on the AICc scores.

Table 5.5. $\bar{R}^2$ values for the selected model of each set

Study Site	Model set	Model	$\bar{R}^2$ value
Africa	ALBs	*Sc*	0.75
	10 km grid	*Sc*	0.81
	50 km grid	*Sc*	0.79
Colombia	Ecoregions	*Sc*	0.69
	ALBs	RST 163	0.41
	10 km grid	*Sc*	0.48
	50 km grid	*Sc*	0.54

The $\bar{R}^2$ values show that the models generally explain a higher amount of variance in the biodiversity data for the African test site than the Colombian Andes (table 5.5) as all the African $\bar{R}^2$ values were greater than the Colombian values. The *Sc* model at the 10 km grid aggregation in Africa has the highest $\bar{R}^2$ (0.81) whilst the RST 163 model in the Colombian ALB set had the lowest ($\bar{R}^2$ = 0.41).

Taylor diagrams can be used to visualise model performance by comparing correlation coefficients and the distribution of modelled and observed data. The "spokes" of the wheel represent different correlation coefficient scores, whilst the standard deviation of the observation data is shown with black contour lines. In order to enable comparison between model runs across different aggregations and for both continents, all data were normalised against the relevant observation results (i.e. the results from the set of models generated using ecoregions in the African tile were normalised against the observations as aggregated to the African ecoregions, whilst the results from the set of models generated using a 10 km grid in the Colombian tile were normalised against the observations as aggregated to the Colombian

10 km grid etc.). This resulted in model assessment of the distribution of results expressed in terms of number of standard deviations away from the relevant observation dataset, thus allowing comparison between aggregations and continents (figure 5.12).

In general, the model runs from the African sets performed better than those in the Colombian sets, with all four model sets producing distributions within 0.5 standard deviations of the corresponding observational dataset and with correlation coefficients greater than 0.85. The set that had the closest distribution to - and highest correlation with - its observation dataset was the ecoregions set within Africa, followed by the African 10km grid. The two worst performing model sets were the 10 km and 50 km grids in the Colombian test site, with correlation coefficients of less than 0.7 and 0.8 respectively, and distributions falling over 0.5 standard deviations away from the observational dataset. All model sets are producing slightly narrower distributions than the observational data (i.e. all model sets fall beneath the 1:1 standard deviation curve in figure 5.12).

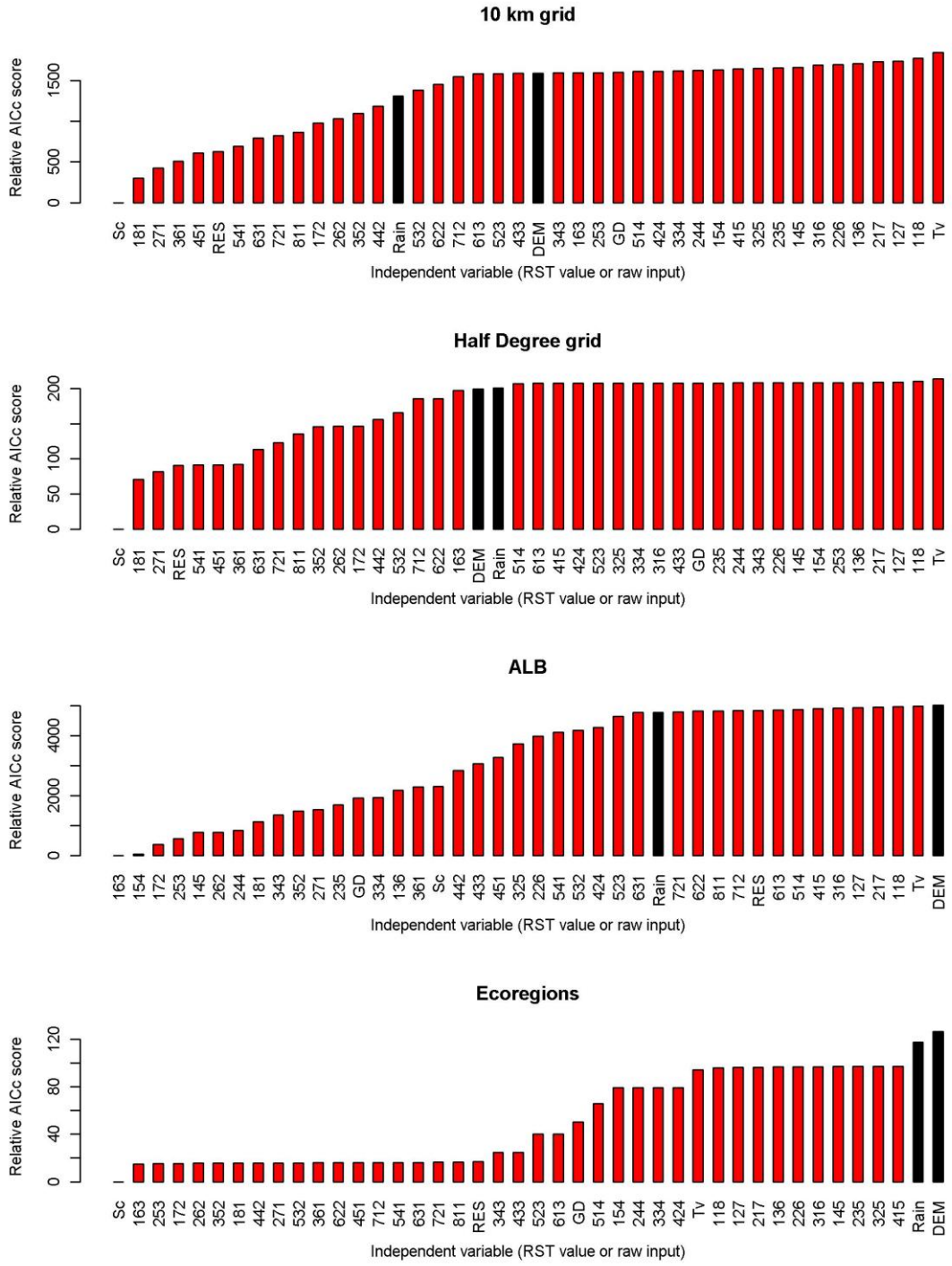

Figure 5.10. AICc scores for GWR models within the Colombian test site, using different parameterisations (weightings) of *GDiv*, as well as elevation and rainfall, as single explanatory variables for total biodiversity (as measured using IUCN distribution data) across four different spatial aggregations. The three digit numbers give the contributions of the three components of geodiversity to the weighted *GDiv* runs as an RST value (see section 5.3.4 for further information).

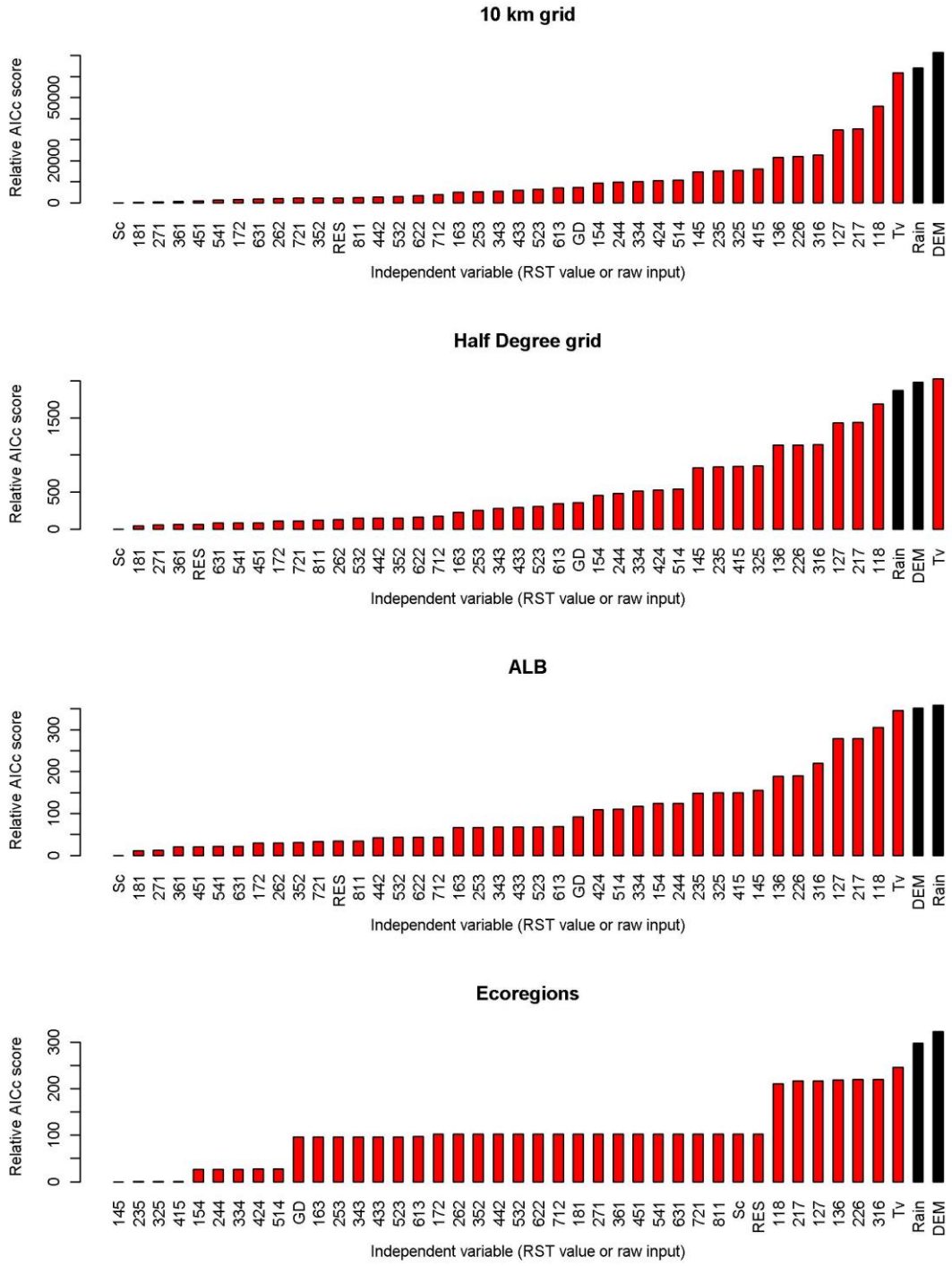

Figure 5.11. AICc scores for GWR models within the African test site, using different parameterisations (weightings) of *GDiv*, as well as elevation and rainfall, as single explanatory variables for total biodiversity (as measured using IUCN distribution data) across four different spatial aggregations. The three digit numbers give the contributions of the three components of geodiversity to the weighted *GDiv* runs as an RST value (see section 5.3.4 for further information).

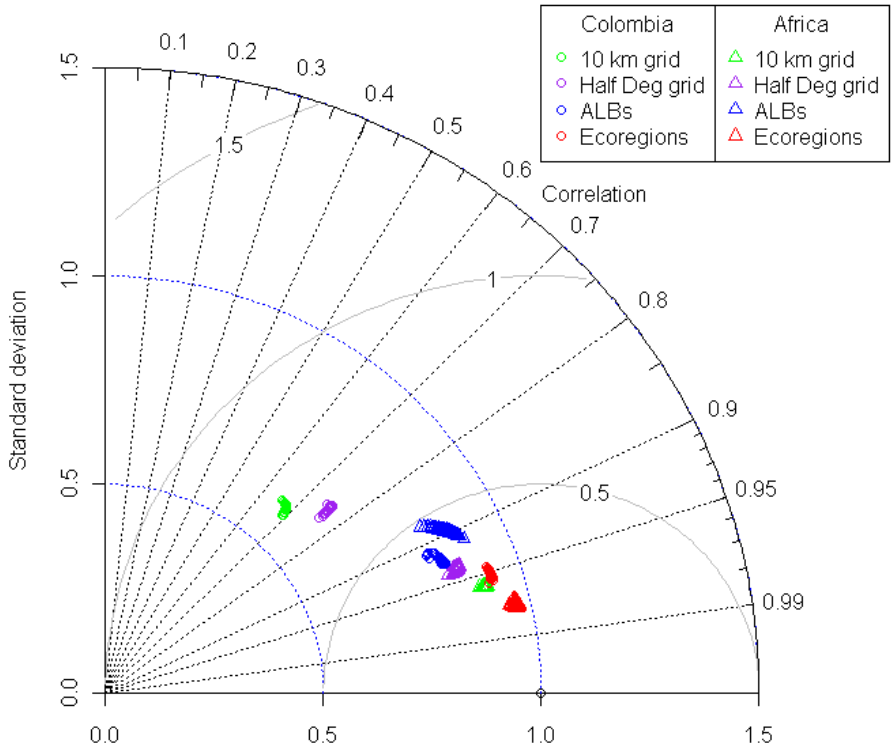

Figure 5.12. Taylor diagram showing results of GWR runs. Correlation coefficients are shown on the "spokes" coming from the origin, whilst the standard deviation of the observed dataset are shown with the blue contour lines. Grey contour lines represent RMSE of the modelled dataset compared to the reference dataset (shown at 1 on the X axis). Each of the 8 sets of simulations was normalised against the observation data relevant to that set (i.e. the overlay of species richness aggregated to the same spatial classification as those models in the model set), thus allowing inter-set comparison. The closer the model run is to the reference dataset (i.e. at the 1 standard deviation on the X axis), the better the model performance in terms of correlation coefficient (r score, black dashed lines), modelled distribution (standard deviations, blue contours) and RMSE (standard deviations, grey contours).

5.5. Discussion

It is important to emphasise that the results set out in this chapter do not provide a true validation of *GDiv* as a model of broad-scale trends in biodiversity but rather a testing against limited observation and interpretation data. Such a task is not possible with currently available biodiversity data. The results from *GDiv* are a true measure of pixel-level geodiversity, according to the theoretical model set out by Mulligan (2000) and Parks and

Mulligan (2010), however there is no equivalent pixel level biodiversity dataset. The data from GBIF would have provided a pixel level measure of biodiversity if it had been considerably more extensive, however there were not enough accessions with an accurate spatial reference to provide a useful validation dataset and there were large areas with no sampling effort. Steps that could be taken to improve this situation are outlined below. The data that was used for testing, i.e. richness calculated from the IUCN distribution surfaces, represents broad scale trends in IUCN redlist species' richness, as defined by 7000 experts governed by the IUCN (IUCN *et al.*, 2008a, IUCN *et al.*, 2008b, Ridgely *et al.*, 2003), however it does not represent pixel-scale biodiversity equivalent to the geodiversity results from *GDiv*. Instead the distribution maps represent "broad-brush" distributions which do not account for fragmented or spatially complex species extents. Furthermore, the dataset only represents a subset of total biodiversity. Whether there is a direct relationship between total biodiversity and this subset is unclear, however the data are widely used as an indicator of biodiversity (e.g. Bass *et al.*, 2010, Assessment, 2005).

Theoretically GBIF occurrence data could provide a suitable validation dataset, however in order for this to be viable then two significant changes would need to be made to the GBIF functionality and available data. First, an estimate of spatial error should be included with georeferenced records; this would allow non-experts to decide whether the data was positioned accurately enough for their purposes. This could be achieved using the technique outlined in section 5.2.1. If possible, the method of recording location should be recorded, along with the precision of the initial measure. Second, the ability to select by functional group would be a marked improvement in terms of downloading a relevant dataset. This would require adding broad functional group classifications (such as "tree", "crop" etc) to the existing data; a task which would require a large investment of effort in the dataset, but would bring about a substantial improvement in terms of usability of the data for non-taxon specific studies. The dataset would remain limited in terms of geographic coverage in tropical montane environments.

An alternative "true validation" dataset to GBIF would be to use tree species richness from detailed plot studies within tropical mountains such as the UNESCO Man And Biosphere permanent plots (Dallmeier *et al.*, 1992). Depending on the total number of studies, this could provide publically available actual species richness point data which could be used as the validation dataset for application at those sites. Whilst this inventory was not possible within the scope of this thesis, the benefit of such an inventory would extend beyond the topic of this thesis and would be a worthwhile investment of future time and research effort. A further

testing method that could be applied pan-tropically would be to use a polygon dataset of major ecosystem types (for example, delimiting the Congo Basin or the Albertine Mountains) and to investigate the degree of congruence between these ecological polygons and polygons obtained by classifying the geodiversity map into an appropriate number of classes. This analysis was not carried out due to time and computing constraints.

In the absence of a suitable validation set, the IUCN data represented the best possible dataset for a validation. The rest of this section discusses the results of the validation efforts and looks into the weight of evidence supporting the hypothesis that there is a relationship between geodiversity and overall levels of biodiversity. It will not be possible to fully quantify this relationship, due to the lack of a suitable validation dataset, and so any conclusions drawn need to be clear regarding what inference can be made from these results. The various spatial aggregations each had a different number of classes and therefore resulted in varying numbers of regression points being used in the model simulations; ecoregions had the fewest (18 in Africa and 20 in Colombia) and so any inference from these model runs must be made with caution.

5.5.1. Comparison of general patterns of geodiversity with general patterns of biodiversity

When comparing the patterns in geodiversity with those found in biodiversity using the results from Gaston (2000), it is important to remember that the patterns in Gaston are taxon specific (birds in the case of latitude, and bats in the case of elevation). Although these were selected as representing known patterns in diversity across all taxa and were therefore considered an acceptable representation of overall biodiversity, it is questionable whether the trends in diversity in these taxa can be generalised to those in others (Araujo *et al.*, 2004), given that one species can often not act as a the best proxy for other species even within a single order (Banks-Leite *et al.*, 2011). The results from the comparison with trends in geodiversity need to be carefully interpreted; similarities suggest that *GDiv* produces spatial patterns similar to the taxon in question for the environmental variable in question (e.g. birds and latitude), however this cannot be generalised to all biodiversity in all settings. Similarly, a lack of congruence between geodiversity patterns and the trends presented in Gaston (2000) do not rule out the validity of *GDiv* as the maps of geodiversity may show trends not captured in the taxon / location specific biodiversity datasets.

The latitudinal trends in bird diversity of Gaston (2000, figure 5.3) have 7 sites that appear to be outliers. It has not been possible to establish the locations of these sites; it is possible they represent mega-diverse island sites which fall outside the bounds of *GDiv*. Ignoring these outliers, there are similarities in the overall pattern between latitudinal bird diversity and latitudinal geodiversity; a peak in diversity just north of the equator, with a steeper decline in diversity towards the north when compared with the south. This steep decline could be due to the species-area relationship, given the smaller landmass of Central compared to Southern America.

The similarities between latitudinal bird diversity and *RES* and *Sc* are more apparent, whilst *Tv* shows few similarities with latitudinal bird diversity. Given that birds are more motile and able to migrate to avoid seasonal resource bottlenecks, it is perhaps unsurprising that bird diversity more closely matches *RES* and *Sc* latitudinal patterns. Since the test sites used for other validation efforts are at the same, equatorial, latitude it is possible that there is no impact of the seasonal resource bottleneck for these sites and that the effect of, and temporal structuring in, resources is to increase the amount of niche space rather than restrict the number of species supported within the region. Were *GDiv* to be developed for use outside the tropics it may be necessary to re-consider the role of *Tv* in the theoretical model; potentially taking the inverse of the current measure to decrease the value of *Tv* as seasonality increases or at least have a more complex relationship that recognises the reduction of biodiversity at very high levels of seasonality.

The variation of geodiversity with elevation within Peru, covering the same region as Gaston's (2000) elevation gradient example, does not show any clear trend in terms of mean geodiversity, whereas there is a clear decline of bat diversity with elevation in Gaston's data. This is a somewhat surprising result given the maps of raw geodiversity shown in chapter 4 (figure 4.8) and the scatter plot (figure 4.28), which show a decline in geodiversity with elevation. However, the map of geodiversity for the region in which this analysis was carried out shows a distinct mid-elevational peak in geodiversity, rather than the decline in geodiversity with elevation as seen in the map for the Colombian test site (figure 5.13). This change in the relationship between geodiversity and the inputs is an interesting discovery and suggests that the controls of overall geodiversity vary with location. This evidence for a mid-elevational peak in geodiversity does tie in with literature review of biodiversity patterns, as outlined in chapter 2 and with previous work with *GDiv* at the regional scale (Mulligan, 2000), however it does not provide validation of a relationship between geodiversity and Gaston's data.

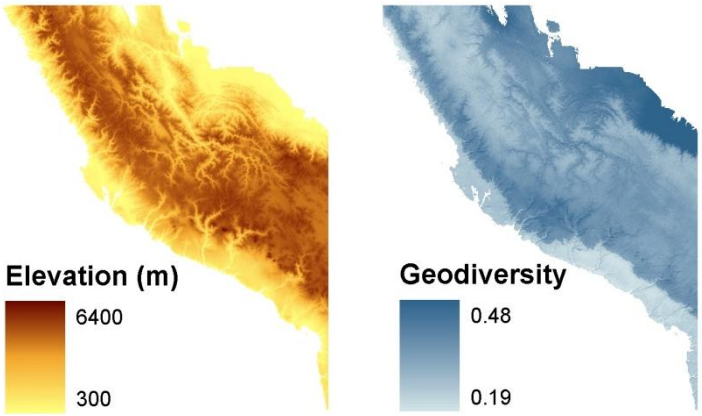

Figure 5.13. Elevation and geodiversity in the Peruvian test site used to validate *GDiv* against Gaston's (2000) data showing bat diversity as a function of elevation.

Whilst use of these patterns of general trends in bird and bat diversity has allowed exploration of the varying relationships between biodiversity and geodiversity, it has not provided a full validation of *GDiv* as a model for biodiversity. Some evidence in support of the capturing of general trends in bird diversity has been found in terms of the latitudinal gradient, however the relationship with the elevational gradient of bat diversity is less clearly established. Further disaggregation of the Gaston datasets would be beneficial, as this would allow greater interpretation of the results - particularly the outliers in the latitudinal bird diversity dataset. *GDiv* shows the weakest correlation with birds and mammals (table 5.4) meaning that generalising these results from taxon specific diversity to overall biodiversity is not a trivial matter.

5.5.2. Correlations between geodiversity and biodiversity

The correlation results enable interpretation of the relationship between geodiversity and biodiversity across a broad range of taxonomic and spatial aggregations, giving an overview of the strengths and weaknesses of the association at a range of scales. This detail of analysis was not possible using more complex analytical techniques, such as GWR, due to computing constraints.

It is clear that the correlation with plants is the weakest of all taxa; this is perhaps surprising given that plants, as structural species, are highly reliant on the physical environment. There are two potential reasons for this; the coarse taxonomic aggregation and the coarse spatial aggregation.

Taxonomically, the dataset used for plant diversity (Kier *et al.*, 2005) includes all plants and makes no effort to distinguish by functional group such as trees, epiphytes or lianas. Within the study site (the Colombian Andes), there are a high number of epiphytes in the mountainous cloud forests, which are more reliant on other plant diversity for their niche space, rather than the physical environment (Jarvis, 2005). Moreover, the datasets used in *GDiv* are based on surface measurements and so represent conditions at the top of the canopy; they do not take into account any canopy storage of water or interception of light for example. The plant dataset represents plant species richness regardless of physical location in the forest; the modelled geodiversity score could be very different to the geodiversity conditions at the forest floor when compared to the top of the canopy.

Spatially, the data was already aggregated to ecoregions, and so did not represent pixel-level diversity. This renders the dataset more susceptible to the modifiable areal unit problem whereby the aggregation of data to pre-defined polygons (i.e. ecoregions) may result in loss of information as the mean value for a region may not be representative for all locations within that region. This is likely to have been confounded by re-aggregating the plant data to alternative spatial aggregations, such as the ALBs or regular grids.

Of the IUCN data, amphibian species richness shows the strongest correlation with geodiversity across a range of spatial aggregations. This could be attributed to the heavy reliance of amphibians on availability of water (Gomez-Rodriguez *et al.*, 2010) - the most influential environmental factor in terms of raw geodiversity, however the strength of correlation between individual environmental inputs and amphibian diversity varies with spatial aggregation suggesting that there are different controls at different spatial scales. As the aggregation becomes finer (i.e. towards the 10 km grid), temperature, rainfall and elevation all have strong correlations with amphibian diversity (albeit a negative relationship with elevation), however the combination of these individual inputs into a measure of geodiversity gives a stronger correlation.

The results of the variance partitioning show that *GDiv* performs more consistently than the individual input variables in terms of explaining variation in the biodiversity surfaces across all taxonomic groups and spatial aggregations. This suggests that the *GDiv* outputs are less sensitive to the underlying structure of the input data (in terms of spatial aggregation and taxanomic group) and so may be less prone to model-overfit than the individual inputs. On the other hand the results could be interpreted as suggesting that, for a known taxonomic group

and a known spatial aggregation, the individual variables provide a more useful model of biodiversity.

This contrast between higher performance for specific taxa / aggragation combinations for some individual inputs (e.g. Rainfall and plant biodiversity at the 10 km aggregation) and the more consistent performance for *GD* across taxa and spatial aggregations ties in with the aim of *GDiv* to model overall trends in biodiversity, rather than to capture trends in specific taxonomic groups. With this in mind, the difference in performance between *GD* and *Tv* can be considered; whilst *GD* has a slightly lower mean explanatory power (16.17%, versus *Tv*'s 18.62%), it also has a lower standard deviation (5.24% versus 8.73%) suggesting that combining the three components into a single metric reduces the sensitivity of the model to the spatial aggregation and / or taxonomic group. Considering the results of the variance partitioning in light of figures 5.4 - 5.7, the use of non-linear regression techniques could improve the model fit, particularly in the case of amphibian richness at the 50 km grid, as well as bird and total IUCN richness at the 10 km grid.

5.5.3. Geographically Weighted Regression

According to the AICc results, *Sc* appears to be the most reliable predictor of biodiversity levels, suggesting that in the regions used in this study, spatial structure is more influential in determining biodiversity than temporal structure or overall resource availability. This could be an artefact of the equatorial location of the two study areas; each site showed very little temporal structure (figure 4.9) so there is little opportunity for seasonal niche differentiation. In terms of overall resource availability, the data presented in figures 3.4 and 3.7 shows some regions within each study site receive very little precipitation. However, within both study sites the regions with low precipitation are predominantly cloud forest (Mulligan, 1999) so a key component of the water supply will be from cloud interception. As this water would not be included in the precipitation dataset used in the *GDiv* runs, this represents a limitation of *GDiv* as the region is unlikely to be experiencing a resource bottleneck in terms of water.

Sc is not the best in-set model for the African ALBs and the Colombian ecoregions. Assuming the inclusion of the ecoregions is valid given the low number (20) of regression points (which may not be a valid assumption), it is possible that some of the spatial structure in the datasets is already captured by the aggregation technique, which are based on physical changes (in altitude or ecosystem) rather than a stratified sampling system. When stratified sampling is

used (i.e. both resolutions of grid aggregation), *Sc* is always the best intra-set model for both study sites.

Comparing the $\bar{R}^2$ results of the selected models for each aggregation across the two study regions, (a comparison that is not valid with the AICc scores) suggests that a greater proportion of biodiversity can be explained in the African study site than in the Colombian site. This can be attributed to the topographical differences in the two study sites; the Colombian Andes are a taller, more topographically diverse chain than the Central African Rift mountains (figure 3.4 and 3.7). As such, the 1 km resolution data is more susceptible to ecological fallacy, meaning the value of each pixel within the Colombian study site is likely to be less representative of the sub-pixel variability than an equivalent pixel in the African study site. The ecological fallacy would also apply to the biodiversity data, as the within-pixel variation in species richness of the Colombian site is likely to be greater than that of the African site (Figure 5.2).

A further difference between the two sites that could explain the difference in explanatory power is that the data used for the African GWR did not include bird species richness, as this was not available in SimTerra at the time. Given that *GDiv* showed weak correlation with bird diversity at all spatial aggregations (table 5.4), it is possible that the explanatory power of *GDiv* in the GWR runs based on all taxa was diluted by the inclusion of the bird data in Colombia. Additional GWR runs examining the taxon specific performance of *GDiv* for mammals and amphibians would be revealing.

This improved performance of *GDiv* in the African versus Colombian site is further highlighted in the Taylor plot (figure 5.12); all African model sets fall within 0.5 standard deviations of their respective validation dataset, whereas only the ALB and Ecoregions do so for the Colombian site. The Taylor plot also highlights the impact of the model weighting; only the ALBs showed a marked systematic response to weighting. With other spatial aggregations, there was a limited or non-systematic response to the varied weightings of the components in the final calculation. This suggests that use of a non-weighted model is justified, particularly in regions where no validation data is available for calibration of model weights.

The different model diagnostics tell different aspects of the story regarding the efficacy of *GDiv* at modelling biodiversity. The AICc scores suggest that *Sc* offers the best model within the majority of model sets, whilst the $\bar{R}^2$ scores suggest that more variation in the validation data can be explained in the African as opposed to Colombian site. The Taylor plot suggests that

there is little systematic response to the varied weightings within the model sets, and so a non-parameterised model may be most appropriate.

All the GWR analysis carried out was done on uni-variate explanatory variables; it was not possible to run multivariate models due to redundancy between *Sc*, *Tv* and *RES* as inputs. The sensitivity analysis presented in chapter 4 established that there was no redundancy at the raw input level (figure 4.28), and so a useful next step would be to run a multivariate GWR based on the raw inputs, prior to combination to *Sc*, *Tv* and *RES*.

5.5.4. Conclusions

The key objective of this chapter was to attempt to verify and validate a quantitative relationship between the results of *GDiv* and broad scale trends in biodiversity. Due to the nature of the problem a full validation was not, and will probably never, be possible; in order for this to be achieved a dataset of pan-tropical species richness at a 1km resolution would be required (in which case the *GDiv* modelling would hardly be necessary). Given this limitation, several smaller scale validations were attempted using a range of validation datasets and comparing the fit of models based on *GDiv* outputs and raw environmental variables. The results from *GDiv* have been demonstrated to provide a closer fit to the validation datasets than raw environmental variables, suggesting that using *GDiv* does provide added value.

Taking the results of all validation efforts into account, it is concluded that there is some degree of substantiation of a quantitative relationship between geodiversity and species richness as a measure of biodiversity, however this relationship varies across taxa and across terrain types with stronger relationships found between geodiversity and amphibians (tested in the Colombian Andes only), and overall stronger relationships between multi-taxon species richness in the less topographically complex African Rift Valley than the Colombian Andes. Therefore it is not possible to fully answer the research question, merely to state that there is some evidence in support of a quantifiable relationship between the *GDiv* and species richness within tropical mountains.

Areas with high overall geodiversity scores are likely to be hot, wet and temporally varied, whereas areas with low overall geodiversity will be relatively cooler, drier and perhaps less seasonal. This characterisation is of potential use in conservation planning as changes to these regimes will have implications for maintenance of biodiversity in protected areas. The next two chapters investigate the potential for applying *GDiv* in planning protected areas, both in terms of the effectiveness of current protected areas at conserving a range of different

habitats as defined by geodiversity and in terms of the robustness of the existing protected areas in the face of climate change that will impact upon geodiversity. Given that the results of the model validation in this chapter demonstrate little systematic benefit from weighting the components of *GDiv*, it was decided to use un-weighted outputs in subsequent experiments.

Chapter 6. Conservation of geodiversity and biodiversity within areas deemed important for conservation under internationally recognised prioritisation schemes.

6.1. Introduction

6.1.1. Prioritising conservation - the current state of affairs

Mountains tend to be highly biodiverse when compared with lowland regions of similar size; the presence of many climatic zones in close proximity, leads to higher habitat heterogeneity and increased niche space (Korner and Spehn, 2002). Biodiversity in the tropics tends to be higher than in temperate regions (e.g.Ding *et al.*, 2006), so tropical mountains tend to be more biodiverse than their temperate counterparts and, when corrected for area, more biodiverse than adjacent lowlands (Hamilton, 2002). Tropical mountains are also of high conservation value due to their a-biotic diversity - this can be termed geodiversity; diversity in overall resource availability, spatial structure in resources and temporal variability in resources (Parks and Mulligan, 2010). The key threats facing tropical mountains are increasing population growth which leads to urbanisation and encroachment of human infrastructure on previously undisturbed habitat (Burgess *et al.*, 2007). In addition to these "local" threats, the increasing global demand for high energy food coupled with technological advances in farming, has resulted in conversion of areas previously economically unviable as agricultural land as a result of global rather than local pressures (Lambin *et al.*, 2003).

These high levels of biodiversity and geodiversity mean tropical mountains are highly important, highly vulnerable ecosystems which, due to the threats of population growth and associated land-use change, are in urgent need of effective and strategic management; as such there is a CBD programme of work targeted specifically at mountain conservation (CBD, 2011). This programme highlights the high species richness and high levels of endemism found in mountain ecosystems, particularly tropical montane forests (TMFs). One of the major threats to mountain ecosystems is climate change. Endemic species tend to exist within a narrow range of environmental parameters; climate change may alter these niches thus squeezing out the highly specialised species since their isolated environment may not connect with other areas of similar characteristics to which they can ‘move’. Mountains are also important because of the services they provide to human beings, notably that of fresh water (providing fresh water to over half the world's human population (CBD, 2011)). Other outcomes of the threats to mountain ecosystems are habitat degradation, which leads to erosion of fertile soil

which in turn led to increased poverty and thus to increased conflict land use (Vanacker *et al.*, 2007).

The CBD Programme of Work for Mountains identifies four characteristics of mountain ecosystems:

- A high number of biodiversity hotspots
- A high level of cultural diversity and indigenous people
- Highly fragile ecosystems, particularly to climate change and land-use change
- The importance of upland / lowland interactions with regards to food production.

In order to tackle the vulnerabilities and importance of mountains arising from these characteristics, the CBD programme of work is divided into three elements, each with its own set of goals and actions:

- Direct actions for conservation / sustainable land use / benefit sharing
- Means of implementing the direct actions
- Supporting actions for the implementation

This clear policy requirement is somewhat restricted in terms of conservation action "on the ground" due to the limited amount of capital to fund conservation efforts, particularly in tropical regions (Macdonald and Service, 2006). As a result, prioritisation of conservation funds is necessary (Myers *et al.*, 2000). Given the wide variety of conservation organisations, there are many different approaches to this prioritisation and these vary according to the remit of the conservation organisation, as outlined in section 2.6.3. Whilst these schemes aid the individual organisations in operational strategy and the allocation of funds, the widely differing maps of prioritised areas (figure 2.11) can result in a confusing picture for non-specialists as to what regions on earth are really the most important for conservation efforts.

One solution to this is to use an overlay of all global conservation schemes in order to assess conservation priority. If an area is prioritised in all conservation schemes, it can be classified as high priority. Inclusion in only one scheme suggests that, whilst the area may be vital to the remit of one scheme it has low overall priority. It is important to note that this is not necessarily a measure of biodiversity, as the prioritisation schemes may not be based on diversity (as outlined below), rather it is a measure of congruence in prioritisation between different conservation organisations.

Mulligan (2011) calculated conservation importance within the tropics based on 1km resolution raster overlays of six prioritisation schemes; WWF G200 Ecoregions (G200), Birdlife

International Endemic Bird Areas (EBAs) and Important Bird Areas (IBAs), the Wildlife Conservation Society's Last of the Wild (LOTW) and Conservation International Biodiversity Hotspots (BH) and Key Biodiversity Areas (KBAs). These were selected to represent a broad range of prioritisation strategies, with measures of endemism (EBAs), conservation operational policy (IBAs and KBAs), importance and threat (Hotspots, G200) and pristineness (LOTW) (summarised in table 6.1). Whilst none of the schemes specifically target conservation of evolutionary processes (Mace and Purvis, 2008), each represents a different aspect of biodiversity and / or threat, so a high score on the combined overlay suggests an area is of conservation priority on a range of criteria.

Table 6.1. Summary of the conservation priority schemes used in (Mulligan, 2011) calculation of conservation importance.

Scheme	Number of regions	Percentage coverage of terrestrial surface	Operational or strategic
G200*	142	33.0	Strategic
EBA	218	4.5	Strategic
IBA	10448	0.3	Operational
LOTW	569	17.0	Strategic
BH	34	2.3	Strategic
KBA	>20000	5.7	Operational

* excluding 53 fresh-water and 43 marine

The aims of this chapter are two-fold. First, the extent to which conservation-important areas consistently prioritise areas of high biodiversity (as estimated by multitaxon species richness) and / or high geodiversity will be investigated. By comparing the proportion of overall biodiversity and geodiversity per unit area for each class of conservation-importance, the effectiveness of the conservation prioritisation scheme in highlighting areas of bio and geo diversity can be assessed. Regions deemed important on many prioritisation schemes would be expected to select a higher proportion of biodiversity and /or geodiversity than would be expected by area alone; if this is found those regions can be deemed conservation efficient. Whilst this does not measure the success at conserving different ecosystems or the ease of enforcing protection, it does enable assessment of conservation efficiency as one of many dimensions of conservation prioritisation success. The second aim of this chapter is to assess the congruence of individual prioritisation schemes with bio and geo diversity - i.e. to establish whether individual conservation prioritisation schemes are conservation efficient for the area which they cover. In this case, KBAs were selected for analysis; this scheme was selected as it is meant to represent operational policy and therefore ought to conserve efficiently in order to make best use of limited funds.

6.2. Methods

6.2.1. Methodological strategy

This chapter will examine the relationship between geodiversity and conservation importance, as outlined above. One of the conditions for success of conservation schemes is to conserve the maximum diversity per unit area efficiently so the sum of geodiversity scores and species richness (in terms of mammals and amphibians) within each level of prioritisation will be calculated in order to establish whether conservation important regions are conserving a greater proportion of geodiversity or biodiversity than would be expected by area alone. In addition to testing the effectiveness of the combined prioritisation schemes (i.e. conservation importance), the efficiency of KBAs alone was also tested. The analyses were run for the three ten degree study areas: the Colombian Andes, the Albertine Rift and Papua New Guinea.

6.2.2. Data

To generate the geodiversity maps for use in these analyses, a *GDiv* simulation using a standard configuration was utilised (i.e. the three components of geodiversity were equally weighted). The resulting geodiversity map for the Colombian Andes has been presented and discussed in chapter 4 (figure 4.8). Geodiversity in the other two test sites follows a similar pattern of decreasing with altitude (figure 4.8). In Papua New Guinea, the highest levels of geodiversity are focused in a hotspot to the south-east of the island's mountainous region, whilst in the Albertine Rift the highest levels are found at the southern end of the tile. This suggests a varying relationship between geodiversity and latitude in the two continents; see chapter 4.4 for further discussion.

Species richness overlays were used based on IUCN distributions for mammals and amphibians, the only datasets available for all study sites at the time of analysis (figure 6.1). According to these data Papua New Guinea is much less species rich than the other two sites, however has a high level of endemism according to Kier *et al.* (2009).

The conservation importance overlays show that the mountains of Papua New Guinea are less highly prioritised than those of Colombia or the Albertine mountain range. The majority of the Colombian Andes are prioritised by three schemes, whilst the majority of the Papua New Guinean mountains score 2. There is no dominant score within the African study region, however the more northern mountains are more highly prioritised than the southern portion.

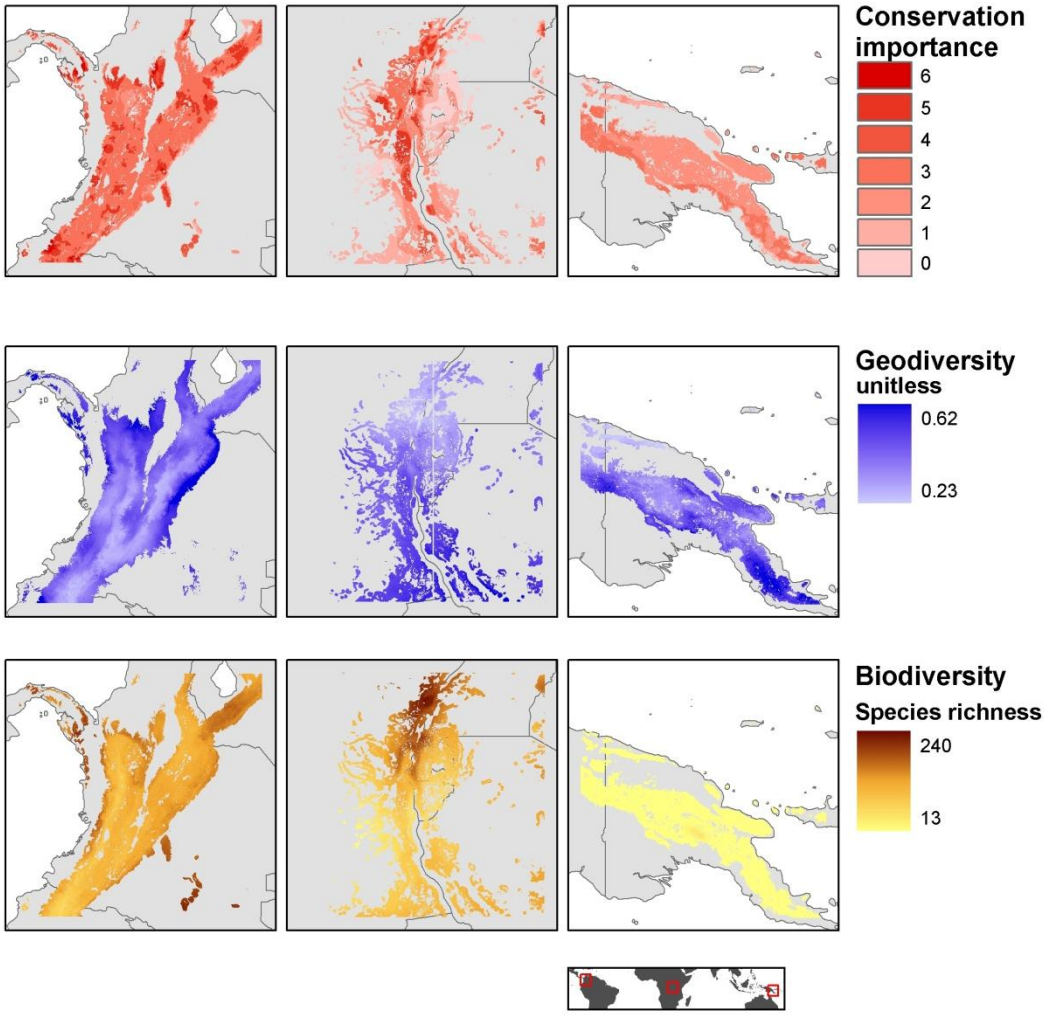

Figure 6.1. Data used in the analyses. The top row shows a measure of conservation-importance (Mulligan, 2011) for each study site, the middle row shows geodiversity scores (as outlined in chapter 4), whilst the bottom row shows species richness (based on IUCN red-list distributions for mammals and amphibians at all threat ranges (IUCN *et al.*, 2008a, IUCN *et al.*, 2008b). Note that, whilst Papua New Guinea appears to have a lower overall species richness, there are high levels of endemism.

Analysis of the efficiency of KBAs alone was only possible for the Colombian Andes and the Albertine Rift (figure 6.2), as no KBAs were present within the Papua New Guinean mountains. 23% of the Colombian Andes tile are within a KBA, compared with 19% of the Albertine Rift mountains tile. KBAs are defined using a multi-criteria approach to identify regions which contain vulnerable and irreplaceable species (Eken *et al.*, 2004):

1. Presence of vulnerable, endangered or critically endangered species (based on IUCN assessments)
2. Range restricted species

3. Biome restricted species
4. Important breeding / roosting sites

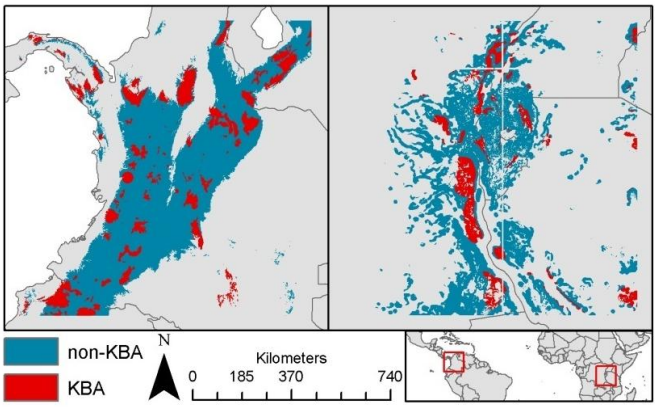

Figure 6.2. KBAs for the Colombian Andes and the Albertine Rift study sites.

6.2.3. GIS Analysis

All GIS processing was carried out using ESRI ArcGIS version 9.3 (ESRI, 2008), whilst the statistical analyses were implemented in R version 2.11.0 (R Team, 2010). The initial GIS processing consisted of preparing the three classes of data; the geodiversity maps, the biodiversity maps and the conservation priority maps. To prepare the geodiversity scores for each study region, the results of an un-weighted simulation on *GDiv* were converted to ESRI grids using ArcGIS 9.3. The species richness maps were calculated by overlaying the IUCN mammal and amphibian richness maps as ESRI grids. In order to prepare the conservation priority data the floating point PCRaster maps were converted to ESRI grids. These were then reclassified to give integer values representing ranked conservation priority scores (between 0 and 6).

For each study region, the proportion of total geodiversity and proportion of biodiversity conserved within each bio-importance class (0 – 6) was calculated. These proportional values were then used to calculate a conservation efficiency ratio for each class of conservation importance

$$CE_c = \frac{\sum D_c}{\sum A_c} \qquad 37$$

where CE_c represents the conservation efficiency for the conservation importance class c, D_c represents the diversity (either bio- or geo) contained within class c and A_c represents the total area of that conservation importance class. *CE* ratios for low conservation importance classes would be expected to have a conservation efficiency ratio of less than 1, whilst higher conservation importance classes would be expected to have a conservation efficiency ratio greater than 1. Similarly, the ratio of geo- and bio-diversity within and outside KBAs were

calculated, allowing the calculation of the conservation efficiency ratios of KBAs. These procedures are summarised in figure 6.3.

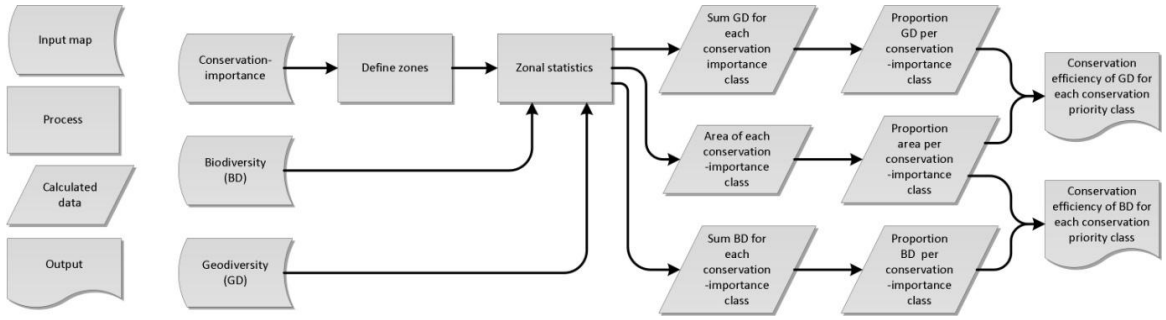

Figure 6.3. Work-flow implemented for each region.

6.3. Results

6.3.1. Efficiency of conservation-important areas in conserving species richness and geodiversity

The conservation efficiency ratio within all classes of conservation importance is approximately 1:1 for both geodiversity and species richness and across all three study regions (Table 6.2). The only exceptions to this are found in Papua New Guinea, where class 1 conserves biodiversity at a ratio of 0.555, whilst class 2 conserves biodiversity at a ratio of 0.876. When the proportions of biodiversity and geodiversity included within each level of conservation priority are compared with the proportion of area covered by each level of conservation priority, there is no significant difference across any of the study regions ($p < 0.99$ in all cases based on t-scores).

Table 6.2. Conservation efficiency ratios of biodiversity and geodiversity conserved per unit area at each of the conservation-importance classes found within the three study sites. Values in brackets give the rank score based on the conservation efficiency ratio.

Conservation-	Colombia		Africa		Papua New Guinea	
importance level	Biodiversity	Geodiversity	Biodiversity	Geodiversity	Biodiversity	Geodiversity
0	1.061 (3)	1.281 (1)	0.952 (6)	0.930 (7)	0.555 (4)	0.992 (2)
1	0.072 (2)	1.102 (2)	0.916 (7)	1.042 (1)	0.876 (3)	0.942 (4)
2	1.038 (5)	1.061 (5)	0.986 (5)	1.036 (3)	1.038 (1)	0.992 (3)
3	0.978 (7)	0.970 (7)	1.133 (1)	0.940 (6)	0.959 (2)	1.048 (1)
4	1.110 (1)	1.094 (3)	1.049 (3)	1.037 (2)	-	-
5	1.017 (6)	1.006 (6)	1.129 (2)	0.971 (4)	-	-
6	1.056 (4)	1.085 (4)	1.046 (4)	0.955 (5)	-	-

When considering the relationship between increasing conservation-importance and conservation efficiency ratios, the strongest rank correlation found was between the conservation efficiency of biodiversity and the conservation-importance class in Papua New Guinea (r_s = 0.800, p = 0.333), Table 6.3). The weakest correlation is found in Africa between conservation-importance and geodiversity conservation efficiency (r_s = 0.036, p = 0.964). In Colombia, negative correlations are found for both biodiversity and geodiversity conservation efficiency (r_s = −0.250, p = 0.595 and r_s = −0.536, p = 0.236 respectively). None of these correlations enabled rejection of the null hypothesis at the 10% level; the most statistically significant correlation came between African species richness and conservation-importance (r_s = 0.643, p = 0.139).

Table 6.3. Spearman Rank Correlation Coefficients (r_s) for ranked conservation efficiency at each conservation-importance class. The value in brackets gives the two tailed p value for accepting the null hypothesis of r_s = 0. There were no significant results at the p < 0.10 level.

Study Region (n)	r_s Biodiversity~ Conservation-importance	r_s Geodiversity~ Conservation-importance
Colombia (7)	-0.250 (0.595)	-0.536 (0.236)
Africa (7)	0.643 (0.139)	0.036 (0.964)
Papua New Guinea (4)	0.800 (0.333)	0.400 (0.750)

6.3.2. Efficiency of KBAs to maximise species richness and geodiversity

Whilst KBAs do maximise biodiversity and geodiversity more efficiently than non KBA regions in both study sites (Table 6.4), this difference is not significant (p > 0.999, based on t-test scores).

Table 6.4. Conservation efficiency for biodiversity and geodiversity within and outside KBAs for Colombia and Africa.

	Colombia		Africa	
	Biodiversity	Geodiversity	Biodiversity	Geodiversity
Non-KBA	0.990	0.993	0.988	0.999
KBA	1.044	1.031	1.061	1.007

6.4. Discussion

The results presented here suggest that conservation-important areas, as a whole, are not conservation efficient in terms of prioritising species richness or geodiversity. Furthermore, KBAs appear to not effectively select for species richness (in terms of mammals and amphibians) or geodiversity (as a measure of abiotic diversity). These findings are somewhat concerning, given the need for economically efficient conservation. Whilst this is not an unprecedented finding (e.g. Williams *et al.*, 2000, Balletto *et al.*, 2010, Rodrigues *et al.*, 2004), it is important to fully explore the limitations of the techniques implemented here before reaching the conclusion that the conservation important areas are not maximising the species richness and geodiversity that should be protected . The following section will consider the potential reasons for the results presented here, issues with using species richness and geodiversity as measures of prioritisation success, the implications of combining very different conservation prioritisation schemes into a single metric and the repercussions for conservation strategy if further support for the findings presented here is found. For a fuller discussion of gap analyses and complementarity in conservation prioritisation, see chapter 2.6.2.

6.4.1. Bio-importance across the three study sites

Limited interpretation can be made from the Papua New Guinean results given the small sample size in terms of different conservation-importance classes (n = 4).

The Colombian Andes are a hotspot of bird diversity in terms of both species richness and endemism (Myers *et al.*, 2000), however the analyses presented here used species richness of amphibians and mammals as the biotic measure of success - a potential reason for the negative correlations between conservation importance and conservation efficiency. As bird richness data was available for the Colombian Andes (Ridgely *et al.*, 2003), the analysis was re-run using both bird richness alone and combined bird, mammal and amphibian richness as success metrics. Negative correlations with conservation importance were still found for species richness across all three taxa (r_s = -0.393, p = 0.396), however a positive correlation was found between conservation importance and bird species richness (r_s = 0.500, p = 0.267). Whilst this is not a significant correlation it does suggest that more conservation important areas are conserving bird richness efficiently, a reassuring finding given that approximately 10% of the birds in the Tropical Andes biodiversity hotspot are classed as "Threatened" (Conservation International, 2011b)

The African site has a higher level of mammalian richness than the other two sites, with 208 species included in the IUCN assessment of the area, compared with 185 in the Colombian Andes and 80 in Papua New Guinea (IUCN *et al.*, 2008b). Given the iconic status of many of these mammals (for example, the mountain gorilla *Gorilla beringei*), it is vital that these areas are efficiently prioritised. The results from these analyses provided the most significant correlation ($r_s = 0.643$, $p = 0.139$) which suggests that for mammals and amphibians the conservation prioritisation schemes are giving prioritisation efficiency.

Given the history of conservation through state owned protected areas in sub-Saharan Africa (Macdonald and Service, 2006), it is perhaps unsurprising that species attractive to tourists are being efficiently conserved. Whilst the prioritisation schemes included in the conservation importance overlay do not actively prioritise touristic regions, they do include measures of current operational sites which tend to fall within national parks, meaning that charismatic species of interest to tourism could have a disproportionate influence over prioritisation schemes. This means that mammals would tend to be effectively conserved, whilst less iconic species may not be. When these analyses were repeated using mammal richness alone as the metric of success a significant correlation between bio-importance and mammalian richness was found ($r_s = 0.786$, $p = 0.048$), further supporting this argument.

Overall, it appears that species richness is being conserved more efficiently than geodiversity across all three continents. Whilst this may seem unsurprising, given the species level focus of the majority of prioritisation schemes, it is nonetheless concerning, given the need to conserve as yet unrecorded species and a range of habitat types. This is of particular pertinence in tropical mountains which, due to their inaccessibility, are one of the most under-sampled ecosystems on Earth. Future conservation prioritisation schemes, or modifications to existing schemes, may wish to incorporate geodiversity into the relevant strategies and consider the prioritization efficiency of geodiversity as a technique for achieving this.

6.4.2. Conservation efficiency of KBAs

Whilst KBAs have been criticised for failing to take local expertise into account, and not considering landscape connectivity (Knight *et al.*, 2007), the results presented here give limited support to the conservation efficiency of KBAs, albeit with a low conservation efficiency ratio across both sites. The fact that species richness is again conserved more efficiently than geodiversity highlights the need for abiotic diversity to be included in conservation planning; conserving geodiversity ought to lead to protection of a wide diversity of species both known

and unknown to science (Parks and Mulligan, 2010). The regions used in these analyses both have challenging socio-political settings which renders effective conservation difficult for differing reasons.

The Colombian Andes are home to two key ecosystems, tropical montane forest and paramo, both of which provide valuable ecosystem services in terms of fresh water production, with over 50% of Colombia's population reliant on water originating from paramo (Nature Conservancy, 2011). The political situation in Colombia plays a complex role in the pressures on the natural environment; whilst the presence of guerrilla groups discourages use of forestland for cattle farming (McLeod, 2010), guerrilla groups such as FARC (the Revolutionary Armed Forces of Colombia) tend to be based in inaccessible mountain regions, and tend to fund their operations through illegal drug trafficking leading to conversion of forest to coca plantations (predominantly in the lowlands, but to some degree in the lower elevations of the mountainous study region of this thesis) and pollution of water courses with chemicals used in the initial stages of cocaine production (Davalos *et al.*, 2011).

The pressure from coca cultivation is, to some degree, lessening through aerial spraying and reduced control by guerrilla groups (Housego, 2005), however the outcomes of this are increased pollution from the herbicides and increasing illegal conversion of forest to agriculture. Thus, regardless of the improved social stability, the pressures on the environment remain or even increase (Davalos *et al.*, 2011), highlighting the need for robust policing in this region to maintain conservation effectiveness of the existing protected area network, including the KBA sites.

The African study site covers parts of Uganda, the Democratic Republic of Congo (DRC), Rwanda, Burundi and the Republic of Tanzania. Of these, only the Republic of Tanzania has remained relatively peaceful over the past 50 years, with the remaining countries being witness to some of the recent past's most horrific civil wars including the Rwandan Genocide of 1994 and Africa's "Great War", the DRC's civil war in which Rwanda, Uganda and Burundi were also involved (along with other nations outside the study area used in these analyses). Due to the civil unrest in the region, there are large numbers of refugees and Internally Displaced People (IDPs) in all countries within the African study site (CIA, 2011).

This high level of conflict has impacted on conservation efforts in a number of ways; whilst the DRC's international wood trading industry collapsed, the high level of IDPs and refugees puts pressure on the remaining forests for firewood and clearance for agriculture, along with an

increase in bushmeat hunting for subsistence and trade (Draulans and Van Krunkelsven, 2002). Whilst it may be expected that conflict causes a decrease in policing of protected areas, research by de Merode *et al.*, (2007) has suggested that the opposite may be the case; during times of conflict the number of anti-poaching patrols remained the same as pre-conflict levels suggesting the increase in bush-meat trade was due to the increased pressure on natural resources. However, the same research also found that within periods of conflict, there is a negative association between the number of anti-poaching patrols (which showed daily variation within each period) and the amount of bushmeat trading, suggesting the relationship between hunting pressure, policing and conflict is complex, and highlighting the need for effective policing (Hanson *et al.*, 2009). The direct and indirect pressures combine to increase the threat to - and vulnerability of - prioritised conservation areas in the region, again highlighting the need to protect conservation efficient areas.

6.4.3. Success metrics

A limitation of the analyses carried out here is that the success metrics used to assess prioritisation efficiency (i.e. mammal / amphibian richness, or geodiversity) may not be the most appropriate metrics to assess the successes of conservation important regions. This is particularly pertinent when considering the taxon based prioritisation schemes included in bio-importance, such as IBAs and EBAs, which may target taxa not included in the measure of biodiversity we are using. However, the fact remains that bio-important areas and KBAs are not more efficient at conserving mammal and amphibian richness than areas not falling in these schemes.

On the other hand, using species richness as a measure of prioritisation success does not take into account levels of endemism, meaning the irreplacability of species is not accounted for by this success metric. To some degree using geodiversity as a success metric tackles this issue by prioritising a variety of habitats and resource regimes, however future research should attempt to include a direct measure of endemism.

In terms of using conservation importance as a technique to assess overall prioritisation efficiency, it is possible that the layers selected for the calculation of conservation importance may not be directly comparable. For example, LOTW covers large tracts of pristine habitats, meaning any given pixel in the dataset is more likely to be included in LOTW than KBA or IBA which are smaller, operational units. Future work evaluating the importance of each prioritisation scheme in determining overall conservation importance, and the impact of

varying the definition of conservation importance on the analysis presented here, would prove valuable in further determining the collective effectiveness of conservation prioritisation schemes.

Furthermore, examining the definition of conservation importance used raises an important philosophical issue; some of the schemes included may cancel each other out as they have different aims and objectives representing pro-active and reactive conservation schemes which have been found to have complimentary spatial distributions (Brooks *et al.*, 2006). This could result in regions with the same conservation importance score not being directly comparable. For example, whilst BH implicitly include "at risk" in their definition, other schemes included in the conservation importance overlay exclusively prioritise pristine environments (LOTW) meaning areas included on these schemes probably do not specifically contain at risk biodiversity. This phenomena will be of greater impact in low - mid scoring regions, meaning that whilst high scoring conservation important regions are considered important on a suite of measures, mid to low scoring regions should not be considered conservation unimportant, depending on which schemes do prioritise them. Recent work by Mulligan (unpub.) has produced an overlay inversely weighting each prioritisation scheme by area so that schemes covering a large area have a smaller influence per pixel than those covering a small area. Development of metric of conservation importance would improve the robustness of the results presented here.

6.5. Conclusions and future directions

The key conclusion that can be drawn from these analyses is that there is a lack of evidence for prioritisation efficiency within areas that are deemed conservation important, as well as within KBAs when measured against mammalian and amphibian species richness or with geodiversity, although there tends to be greater prioritisation efficiency for the species based measures rather than geodiversity. When success metrics appropriate to the region are used individually (i.e. birds in the Colombian Andes and mammals in the Albertine Rift), conservation-important areas are more prioritisation efficient than when tested using the global success metrics. Whilst KBAs did demonstrate some prioritisation efficiency, this was not significant; a worrying finding given that these are operational units. Future analysis should look to further classify the KBAs included in the analyses as some may be watershed or indigenous reserves, rather than areas specifically targeting biodiversity conservation.

Future work should focus on two themes, first creating more sophisticated success metrics and secondly refining the definition of conservation importance. By developing success metrics that combine the important elements of conservation, a more robust analysis of conservation efficiency will be possible. These metrics should make use of new datasets of species richness that are available (for example, threatened bird distribution data is now available for the rest of the world (Birdlife International, 2011a), whilst reptile distribution data is due to become available from the IUCN shortly (IUCN, 2011)), along with measures of endemism that have been derived from these datasets and a measure of ecosystem diversity. A measure of vulnerability could also be included, based on a per-pixel calculation of the number of species within each of the IUCN threat classes. With regards to refining the definition of bio-importance, future work should continue to develop Mulligan's unpublished work changing the weight that each of the prioritisation schemes holds in determining overall conservation importance, and look to ensure that no one scheme is disproportionately influential in determining the final conservation importance score of a region.

Chapter 7 Defining climate change stable conservation corridors for tropical mountains.

7.1. Introduction

7.1.1. Climate change modelling

The Intergovernmental Panel on Climate Change (IPCC) commissioned a Special Report on Emissions Scenarios (SRES). The purpose of the SRES was to develop a suite of future socio-economic scenarios which would enable systematic modelling of a range of possible climate outcomes. SRES devised four storylines, each of which describes a different potential future world, a range of population and economic projections, as well as potential technological developments. The 40 scenarios are different quantitative interpretations of these storylines which cover a range of uncertainties in terms of greenhouse gas emissions. The emissions from each scenario are purely a result of the economic, population and technological developments, as the scenarios do not refer to any specific emission reduction schemes. No probabilities or likelihoods are assigned to the scenarios, they are all considered equally valid (IPCC, 2000). Table 7.1 summarises the four storylines.

Climate change projections based on running General Circulation Models (GCM) on these scenarios result in a range of potential outcomes in terms of overall change in temperature and precipitation, as well as changes in seasonality. As with all models, there are uncertainties associated with each GCM, resulting in differences in model outputs. Work in South America by van Soesbergen (2011) comparing the outputs of 5 GCM models found that differences vary both spatially and temporally. For temperature, there tends to be a generally good agreement between model outcomes in lowlands, with increasing disagreement in mountainous regions - particularly in winter months (figure 7.1). This high level of model uncertainty in mountainous regions can be attributed to the coarse scale at which the GCM models run; the coarse resolution can be downscaled to some extent, however the complex terrain of mountain ranges means a much finer scale is required to reduce the uncertainty. With regards to precipitation, van Soesbergen (2011) found a generally higher level of model disagreement when compared to temperature, and that this was predominantly in the north-east of the region. There was less marked seasonal variation in the precipitation change results, however it is interesting to note that the summer disagreement tends to be focused on the coastal strip whilst the winter disagreement is more wide-spread across the Amazon basin (figure 7.1).

As outlined in chapter 2, the key impacts of climate change are likely to be changes in precipitation, increases in temperature and mean sea-level as well as an increasing number of extreme climate events (Harris *et al.*, 2006). In tropical mountains these effects are likely to be more acute, due to the steep climatic gradients associated with topographic heterogeneity. In general, it is expected that existing habitat and climatic envelopes will exhibit an upwards shift, with high-altitude habitats disappearing (Mansergh *et al.*, 2008). The results of climate change on existing protected areas within mountains would therefore include a shift towards lower-altitude habitats and species compositions being present within the park boundaries.

Table 7.1. Key features of the four SRES storylines (IPCC, 2000).

Storyline	**Population**	**Economic growth (overall)**	**Economic disparity**	**Technological development**
A1 "Technological world"	Peaks 2050	Rapid growth	Converging	Fast. Three sub-storylines: A1F: fossil fuel intensive A1T: non-fossil fuel sources A1B: balanced fuel sources
A2 "Heterogeneous world"	Continues to grow	Regionally fragmented	Diverging	Regionally fragmented
B1 "Global solutions"	Peaks 2050	Moves to a service focus	Converging	Focussed on clean technology
B2 "Local solutions"	Continues to grow (slower than A2)	Intermediate growth	Converging, focus on local solutions	Moderate

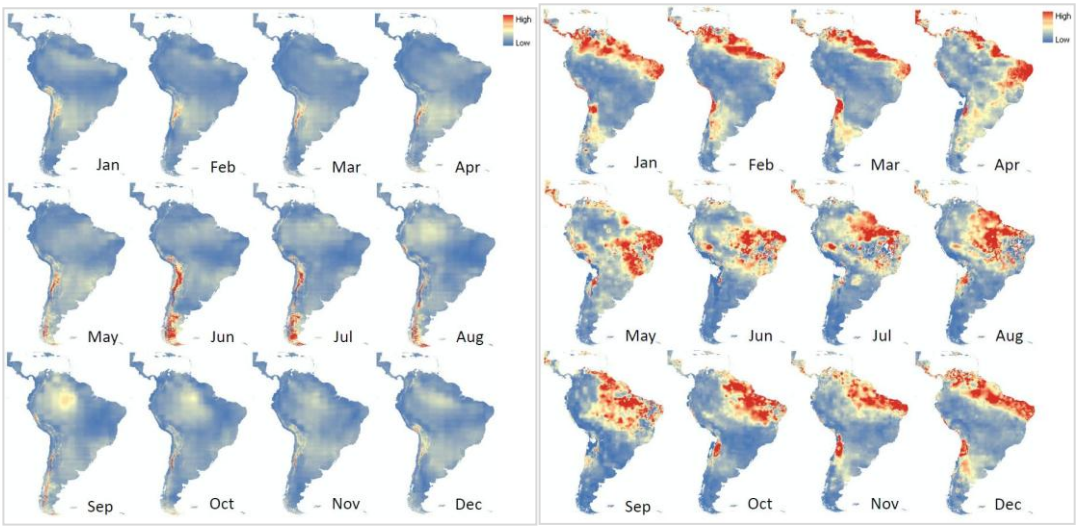

Figure 7.1. From van Soesbergen (2011). Co-efficient of variation (%) for 5 GCM models across South America for temperature (top) and precipitation (bottom). Calculations were based on results for the 2050s from CCCMA_CGCM31, CSIRO_MK30, IPSL_CM4, MPI_ECHAM5 and UKMO_HADCM3 (see text for further details).

7.1.2. Conservation corridors

Conservation efforts need to allow for conservation of both current ecology into the future and provide space for future evolution. As outlined in section 2.1.4, conservation of diverging clades allows for adaptation and evolution as a result of the selection pressure exerted by climatic change, whilst conservation of monophyletic groups ensures rare endemic species are protected (Erwin, 1991). Evolutionary response to anthropogenic environmental change has been recorded in a number of organisms from a variety of geographical regions, for example the dominant phenotype of *Biston betularia* (the UK peppered moth) has changed from white to brown in response to increasing pollution and resultant darkening of its habitat during the industrial revolution (e.g. Haldane, 1956), and has been recognised as occurring on ecologically significant time-frames, i.e. over decades to centuries as opposed to over millennia (Carroll *et al.*, 2007). However, in species with long generation times, such as slow-growing hardwood trees, the ability to evolutionarily adapt to rapid environmental change is reduced; by the time natural selection has had the opportunity to "act", the current climate may have changed again.

Existing protected areas have generally been designed to conserve habitats which are suitable for the target species, ecosystems or landscapes within them as defined under current climate conditions. The fragmented nature of the protected areas network means that – where they become islands in a sea of human-dominated landuse- genetic isolation is more likely to occur, thus further reducing the ability of populations to respond adaptively to climate change and

associated habitat changes within the existing protected area network (Harrison, 1992). One strategy introduced to overcome the problem of fragmentation is that of conservation of habitat corridors - sections of conserved habitat designed to create connectivity between existing protected areas (Halpin, 1997). The design of corridors is a complex issue impacted by physical factors such as corridor shape and size as well as socio-economic issues such as the conflict between conservation and other land uses, as well as local political tensions (Knight *et al.*, 2011). Despite these challenges, they have proven effective tools for conservation of biodiversity under the current climate regime (Damschen *et al.*, 2006) and are currently used as a conservation tool by many organisations (e.g. Conservation International, 2012, Bank, 2011, Wood, 2007) also with a view to long term conservation in the face of climate change.

Given the non-static nature of biodiversity (Pressey *et al.*, 2007) and the likelihood that climate change will "shift" habitats, one strategy which would allow species with a slower reproductive cycle to adapt to climate change is the introduction of corridors that account for these shifting habitats. The term "biolinks" has been used by Mansergh *et al.* (2008) to describe areas of land that are not within existing conservation schemes, but which may prove vital under future climate regimes. This term will not be used here, as the proposed corridors will be targeting geodiversity rather than biodiversity.

This section of the thesis examines future projections of geodiversity within the Colombian Andes study region and aims to answer the third research question of the thesis:
What are the likely impacts of climate change on the spatial distribution of current geodiversity and what are the implications of this in terms of the suitability of the current protected area configuration to protect geodiversity and thus biodiversity?

7.2. Methods

7.2.1. Methodological strategy

In order to achieve the stated aims for this chapter, changes in the three components of geodiversity were examined, along with the changes in the combination of these (rather than looking at only changes in overall geodiversity score) because there could be key differences in the resource regimes of sites with the same pixel-level geodiversity score that render the current assemblage of species within the area untenable under future climates. Current geodiversity was therefore classified to give unique geodiversity classes, each representing a unique combination of *RES*, *Sc* and *Tv*. This classification was then applied to *GDiv* simulations for future distributions of geodiversity based on GCM projected climate data for future

precipitation and temperature for two time periods, allowing a calculation of the changes in geodiversity classes across Colombian mountains from the current baseline over the two time periods. These change maps were used in conjunction with a map of current protected areas to evaluate the vulnerabilities in the existing protected area network to future climate change with respect to protected areas that would change in geodiversity class. Figure 7.2 shows the workflow for the GIS analysis used in this chapter.

7.2.2. Data

Current geodiversity levels were calculated first based on the standard *GDiv* parameterisation outlined in chapter 4, whilst projected geodiversity and *Sc* were calculated using precipitation and temperature data based on the mean of five models, the Canadian Centre for Climate Modelling and Analysis (CGCM3.1, CCCMA, 2010), the Commonwealth Scientific and Industrial Research Organisation's Mk3.0 coupled climate model (CSIRO_MK30, CSIRO, 2005), the Institut Pierre Simon Laplace CM4 (IPSL_CM4, IPSL, 2005), the Max-Planck-Institute for Meteorology ECHAM5 (MPI_ECHAM5, Roeckner *et al.*, 2006) and the United Kingdom Met Office's Hadley Centre Coupled Model v3 (UKMO_HADCM3, MetOffice, 1999). These five models have spatial resolutions ranging between 100 - 300 km^2 and so were statistically downscaled using the delta method, which produces smoothed climate surfaces at a 1 km^2 resolution based on current climate anomalies with WorldClim (Ramirez-Villegas and Jarvis, 2010). Van Soesbergen (2011) then calculated the mean of all 5 models to produce an ensemble forecast for three scenarios and two time periods.

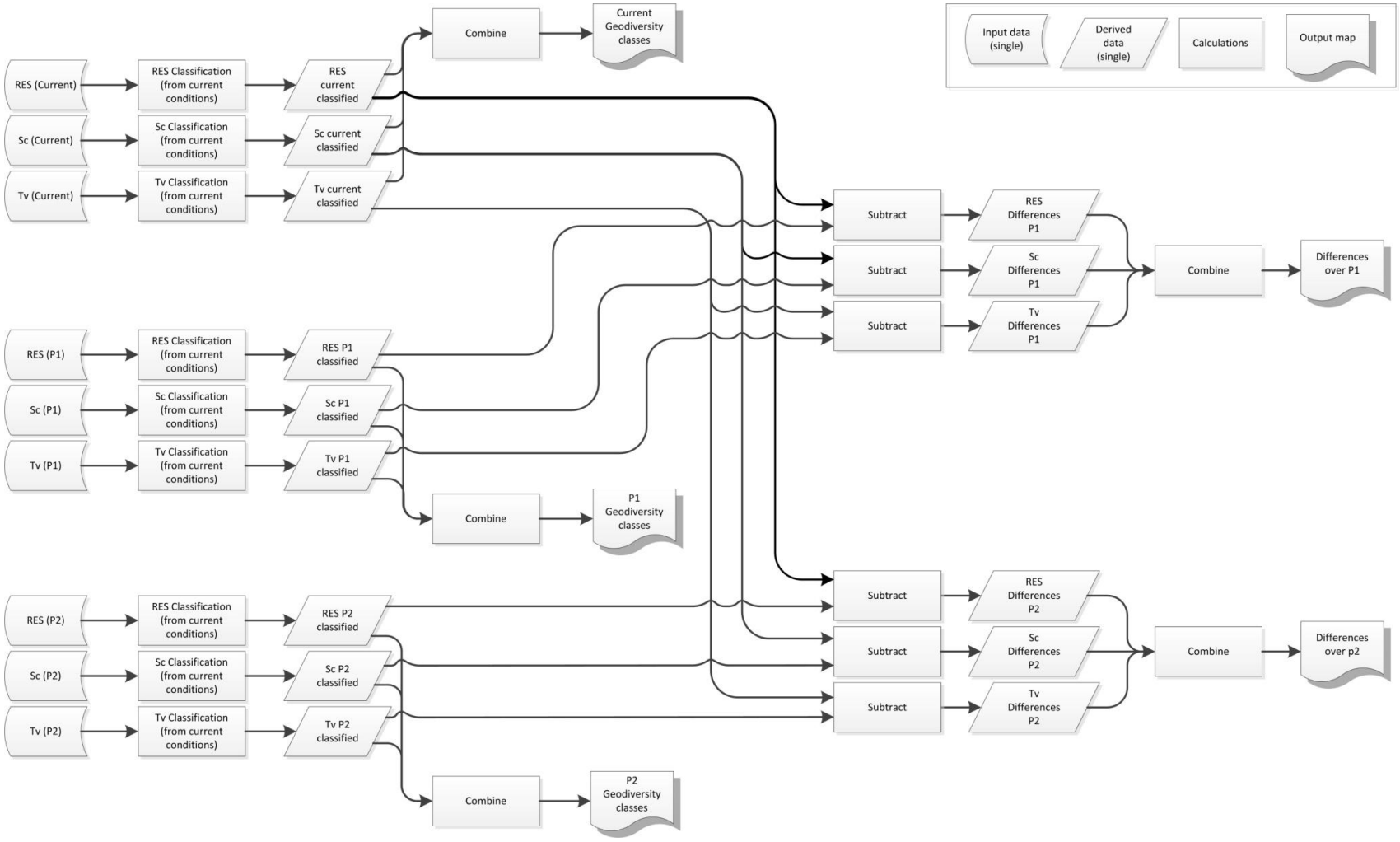

Figure 7.2. GIS workflow for calculation of changes in geodiversity over the two time periods, current to 2041 - 2060 and current to 2081 - 2100.

7.2.3. Model simulations

In order to calculate geodiversity under future climate conditions, *GDiv* was run using the standard model configuration with the input WorldClim rainfall and precipitation input data replaced with the downscaled projected data for the periods 2040 - 2060 and also for 2080 - 2100, for each of the three available SRES scenarios - leading to a total of six projected geodiversity and *Sc* scenarios.

7.2.4. Classifying geodiversity

Using the A2 scenario projections, each of the three components of geodiversity was classified based on the frequency-distribution of values in the baseline to give four classes each for *RES*, *Sc* and *Tv* (Table 7.2). The classification was based on standard deviations from the mean, with class 1 being over one standard deviation below the mean, class 2 being up to one standard deviation below the mean, class three being up to one standard deviation above the mean and class four being greater than one standard deviation above the mean. This classification results in geodiversity classes that can be interpreted in terms of their climatic characteristics (table 7.3).

Table 7.2. Values used for classifying the components of geodiversity. Each component was classified based on current frequency-distribution to give four classes based on standard deviations from the baseline mean value.

RES		*Sc*		*Tv*	
Raw value range	Classified value	Raw value range	Classified value	Raw value range	Classified value
< 0.338	100	< 0.397	10	< 0.203	1
≥ 0.338 < 0.406	200	≥ 0.397 < 0.458	20	≥ 0.203 < 0.280	2
≥ 0.406 < 0.474	300	≥ 0.458 < 0.519	30	≥ 0.280 < 0.357	3
≥ 0.474	400	≥ 0.519	40	≥ 0.357	4

Table 7.3. Climatic characteristics of geodiversity classes

Class	*RES* (pixel level resource context)	*Sc* (wider spatial resource context)	*Tv* (pixel level seasonality)
1	Cold / very dry	Cold / very dry	Not seasonal
2	Cool / dry	Cool / dry	Slightly seasonal
3	Warm / wet	Warm / wet	Somewhat seasonal
4	Hot / very wet	Hot / very wet	Highly seasonal

These classified component maps were then combined to generate a map of geodiversity classes, with each class representing a unique combination of the three classified components. In order to achieve this, the values assigned to the classified component maps were scaled by a factor of 10 for each component (Table 7.2) so that when they were summed the result was a unique three digit number representing the resource regime on a per-pixel basis. For example, a pixel with *RES*, *Sc* and *Tv* scores falling in the lowest class would be assigned to the geodiversity class 111, resulting from a summing of a *RES* classification of 100 (class 1), an *Sc* classification of 10 (class 1) and a *Tv* classification of 1 (class 1).

7.2.5. Calculating changes in geodiversity

Two calculations of changes in geodiversity were carried out - the change in raw geodiversity and the change in classified geodiversity. Changes in raw geodiversity were calculated as

$$\Delta GD_{raw} = GD_{projected} - GD_{current} \quad (38)$$

where $GD_{projected}$ is the future projected geodiversity map and $GD_{current}$ is the current baseline geodiversity map.

The classification system outlined in the previous section enabled clear-cut interpretation of the assigned class labels, as the values are directly linked to the resource regime of each pixel. This meant that, in addition to a calculation of change in current geodiversity class (i.e. identifying pixels that have or have not changed geodiversity class), calculation of the magnitude of that change was also possible (i.e. identifying how many step-changes in class for each of the three components are predicted for each pixel, as outlined below).

The change in current class was determined as change in pixel count for each of the unique geodiversity classes over both future projections. The change in the five most extensive, the five most rapidly declining and the five most rapidly expanding classes was examined in more detail, with most invasive being defined as those geodiversity classes that showed the greatest increase in extent over the period current to 2081 - 2100, and most vulnerable being those that showed the greatest decrease in extent over the period current to 2081 - 2100. Changes in extent were calculated on a per-pixel basis. When defining the rapidly declining geodiversity classes, the change in extent was normalised against current extent and only those classes with a current extent greater then 10 000 pixels were considered, thus avoiding classes with a small current extent that increased by only a few pixels skewing the results.

The magnitude of change was calculated as

$$\Delta_{mag} = \sum \left(\left(Cclass_{projected} - Cclass_{current} \right) / f_{component} \right) \quad 39$$

where $Cclass_{projected}$ is the future projected classified component map, $Cclass_{current}$ is the current classified component map and $f_{component}$ is the correction factor to convert from the classified "labelled" value to the actual class value, so for *RES* is 100, for *Sc* is 10 and for *Tv* is 1 (see table 7.2). This resulted in a potential change on a scale of -9 to +9, with a results of -9 representing a change from 444 to 111 (a decline in 3 classes across all three components) and, conversely, a change result of +9 representing a change from 111 to 444 (an increase in three classes across all three components).

7.2.6. Gap analysis across the protected area network.

The map showing change in geodiversity classes was used as the foundation for a strategic analysis showing gaps in the existing protected area network, both under current conditions and under projected conditions. The extent of each unique geodiversity class was calculated as a proportion of the entire study area as a baseline. Next, the extent of each unique geodiversity class currently represented in the existing protected area network was calculated as a proportion of the total area covered by the protected area network. The difference in representation was then calculated for each geodiversity class as

$$Rep = \frac{Class_{PA}}{Area_{PA}} - \frac{Class_{total}}{Area_{total}} \quad 40$$

where Rep is the representativeness of the geodiversity class in question, $Class_{PA}$ and $Class_{total}$ are the extent of the geodiversity class across the protected area network and the total study region respectively, and $Area_{PA}$ and $Area_{total}$ is the extent of the entire protected area network and study area respectively.

From these *Rep* values, the geodiversity classes were ranked according to current "over-representation" (positive values) and "under-representation" (negative values) in the protected area network - a gap analysis of the effectiveness of the existing protected area network under the current climate -regime. *Rep* values were then calculated for the projected geodiversity classes, allowing for analysis of the change in proportional representation of each of the unique geodiversity classes from the current baseline conditions. Geodiversity classes showing significant decrease in representation, be that from a baseline position of over- or under-representation, were then examined in further detail for changes in spatial distribution and potential protection strategies.

7.3. Results

7.3.1. Spatial changes in unclassified geodiversity

Generally, the majority of the study area shows low levels of change in geodiversity score over both periods (figure 7.3). However, all three scenarios produce similar changes in geodiversity score for both periods (current to 2040 - 2060, and current to 2080 - 2100) in terms of both magnitude and spatial patterns of change. All three scenarios show increases in geodiversity on the north-eastern flank of the Cordillera Oriental by the 2050s, with decreases on the flanks surrounding the Magdalena Valley. Over the second period, there are clear decreases in geodiversity on the mid-slopes of the Cordillera Central and Cordillera Occidental; this is found for all three scenarios, however is more pronounced under A2.

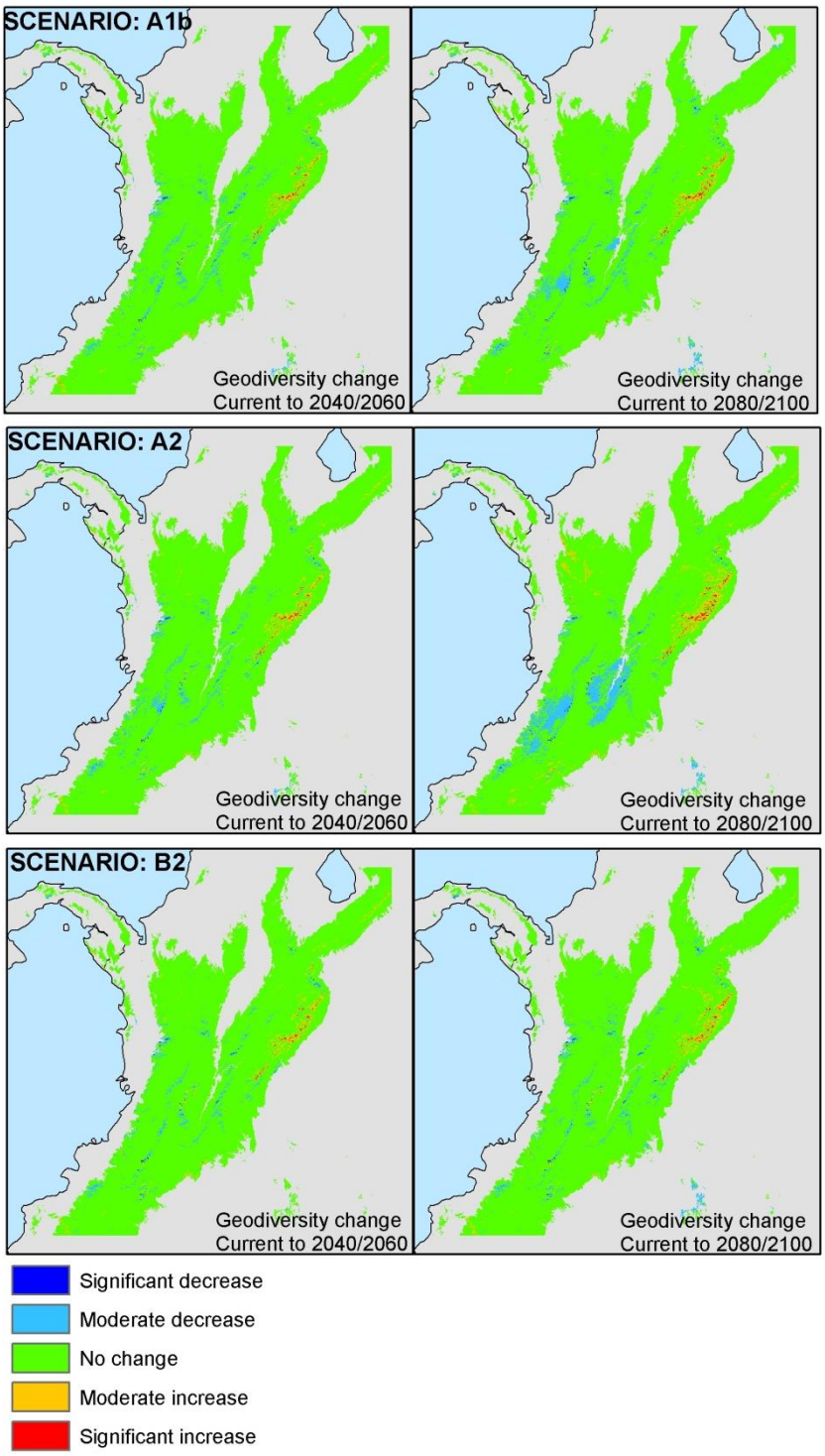

Figure 7.3. Change in geodiversity and components from current to 2040 - 2060 and to 2080 - 2100 for three climate change scenarios (A1B, A2 and B2, as outlined in table 7.1). Areas of no change (green) are defined as falling within ±0.5 standard deviations of the baseline geodiversity score, moderate changes are between 0.5 and 1 standard deviations whilst significant changes are greater than 1 standard deviation.

7.3.2. Changes in geodiversity classes

Figure 7.4 shows changes in extent of each geodiversity class for both the baseline (current) distribution to 2041 - 2060 (period 1) and the baseline to 2081 - 2100 (period 2). This was

calculated as an absolute pixel count, rather than as a normalised value based on the baseline extent, as some geodiversity classes in the baseline consisted of only a few pixels and so any small increase or decrease would be greatly exaggerated in a normalised value. The greatest increases were found in geodiversity classes with relatively high scoring components (i.e. with class scores of 3 and 4 for *RES*, *Sc* and *Tv*). The three geodiversity classes which showed the greatest increase in extent showed an increase over both periods, however the increase in period 2 was not as great as for period 1. Similarly, for the three geodiversity classes exhibiting the greatest decrease in extent there was a larger decrease over period 1 than period 2. Classes 111, 211 and 322 showed a larger increase in extent over period 2 than period 1. Table 7.3 relates the classes to "real world" conditions.

Given that there are 57 unique geodiversity classes, it was deemed inappropriate to map the spatial distribution of all classes. Instead five geodiversity classes for each of three criteria were selected and mapped; the criteria included classes with the greatest extent, the most rapidly declining classes (in terms of extent) and the most rapidly expanding classes. The five largest geodiversity classes were designated by absolute pixel count under baseline (current) conditions. The five most rapidly declining geodiversity classes were designated by taking those with a current pixel count greater than 10 000, as there was a natural break in the frequency distribution at this point (figure 7.5), and then determining which had lost the greatest percentage over period 2. This enabled normalisation of the data for area, without a disproportionate influence for geodiversity classes with a small current extent. The five most rapidly expanding geodiversity classes were designated as those showing the greatest increase in extent (in terms of an absolute pixel count) over period 2.

The five most extensive geodiversity classes (222, 333, 111, 444 and 112) are predominantly equally balanced between the three components, i.e. are either all low, all middle or all high scoring in the three components. The most extensive geodiversity class (222) is found predominantly on the mid-elevations with a large patch on the Cordillera Occidental and around the Magdalena Valley. Geodiversity class 333 is found at the lower elevations, predominantly to the north of the Cordillera Occidental. Classes 111 and 444 are found at high and low elevations respectively, reflecting the resource gradients associated with elevation. In terms of changes in absolute pixel count of these extensive geodiversity classes as a result of climate change, there are noticeable decreases in 333, 222, 444 and 112; only 111 shows an increase.

Interestingly three of the most extensive geodiversity classes (444, 333 and 222) are also among the most declining in extent, on both a percentage and absolute basis. The five classes that lose the greatest proportion of their current area are found at predominantly low to mid elevations within the study area. The most declining of all (332) becomes highly reduced in extent and increasingly fragmented by 2081 - 2100. Class 444 shows the second greatest decrease in extent, however is much less fragmented than 332.

The most expanding geodiversity classes are 232, 212, 434, 111 and 211. As would be expected, these occupy a complimentary distribution to the most vulnerable classes - covering the higher elevations. However, the three most expanding classes (323, 212 and 434) are located at mid elevations.

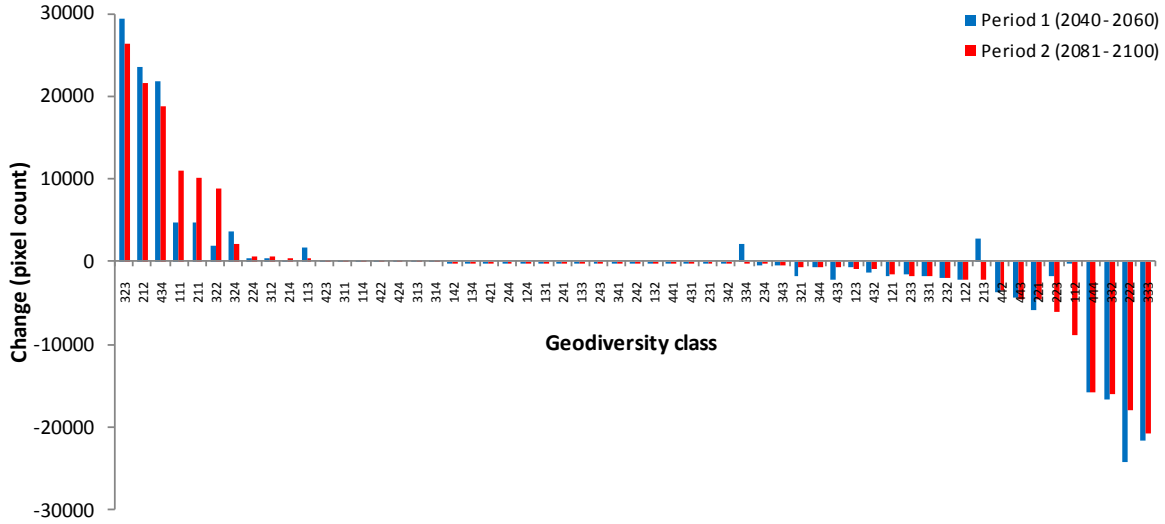

Figure 7.4. Change in extent of current geodiversity classes (expressed as a pixel count) over the two periods (current to 2041 / 2060, and current to 2081 / 2100). Geodiversity class numbers represent the *RES*, *Sc* and *Tv* classification on a per-pixel basis (see section 7.2.4 for further detail).

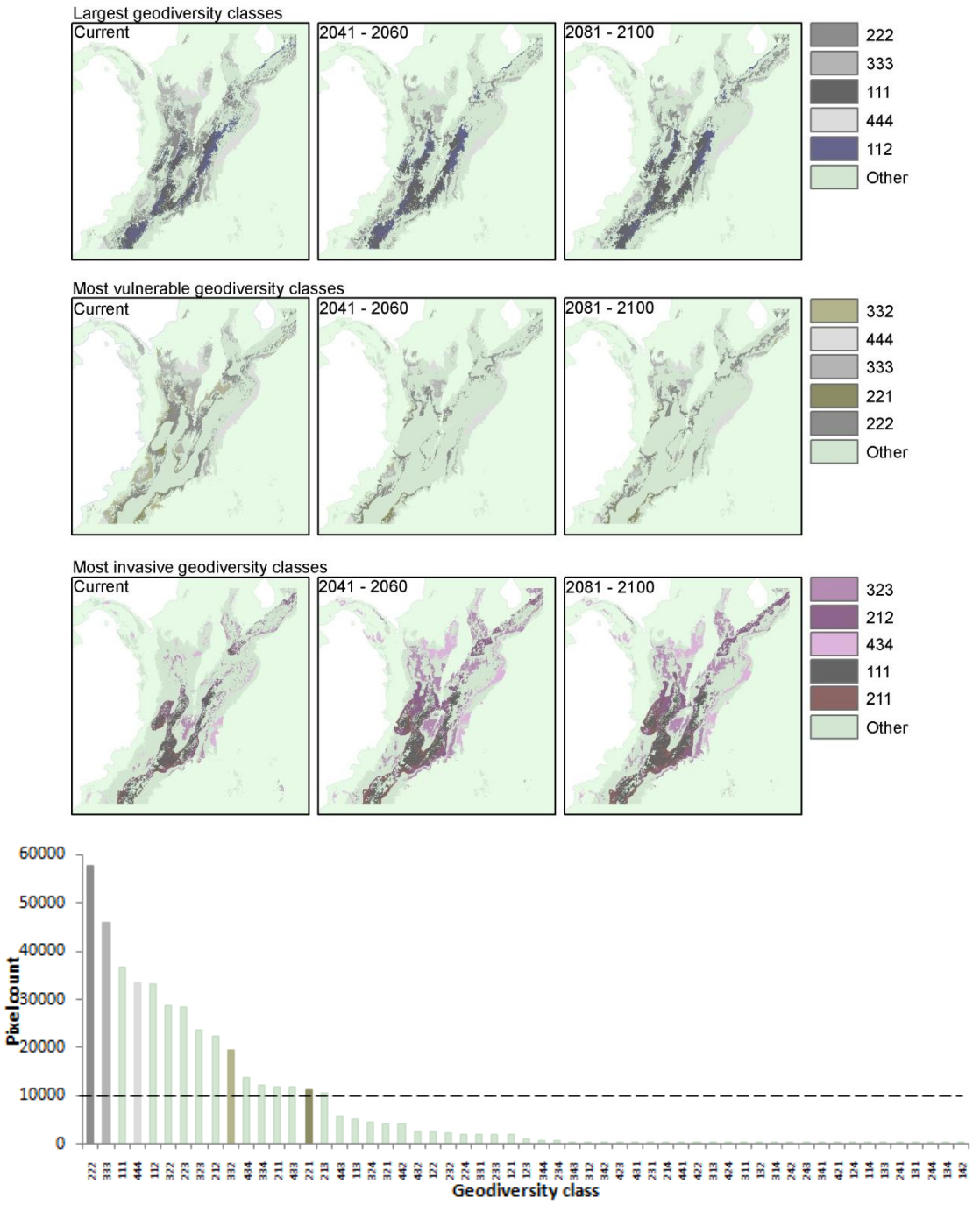

Figure 7.5. Maps show distribution of most extensive (top), most rapidly declining (middle) and most rapidly expanding (bottom) geodiversity classes across the study area for current conditions and both future projections. The bottom panel shows the pixel counts of current geodiversity classes, with the cut-off of 10 000 pixels indicated. The currently most vulnerable classes within this cut-off are (defined as those classes with over 10 000 pixels in current conditions which lost the greatest proportional extent from the current baseline to period 2 (2081 - 2100)). The colours in the legend represent the RST values, with increasing RES, Sc and Tv scores relating to increasing red, green and blue respectively Balanced classes appear grey, with in increasingly light shades of grey representing a more highly scoring geodiversity class number.

7.3.3. Magnitude of changes in geodiversity classes

The majority of pixels show no change in geodiversity class composition (i.e. they fall within the same geodiversity class) across both time periods (figure 7.6 a). This is also found in the changes in the component classes (figure 7.6, b - d). In terms of changes in geodiversity class composition, over period 1 there tends to be a positive Δ_{mag} for geodiversity class (i.e. pixels have generally changed from low scoring component classes to high scoring component classes). This trend is reversed over period two, with more pixels exhibiting a negative Δ_{mag}, representing a decrease of one class level in one or more of the three components.

In terms of Δ_{mag} in the individual components, *RES* shows a symmetrical distribution for both time periods, with the vast majority of pixels remaining in the same *RES* class whilst approximately 50 000 pixels showing a Δ_{mag} of ± a single class level. Changes in *Sc* class are positively skewed; whilst the majority of pixels show no change, approximately 180 000 decrease by one *Sc* class level. This pattern is found in both periods 1 and 2. The Δ_{mag} values for *Tv* are different in each of the two periods; in the first period, there is a slight negative skew, suggesting more pixels will experience an increase in seasonality than will experience a decrease. In the second period the distribution is more symmetrical.

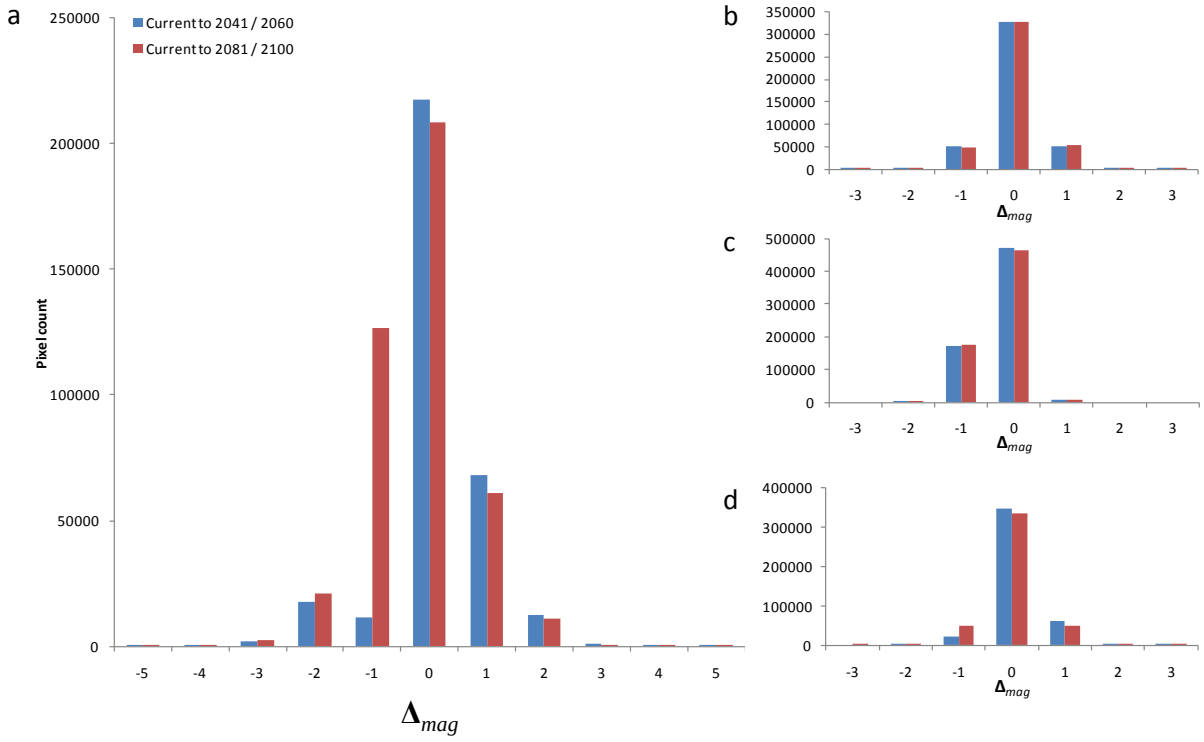

Figure 7.6. Frequency distribution of pixels at each level of Δ_{mag} for geodiversity, *RES*, *Sc* and *Tv* classes over both time periods.

The spatial distribution of Δ_{mag} (figure 7.7) shows that there is generally a greater increase in class levels to the north of the study region, with a decrease found to the south. Of the areas that do exhibit a change ($\Delta_{mag} \neq 0$), the magnitude is generally of 1 to 2 class levels. Δ_{mag} seems to exhibit some relationship with elevation (figure 7.8); negative Δ_{mag} scores tend to be associated with low to mid elevations, with no apparent directional relationship, however positive Δ_{mag} scores are positively correlated with elevation (r^2 = 0.73, r^2 = 0.98 for periods 1 and 2 respectively). Over the entire range of Δ_{mag} values there is also a positive, albeit slightly weaker, correlation for both time periods (r^2 = 0.70, r^2 = 0.87 for periods 1 and 2 respectively)

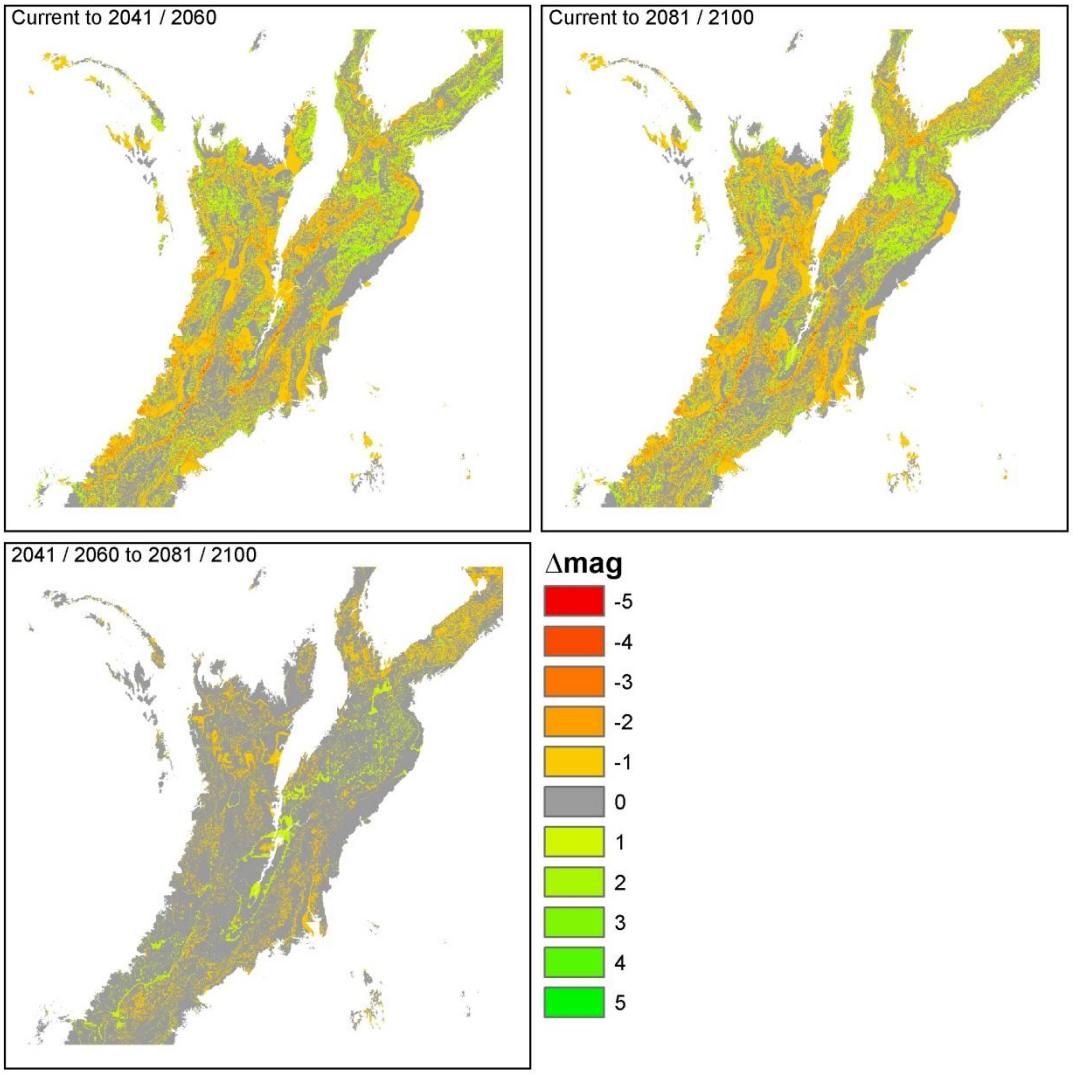

Figure 7.7. Spatial distribution of Δ_{mag} combined for all three components across the study region.

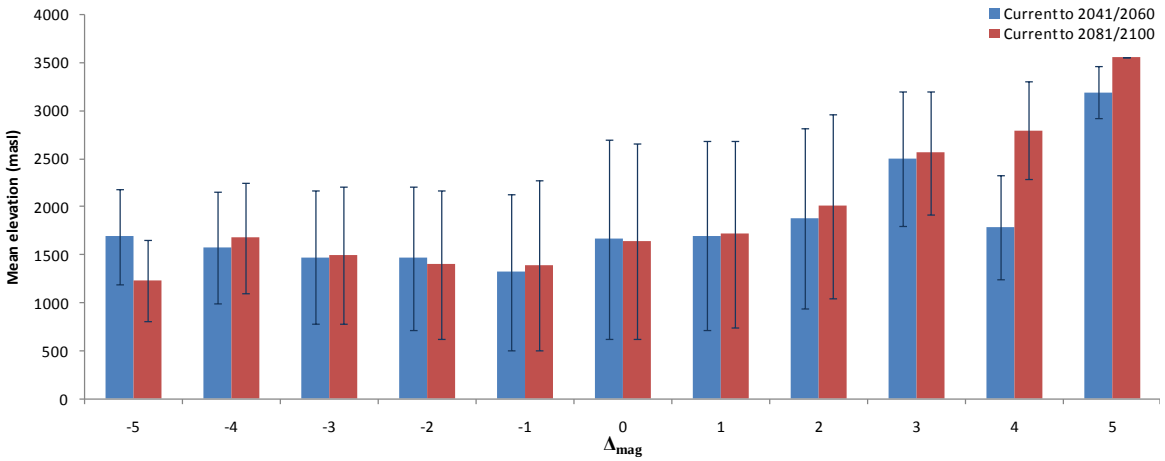

Figure 7.8. Mean elevation for each value of Δ_{mag} in geodiversity class. Error bars show ±1 standard deviation.

7.3.4. Impact of changes in geodiversity on the protected area network

Figure 7.9 shows that the most over represented geodiversity class in the protected area network of the study region is 334, with 4.04% greater coverage in the protected area network when compared with the wider study region. Conversely, the most under-represented geodiversity class is 222, with -3.88% less coverage in the protected area than the wider region. When considering the changes in level of representation as a result of climate change, the two most under represented classes (222 and 322) increase in representation and, over period 2, become over represented in the protected area network by 0.75% and 0.57% respectively. In general terms, the most over-represented classes for the baseline decrease in representation somewhat for the climate scenario - although they are still over represented in 2081 - 2100.

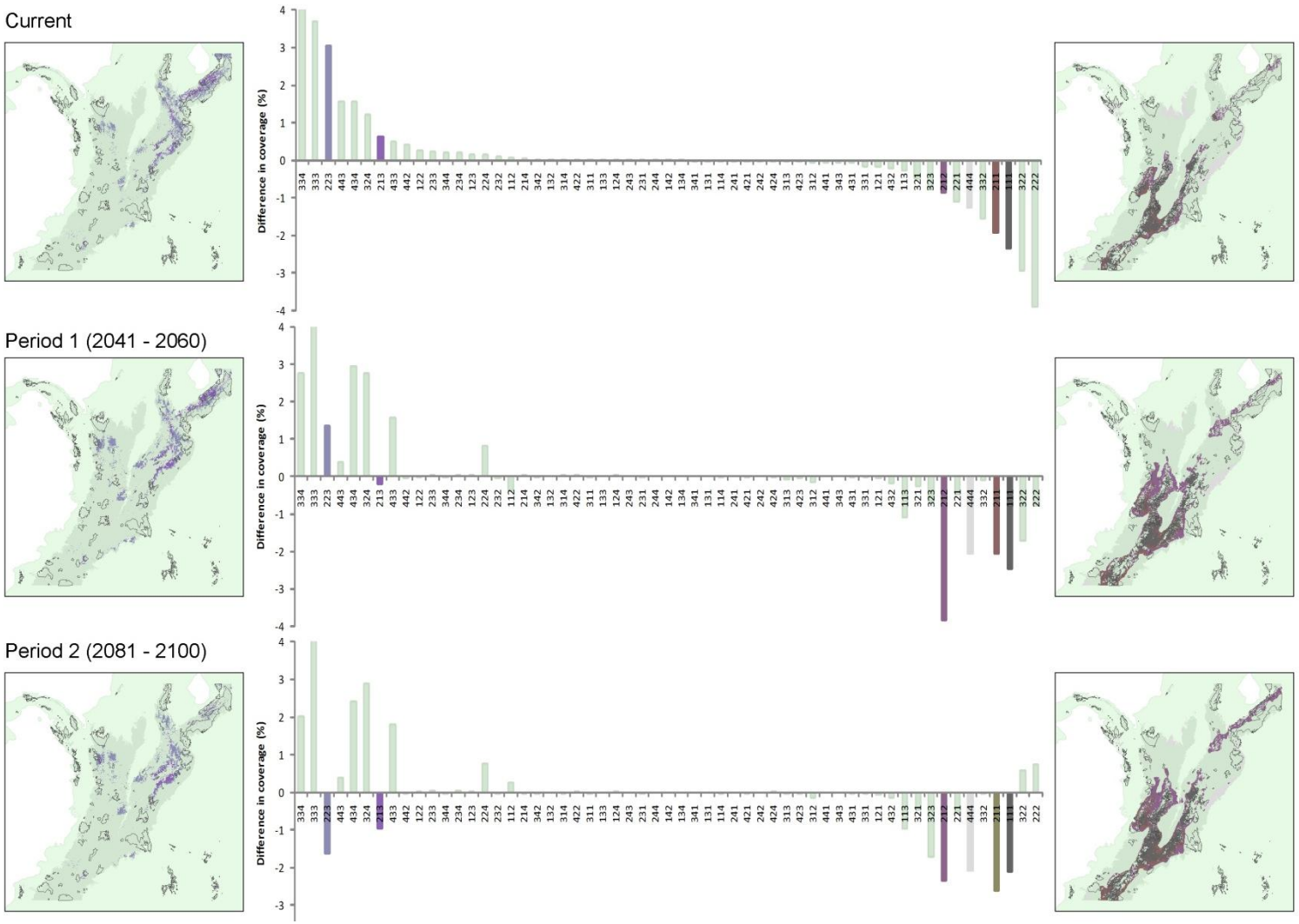

Figure 7.9. Changes in representation of geodiversity classes for each period. Maps show spatial changes in case study classes.

The geodiversity classes selected as case studies are 223 and 213, which are currently over represented in the protected area network and which become under represented by 2081 / 2100. Classes 212, 444, 211 and 111 were also selected; these are currently under represented and become more so over the second period (Table 7.4).

Whilst both 223 and 213, which are currently over represented in the protected area network, decline in extent over period 2 (figure 7.4), there are still patches of both classes to the north east of the study area (figure 7.9); the decline in coverage is due to the migration of the geodiversity classes out of the current protected area system, rather than the wholesale loss of the classes in the landscape, and so carefully planned extensions to the current protected area network could potentially reduce the decline in representation of these classes - and thus the species assumed to be associated with them. This is discussed further in section 7.4.3.

Table 7.4. Representation of the selected case study geodiversity classes under the current protected area network.

Representation (%)		
Current	Period 1 (2041 - 2060)	Period 2 (2081 - 2100)
+3.06	+1.35	-1.63
+0.63	-0.20	-0.96
-0.85	-3.83	-2.34
-1.25	-2.07	-2.08
-1.91	-2.07	-2.62
-2.35	-2.48	-2.12

Of the four case study geodiversity classes which are currently under-represented in the existing protected area network, only 444 is predicted to decrease in extent over period 2 (figure 7.4). However, there are still large un-fragmented patches of this class predicted for the eastern flanks of the Cordillera Oriental by 2081 - 2100 so adaptation of the existing protected area network could counter the under representation of this class. The remaining three case study geodiversity classes (212, 211 and 111) all increase in extent over period 2, and so there is also the potential to adapt the protected area network to offset their under representation.

7.4. Discussion

It is important to note that the areas identified here as potentially providing suitable expansion sites for the existing protected area network are not an absolute solution, rather they are areas that individual government agencies / NGOs may wish to consider for protected area

extension in order to facilitate climate-change-stable conservation for the future. The areas discussed are based purely on physical models, with no consideration of the socio-economic implications; before any decisions could be made based on these proposals, a full socio-economic costing and stakeholder consultation of any actual protected area extension would obviously be necessary, along with verification of the bio-physical conditions on the ground. This work is thus testing the evaluation of a methodology rather than a policy support tool.

7.4.1. Current geodiversity classes

Using raw geodiversity scores to define suitability may not provide the best solution because areas with very different resource regimes (and thus associated biological communities) could potentially have the same geodiversity score. For example, a geodiversity score of 0.6 could arise from different combinations of *RES*, *Sc* and *Tv* scores which then reflect very different physical environments and thus biological assemblages. Whilst classifying a continuous value such as geodiversity can be challenging in terms of determining where to define the class breaks, in this instance the use of geodiversity classes overcame the information limitations associated with using raw geodiversity scores enabling investigation of the potential impacts of projects for climate change on the characteristics as well as the overall magnitude of geodiversity.

The most extensive geodiversity classes all represent "balanced" resource regimes, i.e. the total amount of resource availability, the wider spatial resource context and the temporal variation of resources were all within the same class value. This suggests that, as seen in figure 4.28, there is some correlation between the three components and areas with a low total amount of resource availability are also likely to have low *Sc* and *Tv* scores, as one might expect since the scores are all relevant to the highest within the tile. Of the four balanced classes (111, 222, 333 and 444), the higher resource regimes tended to be found at lower elevations, whilst the lower resource regimes were found at higher elevations. This ties in with the results from chapter 4 which highlighted the decline in geodiversity with elevation, and also with the literature reviewed in chapter 2, and suggests that, as expected, higher elevations will be colder and drier than the lower elevations of this study region.

Considering rare geodiversity classes, there are seven classes that are not present in the study area (141, 143, 144, 411, 412, 413, 414). These all represent classes of extreme differences between *RES* and *Sc*. Looking at the structure of the *GDiv* score can explain why these are highly unlikely to exist - *Sc* is derived using a moving average based on the total annual

resource availability. Thus *RES* and *Sc* are unlikely to show extreme differences. On the other hand, class 142 does exist, albeit with a very small extent of 1 pixel (and which may thus be an artefact), showing that the spatial resource context surrounding the pixel can vary significantly from the overall resource availability of the pixel in question. Of the rare geodiversity classes that are found under current conditions, most have low *RES* scores combined with higher *Tv* and *Sc* scores. Again, this can be explained when *GDiv* structure is considered; as outlined above, it is unlikely to find a pixel with a low *RES* and a high *Sc* score.

With regards to building on this initial classification scheme, further testing of the impact of the definition of the class boundaries will be useful to assess the sensitivity of the geodiversity classes to the definition used. Development of the classification system should look to investigate the impact of both increasing and decreasing the number of component classes from the current level (four per component), as well as using alternative classification techniques based on, for example natural or Jenks breaks, or an equal interval classification. Alternatively, geodiversity classes could be delimited using cluster analysis techniques based on *RES* / *Sc* / *Tv* scores - this would have the advantage of allowing the similarity between geodiversity classes to be quantified

Given that different species evolve to become adapted to specific environmental conditions (Ridley, 1996) it can be hypothesised that unique assemblages of species will be associated with different geodiversity classes. Research into the existence, and potentially strength, of these associations would prove useful for understanding wider patterns of biodiversity. This work would need to be carried out at a more local scale due to the constraints of data availability for species distributions outlined in chapter 5. Alternatively, the datasets used in the analyses for chapters 5 and 6 could be used, although the limitations discussed in those chapters would still apply.

7.4.2. Changes in geodiversity

Two methods for investigating the change in geodiversity were presented, namely investigation of the change in mean geodiversity and investigation into changes in distribution of the unique classes of geodiversity. The changes in raw geodiversity score (figure 7.3) for each of the three climate change scenarios all project increases in geodiversity for the north eastern flank of the Cordillera Oriental, with decreases in geodiversity score for the head of the Magdalena Valley and the western flanks of the Cordillera Occidental (for a discussion of changes in geodiversity class, see section 7.4.3). This suggests that the decision to base the

remainder of the analyses on a single scenario was justified (at least on the basis of geodiversity score) as there was unlikely to be significant differences between the results from different scenarios.

The majority of the study area showed little change in raw geodiversity score with climate change, however further details of the changes that are projected were revealed by considering the magnitude of change in terms of changes in geodiversity class (figure 7.7), demonstrating the advantage of using geodiversity classes as the basis for these analyses. Whilst the majority of pixels still show no change (i.e. they maintain their current geodiversity class over both periods of the analysis), the degree of spatial autocorrelation in the results means that areas that do experience change will experience change at a local to regional scale, rather than isolated pockets of change at the pixel level. This has implications in terms of conservation as it may not be possible for species to migrate far enough, quickly enough or across topographic or artificial barriers in order to adapt to climate change.

There is a positive relationship between increasing positive Δ_{mag} and elevation, i.e. as elevation increases, there is likely to be a greater increase in geodiversity component class value, suggesting that there is likely to be an increase in resource availability, an increase in the wider spatial resource context and an increase in temporal structuring of resources with elevation. This could potentially lead to an increase in invasive species to these regions, as species migrate with the resource regime to which they are adapted. This exerts a double-edged pressure on the existing mountain top ecosystems and species assemblages, which are highly specialised to low energy climates (e.g. paramo), as the resource regime will change and they also become subject to competition from invasive species.

Of the extensive, declining and expanding geodiversity classes highlighted in figure 7.9, it is interesting to note that three of the most extensive classes are among the most declining (444, 333, 222) - despite the fact that the designation as "declining" was based on the number of pixels lost normalised by current area, rather than simply the overall number of pixels lost. These classes are all "balanced" in terms of being at the same class level for *RES*, *Sc* and *Tv*. The fact that these are also declining suggests that there is likely to be a disruption to the composition of the current resource regime; for example it may be that whilst *RES* and *Sc* increase, *Tv* decreases (or vice versa). Interestingly, the other "balanced" geodiversity class (111) is the fourth most expanding geodiversity class. This suggests a possible shift from a balanced resource regime towards a lower level of overall resource availability and a less seasonally structured regime.

Other geodiversity classes designated expanding are 323, 212, 434 and 211. The feature that distinguishes these classes is the lower *Sc* class level compared to *RES* class level; the most vulnerable classes had identical *Sc* and *RES* class levels. This again points to the shift in balance of resource regimes in terms of the three components of geodiversity, with geodiversity classes projected to become less balanced over the next 100 years. The ecological implication of this is that species will not only be exposed to an increase or decrease in resource availability but also a change in the temporal structure of this - again, exerting a double edged pressure on existing ecosystems and communities.

The most expanding geodiversity classes are currently located in the mid-elevations of this study region. They seem to migrate upwards towards the mountain summits, supporting the argument outlined above that associated alpine communities such as paramo are likely to be under most pressure from climate change. With regards to the spatial distribution of the vulnerable geodiversity classes, most are currently located on the low to mid elevations of the study region (figure 7.9). Whilst some of the reduction in extent could be attributed to the migration of these decreasing classes to outside of the extent of this analysis (i.e. outside the mountainous extent), several of the classes which are not directly adjacent to the edge of the study region disappear entirely and do not appear to migrate (for example, 222). This suggests that there is a genuine loss of these geodiversity classes, with the almost total disappearance of class 332. Future work examining the fate of those areas which are currently classed as one of the vulnerable geodiversity classes could reveal further detail regarding precisely how those resource regimes change. Furthermore, investigation into which geodiversity classes are more likely to be replaced by the invasive classes could be illuminating. The application of theory regarding extinction and invasive species could prove useful in understanding the mechanics of this interplay between vulnerable and invasive geodiversity classes.

7.4.3. Robustness of the current protected area network

The current protected area network (figure 7.10) seems to represent current geodiversity classes well; the greatest over- or under- representativeness amounting to only 4%. Interestingly, the representativeness seems to increase under the climate change scenarios investigated here, with most classes moving closer to a representativeness score of 0 (figure 7.9), which suggests that the extent of each class within the protected area network is likely to closely match the extent of that class across the entire study area. This high level of representativeness can be attributed to the dense protected area network within the study

region; regions with fewer protected areas may thus have a protected area network which is not so representative of geodiversity classes.

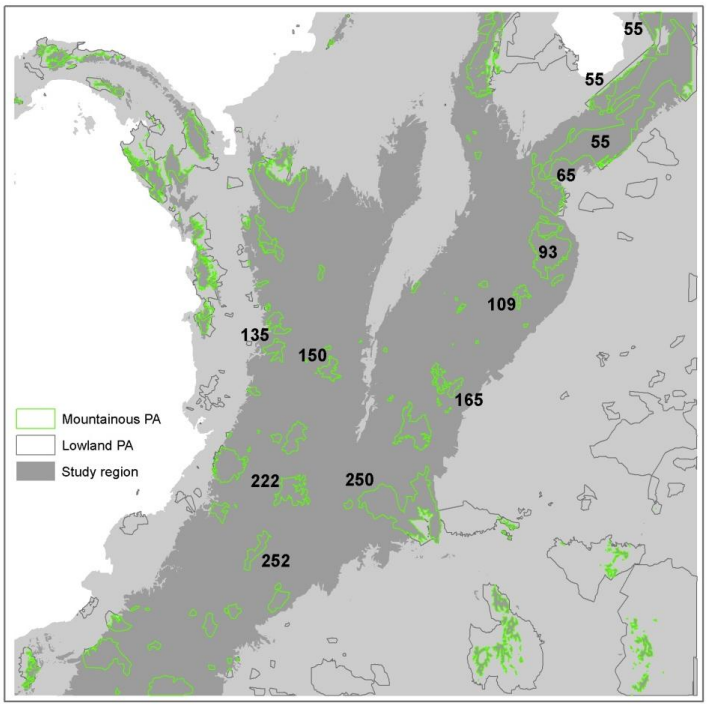

Figure 7.10. Protected area network within the study area and wider region. Labels refer to SimTerra identifier numbers for individual protected areas; those protected areas mentioned in the text are labelled.

An important pattern that emerged from the analyses carried out in this chapter is that the projected changes for period 1 and period 2 are not necessarily uni-directional; a decrease in extent of a given geodiversity class to period 1 does not mean that the class will also a decrease to period 2. For example, class 213 increases in extent over period 1 and then shows a decrease in extent of approximately the same amount over period 2, resulting in very little net change in extent from the baseline conditions. However, the location of the geodiversity class has moved significantly (figure 7.9). This has significant implications for conservation management as it means that expansion of existing protected areas which contain a given geodiversity class may not be an effective long-term conservation solution were that same class to 'migrate' in the longer time. Conservation planning needs to examine a range of potential futures and endeavour to plan for all; these futures should be revisited regularly with the view to adapting strategic plans according to new data and evidence regarding the realisation of alternative future scenarios.

Whilst the current protected area network appears to provide good protection of geodiversity, both under current and projected climate scenarios, future work should look to repeat the

analyses using only the more strict IUCN categories, e.g. I to IV, as these offer greater conservation protection than I to VI. It may be that the apparent representativeness of the current protected area network in the study area does not represent strict protection of current geodiversity classes. For example, whilst Categories Ia and Ib are strictly protected, with limits on human impact, Category VI permits (sustainable) use of natural resources.

Those classes currently over represented, but which are projected to be underrepresented under future climate scenarios (classes 223 and 213), are predominantly situated in the north-east of the study region. The fact that these two classes are currently over represented in the existing protected area network may be indicative of an association of these geodiversity classes with highly valued biodiversity (for example, endangered or endemic species) and are therefore of high importance to conservation. The level of representation decreases because the classes migrate out of PA55 (see figure 7.10 for a map of the numbers allocated to each protected area by SimTerra), a trans-boundary national park in Colombia / Venezuela.

Classes 223 and 213 tend to be found adjacent to each other, a reflection of their similar component profiles - both being cool and dry, and slightly seasonal (table 7.3). This similarity renders a management strategy that considers both classes simultaneously possible; by increasing the coverage of the protected area network to the west of PAs 55, 65, 93 or 109 the migration of classes 213 and 223 would be buffered through time.

PA55 is a combination of twelve adjacent protected areas; as an artefact of rasterisation, these were grouped as a single protected area in the SimTerra database. In reality, SimTerra PA55 is a mosaic of four Category II National Parks (Sierra Nevada, Paramos Del Batallon Y La Negra, Chorro El Indio and Sierra de la Culata), seven Category V Protective Zones (Piedemonte Norte de la Cordillera Andina, Sureste Del Lago de Maracaibo Sto Domingo Motatan, La Marichi, San Cristobal, Rio Torbes Y Sus Alrededores, Las Gonzales and Rio Capaz) and one uncategorised Critical Priority Area (Cuenca Rio Albarregas). These cover tropical rainforest, sub-Andean forest, Andean forest and paramo and represent a varying degree of protection from strictly enforced national parks, to guidelines regarding sustainable use of resources (WDPA, 2012). PA65 is a trans-border reserve, crossing the Colombian - Venezuelan border. Both are designated IUCN Category II (National Park) and the Tama Natural National Park covers 480 km^2 in Colombia, whilst El Tama National Park covers 1390 km^2 in Venezuela and contains tropical rainforest, sub-Andean forest, Andean forest and paramo (WDPA, 2012). PA93 is a Category II National Park, El Cocuy, located in the north east of the study region which was established in 1977 and covers 3060 km^2.

The classes which are currently under represented in the protected area network, and which become more so, are widely distributed across the study area. As such, these will require consideration on a class by class basis.

Class 444 (blue in figure 7.9) can be considered as hot, very wet and highly seasonal. The current level of under-representation is due to the fact that large tracts of this class are located outside the protected area network; one protected area which does contain class 444 is PA165, the Chingaza National Park, which was designated in 1998. The park, predominantly covered in cloud forest, is noted as a region of particular importance for endemic species within Colombia and also as hydrologically important, providing 80% of Bogota's water supply (WDPA, 2012). Given that an un-fragmented band of class 444 is projected to remain to the north-east of PA165, expanding the protected area network in this region would increase the representation of class 444 within the protected area network under the projected climate scenario.

Class 211 (green in figure 7.9) is currently the least extensive of the declining classes, and is highly under-represented in the current protected area network. On a per pixel basis it is cool and dry, with a cold and very dry wider spatial context, and not very seasonal. Interestingly, the class is projected to increase in extent under the climate change scenario, but this does not translate to an increase in representativeness within the protected area network. In order to increase the representativeness for class 211 in the protected area network, an increase in protected areas to the west of PA257 would be beneficial. PA257 is a pair of adjacent protected areas, the Serrania De Los Churumbelos Natural National Park and the Alto Fragua Indiwasi Natural National Park. Both these are IUCN Category II, and were designated in 2007 and 2002 respectively.

The most extensive of the under-represented classes is 111 - representing cold and very dry conditions with no seasonality. This is predominantly located around the mid-slopes of the head of the Magdelena Valley. As with class 211, class 111 increases in extent in both periods. Whilst the representativeness increases slightly, the class is still under represented in period 2, suggesting a need for increased representation within the protected area network in order to ensure effective conservation. Given the large extent of this class there are a wide range of possibilities for expanding the existing protected area network, particularly around PA222, PA250 and PA252.

PA222 is the Nevado Del Huila (WDPA136), a National Park established in 1977 that covers 1580 km^2. The park contains 8 volcanoes including the active Nevado Del Huila after which the park is named, and supports important economic crop production, namely coffee (WDPA, 2012). PA250 covers three protected areas; the Cordillera de los Picachos, Tinigua and Sierra de la Macarena. Together these three cover approximately 12 700 km^2, however only approximately 7700 km^2 is included in these analyses as the remainder falls outside the mountainous study region. All three of these are Category II National Parks, designated in 1988 / 1989 and contain a mix of paramo and Andean forest types. PA252 is Purace National Park, a Category II protected area designated in 1977 (WDPA, 2012).

Geodiversity class 212 (brown in figure 7.9) shows a complex response to the climate scenarios explored here. The class is projected to increase in extent over both periods, with a greater extent projected for period 1 than period 2 (figure 7.9). However, the representativeness in the protected area network is less over period 1 than either baseline conditions or period 2; emphasising the fact that an increase in extent of a given geodiversity class does not equate to an automatic increase in inclusion within the protected area network. In terms of increasing the representation of class 212, there is the potential for expansion between PA150 and PA135. PA 150 is los Nevados National Park, a Category II protected area designated in 1974, whilst PA135 is a combination of one national park (Tatama, designated in 1987) and three indigenous reserves (of which the designation year and IUCN category is unknown) (WDPA, 2012).

Figure 7.11 shows the classes highlighted in the previous section alongside three "impact metrics" that can be used as an initial assessment of protected area expansion on the population in terms of development (represented by night time lights) and agriculture (in terms of crop and pasture coverage). This suggests some of the areas into which under-represented geodiversity classes are projected to migrate may not be suitable for protected area expansion. For example, between PA150 and 135 is a patch of bright lights indicating high levels of development which has implications in both in terms of social conflict between the potential protected area expansion, and in terms of the quality of the habitat that would be conserved by any protected area expansion. Expansion into such a region would cause displacement of a high number of people, with associated economic costs, in order to expand a protected area into a degraded habitat which could have high associated restoration costs. Similarly, expansion into regions used for agriculture may cause loss of livelihood to the farmers and a decrease in food production and thus food security for the region. Furthermore,

agricultural land could also have associated restoration costs to render the land suitable for conservation purposes.

The spatial distribution of the various impact metrics suggest that extending the protected area in the south-eastern portion of the study region would have the lowest impact on currently developed areas and important agricultural areas. Protected area expansion in this region would provide increased representation for classes 111, 212 and 211. Furthermore, given the spatial heterogeneity of the impact metrics, it could be possible to delimit spatio-temporal corridors which avoid regions likely to have a high impact on the population in terms of loss of developed or agricultural land. However, the efficacy of potential corridors may be compromised if the ratio of "edge" to "core" habitat is too high, so careful spatial planning would be required to ensure that the shape and extent of the corridor is able to meet the need of the existing ecosystem without too high an impact on local livelihoods.

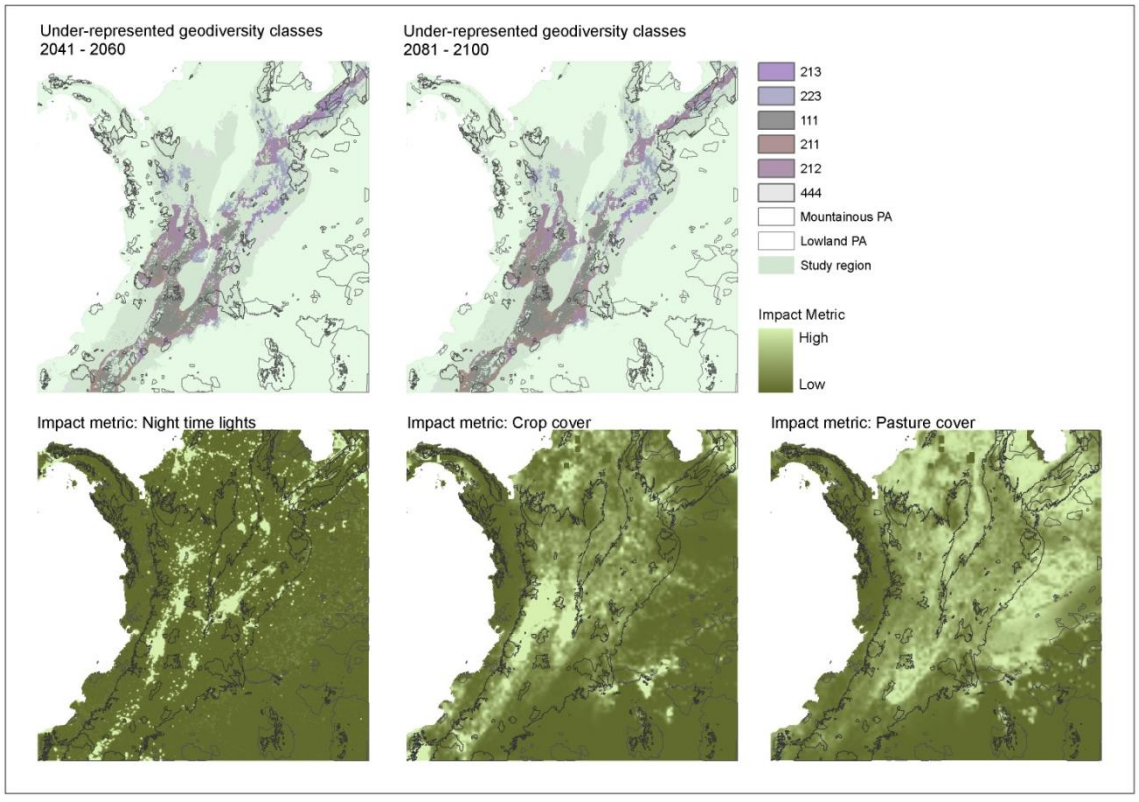

Figure 7.11. Impact metrics for the study region. Night time lights (DMSP, 2004) and Crop / Pasture cover (Monfrede *et al.*, 2008).

7.4.4. Uncertainty

The work presented here has attempted to represent central tendency in the projected climate data by using the mean outputs of 5 GCMs, for the same emissions scenario. However, the uncertainty within each scenario and each GCM means that, as with all research involving

climate projections, there is a large degree of uncertainty associated with the results presented here. Key sources of uncertainty include:

- Emissions scenarios
- The ensemble projections of temperature and precipitation projections
- The uncertainties associated with *GDiv*
- The existence and form of any relationship between geodiversity and species richness
- The spatial uncertainty of the WDPA shapefiles

The analyses presented here are designed to understand process and implications, rather than make specific projections upon which policy decisions can be made; the reader should not interpret outputs as predictions of what will happen.

The SRES storylines may already be underestimating the impact of social and economic change on climate emissions (and therefore climate change); given that the scenarios were devised pre-2000, with less knowledge of the impact of the rapid growth and industrialisation of developing nations such as China and India. Indeed, research has shown that all scenarios have under-estimated actual increases of energy use intensity over the first decade of the 21st century (Pielke *et al.*, 2008). The impact of this on the results presented here is that the extent of declining geodiversity classes may be significantly lower than projected were climate change to be more extreme than envisaged in the A2 scenario.

Ensemble modelling, such as the "mean of models" approach used by van Soesbergen (2011) to produce the projected climate change data used in these analyses, has been used to assess the uncertainty associated with GCMs; the mean value across the ensemble of models representing the central tendency of projected values, whilst the variation between models in the ensemble give a measure of the uncertainty associated with the models (Barnett *et al.*, 2006).

In the case of the model ensemble used for these analyses, figure 7.1 shows a greater level of agreement with regards to temperature projections than precipitation, suggesting that there is a higher level of uncertainty associated with the precipitation data used herein. Given that *GDiv* is more sensitive to precipitation than temperature (section 4.3.1), the implications of this are important as a wide range of uncertainty in the projected geodiversity classes reduces the chance that the projected values represent the true current or future distribution of these classes. A fully quantified estimation of the impact of uncertainty arising from the use of including different GCMs in the ensemble would be valuable.

Aside from the uncertainties associated with the modelling of both geodiversity and climate projections, there is also a degree of uncertainty associated with the WDPA data. In some regions it is possible to validate the WDPA polygons based on forest cover from satellite imagery, however many of the protected areas in these analyses have a high level of cloud cover which obscures the land surface beneath. Were the PEZs to be used to guide conservation planning, it would be necessary to further validate the accuracy of the WDPA protected area polygons of interest. The same is true for all input datasets to the *GDiv* baseline and upon which the climate change factors are added including the DEM, temperature and precipitation maps as well as the global datasets used to understand the distribution of human occupancy (night time lights).

7.4.5. Future considerations

An artefact of the definition of "mountains" as the study region is that some of the existing protected areas were clipped to the study area; as a result, vulnerability to changes in geodiversity may have been overestimated. For example, PA250 is part of a larger conglomeration of three protected areas which extend eastward into the lowlands; this "edge effect" impacts several of the protected areas included in these analyses. Geodiversity classes currently contained within lowland protected areas or projected to be found in these protected areas in future climate scenarios are excluded from these analyses. Future work should look to overcome this limitation by running the analysis over a greater extent.

A further consideration is the need to ensure the connectivity of any protected area extension in terms of geodiversity classes. Working on the assumption that unique geodiversity classes are associated with unique species assemblages (an assumption that needs further investigation), any protected area extension should attempt to provide connectivity with similar, existing geodiversity classes to enable natural migration of the species with climate change. Increased connectivity ought to further increase the robustness of the protected area network, increasing the potential for natural re-colonisation and migration to areas of more favourable habitat. Again, factors other than the physical habitat would need to be taken into consideration; for example examining the impact metrics reveals the areas of high development which would prevent connectivity between some protected areas within close proximity to each other.

A final avenue that should be carefully explored is the assumed relationship between unique geodiversity classes and unique species assemblages. According to niche theory, species are

able to co-exist by carving out an individual niche consisting of a unique combination of "tolerances" of environmental conditions (Hutchinson, 1957, Schoener, 1974). It thus follows that unique combinations of environmental conditions (i.e. unique geodiversity classes) ought to be associated with unique groups of species, adapted to those conditions. This has important implications in terms of the protection of rare geodiversity classes, as these would be expected to contain rare and / or endemic species. If this relationship can be demonstrated to hold, conservation of geodiversity classes would provide a valuable alternative to costly inventory and collection expeditions.

7.5. Conclusions

This chapter set out to answer the question "what are the likely impacts of climate change on the spatial distribution of current geodiversity and what are the implications of this in terms of the suitability of the current protected area configuration to protect geodiversity and thus biodiversity?". *GDiv* simulations under a range of SRES climate change scenarios over two time periods revealed that, whilst the majority of the study area will remain within one standard deviation of the baseline score there is likely to be a change in overall geodiversity in some areas. However, when the three components of geodiversity are classified and combined to give unique geodiversity classes and these are projected under a climate change scenario (SRES A2), more extensive change is revealed with higher elevations experiencing a greater magnitude of change than lower elevations. Furthermore projections for two time periods revealed that there is not a single "future", with some geodiversity classes having very different extents under the two projected scenarios.

The current protected area network seems to be effective at conserving unique geodiversity classes, with a maximum over / under representation of ± 4% for geodiversity classes within the protected areas compared to across the entire study region. Future work is needed to test whether this robustness is true when only the higher IUCN protection categories are considered since these may be the protected areas that have a greater level of protection in the long-term. The robustness of the protected area network under the future scenarios, when considered over all geodiversity classes, improves in terms of protected area representativeness of geodiversity classes for both periods (i.e. more classes are closer to a representativeness score of 0 than under baseline conditions and therefore have the same proportion of coverage within the protected area network as across the wider study region). However, some classes do decline in representativeness. Whilst there are potential opportunities to expand the current protected area network to conserve these classes, any

expansions will need full social and economic costing with high levels of engagement with local stakeholders before any concrete recommendations can be made.

Chapter 8: Conclusions

8.1. Research questions

This thesis set out to answer three research questions:

Question one: Is there a quantifiable relationship between geodiversity, as defined in Parks and Mulligan (2010), and biodiversity as measured by overlay of the available mapped estimates of IUCN redlist species distributions for key taxonomic groups?

Question two: Do areas that are consistently prioritised by conservation organisations offer protection to a higher proportion of geodiversity than would be expected by chance alone?

Question three: What are the likely impacts of climate change on the spatial distribution of current geodiversity scores and classes of geodiversity and what might be the implications of this in terms of the suitability of current protected area configuration in tropical mountains to protect geodiversity and thus biodiversity into the future?

8.1.1. Question one

With regards to question one, chapter 5 presented some support for a relationship between the geodiversity metric developed in this thesis and a species richness overlay based on mammal and amphibian species richness using comparisons based on uni-variate GWR analysis. The most powerful explanatory variable for the majority of spatial aggregation techniques was the spatial context of resources (*Sc*), suggesting that the wider spatial context of resources is the most relevant of the three components of geodiversity to biodiversity patterns for the taxa and regions in which the analyses were run. It is important to remember that these relationships may vary from region to region, so further work is necessary to establish whether the importance of *Sc* is a general trend or unique to the taxa and study sites across three continents that were chosen. A further development of the analyses presented in chapter 5 would be to move to multi-variate analyses with the aim of better describing the trends in species richness. A combination of either the components of geodiversity (*RES*, *Sc* and *Tv*) or the scaled elements for the environmental inputs (i.e. the maps presented in figures 4.9 – 4.11) could be used as explanatory variables in a multi-variate GWR analysis.

The species richness overlay used was based on IUCN redlist distribution maps, which provide a binary classification of range size for each species that has been assessed. Whilst this represents the best global biodiversity dataset that is currently available, there are major weaknesses inherent in the data. There is potential to improve the biodiversity overlay to some degree by moving from a binary to a fuzzy classification of extent, which would reflect the uncertainty associated with delimiting species' extents. This could be based on a simple distance decay, or include climate and environmental co-variates as a measure of the rate of change. Whilst an improved species richness overlay would be useful in terms of assessing the relationship between biodiversity and geodiversity, as well as assessing conservation efficiency, it would still not represent a true pixel based measure of global species richness.

8.1.2. Question two

Question two was investigated in chapter 6, where a worrying lack of conservation efficiency of species richness and geodiversity within consistently prioritised regions was found. Whilst further refinement of the success metric is required, along with refinement of the conservation priority metric, the general trend of a lack of conservation efficiency is unequivocal. This can be attributed to the datasets used to measure success as the species richness datasets represent all classes of the IUCN redlist data, including those of "least concern". Given that the "least concern" threat category was the largest category for each of the taxanomic groups used in these analyses (55% of the mammal species and 37% of amphibian species), it is perhaps unsurprising that the prioritisation schemes are not efficient when tested against this metric as most of the prioritisation schemes aimed to prioritise vulnerable species.

Future work developing species richness overlays for each of the IUCN threat classes would thus enable consideration of the conservation efficiency of prioritised areas for each threat class. Given that these areas are a key method of in-situ conservation, it is of vital importance that they are conservation efficient, especially for threatened species. If this is not the case, then swift action would be needed to ensure that any newly designated protected areas are conservation efficient and that any extensions to existing protected areas increase overall conservation efficiency. This can be achieved by combining regional hotspot analyses such as those presented here with detailed on the ground monitoring and evaluation.

It is important to note that these analyses were based on species richness, with no measure of species turnover included. Thus there was no distinction between areas with a high level of species richness but low endemism and areas which may have had lower species richness but contain many endemic species. Future work should look to include a measure of endemism when assessing the efficiency of protected areas and prioritisation schemes.

The analyses carried out in chapter 6 were based on a multi-taxa species richness overlay and were aimed at giving an overall assessment of conservation efficiency for a broad range of conservation prioritisation schemes. However, the method developed here has the potential to be further developed to support conservation prioritisation in addition to the existing schemes such as hotspots and the global 200.

8.1.3. Question three

In answer to question three, it was found that, on the basis of scenarios for climate change to the 2050s and 2080s, the majority of the study area remained within one standard deviation of the current geodiversity score and remained in the same geodiversity class. The protected area network across the test site is generally effective at representing all classes of geodiversity in similar proportions to those found across the whole study area. The overall representativeness of geodiversity classes within the protected areas of the study area improves over both future periods considered in the analyses. However, some geodiversity classes switch from being over-represented under the current regime to being under-represented in both the 2050s and 2080s, whilst some of the classes that are currently under-represented become more so for both periods. The results of the classifying system used are dependent on the initial boundaries set; future work should involve a sensitivity analysis into the impact of varying this on the results.

Bearing in mind that these analyses were based on only one of many potential future emissions scenarios (though several GCMs), it was not deemed appropriate to make specific recommendations in terms of precisely defined extensions to named protected areas. Instead, it is recommended that the techniques developed in this thesis could contribute to more fully exploring the potential changes in geodiversity representation within the protected area network as a result of a wide range of climate change scenarios.

8.2. Future model development

GDiv has been demonstrated to be robust within the boundaries of the testing presented in this thesis. However, this version of the model would benefit from further development including work on the following:

1. The components and elements of geodiversity included in *GDiv*, for example combining the *Sc* and *RES* components or adding in measures of the soil / geology element of geodiversity.
2. Improving the scaling of the final geodiversity score, for example scaling to the 90th percentile rather than the maximum.
3. Moving from a measure of raw natural geodiversity to one including human influence on the environment incorporating factors such as land use.
4. Refinement of the calculation of unique geodiversity classes presented in chapter 7 and further testing of the potential relationship with unique species assemblages.

The results from chapter 4 show that *Sc* and *RES* are correlated (r = 0.95, figure 4.28) suggesting that, whilst there is no model redundancy at the element level (i.e. between the raw model inputs such as rainfall and temperature) there is some model redundancy in terms of the components (i.e. *RES, Sc* and *Tv*). The results from chapter 5 suggest that, in terms of modelling biodiversity, *Sc* provides the strongest predictive variable (at least for the study areas included in the analyses) and so redundancy in *GDiv* could be reduced by removing *RES* and simply including *Sc* and *Tv* only.

Much of the literature cited suggests that spatial heterogeneity is also an important control of biodiversity and future development of *GDiv* should look to include a measure of this. Potential measures include a kernel based measure of either standard deviation or diversity of resources. An alternative to both of these would be to use the environmental roughness index, *G*, proposed by Dufour et al. (2006) and outlined in chapter 2.4.3. *G* was originally intended to quantify topographic heterogeneity across two planes (north – south and east – west slopes), based on the standard deviation of slopes in these two orientations. This measure could be adapted for use with any continuous environmental variable and, within *GDiv* would need to be calculated within a moving kernel in order to provide a map-surface showing how *G* changes over the study area, rather than calculating a single value of *G* for the entire study region.

The current version of *GDiv* scales the components and geodiversity metric by the maximum value in the study area, which means that the results are highly dependent on this maximum

and therefore sensitive to outliers. Future model improvements should look to develop this into a more robust method that is less dependent on the "tails" of the distribution of values within the study area, for example scale the component and geodiversity maps to a high percentile value (e.g. the 90th percentile).

Newer versions of *GDiv* should also aim to move away from measuring "raw" geodiversity, as in geodiversity in a pristine environment, to providing a measure of geodiversity in the human impacted world. This could be achieved by overlaying the raw geodiversity metric, as calculated by the current version of *GDiv*, with a measure of agriculturisation and urbanisation. This development will allow investigation of the impact of land-use change on geodiversity (noting that both urban areas and agriculture maintain elements of geodiversity) and thus enable analyses into the combined impact of both climate and land-use change.

As outlined in chapter 7.4.1, the unique geodiversity classes used in chapter 7 would benefit from further refinement in terms of delimiting the classes. Theoretically, these classes should be associated with unique species assemblages. It would be interesting to test this hypothesis using the IUCN species extent polygons. Furthermore, these polygons have been used to calculate a surface of endemism (Mulligan, 2009) which could be used to assess whether or not rare geodiversity classes are associated with hotspots of endemism.

Whilst the sensitivity analyses presented in Chapter 4 increased understanding of the impact of utilising different data sources and spatial resolutions on the results of *GDiv* it is important to remember that the results presented in chapters 5 to 7 are (necessarily) based on a single set of data inputs at a single resolution; these results may be very different had alternative input datasets at varying resolutions been used in the analyses. Future work should look to further investigate and quantify the impact of using alternative datasets at different spatial resolutions.

8.3. Applications of *GDiv*

The techniques presented in this thesis have great potential in terms of enabling policy makers to improve the conservation of the natural world, be that bio- or geodiversity. In order to enable the dissemination of these findings, it is proposed that a web-interface is developed in order to provide an online tool to support conservation decisions. This could either form part of the wider suite of tools available at www.policysupport.org (for example Costing Nature), or

form the basis of a new website. The tool should focus on providing access to the techniques presented in chapters 6 and 7, namely to enable the interested party to:

- Establish the conservation efficiency of a suite of protected areas
- Investigate the robustness of the protected area network under climate change scenarios.

To meet the first of these, the website should enable the interested party to define their own priority system (through drawing a polygon on a map or uploading an existing file), and then assess the efficiency of these polygons at conserving geodiversity. The ability to test the efficiency of prioritisation schemes will enable conservation organisations to gain the most "bang per buck".

The second facility should enable the policy maker to define the study extent and then carry out a gap analysis of the protected areas within that region for both current and future projections of classified geodiversity; the ability to select the categories of protected area to include in the analyses would be advantageous. This tool must allow users to explore a wide range of climate and land-use scenarios and ideally would enable policy makers to test a range of potential protected area extensions to determine the optimal solution to the potential impacts of climate and land-use change.

In order to ensure the most effective continuation of the research presented in this thesis *GDiv* should first be improved as outlined in section 8.2, before being made available for wider use.

References

ABRAMS, P. 1983. THE THEORY OF LIMITING SIMILARITY. *Annual Review of Ecology and Systematics,* 14**,** 359-376.

ABRAMS, P. A. 1995. MONOTONIC OR UNIMODAL DIVERSITY PRODUCTIVITY GRADIENTS - WHAT DOES COMPETITION THEORY PREDICT. *Ecology,* 76**,** 2019-2027.

ANALYSIS, C. C. F. C. M. A. 2010. *CGCM3.1 Model Output* [Online]. Available: http://www.cccma.ec.gc.ca/data/cgcm3/cgcm3.shtml [Accessed 12/01 2012].

ANDELMAN, S. J. & FAGAN, W. F. 2000. Umbrellas and flagships: Efficient conservation surrogates or expensive mistakes? *Proceedings of the National Academy of Sciences of the United States of America,* 97**,** 5954-5959.

ARAUJO, M. B. & PEARSON, R. G. 2005. Equilibrium of species' distributions with climate. *Ecography,* 28**,** 693-695.

ARAUJO, M. B. & RAHBEK, C. 2006. How does climate change affect biodiversity? *Science,* 313**,** 1396-1397.

ARAUJO, M. B., DENSHAM, P. J. & WILLIAMS, P. H. 2004. Representing species in reserves from patterns of assemblage diversity. *Journal of Biogeography,* 31**,** 1037-1050.

ARMENTERAS, D. & MULLIGAN, M. 2010. Modelling the potential distribution of tree species on a national scale in Colombia: Application to *Palicourea angustifolia* kunth and *Palicourea guianensi* aubl. *Botanica Fitogeografia,* 32**,** 355 - 380.

ARRHENIUS, O. 1921. Species and area. *Journal of Ecology,* 9**,** 95-99.

ASSESSMENT, M. E. 2005. *Ecosystems and Human Wellbeing* [Online]. Available: http://www.millenniumassessment.org/documents/document.356.aspx.pdf [Accessed 2nd June 2009].

AUBRY, S., MAGNIN, F., BONNET, V. & PREECE, R. C. 2005. Multi-scale altitudinal patterns in species richness of land snail communities in south-eastern France. *Journal of Biogeography,* 32**,** 985-998.

BALDI, A. 2008. Habitat heterogeneity overrides the species-area relationship. *Journal of Biogeography,* 35**,** 675-681.

BALEK, J. 1983. *Hydrology and Water Resources in Tropical Regions,* New York, Elsevier.

BALLETTO, E., BONELLI, S., BORGHESIO, L., CASALE, A., BRANDMAYR, P. & TAGLIANTI, A. V. 2010. Hotspots of biodiversity and conservation priorities: A methodological approach. *Italian Journal of Zoology,* 77**,** 2-13.

BANK, A. D. 2011. *Greater Mekong Subregion Biodiversity Conservation Corridors* [Online]. Available: http://www.adb.org/projects/project.asp?id=40253 [Accessed 12/01 2012].

BANKS-LEITE, C., EWERS, R. M., KAPOS, V., MARTENSEN, A. C. & METZGER, J. P. 2011. Comparing species and measures of landscape structure as indicators of conservation importance. *Journal of Applied Ecology,* 48**,** 706-714.

BARNARD, P., BROWN, C. J., JARVIS, A. M., ROBERTSON, A. & VAN ROOYEN, L. 1998. Extending the Namibian protected area network to safeguard hotspots of endemism and diversity. *Biodiversity and Conservation,* 7**,** 531-547.

BARNETT, D. N., BROWN, S. J., MURPHY, J. M., SEXTON, D. M. H. & WEBB, M. J. 2006. Quantifying uncertainty in changes in extreme event frequency in response to doubled CO2 using a large ensemble of GCM simulations. *Climate Dynamics,* 26**,** 489-511.

BARTHLOTT, W., KIER, G. & MUTKE, J. 1999. Global biodiversity and its uneven distribution. *In:* WALOSSEK, D. (ed.) *Shakeup in Systematics.* Frankfurt: Senckenbergische Naturforschende Gesellschaft.

BARWICK, M. 2004. Tropical and Subtropical trees. A worldwide encyclopaedia. London: Thames and Hudson.

BASS, M. S., FINER, M., JENKINS, C. N., KREFT, H., CISNEROS-HEREDIA, D. F., MCCRACKEN, S. F., PITMAN, N. C. A., ENGLISH, P. H., SWING, K., VILLA, G., DI FIORE, A., VOIGT, C. C. & KUNZ, T. H. 2010. Global Conservation Significance of Ecuador's Yasuni National Park. *Plos One,* 5.

BATES, J. M., HAFFER, J. & GRISMER, E. 2004. Avian mitochondrial DNA sequence divergence across a headwater stream of the Rio Tapajos, a major Amazonian river. *Journal of Ornithology,* 145**,** 199-205.

BEAUMONT, L. J., HUGHES, L. & POULSEN, M. 2005. Predicting species distributions: use of climatic parameters in BIOCLIM and its impact on predictions of species' current and future distributions. *Ecological Modelling,* 186**,** 250-269.

BECK, J. & KITCHING, I. J. 2007. Estimating regional species richness of tropical insects from museum data: a comparison of a geography-based and sample-based methods. *Journal of Applied Ecology,* 44**,** 672-681.

BECK, J., KITCHING, I. J. & LINSENMAIR, K. E. 2006. Determinants of regional species richness: an empirical analysis of the number of hawkmoth species (Lepidoptera : Sphingidae) on the Malesian archipelago. *Journal of Biogeography,* 33**,** 694-706.

BEGON, M., HARPER, J. L. & TOWNSEND, C. R. 1996. *Ecology,* Oxford, Blackwell Science.

BELBIN, L. 1993. ENVIRONMENTAL REPRESENTATIVENESS - REGIONAL PARTITIONING AND RESERVE SELECTION. *Biological Conservation,* 66**,** 223-230.

BENTON, M. J. 2009. The Red Queen and the Court Jester: Species Diversity and the Role of Biotic and Abiotic Factors Through Time. *Science,* 323**,** 728-732.

BIRDLIFE INTERNATIONAL. 2009a. *Endemic Bird Areas* [Online]. Available: http://www.birdlife.org/action/science/endemic_bird_areasindex.html [Accessed 2nd June 2009].

BIRDLIFE INTERNATIONAL. 2009b. *Important Bird Areas* [Online]. Available: http://www.birdlife.org/action/science/sites/ [Accessed 2nd June 2009].

BIRDLIFE INTERNATIONAL. 2011a. *Species Distribution Data Download* [Online]. Available: http://www.birdlife.org/datazone/info/spcdownload [Accessed 20/12 2011].

BONN, A. & GASTON, K. J. 2005. Capturing biodiversity: selecting priority areas for conservation using different criteria. *Biodiversity and Conservation,* 14**,** 1083-1100.

BOTKIN, D. B., SAXE, H., ARAUJO, M. B., BETTS, R., BRADSHAW, R. H. W., CEDHAGEN, T., CHESSON, P., DAWSON, T. P., ETTERSON, J. R., FAITH, D. P., FERRIER, S., GUISAN, A., HANSEN, A. S., HILBERT, D. W., LOEHLE, C., MARGULES, C., NEW, M., SOBEL, M. J. & STOCKWELL, D. R. B. 2007. Forecasting the effects of global warming on biodiversity. *Bioscience,* 57**,** 227-236.

BOWEN, B. W. & ROMAN, J. 2005. Gaia's handmaidens: the Orlog model for conservation biology. *Conservation Biology,* 19**,** 1037-1043.

BRITISH ATMOSPHERIC DATA CENTRE, 2000. Mean sea level pressure derived from UK Meteorological Office, Hadley Centre, CSIRO (Scientific and Industrial Research for Australia), Australia and NIWA (National Institute of Water and Atmospheric Research), New Zealand. Met Office - Global Mean Sea-Level Pressure datasets (GMSLP and HadSLP1).

BROOKS, T. M., MITTERMEIER, R. A., DA FONSECA, G. A. B., GERLACH, J., HOFFMANN, M., LAMOREUX, J. F., MITTERMEIER, C. G., PILGRIM, J. D. & RODRIGUES, A. S. L. 2006. Global biodiversity conservation priorities. *Science,* 313**,** 58-61.

BROWN, J. S. 1989. COEXISTENCE ON A SEASONAL RESOURCE. *American Naturalist,* 133**,** 168-182.

BRUIJNZEEL, L., MULLIGAN, M. & SCATENA, F. 2011. Hydrometeorology of tropical montane cloud forests: emerging patterns. *Hydrological Processes,* 25**,** 465-498.

BRYANT, D., NIELSON, D. & TANGLEY, L. 1997. *Last Frontier Forests,* Washington DC, World Resources Institute.

BUCHHOLZ, R. 2007. Behavioural biology: an effective and relevant conservation tool. *Trends in Ecology & Evolution,* 22**,** 401-407.

BUCKLAND, S. T., MAGURRAN, A. E., GREEN, R. E. & FEWSTER, R. M. 2005. Monitoring change in biodiversity through composite indices. *Philosophical Transactions of the Royal Society B-Biological Sciences,* 360**,** 243-254.

BURGESS, N. D., BALMFORD, A., CORDEIRO, N. J., FJELDSA, J., KUPER, W., RAHBEK, C., SANDERSON, E. W., SCHARLEMANN, J. P. W., SOMMER, J. H. & WILLIAMS, P. H. 2007. Correlations among species distributions, human density and human infrastructure across the high biodiversity tropical mountains of Africa. *Biological Conservation,* 134**,** 164-177.

BURNHAM, K. P. & ANDERSON, D. R. 2002. Model selection and multimodel inference. Second edition ed. New York: Springer.

BURRIDGE, D. M. & GADD, A. J. 1977. The Meteorological Office operational 10-level numerical weather prediction model (December 1975). *The Meteorological Office operational 10-level numerical weather prediction model (December 1975)***,** 39.

CALLICOTT, J. B., ROZZI, R., DELGADO, L., MONTICINO, M., ACEVEDO, M. & HARCOMBE, P. 2007. Biocomplexity and conservation of biodiversity hotspots: three case studies from the Americas. *Philosophical Transactions of the Royal Society B-Biological Sciences,* 362**,** 321-333.

CARROLL, S. P., HENDRY, A. P., REZNICK, D. N. & FOX, C. W. 2007. Evolution on ecological time-scales. *Functional Ecology,* 21**,** 387-393.

CATULLO, G., MASI, M., FALCUCCI, A., MAIORANO, L., RONDININI, C. & BOITANI, L. 2008. A gap analysis of Southeast Asian mammals based on habitat suitability models. *Biological Conservation,* 141**,** 2730-2744.

CBD. 1992. *Text of the Convention on Biological Diversity* [Online]. Available: http://www.cbd.int/convention/convention.shtml [Accessed 2nd June 2009].

CBD. 2006. *Article 2. Use of Terms* [Online]. [Accessed 2nd June 2009].

CBD. 2009. *The 2010 Biodiversity Target* [Online]. Available: http://www.dbc.int/doc/publications/cbd-2010-brochure-en.pdf [Accessed 2nd June 2009].

CBD. 2010. *List of Parties* [Online]. Available: http://www.cbd.int/convention/parties/list [Accessed 8th October 2010].

CBD. 2011. *Mountain Biodiversity* [Online]. Available: http://www.cbd.in/mountain [Accessed 25/11 2011].

CGIAR-CSI. 2004. *Void filled seamless SRTM data V1, International Centre for Tropical Agriculture (CIAT)* [Online]. Available: http://www.ambiotek.com/topoview [Accessed 2nd June 2009].

CHESSON, P. 2000. Mechanisms of maintenance of species diversity. *Annual Review of Ecology and Systematics,* 31**,** 343-+.

CIA. 2011. *The World Factbook* [Online]. Available: https://www.cia.gov/library/publications/the-world-factbook/ [Accessed 18/12 2011].

CITES. 2008. *What is CITES?* [Online]. Available: http://www.cites.org/eng/disc/what.shtml [Accessed 2nd June 2009].

CONDIT, R. 1998. Ecological implications of changes in drought patterns: Shifts in forest composition in Panama. *Climatic Change,* 39**,** 413-427.

CONNELL, J. H. 1978. DIVERSITY IN TROPICAL RAIN FORESTS AND CORAL REEFS - HIGH DIVERSITY OF TREES AND CORALS IS MAINTAINED ONLY IN A NON-EQUILIBRIUM STATE. *Science,* 199**,** 1302-1310.

CONSERVATION INTERNATIONAL. 2007. *Tumbes-Chocos-Magdalena Hotspot* [Online]. Available: http://www.biodiversityhotspots.org/xp/hotspots/tumbes_choco/Pages/default.aspx [Accessed 2nd June 2009].

CONSERVATION INTERNATIONAL. 2011b. *Tropical Andes Hotspot* [Online]. Available: http://www.biodiversityhotspots.org/xp/hotspots/andes/Pages/default.aspx [Accessed 16/12/2011 2011].

CONSERVATION INTERNATIONAL. 2012. *Corridors* [Online]. Available: http://www.conservation.org/FMG/Articles/Pages/conservation_corridors_for_pandas_people.aspx [Accessed 12/01 2012].

CORRAL, A., TELESCA, L. & LASAPONARA, R. 2008. Scaling and correlations in the dynamics of forest-fire occurrence. *Physical Review E,* 77.

COSTANZA, R., DARGE, R., DEGROOT, R., FARBER, S., GRASSO, M., HANNON, B., LIMBURG, K., NAEEM, S., ONEILL, R. V., PARUELO, J., RASKIN, R. G., SUTTON, P. & VANDENBELT, M. 1997. The value of the world's ecosystem services and natural capital. *Nature,* 387**,** 253-260.

CSIRO. 2005. *CSIRO-Mk3.0. Model Information of Potential Use to the IPCC Lead Authors and the AR4.* [Online]. Available: http://www-pcmdi.llnl.gov/ipcc/model_documentation/CSIRO-Mk3.0.htm [Accessed 12/01 2012].

DALLMEIER, F., KABEL, M., MAYNE, J. C., RICE, R. & TAYLOR, C. M. 1992. *Long-term monitoring of biological diversity in tropical forest areas. Methods for establishment and inventory of permanent plots.,* Paris, UNESCO.

DALY, C., NEILSON, R. P. & PHILLIPS, D. L. 1994. A STATISTICAL TOPOGRAPHIC MODEL FOR MAPPING CLIMATOLOGICAL PRECIPITATION OVER MOUNTAINOUS TERRAIN. *Journal of Applied Meteorology,* 33**,** 140-158.

DAMSCHEN, E. I., HADDAD, N. M., ORROCK, J. L., TEWKSBURY, J. J. & LEVEY, D. J. 2006. Corridors increase plant species richness at large scales. *Science,* 313**,** 1284-1286.

DAVALOS, L., BEJARANO, A., HALL, M., CORREA, H., CORTHALS, A. & ESPEJO, O. 2011. Forests and Drugs: Coca-Driven Deforestation in Tropical Biodiversity Hotspots. *Environmental Science & Technology,* 45**,** 1219-1227.

DE MERODE, E., SMITH, K. H., HOMEWOOD, K., PETTIFOR, R., ROWCLIFFE, M. & COWLISHAW, G. 2007. The impact of armed conflict on protected-area efficacy in Central Africa. *Biology Letters,* 3**,** 299-301.

DIAZ, S., FARGIONE, J., CHAPIN, F. S. & TILMAN, D. 2006. Biodiversity loss threatens human well-being. *Plos Biology,* 4**,** 1300-1305.

DING, T. S., YUAN, H. W., GENG, S., KOH, C. N. & LEE, P. F. 2006. Macro-scale bird species richness patterns of the East Asian mainland and islands: energy, area and isolation. *Journal of Biogeography,* 33**,** 683-693.

DINIZ, J. A. F. 2004. Phylogenetic diversity and conservation priorities under distinct models of phenotypic evolution. *Conservation Biology,* 18**,** 698-704.

DMSP 2004. Night-time lights of the world.

DOLMAN, A. J., VERHAGEN, A. & ROVERS, C. A. 2003. *Global Environmental Change and Land Use Change,* Dordrecht, Kluwer Academic Publishers.

DRAULANS, D. & VAN KRUNKELSVEN, E. 2002. The impact of war on forest areas in the Democratic Republic of Congo. *Oryx,* 36**,** 35-40.

DUFOUR, A., GADALLAH, F., WAGNER, H. H., GUISAN, A. & BUTTLER, A. 2006. Plant species richness and environmental heterogeneity in a mountain landscape: effects of variability and spatial configuration. *Ecography,* 29**,** 573-584.

EKEN, G., BENNUN, L., BROOKS, T. M., DARWALL, W., FISHPOOL, L. D. C., FOSTER, M., KNOX, D., LANGHAMMER, P., MATIKU, P., RADFORD, E., SALAMAN, P., SECHREST, W., SMITH, M. L., SPECTOR, S. & TORDOFF, A. 2004. Key biodiversity areas as site conservation targets. *Bioscience,* 54**,** 1110-1118.

ELITH, J., GRAHAM, C. H., ANDERSON, R. P., DUDIK, M., FERRIER, S., GUISAN, A., HIJMANS, R. J., HUETTMANN, F., LEATHWICK, J. R., LEHMANN, A., LI, J., LOHMANN, L. G., LOISELLE, B. A., MANION, G., MORITZ, C., NAKAMURA, M., NAKAZAWA, Y., OVERTON, J. M., PETERSON, A. T., PHILLIPS, S. J., RICHARDSON, K., SCACHETTI-PEREIRA, R., SCHAPIRE, R. E., SOBERON, J., WILLIAMS, S., WISZ, M. S. & ZIMMERMANN, N. E. 2006. Novel methods improve prediction of species' distributions from occurrence data. *Ecography,* 29**,** 129-151.

ENGLAND, N. 2009. *Local geodiversity action plans* [Online]. Available: http://www.english-nature.org.uk/special/geological/lgap/default.htm [Accessed 2nd June 2009].

ERWIN, T. L. 1991. AN EVOLUTIONARY BASIS FOR CONSERVATION STRATEGIES. *Science,* 253**,** 750-752.

ESRI. 2008. ArcMap (Info) 9.3. Redlands, California: ESRI.

EVANS, K. L., WARREN, P. H. & GASTON, K. J. 2005. Species-energy relationships at the macroecological scale: a review of the mechanisms. *Biological Reviews,* 80**,** 1-25.

FAITHS, D. P., FERRIER, S. & WILLIAMS, K. J. 2008. Getting biodiversity intactness indices right: ensuring that 'biodiversity' reflects 'diversity'. *Global Change Biology,* 14**,** 207-217.

FAO. 2009a. *Crop evapotranspiration - Guidelines for computing crop water requirements - FAO irrigation and drainage paper 56* [Online]. Available: http://www.fao.org/docrep/Z0490E/x0490e00/htm#Contents [Accessed 2nd June 2009].

FAO. 2009b. *Irrigation water management: Irrigation water needs* [Online]. Available: http://www.fao.org/docrep/s2022e/2022e00.htm#Contents [Accessed 2nd June 2009].

FAO. 2010. *Global Forest Resources Assessment* [Online]. Available: http://www.fao.org/forestry/fra/fra2010/en/ [Accessed 21/01 2012].

FATTORINI, S. 2007. Are planar areas adequate for the species-area relationship? *Italian Journal of Zoology,* 74**,** 259-264.

FEDDEMA, J. J., OLESON, K. W., BONAN, G. B., MEARNS, L. O., BUJA, L. E., MEEHL, G. A. & WASHINGTON, W. M. 2005. The importance of land-cover change in simulating future climates. *Science,* 310**,** 1674-1678.

FERREIRA DE LIMA, R. A. & DE MOURA, L. C. 2008. Gap disturbance regime and composition in the Atlantic Montane Rain Forest: the influence of topography. *Plant Ecology,* 197**,** 239-253.

FERRIER, S. & WATSON, G. 1997. An evaluation of the effectiveness of environmental surrogates and modelling techniques in predicting the distribution of biological diversity. Consultancy report to the Biodiversity Convention and Strategy Section of the Biodiversity Group, Environment Australia. Australia: Environment Australia.

FERRIER, S., WATSON, G., PEARCE, J. & DRIELSMA, M. 2002. Extended statistical approaches to modelling spatial pattern in biodiversity in northeast New South Wales. I. Species-level modelling. *Biodiversity and Conservation,* 11**,** 2275-2307.

FIELD, R., HAWKINS, B. A., CORNELL, H. V., CURRIE, D. J., DINIZ-FILHO, J. A. F., GUEGAN, J. F., KAUFMAN, D. M., KERR, J. T., MITTELBACH, G. G., OBERDORFF, T., O'BRIEN, E. M. & TURNER, J. R. G. 2009. Spatial species-richness gradients across scales: a meta-analysis. *Journal of Biogeography,* 36**,** 132-147.

FLETCHER, R. J., RIES, L., BATTIN, J. & CHALFOUN, A. D. 2007. The role of habitat area and edge in fragmented landscapes: definitively distinct or inevitably intertwined? *Canadian Journal of Zoology-Revue Canadienne De Zoologie,* 85**,** 1017-1030.

FOTHERGILL, A. 2006. Planet Earth. BBC Books, Ebury Publishing.

FOTHERINGHAM, A. S., BRUNSDON, C. & CHARLTON, M. 2002. *Geographically Weighted Regression; the analysis of spatially varying relationships.,* Chichester, Wiley.

FRETWELL, S. D. 1987. FOOD-CHAIN DYNAMICS - THE CENTRAL THEORY OF ECOLOGY. *Oikos,* 50**,** 291-301.

GASTON, K. J. & SPICER, J. I. 2004. *Biodiversity. An Introduction.,* Oxford, Blackwell Science.

GASTON, K. J. 2000. Global patterns in biodiversity. *Nature,* 405**,** 220-227.

GBIF. 2009. *Global Biodiversity Information Facility Data Portal* [Online]. Available: data.gbif.org [Accessed 2nd June 2009].

GLEASON, H. A. 1922. On the relation between species and area. *Ecology,* 3**,** 158-162.

GOMEZ-RODRIGUEZ, C., DIAZ-PANIAGUA, C., BUSTAMANTE, J., SERRANO, L. & PORTHEAULT, A. 2010. Relative importance of dynamic and static environmental variables as predictors of amphibian diversity patterns. *Acta Oecologica-International Journal of Ecology,* 36**,** 650-658.

GORELICK, R. 2008. Species richness and the analytic geometry of latitudinal and altitudinal gradients. *Acta Biotheoretica,* 56**,** 197-203.

GRAU, H. R. 2002. Scale-dependent relationships between treefalls and species richness in a neotropical montane forest. *Ecology,* 83**,** 2591-2601.

GRAY, M. 2004. *Geodiversity. Valuing and conserving abiotic nature.,* Chichester, Wiley.

GRAY, M. 2008. Geodiversity: developing the paradigm. *Proceedings of the Geologists Association,* 119**,** 287-298.

GRAY, M. 2011. Other nature: geodiversity and geosystem services. *Environmental Conservation,* 38**,** 271-274.

GUISAN, A. & ZIMMERMANN, N. E. 2000. Predictive habitat distribution models in ecology. *Ecological Modelling,* 135**,** 147-186.

GULBRANDSEN, L. H. 2009. The emergence and effectiveness of the Marine Stewardship Council. *Marine Policy,* 33**,** 654-660.

GUPTA, A. 2005. *The Physical Geography of Southeast Asia,* Oxford, Oxford University Press.

GUTTAL, V. & JAYAPRAKASH, C. 2007. Self-organization and productivity in semi-arid ecosystems: Implications of seasonality in rainfall. *Journal of Theoretical Biology,* 248**,** 490-500.

HAIRSTON, N. G., SMITH, F. E. & SLOBODKIN, L. B. 1960. COMMUNITY STRUCTURE, POPULATION CONTROL, AND COMPETITION. *American Naturalist,* 94**,** 421-425.

HALDANE, J. B. S. 1956. THE THEORY OF SELECTION FOR MELANISM IN LEPIDOPTERA. *Proceedings of the Royal Society of London Series B-Biological Sciences,* 145**,** 303-306.

HALPIN, P. N. 1997. Global climate change and natural-area protection: Management responses and research directions. *Ecological Applications,* 7**,** 828-843.

HAMILTON, L. S. 2002. Conserving mountain biodiversity in protected areas. *In:* KORNER, C. & SPEHN, E. M. (eds.) *Mountain Biodiversity, a global assessment.* London: Parthenon.

HAMPE, A. 2004. Bioclimate envelope models: what they detect and what they hide. *Global Ecology and Biogeography,* 13**,** 469-471.

HANNAH, L. 2001. The role of a global protected areas system in conserving biodiversity in the face of climate change. *Global Change and Protected Areas,* 9**,** 413-422.

HANSON, T., BROOKS, T. M., DA FONSECA, G. A. B., HOFFMANN, M., LAMOREUX, J. F., MACHLIS, G., MITTERMEIER, C. G., MITTERMEIER, R. A. & JOHN, D. P. 2009. Warfare in Biodiversity Hotspots. *Conservation Biology,* 23**,** 578-587.

HARRIS, J. A., HOBBS, R. J., HIGGS, E. & ARONSON, J. 2006. Ecological restoration and global climate change. *Restoration Ecology,* 14**,** 170-176.

HARRISON, R. L. 1992. TOWARD A THEORY OF INTER-REFUGE CORRIDOR DESIGN. *Conservation Biology,* 6**,** 293-295.

HAWKINS, B. A. & DINIZ, J. A. F. 2004. 'Latitude' and geographic patterns in species richness. *Ecography,* 27**,** 268-272.

HE, F. L. & LEGENDRE, P. 1996. On species-area relations. *American Naturalist,* 148**,** 719-737.

HIJMANS, R. J., CAMERON, S. E., PARRA, J. L., JONES, P. G. & JARVIS, A. 2005. Very high resolution interpolated climate surfaces for global land areas. *International Journal of Climatology,* 25**,** 1965-1978.

HILLERISLAMBERS, R., RIETKERK, M., VAN DEN BOSCH, F., PRINS, H. H. T. & DE KROON, H. 2001. Vegetation pattern formation in semi-arid grazing systems. *Ecology,* 82**,** 50-61.

HOEKSTRA, J. M., BOUCHER, T. M., RICKETTS, T. H. & ROBERTS, C. 2005. Confronting a biome crisis: global disparities of habitat loss and protection. *Ecology Letters,* 8**,** 23-29.

HOLE, D. G., WILLIS, S. G., PAIN, D. J., FISHPOOL, L. D., BUTCHART, S. H. M., COLLINGHAM, Y. C., RAHBEK, C. & HUNTLEY, B. 2009. Projected impacts of climate change on a continent-wide protected area network. *Ecology Letters,* 12**,** 420-431.

HONKANEN, M., ROBERGE, J. M., RAJASARKKA, A. & MONKKONEN, M. 2010. Disentangling the effects of area, energy and habitat heterogeneity on boreal forest bird species richness in protected areas. *Global Ecology and Biogeography,* 19**,** 61-71.

HORN, H. S. 1975. FOREST SUCCESSION. *Scientific American,* 232**,** 90-98.

HOUSEGO, K. 2005. *Cocaine is killing Colombian Nature Parks* [Online]. Available: http://www.enn.com/wildlife/article/2717/print [Accessed 18/12 2011].

HSIUNG, W. & SUNSTEIN, C. R. 2007. Climate change and animals. *University of Pennsylvania Law Review,* 155**,** 1695-1740.

HUBALEK, Z. 2000. Measures of species diversity in ecology: an evaluation. *Folia Zoologica,* 49**,** 241-260.

HUTCHINSON, G. E. 1957. POPULATION STUDIES - ANIMAL ECOLOGY AND DEMOGRAPHY - CONCLUDING REMARKS. *Cold Spring Harbor Symposia on Quantitative Biology,* 22**,** 415-427.

IMBACH, P., MOLINA, L., LOCATELLI, B., ROUPSARD, O., CIAIS, P., CORRALES, L. & MAHE, G. 2010. Climatology-based regional modelling of potential vegetation and average annual long-term runoff for Mesoamerica. *Hydrology and Earth System Sciences,* 14**,** 1801-1817.

IPCC. 2000. *Special Report on Emissions Scenarios (SRES)* [Online]. Available: http://www.grida.no/publications/other/ipcc_sr/ [Accessed 12/01 2012].

IPCC. 2007. *Climate Change 2007: Synthesis Report* [Online]. Available: http://www.ipcc.ch/pdf/assessment-report/ar4/syr/ar4_syr.pdf [Accessed 2nd June 2009].

IPSL. 2005. *IPSL-CM4 model. Model Information of Potential Use to the IPCC Lead Authors and the AR4.* [Online]. Available: http://dods.ipsl.jussieu.fr/omamce/IPSLCM4/DocIPSLCM4/FILES/DocIPSLCM4.pdf [Accessed 12/01 2012].

IQBAL, M. 1983. *Introduction to Solar Radiation,* London, Academic Press.

IUCN, CONSERVATION INTERNATIONAL, ARIZONA STATE UNIVERSITY, TEXAS A&M UNIVERSITY, UNIVERSITY OF ROME, UNIVERSITY OF VIRGINIA & ZOOLOGICAL SOCIETY OF LONDON 2008b. An analysis of mammals on the 2008 IUCN Red List. www.iucnredlist.org/mammals [downloaded 9th May, 2009].

IUCN, CONSERVATION INTERNATIONAL. & NATURESERVE 2008a. An analysis of amphibians on the 2008 IUCN Red List. www.iucnredlist.org/amphibians [downloaded 9th May, 2009].

IUCN. 1994. *Defining protected area management categories* [Online]. [Accessed 2nd June 2009].

IUCN. 2010a. *IUCN Red List of Threatened Species. Summary Statistics for Globally Threatened Species, Table 1: Numbers of threatened species by major groups of organisms (1996 - 2010).* [Online]. Available: www.iucnredlist.org/documents/summarystatistics/2010_1RL_stats_Table_1.pdf [Accessed 03/03 2012].

IUCN. 2010b. *Spatial Data Download* [Online]. Available: http://www.iucnredlist.org/technical-documents/spatial-data [Accessed 11/01 2012].

IUCN. 2011. *Spatial Data Download - Reptiles* [Online]. Available: http://www.iucnredlist.org/technical-documents/spatial-data#reptiles [Accessed 20/12 2011].

JANZEN, D. H. 1970. HERBIVORES AND NUMBER OF TREE SPECIES IN TROPICAL FORESTS. *American Naturalist,* 104**,** 501-&.

JARVIS, A. J. 2005. *Terrain controls on the distribution of tree species diversity and structure in tropical lowland and tropical montane forest.* PhD, King's College.

JAX, K. 2005. Function and "functioning" in ecology: what does it mean? *Oikos,* 111**,** 641-648.

JETZ, W., WILCOVE, D. S. & DOBSON, A. P. 2007. Projected impacts of climate and land-use change on the global diversity of birds. *Plos Biology,* 5**,** 1211-1219.

JIN, C. H. 2008. Biodiversity dynamics of freshwater wetland ecosystems affected by secondary salinisation and seasonal hydrology variation: a model-based study. *Hydrobiologia,* 598**,** 257-270.

JONES, M. M., TUOMISTO, H., BORCARD, D., LEGENDRE, P., CLARK, D. B. & OLIVAS, P. C. 2008. Explaining variation in tropical plant community composition: influence of environmental and spatial data quality. *Oecologia,* 155**,** 593-604.

KAREIVA, P. & MARVIER, M. 2003. Conserving biodiversity coldspots - Recent calls to direct conservation funding to the world's biodiversity hotspots may be bad investment advise. *American Scientist,* 91**,** 344-351.

KAUNZINGER, C. M. K. & MORIN, P. J. 1998. Productivity controls food-chain properties in microbial communities. *Nature,* 395**,** 495-497.

KESSLER, M. 2001. Patterns of diversity and range size of selected plant groups along an elevational transect in the Bolivian Andes. *Biodiversity and Conservation,* 10**,** 1897-1921.

KHAROUBA, H. M. & KERR, J. T. 2010. Just passing through: Global change and the conservation of biodiversity in protected areas. *Biological Conservation,* 143**,** 1094-1101.

KHOMO, L. & ROGERS, K. H. 2009. Stream order controls geomorphic heterogeneity and plant distribution in a savanna landscape. *Austral Ecology,* 34**,** 170-178.

KIER, G. & BARTHLOTT, W. 2001. Measuring and mapping endemism and species richness: a new methodological approach and its application on the flora of Africa. *Biodiversity and Conservation,* 10**,** 1513-1529.

KIER, G., KREFT, H., LEE, T. M., JETZ, W., IBISCH, P. L., NOWICKI, C., MUTKE, J. & BARTHLOTT, W. 2009. A global assessment of endemism and species richness across island and mainland regions. *Proceedings of the National Academy of Sciences of the United States of America,* 106**,** 9322-9327.

KIER, G., MUTKE, J., DINERSTEIN, E., RICKETTS, T. H., KUPER, W., KREFT, H. & BARTHLOTT, W. 2005. Global patterns of plant diversity and floristic knowledge. *Journal of Biogeography,* 32**,** 1107-1116.

KINNISON, M. T. & HAIRSTON, N. G. 2007. Eco-evolutionary conservation biology: contemporary evolution and the dynamics of persistence. *Functional Ecology,* 21**,** 444-454.

KNIGHT, A. T., COWLING, R. M., BOSHOFF, A. F., WILSON, S. L. & PIERCE, S. M. 2011. Walking in STEP: Lessons for linking spatial prioritisations to implementation strategies. *Biological Conservation,* 144**,** 202-211.

KNIGHT, A., SMITH, R., COWLING, R., DESMET, P., FAITH, D., FERRIER, S., GELDERBLOM, C., GRANTHAM, H., LOMBARD, A., MAZE, K., NEL, J., PARRISH, J., PENCE, G., POSSINGHAM, H., REYERS, B., ROUGET, M., ROUX, D. & WILSON, K. 2007. Improving the key biodiversity areas approach for effective conservation planning. *Bioscience,* 57**,** 256-261.

KORNER, C. & SPEHN, E. M. 2002. *Mountain biodiversity, a global assessment,* London, Parthenon.

KORNER, C. 2002. Mountain biodiversity, its causes and function: an overview. *In:* KORNER, C. & SPEHN, E. M. (eds.) *Mountain Biodiversity, a global assessment.* London: Parthenon.

KUJALA, H., ARAUJO, M. B., THUILLER, W. & CABEZA, M. 2011. Misleading results from conventional gap analysis - Messages from the warming north. *Biological Conservation,* 144**,** 2450-2458.

LAMBERT, L. & CHITRAKAR, B. D. 1989. VARIATION OF POTENTIAL EVAPOTRANSPIRATION WITH ELEVATION IN NEPAL. *Mountain Research and Development,* 9**,** 145-152.

LAMBIN, E. F. 2005. Modelling Land-Use Change. *In:* WAINWRIGHT, J. & MULLIGAN, M. (eds.) *Environmental Modelling. Finding simplicity in complexity.* Chichester: Wiley.

LAMBIN, E. F., GEIST, H. J. & LEPERS, E. 2003. Dynamics of land-use and land-cover change in tropical regions. *Annual Review of Environment and Resources,* 28**,** 205-241.

LAMOREUX, J. F., MORRISON, J. C., RICKETTS, T. H., OLSON, D. M., DINERSTEIN, E., MCKNIGHT, M. W. & SHUGART, H. H. 2006. Global tests of biodiversity concordance and the importance of endemism. *Nature,* 440**,** 212-214.

LENNON, J. J., KOLEFF, P., GREENWOOD, J. J. D. & GASTON, K. J. 2001. The geographical structure of British bird distributions: diversity, spatial turnover and scale. *Journal of Animal Ecology,* 70**,** 966-979.

LEVIN, N., SHMIDA, A., LEVANONI, O., TAMARI, H. & KARK, S. 2007. Predicting mountain plant richness and rarity from space using satellite-derived vegetation indices. *Diversity and Distributions,* 13**,** 692-703.

LEVINS, R. 1979. COEXISTENCE IN A VARIABLE ENVIRONMENT. *American Naturalist,* 114**,** 765-783.

LIEBIG, J. V. 1855. Die Grundsatze der agricultur-chemie mit Rucksicht auf die in Englent angestellten Untersuchchungen. Braunschweig, Germany: Friedrich Vieweg and Sohn.

LOMOLINO, M. V. & WEISER, M. D. 2001. Towards a more general species-area relationship: diversity on all islands, great and small. *Journal of Biogeography,* 28**,** 431-445.

LORIMER, J. 2006. Nonhuman charisma: which species trigger our emotions and why? *ECOS,* 27**,** 20 - 27.

LUNDHOLM, J. T. 2009. Plant species diversity and environmental heterogeneity: spatial scale and competing hypotheses. *Journal of Vegetation Science,* 20**,** 377-391.

LUOTO, M., TOIVONEN, T. & HEIKKINEN, R. K. 2002. Prediction of total and rare plant species richness in agricultural landscapes from satellite images and topographic data. *Landscape Ecology,* 17**,** 195-217.

LUOTO, M., VIRKKALA, R., HEIKKINEN, R. K. & RAINIO, K. 2004. Predicting bird species richness using remote sensing in boreal agricultural-forest mosaics. *Ecological Applications,* 14**,** 1946-1962.

MAC NALLY, R. & FLEISHMAN, E. 2002. Using "indicator" species to model species richness: Model development and predictions. *Ecological Applications,* 12**,** 79-92.

MAC NALLY, R. & WATSON, D. M. 1997. Distinguishing area and habitat heterogeneity effects on species richness: Birds in Victorian buloke remnants. *Australian Journal of Ecology,* 22**,** 227-232.

MACDONALD, D. W. & SERVICE, K. 2006. *Key topics in conservation biology,* Malden, MA. ; Oxford, Blackwell.

MACE, G. M. & PURVIS, A. 2008. Evolutionary biology and practical conservation: bridging a widening gap. *Molecular Ecology,* 17**,** 9-19.

MACE, G. M. 2004. The role of taxonomy in species conservation. *Philosophical Transactions of the Royal Society of London Series B-Biological Sciences,* 359**,** 711-719.

MAGURRAN, A. 2004. *Measuring biological diversity.,* New York, Blackwell.

MALAMUD, B. D., TURCOTTE, D. L., GUZZETTI, F. & REICHENBACH, P. 2004. Landslide inventories and their statistical properties. *Earth Surface Processes and Landforms,* 29**,** 687-711.

MALCOLM, J. R., LIU, C. R., NEILSON, R. P., HANSEN, L. & HANNAH, L. 2006. Global warming and extinctions of endemic species from biodiversity hotspots. *Conservation Biology,* 20**,** 538-548.

MANSERGH, I., CHEAL, D. & FITZSIMONS, J. A. 2008. Future landscapes in south-eastern Australia: the role of protected areas and biolinks in adaptation to climate change. *Biodiversity (Ottawa),* 9**,** 59-70.

MARINI, L., PROSSER, F., KLIMEK, S. & MARRS, R. H. 2008. Water-energy, land-cover and heterogeneity drivers of the distribution of plant species richness in a mountain region of the European Alps. *Journal of Biogeography,* 35**,** 1826-1839.

MCLEOD, B. 2010. *The private companies helping conservation in Colombia* [Online]. Available: http://www.bbc.co.uk/news/science-environment-11532877 [Accessed 18/12 2011].

MENGE, B. A. & SUTHERLAND, J. P. 1976. SPECIES-DIVERSITY GRADIENTS - SYNTHESIS OF ROLES OF PREDATION, COMPETITION, AND TEMPORAL HETEROGENEITY. *American Naturalist,* 110**,** 351-369.

METOFFICE, U. 1999. *Met Office climate prediction model: HadCM3* [Online]. Available: http://www.metoffice.gov.uk/research/modelling-systems/unified-model/climate-models/hadcm3 [Accessed 12/01 2012].

MITTELBACH, G. G., SCHEMSKE, D. W., CORNELL, H. V., ALLEN, A. P., BROWN, J. M., BUSH, M. B., HARRISON, S. P., HURLBERT, A. H., KNOWLTON, N., LESSIOS, H. A., MCCAIN, C. M., MCCUNE, A. R., MCDADE, L. A., MCPEEK, M. A., NEAR, T. J., PRICE, T. D., RICKLEFS, R. E., ROY, K., SAX, D. F., SCHLUTER, D., SOBEL, J. M. & TURELLI, M. 2007. Evolution and the latitudinal diversity gradient: speciation, extinction and biogeography. *Ecology Letters,* 10**,** 315-331.

MITTERMEIER, R. A., MITTERMEIER, C. G., BROOKS, T. M., PILGRIM, J. D., KONSTANT, W. R., DA FONSECA, G. A. B. & KORMOS, C. 2003. Wilderness and biodiversity conservation. *Proceedings of the National Academy of Sciences of the United States of America,* 100**,** 10309-10313.

MITTERMEIER, R. A., ROBLES-GIL, P. & MITTERMEIER, C. G. 1997. *Megadiversity,* Mexico City, CEMEX.

MODIS. 2009. *Product description* [Online]. Available: http://modis-atmos.gsfc.nasa.gov/MOD06_L2/index.html [Accessed 2nd June 2009].

MONFREDA, C., RAMANKUTTY, N. & FOLEY, J. A. 2008. Farming the planet: 2. Geographic distribution of crop areas, yields, physiological types, and net primary production in the year 2000. *Global Biogeochemical Cycles,* 22.

MORA, C., TITTENSOR, D. P., ADL, S., SIMPSON, A. G. B. & WORM, B. 2011. How Many Species Are There on Earth and in the Ocean? *Plos Biology,* 9.

MOSER, D., DULLINGER, S., ENGLISCH, T., NIKLFELD, H., PLUTZAR, C., SAUBERER, N., ZECHMEISTER, H. G. & GRABHERR, G. 2005. Environmental determinants of vascular plant species richness in the Austrian Alps. *Journal of Biogeography,* 32**,** 1117-1127.

MSC. 2009. *Marine Stewardship Council* [Online]. Available: http://www.msc.org/about-us/ [Accessed 2nd June 2009].

MULLIGAN, M. & BURKE, S. M. 2005. *FIESTA Fog Interception for the Enhancement of Streamflow in Tropical Areas. Final Technical report for AMBIOTEK contribution to DFID FRP R7991. "This publication is an output from a research project funded by the United Kingdom Department for International Development (DFID) for the benefit of developing countries. The views expressed are not necessarily those of DFID. R7991 [Forestry Research Programme]."* [Online]. Available: www.ambiotek.com/fiesta [Accessed 2nd June 2009].

MULLIGAN, M. 1999. *A simple distributed hydrological model for tropical montane cloud forests (TAMBITO V1.0)* [Online]. Available: www.ambiotek.com/publicaations/tambitomod.pdf [Accessed 2nd June 2009].

MULLIGAN, M. 2000. A model for characterising the geo-environmental drivers of biodiversity in tropical mountains. Unpublished.

MULLIGAN, M. 2006a. MODIS MOD35 pan-tropical cloud climatology. Version 1 [online]. Available from http://www.ambiotek.com/clouds.

MULLIGAN, M. 2006b. *TRMM 2b31-based rainfall climatology, version 1.0* [Online]. Available: www.ambiotek.com/1kmrainfall [Accessed 2nd June 2009].

MULLIGAN, M. 2007. *Hydrology.,* London, University of London Press.

MULLIGAN, M. 2008. *Geodiversity model description*, (personal communication).

MULLIGAN, M. 2009. *SimTerra: A gridded global database of climate, terrain and land cover maps at 1 km and 100 m resolution for modelling studies.* [Online]. Available: www.ambiotek.com/simterra [Accessed 2nd June 2009].

MULLIGAN, M. 2011. *Co$ting Nature Conservation Priority Layer (Online)* [Online]. Available: www.policysupport.org [Accessed 01/06 2011].

MYERS, N., MITTERMEIER, R. A., MITTERMEIER, C. G., DA FONSECA, G. A. B. & KENT, J. 2000. Biodiversity hotspots for conservation priorities. *Nature,* 403**,** 853-858.

NASA. 2008. *TRMM product level 2B combined (PR, TMI) Rainfall Profile* [Online]. Available: http://disc.sci.gsfc.nasa.gov/precipitation/documentation/TRMM_README/TRMM_2B31_readme.shtml [Accessed 2nd June 2009].

NASA. 2009. *Shuttle Radar Topography Mission* [Online]. Available: http://www2.jpl.nasa.gov/srtm/ [Accessed 2nd June 2009].

NATURE CONSERVANCY. 2008. *Consolidated financial statements as of June 30 2008 and 2007.* [Online]. Available: http://www.nature.org/aboutus/annualreport/files/fs_fy08.pdf [Accessed 2nd June 2009].

NATURE CONSERVANCY. 2011. *Colombia* [Online]. Available: http://www.nature.org/ourinitiatives/regions/southamerica/colombia/index.htm [Accessed 18/12 2011].

NELSON, A. & CHOMITZ, K. M. 2011. Effectiveness of Strict vs. Multiple Use Protected Areas in Reducing Tropical Forest Fires: A Global Analysis Using Matching Methods. *Plos One,* 6**,** 14.

NEW, M., LISTER, D., HULME, M. & MAKIN, I. 2002. A high-resolution data set of surface climate over global land areas. *Climate Research,* 21**,** 1-25.

NOBIS, M. & WOHLGEMUTH, T. 2004. Trend words in ecological core journals over the last 25 years (1978-2002). *Oikos,* 106**,** 411-421.

NOGUES-BRAVO, D., ARAUJO, M. B., ROMDAL, T. & RAHBEK, C. 2008. Scale effects and human impact on the elevational species richness gradients. *Nature,* 453**,** 216-U8.

OED. 2010. *Oxford English Dictionary* [Online]. Available: dictionary.oed.com [Accessed 22/10 2010].

OKSANEN, L., FRETWELL, S. D., ARRUDA, J. & NIEMELA, P. 1981. EXPLOITATION ECOSYSTEMS IN GRADIENTS OF PRIMARY PRODUCTIVITY. *American Naturalist,* 118**,** 240-261.

OLSON, D. M. & DINERSTEIN, E. 1998. The global 200: A representation approach to conserving the Earth's most biologically valuable ecoregions. *Conservation Biology,* 12**,** 502-515.

ORME, C. D. L., DAVIES, R. G., BURGESS, M., EIGENBROD, F., PICKUP, N., OLSON, V. A., WEBSTER, A. J., DING, T. S., RASMUSSEN, P. C., RIDGELY, R. S., STATTERSFIELD, A. J., BENNETT, P. M., BLACKBURN, T. M., GASTON, K. J. & OWENS, I. P. F. 2005. Global hotspots of species richness are not congruent with endemism or threat. *Nature,* 436**,** 1016-1019.

OVASKAINEN, O. 2002. Long-term persistence of species and the SLOSS problem. *Journal of Theoretical Biology,* 218**,** 419-433.

OWENS, I. P. F. & BENNETT, P. M. 2000. Quantifying biodiversity: a phenotypic perspective. *Conservation Biology,* 14**,** 1014-1022.

PAINE, R. T. 1966. FOOD WEB COMPLEXITY AND SPECIES DIVERSITY. *American Naturalist,* 100**,** 65-&.

PALMER, M. W. 1992. THE COEXISTENCE OF SPECIES IN FRACTAL LANDSCAPES. *American Naturalist,* 139**,** 375-397.

PARKS, K. E. & MULLIGAN, M. 2010. On the relationship between a resource based measure of geodiversity and broad scale biodiversity patterns. *Biodiversity and Conservation,* 19**,** 2751-2766.

PARMESAN, C. & YOHE, G. 2003. A globally coherent fingerprint of climate change impacts across natural systems. *Nature,* 421**,** 37-42.

PARMESAN, C. 2006. Ecological and evolutionary responses to recent climate change. *Annual Review of Ecology Evolution and Systematics.* Palo Alto: Annual Reviews.

PATTERSON, B. D., STOTZ, D. F., SOLARI, S., FITZPATRICK, J. W. & PACHECO, V. 1998. Contrasting patterns of elevational zonation for birds and mammals in the Andes of southeastern Peru. *Journal of Biogeography,* 25**,** 593-607.

PEARCE, D. 2007. Do we really care about Biodiversity? *Environmental & Resource Economics,* 37**,** 313-333.

PEARSON, R. G. & DAWSON, T. P. 2003. Predicting the impacts of climate change on the distribution of species: are bioclimate envelope models useful? *Global Ecology and Biogeography,* 12**,** 361-371.

PEREIRA, A. R. & PRUITT, W. O. 2004. Adaptation of the Thornthwaite scheme for estimating daily reference evapotranspiration. *Agricultural Water Management,* 66**,** 251-257.

PETCHEY, O. L. & GASTON, K. J. 2006. Functional diversity: back to basics and looking forward. *Ecology Letters,* 9**,** 741-758.

PHILLIPS, S. J. & DUDIK, M. 2008. Modeling of species distributions with Maxent: new extensions and a comprehensive evaluation. *Ecography,* 31**,** 161-175.

PHILLIPS, S. J., ANDERSON, R. P. & SCHAPIRE, R. E. 2006. Maximum entropy modeling of species geographic distributions. *Ecological Modelling,* 190**,** 231-259.

PIANKA, E. R. 1966. LATITUDINAL GRADIENTS IN SPECIES DIVERSITY - A REVIEW OF CONCEPTS. *American Naturalist,* 100**,** 33-&.

PIELKE, R., WIGLEY, T. & GREEN, C. 2008. Dangerous assumptions. *Nature,* 452**,** 531-532.

PIMM, S. L., RUSSELL, G. J., GITTLEMAN, J. L. & BROOKS, T. M. 1995. THE FUTURE OF BIODIVERSITY. *Science,* 269**,** 347-350.

PRESSEY, R. L., CABEZA, M., WATTS, M. E., COWLING, R. M. & WILSON, K. A. 2007. Conservation planning in a changing world. *Trends in Ecology & Evolution,* 22**,** 583-592.

PRESTON, F. W. 1948. THE COMMONNESS, AND RARITY, OF SPECIES. *Ecology,* 29**,** 254-283.

R DEVELOPMENT CORE TEAM, 2010. R: A language and environment for statistical computing. Vienna, Austria: R Foundation for Statistical Computing.

RAHBEK, C. 1995. THE ELEVATIONAL GRADIENT OF SPECIES RICHNESS - A UNIFORM PATTERN. *Ecography,* 18**,** 200-205.

RAHBEK, C. 1997. The relationship among area, elevation, and regional species richness in neotropical birds. *American Naturalist,* 149**,** 875-902.

RAMIREZ-VILLEGAS, J. & JARVIS, A. 2010. Downscaling Global Circulation Model Outputs: The Delta Method Decision and Policy Analysis Working Paper No. 1. Cali, Colombia: CIAT.

REDFORD, K. H., COPPOLILLO, P., SANDERSON, E. W., DA FONSECA, G. A. B., DINERSTEIN, E., GROVES, C., MACE, G., MAGINNIS, S., MITTERMEIER, R. A., NOSS, R., OLSON, D.,

ROBINSON, J. G., VEDDER, A. & WRIGHT, M. 2003. Mapping the conservation landscape. *Conservation Biology,* 17**,** 116-131.

REED, D. N., ANDERSON, T. M., DEMPEWOLF, J., METZGER, K. & SERNEELS, S. 2009. The spatial distribution of vegetation types in the Serengeti ecosystem: the influence of rainfall and topographic relief on vegetation patch characteristics. *Journal of Biogeography,* 36**,** 770-782.

RESTREPO, C. & ALVAREZ, N. 2006. Landslides and their contribution to land-cover change in the mountains of Mexico and Central America. *Biotropica,* 38**,** 446-457.

RIDGELY, R. S., ALLNUTT, T. F., BROOKS, D. K., MCNICOL, D. W., YOUNG, B. E. & ZOOK, J. R. 2003. Digital distribution maps of the birds of the Western Hemisphere, version 1.0. NatureServe, Arlington, Virginia, USA.

RIDLEY, M. 1996. *Evolution,* USA, Blackwell Science.

RIETKERK, M., BOERLIJST, M. C., VAN LANGEVELDE, F., HILLERISLAMBERS, R., VAN DE KOPPEL, J., KUMAR, L., PRINS, H. H. T. & DE ROOS, A. M. 2002. Self-organization of vegetation in arid ecosystems. *American Naturalist,* 160**,** 524-530.

RODRIGUES, A. S. L. & BROOKS, T. M. 2007. Shortcuts for biodiversity conservation planning: The effectiveness of surrogates. *Annual Review of Ecology Evolution and Systematics,* 38**,** 713-737.

RODRIGUES, A. S. L. & GASTON, K. J. 2001. How large do reserve networks need to be? *Ecology Letters,* 4**,** 602-609.

RODRIGUES, A. S. L., ANDELMAN, S. J., BAKARR, M. I., BOITANI, L., BROOKS, T. M., COWLING, R. M., FISHPOOL, L. D. C., DA FONSECA, G. A. B., GASTON, K. J., HOFFMANN, M., LONG, J. S., MARQUET, P. A., PILGRIM, J. D., PRESSEY, R. L., SCHIPPER, J., SECHREST, W., STUART, S. N., UNDERHILL, L. G., WALLER, R. W., WATTS, M. E. J. & YAN, X. 2004. Effectiveness of the global protected area network in representing species diversity. *Nature,* 428**,** 640-643.

ROECKNER, E., BROKOPF, R., ESCH, M., GIORGETTA, M., HAGEMANN, S., KORNBLUEH, L., MANZINI, E., SCHLESE, U. & SCHULZWEIDA, U. 2006. Sensitivity of simulated climate to horizontal and vertical resolution in the ECHAM5 atmosphere model. *Journal of Climate,* 19**,** 3771-3791.

ROHDE, K. 1992. LATITUDINAL GRADIENTS IN SPECIES-DIVERSITY - THE SEARCH FOR THE PRIMARY CAUSE. *Oikos,* 65**,** 514-527.

ROMDAL, T. S. & GRYTNES, J. A. 2007. An indirect area effect on elevational species richness patterns. *Ecography,* 30**,** 440-448.

ROOT, T. L., PRICE, J. T., HALL, K. R., SCHNEIDER, S. H., ROSENZWEIG, C. & POUNDS, J. A. 2003. Fingerprints of global warming on wild animals and plants. *Nature,* 421**,** 57-60.

ROSENZWEIG, M. L. & ROSENZWEIG, M. L. 1995. Species diversity in space and time. *Species diversity in space and time*, xxi+436p.

RUEL, J. C., MITCHELL, S. J. & DORNIER, M. 2002. A GIS based approach to map wind exposure for windthrow hazard rating. *Northern Journal of Applied Forestry,* 19, 183-187.

SANDERSON, E. W., JAITEH, M., LEVY, M. A., REDFORD, K. H., WANNEBO, A. V. & WOOLMER, G. 2002. The human footprint and the last of the wild. *Bioscience,* 52, 891-904.

SARKAR, S., PRESSEY, R. L., FAITH, D. P., MARGULES, C. R., FULLER, T., STOMS, D. M., MOFFETT, A., WILSON, K. A., WILLIAMS, K. J., WILLIAMS, P. H. & ANDELMAN, S. 2006. Biodiversity conservation planning tools: Present status and challenges for the future. *Annual Review of Environment and Resources,* 31, 123-159.

SCHERER-LORENZEN, M., BONILLA, J. L. & POTVIN, C. 2007. Tree species richness affects litter production and decomposition rates in a tropical biodiversity experiment. *Oikos,* 116, 2108-2124.

SCHOENER, T. W. 1974. RESOURCE PARTITIONING IN ECOLOGICAL COMMUNITIES. *Science,* 185, 27-39.

SCHOENER, T. W. 1989. THE ECOLOGICAL NICHE. *Cherrett, J. M. (Ed.). Ecological Concepts: the Contribution of Ecology to an Understanding of the Natural World; 29th Symposium of the British Ecological Society, London, England, Uk, April 12-13, 1988. Viii+385p. Blackwell Scientific Publications: Cambridge, Massachusetts, USA; Oxford, England, Uk. Illus. Paper*, 79-114.

SCHOLES, R. J. & BIGGS, R. 2005. A biodiversity intactness index. *Nature,* 434, 45-49.

SEYLER, F., MULLER, F., COCHONNEAU, G., GUIMARAES, L. & GUYOT, J. L. 2009. Watershed delineation for the Amazon sub-basin system using GTOPO30 DEM and a drainage network extracted from JERS SAR images. *Hydrological Processes,* 23, 3173-3185.

SHANNON, C. E. 1948. A MATHEMATICAL THEORY OF COMMUNICATION. *Bell System Technical Journal,* 27, 379-423.

SHEA, K., ROXBURGH, S. H. & RAUSCHERT, E. S. J. 2004. Moving from pattern to process: coexistence mechanisms under intermediate disturbance regimes. *Ecology Letters,* 7, 491-508.

SHERWIN, W. B., JABOT, F., RUSH, R. & ROSSETTO, M. 2006. Measurement of biological information with applications from genes to landscapes. *Molecular Ecology,* 15, 2857-2869.

SIMPSON, E. H. 1949. MEASUREMENT OF DIVERSITY. *Nature,* 163, 688-688.

SKELLY, D. K., JOSEPH, L. N., POSSINGHAM, H. P., FREIDENBURG, L. K., FARRUGIA, T. J., KINNISON, M. T. & HENDRY, A. P. 2007. Evolutionary responses to climate change. *Conservation Biology,* 21, 1353-1355.

SOUTULLO, A. & GUDYNAS, E. 2006. How effective is the MERCOSUR's network of protected areas in representing South America's ecoregions? *Oryx,* 40**,** 112-116.

SPATHELF, M. & WAITE, T. A. 2007. Will hotspots conserve extra primate and carnivore evolutionary history? *Diversity and Distributions,* 13**,** 746-751.

SPRENGEL, C. 1828. Von den Substanzen der Ackerkrume und des Untergrundes. *Journal fur Tecnische und Okonomische Chemie,* 2**,** 423 - 474.

STANLEY, W. G. & MONTAGNINI, F. 1999. Biomass and nutrient accumulation in pure and mixed plantations of indigenous tree species grown on poor soils in the humid tropics of Costa Rica. *Forest Ecology and Management,* 113**,** 91-103.

STATTERSFIELD, A. J., CROSBY, M. J., LONG, A. J. & WEGE, D. C. 1998. *Endemic Bird Areas of the world,* Cambridge, BirdLife International.

STEVENS, M. H. H., SANCHEZ, M., LEE, J. & FINKEL, S. E. 2007. Diversification rates increase with population size and resource concentration in an unstructured habitat. *Genetics,* 177**,** 2243-2250.

STORCH, D., EVANS, K. L. & GASTON, K. J. 2005. The species-area-energy relationship. *Ecology Letters,* 8**,** 487-492.

STORCH, D., SIZLING, A. L. & GASTON, K. J. 2003. Geometry of the species-area relationship in central European birds: testing the mechanism. *Journal of Animal Ecology,* 72**,** 509-519.

STRAHLER, A. & STRAHLER, A. 2005. *Physical Geography,* USA, Von Hoffmann.

STRAHLER, A. N. 1952. HYPSOMETRIC (AREA-ALTITUDE) ANALYSIS OF EROSIONAL TOPOGRAPHY. *Geological Society of America Bulletin,* 63**,** 1117-&.

TAKAFUMI, H. & HIURA, T. 2009. Effects of disturbance history and environmental factors on the diversity and productivity of understory vegetation in a cool-temperate forest in Japan. *Forest Ecology and Management,* 257**,** 843-857.

THACKWAY, R. & CRESSWELL, I. D. 1995. An Interim Biogeographic REgionalisation for Australia. Canberra: Australian Nature Conservation Agency.

THOMAS, C. D., CAMERON, A., GREEN, R. E., BAKKENES, M., BEAUMONT, L. J., COLLINGHAM, Y. C., ERASMUS, B. F. N., DE SIQUEIRA, M. F., GRAINGER, A., HANNAH, L., HUGHES, L., HUNTLEY, B., VAN JAARSVELD, A. S., MIDGLEY, G. F., MILES, L., ORTEGA-HUERTA, M. A., PETERSON, A. T., PHILLIPS, O. L. & WILLIAMS, S. E. 2004. Extinction risk from climate change. *Nature,* 427**,** 145-148.

THOMPSON, R. & STARZOMSKI, B. M. 2007. What does biodiversity actually do? A review for managers and policy makers. *Biodiversity and Conservation,* 16**,** 1359-1378.

THORNTHWAITE, C. W. 1948. An approach toward a rational classification of climate. *Geographical Review,* 38**,** 55 - 94.

TILMAN, D. 1994. COMPETITION AND BIODIVERSITY IN SPATIALLY STRUCTURED HABITATS. *Ecology,* 75**,** 2-16.

TILMAN, D. 1999. The ecological consequences of changes in biodiversity: A search for general principles. *Ecology,* 80**,** 1455-1474.

TOBLER, W. R. 1970. COMPUTER MOVIE SIMULATING URBAN GROWTH IN DETROIT REGION. *Economic Geography,* 46**,** 234-240.

TRABUCCO, A., ACHTEN, W. M. J., BOWE, C., AERTS, R., VAN ORSHOVEN, J., NORGROVE, L. & MUYS, B. 2010. Global mapping of Jatropha curcas yield based on response of fitness to present and future climate. *Global Change Biology Bioenergy,* 2**,** 139-151.

TRIANTIS, K. A., NOGUES-BRAVO, D., HORTAL, J., BORGES, P. A. V., ADSERSEN, H., FERNANDEZ-PALACIOS, J. M., ARAUJO, M. B. & WHITTAKER, R. J. 2008. Measurements of area and the (island) species-area relationship: new directions for an old pattern. *Oikos,* 117**,** 1555-1559.

TRISURAT, Y. 2007. Applying gap analysis and a comparison index to evaluate protected areas in Thailand. *Environmental Management,* 39**,** 235-245.

TRIVEDI, M. R., BERRY, P. M., MORECROFT, M. D. & DAWSON, T. P. 2008. Spatial scale affects bioclimate model projections of climate change impacts on mountain plants. *Global Change Biology,* 14**,** 1089-1103.

TURNER, J. R. G., LENNON, J. J. & LAWRENSON, J. A. 1988. BRITISH BIRD SPECIES DISTRIBUTIONS AND THE ENERGY THEORY. *Nature,* 335**,** 539-541.

TUVI, E. L., VELLAK, A., REIER, U., SZAVA-KOVATS, R. & PARTEL, M. 2011. Establishment of protected areas in different ecoregions, ecosystems, and diversity hotspots under successive political systems. *Biological Conservation,* 144**,** 1726-1732.

UN. 1997. *UN Conference on Environment and Development* [Online]. Available: http://www.un.org/geninfo/bp/enviro.html [Accessed 2nd June 2009].

UNEP. 1995. *Global Biodiversity Assessment* [Online]. Cambridge: Cambridge University Press.

UNEP-WCMC 2005. *Millennium Ecosystem Assessment, systems_mountain raster digital data,* USA, Washington DC.

UNEP-WCMC. 2002. *Mountain Watch* [Online]. UK: UNEP-WCMC.

UNEP-WCMC. 2006. *Rwenzori Mountains National Park, Uganda* [Online]. Available: http://www.unep-wcmc.org/sites/wh/pdf/Rwenzori.pdf [Accessed 20/10 2010].

UNESCO-MAB. 2008. *UNESCO's Man and Biosphere Programme (MAB)* [Online]. [Accessed 2nd June 2009].

USGS. 2009a. *Hydro 1k documentation* [Online]. Available: http://edc.usgs.gov/products/elevation/gtopo30/hydro/readme.html [Accessed 2nd June 2009].

USGS. 2009b. *Shuttle Radar Topography Mission* [Online]. Available: http://eros.usgs.gov/productselevation/srtmted.php [Accessed 2nd June 2009].

VAN SOESBERGEN, A. 2011. Global 1km gridded multimodal climate dataset based on CIAT statistically downscaled data (CIAT data available at http://gisweb.ciat.cgiar.org/GCMPage/download_sres.html).

VANACKER, V., VON BLANCKENBURG, F., GOVERS, G., MOLINA, A., POESEN, J., DECKERS, J. & KUBIK, P. 2007. Restoring dense vegetation can slow mountain erosion to near natural benchmark levels. *Geology,* 35**,** 303-306.

VERHELST, J. C. & MULLIGAN, M. submitted. Methods for filtering erroneous records in point observation data: an application to museaum bird collections from Colombia. *International Journal of Geographical Information science*.

VERHELST, J.C. 2011. Distribution in Colombia: Current Diversity and Potential Refugia Under Climate Change. PhD Thesis, King's College London – University of London, London.

WDPA 2011. Regional and global stats for 1990 - 2010 from the 2011 MDG analysis. WDPA.

WDPA. 2012. *Protected Planet* [Online]. Available: www.protectedplanet.net [Accessed 12/01 2012].

WHITMORE, T. C. 1998. *An introduction to tropical rain forests.,* Oxford, Oxford University Press.

WHITTAKER, R. H. & NIERING, W. A. 1975. VEGETATION OF SANTA CATALINA MOUNTAINS, ARIZONA .5. BIOMASS, PRODUCTION, AND DIVERSITY ALONG ELEVATION GRADIENT. *Ecology,* 56**,** 771-790.

WHITTAKER, R. J., ARAUJO, M. B., PAUL, J., LADLE, R. J., WATSON, J. E. M. & WILLIS, K. J. 2005. Conservation Biogeography: assessment and prospect. *Diversity and Distributions,* 11**,** 3-23.

WILLIAMS, P. H., BURGESS, N. D. & RAHBEK, C. 2000. Flagship species, ecological complementarity and conserving the diversity of mammals and birds in sub-Saharan Africa. *Animal Conservation,* 3**,** 249-260.

WILLIAMS, S. E. & MIDDLETON, J. 2008. Climatic seasonality, resource bottlenecks, and abundance of rainforest birds: implications for global climate change. *Diversity and Distributions,* 14**,** 69-77.

WILLIAMSON, M., GASTON, K. J. & LONSDALE, W. M. 2001. The species-area relationship does not have an asymptote! *Journal of Biogeography,* 28**,** 827-830.

WILLIS, S. G., HOLE, D. G., COLLINGHAM, Y. C., HILTON, G., RAHBEK, C. & HUNTLEY, B. 2009. Assessing the Impacts of Future Climate Change on Protected Area Networks: A Method to Simulate Individual Species' Responses. *Environmental Management,* 43**,** 836-845.

WILSON, E. O. 1984. *Biophilia,* USA, Harvard Press.

WOOD, J. & GUTH, A. 2010. *East Africa's Great Rift Valley: a complex rift system* [Online]. Available: http://geology.com/articles/east-africa-rift.shtml [Accessed 20/10/2010 2010].

WOOD, S. 2007. Australia plans massive conservation corridor. *Cosmos* [Online]. Available: http://www.cosmosmagazine.com/node/1083.

WRIGHT, D. H. 1983. SPECIES-ENERGY THEORY - AN EXTENSION OF SPECIES-AREA THEORY. *Oikos,* 41**,** 496-506.

WWF. 2008. *Living Planet Report* [Online]. Available: http://assets.panda.org/downloads/living_planet_report_2008.pdf [Accessed 2nd June 2009].

WWF. 2009. *Ecoregions* [Online]. Available: http://www.panda.org/about_our_earth/ecoregions/ [Accessed 2nd June 2009].

WWF-IUCN 1994 - 1997. *Centres of Plant Diversity,* Gland, Switzerland, WWF and IUCN.

WYLIE, D. P., MENZEL, W. P., WOOLF, H. M. & STRABALA, K. I. 1994. 4 YEARS OF GLOBAL CIRRUS CLOUD STATISTICS USING HIRS. *Journal of Climate,* 7**,** 1972-1986.

ZHANG, Q. G. & ZHANG, D. Y. 2007. Consequences of individual species loss in biodiversity experiments: An essentiality index. *Acta Oecologica-International Journal of Ecology,* 32**,** 236-242.

ZINKO, U., SEIBERT, J., DYNESIUS, M. & NILSSON, C. 2005. Plant species numbers predicted by a topography-based groundwater flow index. *Ecosystems,* 8**,** 430-441.

Appendix 1.

Convention on Biodiversity Targets, from http://www.cbd.int/sp/targets/

Strategic Goal A:

Address the underlying causes of biodiversity loss by mainstreaming biodiversity across government and society

Target 1

By 2020, at the latest, people are aware of the values of biodiversity and the steps they can take to conserve and use it sustainably.

Target 2

By 2020, at the latest, biodiversity values have been integrated into national and local development and poverty reduction strategies and planning processes and are being incorporated into national accounting, as appropriate, and reporting systems.

Target 3

By 2020, at the latest, incentives, including subsidies, harmful to biodiversity are eliminated, phased out or reformed in order to minimize or avoid negative impacts, and positive incentives for the conservation and sustainable use of biodiversity are developed and applied, consistent and in harmony with the Convention and other relevant international obligations, taking into account national socio economic conditions.

Target 4

By 2020, at the latest, Governments, business and stakeholders at all levels have taken steps to achieve or have implemented plans for sustainable production and consumption and have kept the impacts of use of natural resources well within safe ecological limits.

Strategic Goal B:

Reduce the direct pressures on biodiversity and promote sustainable use

Target 5

By 2020, the rate of loss of all natural habitats, including forests, is at least halved and where feasible brought close to zero, and degradation and fragmentation is significantly reduced.

Target 6

By 2020 all fish and invertebrate stocks and aquatic plants are managed and harvested sustainably, legally and applying ecosystem based approaches, so that overfishing is avoided, recovery plans and measures are in place for all depleted species, fisheries have no significant adverse impacts on threatened species and vulnerable ecosystems and the impacts of fisheries on stocks, species and ecosystems are within safe ecological limits.

Target 7

By 2020 areas under agriculture, aquaculture and forestry are managed sustainably, ensuring conservation of biodiversity.

Target 8

By 2020, pollution, including from excess nutrients, has been brought to levels that are not detrimental to ecosystem function and biodiversity.

Target 9

By 2020, invasive alien species and pathways are identified and prioritized, priority species are controlled or eradicated, and measures are in place to manage pathways to prevent their introduction and establishment.

Target 10

By 2015, the multiple anthropogenic pressures on coral reefs, and other vulnerable ecosystems impacted by climate change or ocean acidification are minimized, so as to maintain their integrity and functioning.

Strategic Goal C:

To improve the status of biodiversity by safeguarding ecosystems, species and genetic diversity

Target 11

By 2020, at least 17 per cent of terrestrial and inland water, and 10 per cent of coastal and marine areas, especially areas of particular importance for biodiversity and ecosystem services, are conserved through effectively and equitably managed, ecologically representative and well connected systems of protected areas and other effective area-based conservation measures, and integrated into the wider landscapes and seascapes.

Target 12

By 2020 the extinction of known threatened species has been prevented and their conservation status, particularly of those most in decline, has been improved and sustained.

Target 13

By 2020, the genetic diversity of cultivated plants and farmed and domesticated animals and of wild relatives, including other socio-economically as well as culturally valuable species, is maintained, and strategies have been developed and implemented for minimizing genetic erosion and safeguarding their genetic diversity.

Strategic Goal D: Enhance the benefits to all from biodiversity and ecosystem services

Target 14

By 2020, ecosystems that provide essential services, including services related to water, and contribute to health, livelihoods and well-being, are restored and safeguarded, taking into account the needs of women, indigenous and local communities, and the poor and vulnerable.

Target 15

By 2020, ecosystem resilience and the contribution of biodiversity to carbon stocks has been enhanced, through conservation and restoration, including restoration of at least 15 per cent of degraded ecosystems, thereby contributing to climate change mitigation and adaptation and to combating desertification.

Target 16

By 2015, the Nagoya Protocol on Access to Genetic Resources and the Fair and Equitable Sharing of Benefits Arising from their Utilization is in force and operational, consistent with national legislation.

Strategic Goal E: Enhance implementation through participatory planning, knowledge management and capacity building

Target 17

By 2015 each Party has developed, adopted as a policy instrument, and has commenced implementing an effective, participatory and updated national biodiversity strategy and action plan.

Target 18

By 2020, the traditional knowledge, innovations and practices of indigenous and local communities relevant for the conservation and sustainable use of biodiversity, and their customary use of biological resources, are respected, subject to national legislation and relevant international obligations, and fully integrated and reflected in the implementation of the Convention with the full and effective participation of indigenous and local communities, at all relevant levels.

Target 19

By 2020, knowledge, the science base and technologies relating to biodiversity, its values, functioning, status and trends, and the consequences of its loss, are improved, widely shared and transferred, and applied.

Target 20

By 2020, at the latest, the mobilization of financial resources for effectively implementing the Strategic Plan for Biodiversity 2011-2020 from all sources, and in accordance with the consolidated and agreed process in the Strategy for Resource Mobilization, should increase substantially from the current levels. This target will be subject to changes contingent to resource needs assessments to be developed and reported by Parties.

Appendix 2

Part 1: Code for *GDiv* control

```
# Runs model by calling python modules in correct order.
# Edit top section to assign correct variables and parameters.

# Import necessary modules
from pcraster import *
from multi_tile_functions import *

################################################################################################################################
###  MODEL SET UP
################################################################################################################################
# Set user input variables
convert_temp = int(input('Is it necessary to convert the temperature data from deg*10? 1 / 0: '))
correct_rain = int(input('Is it necessary to correct rainfall data for outliers? 1 / 0: '))
modify = int(input('Do you wish to modify the standard model set-up? 1 / 0: '))
calibrate = int(input('Do you wish to calibrate the model? 1 / 0: '))
SA = int(input('Do you wish to run a sensitivity analysis? 1 / 0: '))
SA_modules = {} # 1s and 0s (user defined) for one-off SAs.
SAm_modules = {} # 1s and 0s (user defined) for monthly SAs
SAd_modules = {} # 1s and 0s (user defined) for directional SAs
PC_change = [0] # Used in PC_change_calcs function

# Standard setup:
run_temp = 1
run_SR = 1
run_rain = 1
run_ET = 1
run_WET = 1
run_landslide = 1
run_tree = 1
run_WB = 1
run_SD = 1
run_DL = 1
run_RIV = 1
```

```
run_Dist = 1
run_TV = 1
run_SV = 1
run_RES = 1
inc_temp = 1
inc_SR = 1
inc_rain = 1
inc_ET = 1
inc_WET = 1
inc_landslide = 1
inc_tree = 1
inc_WB = 1
inc_SD = 1
inc_DL = 1
inc_RIV = 1
inc_Dist = 1
inc_TV = 1
inc_SV = 1
inc_RES = 1
RESweight = 1.0/3.0
Svweight = 1.0/3.0
Tvweight =1.0/3.0

# User defined setup:
if (calibrate) == 1:
    RESweight = float(input("Enter RES weighting as float: "))
    Svweight = float(input("Enter Sv weighting as float: "))
    Tvweight = float(input("Enter Tv weighting as float: "))

if (modify) == 1:
    inc_temp = input("Include temperature in final calculations? 1 / 0: ")
    inc_SR = input("Include solar radiation in final calculations? 1 / 0: ")
    inc_rain = input("Include rain in final calculations? 1 / 0: ")
    inc_ET = input("Include evapotranspiration in final calculations? 1 / 0: ")
    inc_WET = input("Include topo-wet in final calculations? 1 / 0: ")
    inc_landslide = input("Include landslide in final calculations? 1 / 0: ")
    inc_tree = input("Include treefall in final calculations? 1 / 0: ")
    inc_WB = input("Include water balances in final calculations? 1 / 0: ")
    inc_SD = input("Include seasonal drought in final calculations? 1 / 0: ")
    inc_DL = input("Include drought length in final calculations? 1 / 0: ")
    inc_RIV = input("Include rivers in final calculations? 1 / 0: ")
```

```
    inc_Dist = input("Include disturbance in final calculations? 1 / 0: ")
    inc_TV = input("Include Tv in final calculations? 1 / 0: ")
    inc_SV = input("Include Sv in final calculations? 1 / 0: ")
    inc_RES = input("Include RES in final calculations? 1 / 0: ")

if (SA) == 1:
    SAm_modules['SA_temp'] = int(input("Run temperature sensitivity analysis? 1 / 0: "))
    SAm_modules['SA_sr'] = int(input("Run solar radiation sensitivity analysis? 1 / 0: "))
    SAm_modules['SA_rain'] = int(input("Run rain sensitivity analysis? 1 / 0: "))
    SAm_modules['SA_blwind'] = int(input("Run boundary layer wind direction sensitivity analysis? 1 / 0: "))
    SAm_modules['SA_wind'] = int(input("Run wind speed sensitivity analysis? 1 / 0: "))
    SAm_modules['SA_cloud'] = int(input("Run fractional cloud cover sensitivity analysis? 1 / 0: "))
    SA_modules['SA_dem'] = int(input("Run DEM sensitivity analysis? 1 / 0: "))
    SAd_modules['SA_topex'] = int(input("Run Topex sensitivity analysis? 1 / 0:"))
    number_changes = int(input('How many percent changes are there? '))
    for i in range(0, number_changes):
        PC = float(input('Enter percentage change: '))
        PC_change.append(PC)

if (SA) == 0:
    SAm_modules['SA_temp'] = 0
    SAm_modules['SA_sr'] = 0
    SAm_modules['SA_rain'] = 0
    SAm_modules['SA_blwind'] = 0
    SAm_modules['SA_wind'] = 0
    SAm_modules['SA_cloud'] = 0
    SA_modules['SA_dem'] = 0
    SAd_modules['SA_topex'] = 0

# Set up the tile variables
Tiles = set_tiles()

Drought_severity = 1

SV_window = int(input('Enter the size of the spatial variation window (in m): '))

print('defining variables')

# Define remaining variables
RES = []
Sv = []
```

```
Tv = []
GD = []
write_components(RES, Sv, Tv, GD, inc_temp, inc_SR, inc_rain, inc_WET, inc_WB, inc_SD, inc_DL, inc_RIV, inc_Dist, inc_TV, inc_SV,
inc_RES)
outputs = GD
outputs.append('GD')
inputs = ['blwind', 'cloud', 'dem', 'rain', 'sr', 'temp', 'topex', 'wind']

# Set run number and write run_record file
rawfile = open("RunRecord.txt")
text = rawfile.read()
number = text.count('<>')
run_number = 1 + number
rawfile.close()

rawfile = open("RunModel.sh")
text = rawfile.read()
start_var = text.find('<>')
end_var = text.find('<<>>')
var1 = start_var + 2
var2 = end_var - 2

variables = text[var1:var2]

run_record(variables, run_number, Tiles, SV_window, RES, Sv, Tv, SAm_modules, SA_modules, PC_change)

#########################################################################################################################
###  RUN MODEL
#########################################################################################################################

# Correct temperature if necessary
tiles = Tiles
for tiles in tiles:
    print("Correcting inputs")
    if int(convert_temp) == 1:
        temp_convert(tiles)
    elif int(convert_temp) != 1:
        for m in range(0,12):
            Map = readmap('RAW_Temp_' + str(m + 1) + '__' + str(tiles) + '.map')
            report(Map, 'RAW_temp_' + str(m+1) + '__' + str(tiles) + '.map')
```

```
    if int(correct_rain) == 1:
        rm_outliers(tiles)
    elif int(correct_rain) != 1:
       for m in range(0,12):
            Map = readmap('RAW_Rain_' + str(m + 1) + '__' + str(tiles) + '.map')
            report(Map, 'RAW_rain_' + str(m+1) + '__' + str(tiles) + '.map')

    if int(run_SR) == 1:
        SR_corr(tiles)

# Set up loop for SA calculations and calculate inputs accordingly
tiles = Tiles
for changes in PC_change:
    for tiles in tiles:
        PC_change_calcs(SA_modules, SAm_modules, SAd_modules, changes, tiles)

        # Run model:
        # Set clone and set up empty map
        setclone('cloneMETRES__' + str(tiles) + '.map')
        EmptyMap = readmap('cloneMETRES__' + str(tiles) + '.map')
        EmptyMap = 1 - (abs(EmptyMap) / abs(EmptyMap))

            # Run functions in correct order for individual tiles
        if int(run_rain) == 1:
            Rain(tiles, EmptyMap)
        if int(run_temp) == 1:
            Temp(tiles, EmptyMap)
        if int(run_SR) == 1:
            SR(tiles, EmptyMap)
        if int(run_ET) == 1:
            ET(tiles)
        if int(run_WET) == 1:
            WET(tiles)
        if int(run_landslide) == 1:
            landslide(tiles)
        if int(run_tree) == 1:
            tree(tiles, EmptyMap)
        if int(run_WB) == 1:
            WB(tiles, EmptyMap)
        if int(run_SD) == 1:
            SD(tiles, EmptyMap)
```

```
    if int(run_DL) == 1:
        DL(tiles, Drought_severity, EmptyMap)
    if int(run_RIV) == 1:
        RIV(tiles)
tiles = Tiles

# Calculate disturbance across the region (loops through tiles in function)
if int(run_Dist) == 1:
    Dist(tiles)

# Calculate raw spatial variation across the region
print("Calculating spatial variation for region")
spatial_variation(tiles, Sv, SV_window)

# Calculate map maximums across the region
print('Calculating map maximums for region')
tvmaxvals = maxmaps(tiles, Tv)
resmaxvals = maxmaps(tiles, RES)
svmaxvals = maxmaps(tiles, Sv)

# Calculate map minimums across the region
print('Calculating map minimums for region')
tvminvals = minmaps(tiles, Tv)
resminvals = minmaps(tiles, RES)
svminvals = minmaps(tiles, Sv)

# Scale maps across the region
print('Scaling maps 0 - 1')
scale_maps(Tv, tiles, tvminvals, tvmaxvals)
scale_maps(Sv, tiles, svminvals, svmaxvals)
scale_maps(RES, tiles, resminvals, resmaxvals)

# Set up new "tiles" loop to calculate components across the region
for tiles in tiles:
    # Set clone and set up empty map
    setclone('RAW_dem__' + str(tiles) + '.map')
    EmptyMap = readmap('RAW_dem__' + str(tiles) + '.map')
    EmptyMap = 1 - (abs(EmptyMap) / abs(EmptyMap))

    # Calculate components
    print('Calculating components for tile ' + str(tiles))
```

```
        if int(inc_TV) == 1:
            components(EmptyMap, Tv, 'TV__', tiles, run_number, changes)
        elif int(inc_TV) !=1:
            report(EmptyMap, 'run_' + str(run_number) + '_TV__' + str(tiles) + '_SA' + str(int(changes)) + '.map')
        if int(inc_SV) == 1:
            components(EmptyMap, Sv, 'SV__', tiles, run_number, changes)
        elif int(inc_SV) !=1:
            report(EmptyMap, 'run_' + str(run_number) + '_SV__' + str(tiles) + '_SA' + str(int(changes)) + '.map')
        if int(inc_RES) == 1:
            components(EmptyMap, RES, 'RES__', tiles, run_number, changes)
        elif int(inc_RES) !=1:
            report(EmptyMap, 'run_' + str(run_number) + '_RES__' + str(tiles) + '_SA' + str(int(changes)) + '.map')
        # Calculate geodiversity
        print('Calculating geodiversity for tile ' + str(tiles))
        Geodiversity(tiles, run_number, changes, RESweight, Svweight, Tvweight)
    tiles = Tiles
print('Done')
```

Part 2: Code for functions used in *GDiv*

```
#########################################################################################################################
###  ALL FUNCTIONS USED TO RUN GDIV
#########################################################################################################################

def AnnTot(MonthlyComponents, EmptyMap, tiles):
    # Calculates raw annual totals and monthly means for monthly variables
    print('Calculating annual totals and monthly means for monthly variables ' + str(tiles))
    from pcraster import readmap, report
    for i in MonthlyComponents:
        total = EmptyMap
        for m in range(0, 12):
            Map = readmap(i + str(m + 1) + '__' + str(tiles) + '.map')
            total = Map + total
        mean = total / 12
        report(total, 'TOT_' + i + '__' + str(tiles) + '.map')
        report(mean, 'AV_' + i + '__' + str(tiles) + '.map')

#########################################################################################################################
```

```
def components(EmptyMap, component, label, tiles, run_number, changes):
    # Calculates componentes for specified tiles
    from pcraster import readmap, report
    summap = EmptyMap
    for i in range(0,len(component)):
        in_map = readmap('SCALED_' + str(component[i]) + '__' + str(tiles) + '.map')
        summap = in_map + summap
    finalmap = summap / (int(len(component)))
    report(finalmap, 'run_' + str(run_number) + '_' + label + str(tiles)  + '_SA' + str(int(changes)) + '.map')

#########################################################################################################################

def create_clones_mountains(tiles):
    # Creates clone map of mountainous areas according to UNEP-WCMC Mountain Watch
    from pcraster import readmap, ifthen, scalar, atan, slope, windowmaximum, windowminimum, ifthenelse, pcrge, report
    import os
    cellsizes = [1000, 0.00833333]
    length = [1000]

    print("Creating clones for tile " + str(tiles))
    name = 'dem__' + str(tiles) + '.map'
    command = 'mapattr -s -l 1000 %s' %(name)
    os.popen(command)
    dem = readmap('dem__' + str(tiles) + '.map')

    slope = scalar(atan(slope(dem)))
    demrange = windowmaximum(dem, 70000) - windowminimum(dem, 7000)
    classes123 = scalar(ifthenelse(pcrge(dem, 2500), scalar(1), scalar(0)))
    map2 = scalar(ifthenelse(pcrge(dem, 1500), scalar(1), scalar(0)))
    map3 = scalar(ifthenelse(pcrge(slope, 2), scalar(1), scalar(0)))
    map4 = scalar(ifthenelse(pcrge(dem, 1000), scalar(1), scalar(0)))
    map5 = scalar(ifthenelse(pcrge(slope, 5), scalar(1), scalar(0)))
    map6 = scalar(ifthenelse(pcrge(dem, 300), scalar(1), scalar(0)))
    map7 = scalar(ifthenelse(pcrge(demrange, 300), scalar(1), scalar(0)))
    map8 = map2 + map3
    map9 = map4 + map5
    map10 = map6 + map7
    map11 = map7 + map4
    class4 = scalar(ifthenelse(map8 == 2, scalar(1), scalar(0)))
    class5 = scalar(ifthenelse(map9 == 2, scalar(1), scalar(0)))
    class5alt = scalar(ifthenelse(map11 == 2, scalar(1), scalar(0)))
```

```
    class6 = scalar(ifthenelse(map10 == 2, scalar(1), scalar(0)))
    map12 = classes123 + class4 + class5 + class5alt + class6
    mountains = scalar(ifthen(pcrge(map12, 1), dem))
    report(mountains, "cloneMETRES__" + str(tiles) + ".map")
    report(mountains, "cloneDD__" + str(tiles) + ".map")
    name = 'cloneDD__' + str(tiles) + '.map'
    command = 'mapattr -s -l 0.008333 %s' %(name)
    os.popen(command)

##########################################################################################################################################

def Dist(tiles):
    # Calculates disturbance, scaled across all tiles
    from pcraster import readmap, report, cellvalue, setclone
    treemaxval = 0
    treeminval = 0
    landslidemaxval = 0
    landslideminval = 0

    for i in range(0, len(tiles)):
        setclone('cloneMETRES__' + str(tiles[i]) + '.map')
        maxmap = readmap('MAX_tree' + '__' + str(tiles[i]) + '.map')
        treemax = cellvalue(maxmap, 1, 1)
        minmap = readmap('MIN_tree' + '__' + str(tiles[i]) + '.map')
        treemin = cellvalue(minmap, 1, 1)
        if treemax[0] > treemaxval:
            treemaxval = treemax[0]
        if treemin[0] < treeminval:
            treeminval = treemin[0]

    for i in range(0, len(tiles)):
        setclone('cloneMETRES__' + str(tiles[i]) + '.map')
        maxmap = readmap('MAX_landslide' + '__' + str(tiles[i]) + '.map')
        landslidemax = cellvalue(maxmap, 1, 1)
        minmap = readmap('MIN_landslide' + '__' + str(tiles[i]) + '.map')
        landslidemin = cellvalue(minmap, 1, 1)
        if landslidemax[0] > landslidemaxval:
            landslidemaxval = landslidemax[0]
        if landslidemin[0] < landslideminval:
            landslideminval = landslidemin[0]
```

```
    for tiles in tiles:
        setclone('cloneMETRES__' + str(tiles) + '.map')
        tree = readmap('tree__' + str(tiles) + '.map')
        treescaled = (tree + abs(treeminval + 0.000000001)) / (treemaxval + abs(treeminval + 0.000000001))
        report(treescaled, 'treescaled__' + str(tiles) + '.map')

        landslide = readmap('landslide__' + str(tiles) + '.map')
        landslidescaled = (landslide + abs(landslideminval + 0.000000001)) / (landslidemaxval + abs(landslideminval + 0.000000001))
        report(landslidescaled, 'landslidescaled__' + str(tiles) + '.map')

        Dist = treescaled + landslidescaled
        report(Dist, 'TOT_Dist__' + str(tiles) + '.map')
        report(Dist, 'AV_Dist__' + str(tiles) + '.map')

##########################################################################################################################

def DL(tiles, Drought_severity, EmptyMap):
    # Calculates the length of the dry season based on monthly waterbalance
    from pcraster import readmap, sqr, sqrt, report, scalar, ifthenelse, pcrle
    # Define necessary variables
    DinM = [31, 28, 31, 20, 31, 30, 31, 31, 30, 31, 30, 31]  # Days in month

    DL = EmptyMap
    stdev2 = EmptyMap
    ann_drought = EmptyMap

    # Calculate mean monthly drought and standard deviation
    print('Calculating Drought Length ' + str(tiles))
    for m in range(0, 12):
        droughtm = readmap('WB' + str(m + 1) + '__' + str(tiles) + '.map')
        ann_drought = ann_drought + droughtm
    for m in range (0, 12):
        droughtm = readmap('WB' + str(m + 1) + '__' + str(tiles) + '.map')
        stdev1 = sqr(droughtm - ann_drought)
        stdev2 = stdev2 + stdev1
    stdev3 = stdev2 / 11
    StDev = sqrt(stdev3)

    # Create 'yard-stick' against which to check water balance for drought
    drought_level = StDev * Drought_severity
    drought_check = ann_drought - drought_level
```

```
    # Check whether the month is a drought month or not, and sum the number of days in drought
    for m in range(0, 12):
        droughtm = readmap('WB' + str(m + 1) + '__' + str(tiles) + '.map')
        days = scalar(DinM[m])
        DLm = ifthenelse(pcrle(droughtm, drought_check), days, 0)
        DL = DL + DLm
    report(DL, 'TOT_DL__' + str(tiles) + '.map')
    report(DL, 'AV_DL__' + str(tiles) + '.map')

##########################################################################################################################

def ET(tiles):
    # Calculates potential monthly evapotranspiration (ET) based on solar radiation (SR) / latent heat
    # for the vaporisation of water.  Assumes a wet environment where most incoming energy is used
    # in evaporating water, rather than heating air.
    from pcraster import readmap, report
    print('Calculating evapotranspiration ' + str(tiles))
    for i in range (0,12):
        SR = readmap('SR' + str(i + 1) + '__' + str(tiles) + '.map')
        SRa = SR / 1000000
        ET = SR / 2260
        report(ET, 'ET' + str(i + 1) + '__' + str(tiles) + '.map')

##########################################################################################################################

def Geodiversity(tiles, run_number, changes, RESweight, Svweight, Tvweight):
    # Calculates overall geodiversity scaled across all tiles
    from pcraster import readmap, report
    res_map = readmap('run_' + str(run_number) + '_' + 'RES__' + str(tiles)  + '_SA' + str(int(changes)) + '.map')
    sv_map = readmap('run_' + str(run_number) + '_' + 'SV__' + str(tiles)  + '_SA' + str(int(changes)) + '.map')
    tv_map = readmap('run_' + str(run_number) + '_' + 'TV__' + str(tiles)  + '_SA' + str(int(changes)) + '.map')
    GD = ((res_map * RESweight) + (sv_map * Svweight) + (tv_map * Tvweight))
    report(GD, 'run_' + str(run_number) + '_' + 'GD' + '__' + str(tiles)  + '_SA' + str(int(changes)) + '.map')

##########################################################################################################################

def landslide(tiles):
    # Calculates the likelihood of landslide for each cell based on topographic wetness and slope.
    from pcraster import readmap, report, mapmaximum, mapminimum
    print('Calculating landslide likelihood ' + str(tiles))
```

```
    Wetness = readmap('TOT_WET__' + str(tiles) + '.map')
    Slope = readmap('Slope__' + str(tiles) + '.map')
    landslide = Wetness * Slope
    maxlandslide = mapmaximum(landslide)
    minlandslide = mapminimum(landslide)
    report(landslide, 'landslide__' + str(tiles) + '.map')
    report(minlandslide, 'MIN_landslide__' + str(tiles) + '.map')
    report(maxlandslide, 'MAX_landslide__' + str(tiles) + '.map')

#############################################################################################################################

def mapattr_edit(inputs, tiles):
    # This script uses the PCRaster mapattr application to change the attributes of existing PCRaster maps.
    # The file-name format in this case is 'variable''month'__'tile'.map, e.g. tmean1__9__11.map, dem__9__11.map etc.

    # Import necessary modules:
    import os
    month = ['', '1', '2', '3', '4', '5', '6', '7', '8', '9', '10', '11', '12']
    # Run mapattr for all combinations of inputs, months and tiles.
    # When the script runs you will get error messages as mapattr tries to calculate for non-existent maps (e.g. monthly DEMs).
    # This doesn't affect the results.
    # See PCRaster (non-python) documentation for more info on mapattr options used when defining 'command' variable.

    for i in range (0,len(inputs)):
        print('Editing attributes for ' + str(inputs[i]))
        for j in range (0,len(month)):
            for k in range (0,len(tiles)):
                name = inputs[i] + month[j] + '__' + tiles[k] + '.map'
                command='mapattr -s -l 1000 %s' %(name)
                os.popen(command)

#############################################################################################################################

def maxmaps(tiles, component):
    # Calculates maximum values for each input and returns as a hash
    # keys are input names, scores are max vals.

    from pcraster import readmap, mapmaximum, cellvalue, report, setclone
    inputmaxval = 0
```

```
    maxvals = {}

    for j in range (0, len(component)):
        for i in range (0, len(tiles)):
            setclone('cloneMETRES__' + str(tiles[i]) + '.map')
            rawmap = readmap(str(component[j]) + '__' + str(tiles[i]) + '.map')
            maxmap = mapmaximum(rawmap)
            maxval = cellvalue(maxmap, 1, 1)
            if maxval[0] > inputmaxval:
                inputmaxval = maxval[0]
        maxvals[component[j]] = inputmaxval
        inputmaxval = 0

    return maxvals
    maxvals = {}

#########################################################################################################################

def minmaps(tiles, component):
    # Calculates minimum values for each input and returns as a hash
    # keys are input names, scores are min vals.

    from pcraster import readmap, mapminimum, cellvalue, report, setclone
    inputminval = 0

    minvals = {}

    for j in range (0, len(component)):
        for i in range (0, len(tiles)):
            setclone('cloneMETRES__' + str(tiles[i]) + '.map')
            rawmap = readmap(str(component[j]) + '__' + str(tiles[i]) + '.map')
            minmap = mapminimum(rawmap)
            minval = cellvalue(minmap, 1, 1)
            if minval[0] < inputminval:
                inputminval = minval[0]
        minvals[component[j]] = inputminval
        inputminval = 0

    return minvals
    minvals = {}
```

```
#########################################################################################################################

def PC_change_calcs(SA_modules, SAm_modules, SAd_modules, changes, tiles):
    # Writes maps for the model run with varied values according to user specified values
    from pcraster import readmap, report
    month = [1,2,3,4,5,6,7,8,9,10,11,12]
    direction = [1, 2, 3, 4, 6, 7, 8, 9]
    # Calculate necessary inputs for one-off inputs (e.g. dem)
    for i in SA_modules:
        if SA_modules[i] == 1:
            start_component = i.find('_')
            component = i[(start_component + 1):len(i)]
            in_map = readmap('RAW_' + str(component) + '__' + str(tiles) + '.map')
            step1 = changes / 100.0
            step2 = step1 * in_map
            step3=in_map + step2
            report(step3, str(component) + '__' + str(tiles) + '.map')
            # Maps are reported with the RAW_ prefix removed (i.e. blah__X__Y.map)
        if SA_modules[i] == 0:
            start_component = i.find('_')
            component = i[(start_component + 1):len(i)]
            in_map = readmap('RAW_' + str(component) + '__' + str(tiles) + '.map')
            report(in_map, str(component) + '__' + str(tiles) + '.map')
            # Maps are reported with the RAW_ prefix removed (i.e. blah__X__Y.map)
    # Calculate necessary inputs for monthly inputs (e.g. temp)
    for i in SAm_modules:
        for m in month:
            if SAm_modules[i] == 1:
                start_component = i.find('_')
                component = i[(start_component + 1):len(i)]
                in_map = readmap('RAW_' + str(component) + '_' + str(m) + '__' + str(tiles) + '.map')
                step1 = changes / 100.0
                step2 = step1 * in_map
                step3=in_map + step2
                report(step3, str(component) + str(m) + '__' + str(tiles) + '.map')
            # Maps are reported with the RAW_ prefix removed (i.e. blahm__X__Y.map)
            if SAm_modules[i] == 0:
                start_component = i.find('_')
                component = i[(start_component + 1):len(i)]
                in_map = readmap('RAW_' + str(component) + '_' + str(m) + '__' + str(tiles) + '.map')
                report(in_map, str(component) + str(m) + '__' + str(tiles) + '.map')
```

```
            # Maps are reported with the RAW_ prefix removed (i.e. blahm__X__Y.map)

    # Calculate necessary inputs for directional inputs (e.g. temp)
    for i in SAd_modules:
        for d in direction:
            if SAd_modules[i] == 1:
                start_component = i.find('_')
                component = i[(start_component + 1):len(i)]
                in_map = readmap('RAW_' + str(component) + '_' + str(d) + '__' + str(tiles) + '.map')
                step1 = changes / 100.0
                step2 = step1 * in_map
                step3=in_map + step2
                report(step3, str(component) + str(d) + '__' + str(tiles) + '.map')
            # Maps are reported with the RAW_ prefix removed (i.e. blahm__X__Y.map)
            if SAd_modules[i] == 0:
                start_component = i.find('_')
                component = i[(start_component + 1):len(i)]
                in_map = readmap('RAW_' + str(component) + '_' + str(d) + '__' + str(tiles) + '.map')
                report(in_map, str(component) + str(d) + '__' + str(tiles) + '.map')
            # Maps are reported with the RAW_ prefix removed (i.e. blahm__X__Y.map)

##########################################################################################################################################

def Rain(tiles, EmptyMap):
    # Calculates total annual and mean monthly rainfall.
    from pcraster import readmap, report
    print('Calculating rainfall variables for ' + str(tiles))
    total = EmptyMap
    for m in range(0, 12):
        Map = readmap('rain' + str(m + 1) + '__' + str(tiles) + '.map')
        total = Map + total
    mean = total / 12
    report(total, 'TOT_Rain' + '__' + str(tiles) + '.map')
    report(mean, 'AV_Rain' + '__' + str(tiles) + '.map')

##########################################################################################################################################

def RIV(tiles):
    # Calculates drainage channels with a stream order greater than 3
    from pcraster import readmap, streamorder, ifthenelse, pcrgt, scalar, report
    # Read LDD, calculate streams then convert to scalar
```

```
    print('Calculating Rivers ' + str(tiles))
    LDD = readmap('LDD__' + str(tiles) + '.map')
    streams = streamorder(LDD)
    rivLDD = ifthenelse(pcrgt(streams, 3), streams, 0)
    Rivers = scalar(rivLDD)
    report(Rivers, 'AV_RIV__' + str(tiles) + '.map')

#########################################################################################################################

def rm_outliers(tiles):
    from pcraster import readmap, windowaverage, setclone, windowtotal, pcrgt, ifthenelse, report, sqr, sqrt
    for m in range(0,12):
        print("Removing TRMM outliers, month " + str(m + 1))
        setclone('cloneMETRES__' + str(tiles) + '.map')
        Map = readmap('RAW_Rain_' + str(m + 1) + '__' + str(tiles) + '.map')
        Mean = windowaverage(Map, 50000)
        stdev1 = sqr(Map - Mean)
        stdev2 = windowtotal(stdev1, 50000)
        stdev3 = stdev2 / ((windowtotal ((stdev2 / stdev2), 10000)) - 1)
        StDev = sqrt(stdev3)
        corr_map = ifthenelse(pcrgt(Map, (3 * StDev)), Mean, Map)
        report(corr_map, 'RAW_rain_' + str(m + 1) + '__' + str(tiles) + '.map')

#########################################################################################################################

def run_record(variables, run_number, Tiles, SV_window, RES, Sv, Tv, SAm_modules, SA_modules, PC_change):
    # Writes to run_record.txt with run number, tiles, sv window and data resolution.
    file = open("/users/kate/working/RunRecord.txt", "a")
    file.write('#############################################################\n')
    file.write('RUN NUMBER:         <>%s\n' % (str(run_number)))
    file.write('Raw inputs used:      %s\n' % (str(variables)))
    file.write('Tiles:                %s\n' % (str(Tiles)))
    file.write('RES:                  %s\n' % (str(RES)))
    file.write('Sv:                   %s\n' % (str(Sv)))
    file.write('Tv:                   %s\n' % (str(Tv)))
    file.write('Sv window (m):        %s\n' % (str(SV_window)))
    file.write('Sensitivity analysis:\n')
    file.write('Modules changed:      %s\n' % (str(SAm_modules)))
    file.write('Modules changed:      %s\n' % (str(SA_modules)))
    file.write('Percent changes:      %s\n' % (str(PC_change)))
    file.close()
```

```
#########################################################################################################################

def scale_maps(component, tiles, componentmins, componentmaxs):
    from pcraster import readmap, report, setclone
    for i in range(0, len(component)):
        for j in range(0, len(tiles)):
            setclone('cloneMETRES__' + str(tiles[j]) + '.map')
            in_map = readmap(str(component[i]) + '__' + str(tiles[j]))
            map_min = componentmins[component[i]]
            map_max = componentmaxs[component[i]]
            scaled = (in_map + (float(abs(map_min + 0.000000000001)))) / (map_max + (float(abs(map_min + 0.000000000001))))
            # if have 0 as map max and map min, get domain error.  try adding 1 to each side, then subtracting 1 from the result?
            report(scaled, 'SCALED_' + str(component[i]) + '__' + str(tiles[j]) + '.map')

#########################################################################################################################

def SD(tiles, EmptyMap):
    # Calculates the drought severity for the most water-stressed month, based on monthly
    # rainfall data and modelled evapotranspiration
    from pcraster import readmap, ifthenelse, report, pcrgt
    # Set up empty map
    SD = EmptyMap

    print('Calculating Seasonal Drought stress ' + str(tiles))
    for m in range (0,12):
        compare = readmap('WB' + str(m + 1) + '__' + str(tiles) + '.map')
        SD = ifthenelse(pcrgt(SD, compare), SD, compare)
    report(SD, 'TOT_SD__' + str(tiles) + '.map')
    report(SD, 'AV_SD__' + str(tiles) + '.map')

#########################################################################################################################

def SR_corr(tiles):
    # Corrects raw solar radiation modelled data for cloud coverage
    # using fractional cloud coverage (from Burridge and Gadd, 1974).
    from pcraster import readmap, report, sqr, sqrt
    print('Correcting solar radiation for cloud cover ' + str(tiles))

    for i in range(0,12):
        SRRAw = readmap('RAW_sr_' + str(i + 1) + '__' + str(tiles) + '.map')
```

```
        Cloud = readmap('RAW_cloud_' + str(i + 1) + '__' + str(tiles) + '.map')
        Tk = ((1-(0.4 * (0.333 * Cloud))) * (1-(0.7 * (0.333 * Cloud)))*(1-(0.4 * (0.333 * Cloud))))
        SRcorr = SRRAw * Tk
        report(SRcorr, 'SR' + str(i + 1) + '__' + str(tiles) + '.map')

#########################################################################################################################################

def SR(tiles, EmptyMap):
    # Calculate annual total and monthly mean
    from pcraster import readmap, report, sqr, sqrt
    print('Calculating SR totals and means for ' + str(tiles))
    total = EmptyMap
    for m in range(0, 12):
        Map = readmap('SR' + str(m + 1) + '__' + str(tiles) + '.map')
        total = Map + total
    mean = total / 12
    report(total, 'TOT_SR' + '__' + str(tiles) + '.map')
    report(mean, 'AV_SR' + '__' + str(tiles) + '.map')

    # Step 3.  Calculate standard deviation
    stdev2 = EmptyMap
    for m in range (0, 12):
        Map = readmap('SR' + str(m + 1) + '__' + str(tiles) + '.map')
        Mean = readmap('AV_SR__' + str(tiles) + '.map')
        stdev1 = sqr(Map - Mean)
        stdev2 = stdev2 + stdev1
    stdev3 = stdev2 / 11
    StDev = sqrt(stdev3)
    report(StDev, 'SDEV_SR__' + str(tiles) + '.map')

#########################################################################################################################################

def spatial_variation(tiles, Sv, SV_window):
    from pcraster import readmap, windowaverage, report, setclone

    for tiles in tiles:
        setclone('cloneMETRES__' + str(tiles) + '.map')
        for i in Sv:
            Map = readmap(str(i) + '__' + str(tiles) + '.map')
            Svmap = windowaverage(Map, SV_window)
            report(Svmap, str(i) + '__' + str(tiles) + '.map')
```

```
#########################################################################################################################

def temp_convert(tiles):
    from pcraster import readmap, report
    print("Converting temperature")
    for m in range(0,12):
        Map = readmap('RAW_Temp_' + str(m + 1) + '__' + str(tiles) + '.map')
        temp_converted = Map / 10
        report(temp_converted, 'RAW_temp_' + str(m+1) + '__' + str(tiles) + '.map')

#########################################################################################################################

def Temp(tiles, EmptyMap):
    # Calculates annual total and monthly mean
    from pcraster import readmap, report, sqr, sqrt
    print('Deriving necessary temperature maps for ' + str(tiles))

    # Step 1.  Calculate annual total and mean monthly temperature.
    total = EmptyMap
    for m in range(0, 12):
        Map = readmap('temp' + str(m + 1) + '__' + str(tiles) + '.map')
        total = Map + total
    mean = total / 12
    report(total, 'TOT_Temp' + '__' + str(tiles) + '.map')
    report(mean, 'AV_' + 'Temp' + '__' + str(tiles) + '.map')

    # Step 2.  Calculate standard deviation
    stdev2 = EmptyMap
    for m in range (0, 12):
        Map = readmap('temp' + str(m + 1) + '__' + str(tiles) + '.map')
        Mean = readmap('AV_Temp__' + str(tiles) + '.map')
        stdev1 = sqr(Map - Mean)
        stdev2 = stdev2 + stdev1
    stdev3 = stdev2 / 11
    StDev = sqrt(stdev3)
    report(StDev, 'SDEV_Temp__' + str(tiles) + '.map')

#########################################################################################################################

def set_tiles():
```

```
    # returns tile variable to calling module
    tile_number = input('Enter number of tiles: ')
    Tiles = []
    for i in range(0,int(tile_number)):
        tile = raw_input('Enter tile reference number: ')
        Tiles.append(tile)
    return(Tiles)

#########################################################################################################################

def tree(tiles, EmptyMap):
# Step 2.  Calculate likelihood of treefall at each cell based on topex and predominant wind conditions
    # Step 2a.  Set variables: top_dir =  topographic directions, m_weighted_topex will be
    # the monthly weighted topex but is set to a map of 0.  tree will be likelihood of treefall
    # but here is an empty map (0s).
    from pcraster import readmap, mapmaximum, mapminimum, ifthenelse, pcreq, abs, mapminimum, report

    print('Calculating treefall likelihood ' + str(tiles))
    top_dir = [1, 2, 3, 4, 6, 7, 8, 9]

    m_weighted_topex = EmptyMap
    tree = EmptyMap

    # Step 2b.  For each month, create a map of topex values based on the predominant wind direction
    # and normalise it
    for m in range(0,12):
        for d in (top_dir):
            blwind = readmap('blwind' + str(m + 1) + '__' + str(tiles) + '.map')
            topex = readmap('topex' + str(d) + '__' + str(tiles) + '.map')
            mtopex_d = ifthenelse(pcreq(blwind, (d)), topex, 0)
            m_weighted_topex = m_weighted_topex + mtopex_d
        norm_weighted_topex = (m_weighted_topex + (abs(mapminimum(m_weighted_topex + 0.000000001))))/(mapmaximum(m_weighted_topex +
(abs(mapminimum(m_weighted_topex + 0.000000001)))))
    # Step 2c.  For each month, correct the wind speed then weight it by the weighted topex and normalise to give
    # a measure of treefall likelihood.
        wind = readmap('wind' + str(m + 1) + '__' + str(tiles) + '.map')
        wind = wind / 10
        wind_weighted = wind * norm_weighted_topex
        tree = tree + wind_weighted
    maxtree = mapmaximum(tree)
    mintree = mapminimum(tree)
```

```
    report(maxtree, 'MAX_tree__' + str(tiles) + '.map')
    report(mintree, 'MIN_tree__' + str(tiles) + '.map')
    report(tree, 'tree__' + str(tiles) + '.map')

#########################################################################################################################################

def WB(tiles, EmptyMap):
    # Calculates the raw monthly, standard deviation, monthly mean and annual water balances based on rainfall data and
    # modelled evapotranspiration
    from pcraster import readmap, report, sqr, sqrt
    # Set up empty map
    WBtot = EmptyMap

    # Calculate monthly balances, and keep running total.
    print('Calculating water balances ' + str(tiles))
    for m in range (0, 12):
        rain = readmap('rain' + str(m + 1) + '__' + str(tiles) + '.map')
        ET = readmap('ET' + str(m + 1) + '__' + str(tiles) + '.map')
        WBm = rain - ET
        report(WBm, 'WB' + str(m + 1) + '__' + str(tiles) + '.map')
        WBtot = WBtot + WBm
    report(WBtot, 'TOT_WB__' + str(tiles) + '.map')
    Av_WB = WBtot / 12
    report(Av_WB, 'AV_WB__' + str(tiles) + '.map')

    # Calculate standard deviation
    stdev2 = EmptyMap
    for m in range (0, 12):
        Map = readmap('WB' + str(m + 1) + '__' + str(tiles) + '.map')
        Mean = readmap('AV_WB__' + str(tiles) + '.map')
        stdev1 = sqr(Map - Mean)
        stdev2 = stdev2 + stdev1
    stdev3 = stdev2 / 11
    StDev = sqrt(stdev3)
    report(StDev, 'SDEV_WB__' + str(tiles) + '.map')

#########################################################################################################################################

def WET(tiles):
    # Calculates the ldd, slope and topographic wetness index for each cell.
    from pcraster import readmap, lddcreate, report, slope, catchmenttotal, ifthenelse, pcrle, scalar, atan, tan, ln
```

```
    # Calculate ldd
    print('Calculating LDD ' + str(tiles))
    DEM = readmap('dem__' + str(tiles) + '.map')
    LDD = lddcreate(DEM, 1e31, 1e31, 1e31, 1e31)
    report(LDD, 'LDD__' + str(tiles) + '.map')

    # Calculate slope
    print('Calculating Slope ' + str(tiles))
    Slope = scalar(atan(slope(DEM)))
    report(Slope, 'Slope__' + str(tiles) + '.map')


    # Calculate Topographic Wetness Index as ln(area upslope / (tan(slope)))
    print('Calculating TopoWet ' + str(tiles))
    catchment = (catchmenttotal(1, LDD)) * 1000
    tan_slope = tan(Slope)
    tan_slope_noneg = ifthenelse(pcrle(tan_slope, scalar(0)), 0.00000001, tan_slope)
    catchment_slope = catchment / tan_slope_noneg
    Wetness = ln(catchment_slope)
    report(Wetness, 'TOT_WET__' + str(tiles) + '.map')
    report(Wetness, 'AV_WET__' + str(tiles) + '.map')

#########################################################################################################################

def write_components(RES, Sv, Tv, GD, inc_temp, inc_SR, inc_rain, inc_WET, inc_WB, inc_SD, inc_DL, inc_RIV, inc_Dist, inc_TV, inc_SV,
inc_RES):
    if int(inc_temp) == 1:
        RES.append('TOT_Temp')
        Sv.append('AV_Temp')
        Tv.append('SDEV_Temp')

    if int(inc_SR) == 1:
        RES.append('TOT_SR')
        Sv.append('AV_SR')
        Tv.append('SDEV_SR')

    if int(inc_rain) == 1:
        RES.append('TOT_Rain')
        Sv.append('AV_Rain')

    if int(inc_WET) == 1:
```

```
        RES.append('TOT_WET')
        Sv.append('AV_WET')

    if int(inc_WB) == 1:
        RES.append('TOT_WB')
        Sv.append('AV_WB')
        Tv.append('SDEV_WB')

    if int(inc_SD) == 1:
        RES.append('TOT_SD')
        Sv.append('AV_SD')

    if int(inc_DL) == 1:
        RES.append('TOT_DL')
        Sv.append('AV_DL')

    if int(inc_RIV) == 1:
        Sv.append('AV_RIV')

    if int(inc_Dist) == 1:
        RES.append('TOT_Dist')
        Sv.append('AV_Dist')

    if int(inc_TV) == 1:
        GD.append('Tv')

    if int(inc_SV) == 1:
        GD.append('Sv')

    if int(inc_RES) == 1:
        GD.append('RES')

    return(RES)
    return(Sv)
    return(Tv)
    return(GD)
#########################################################################################################################
```

Part 3: Code to calculate Solar Radiation maps according to Iqbal (1983)

```
#########################################################################################################################
```

```
# Import modules
from pcraster import *
import math

# Set clone and input map
setclone("cloneMETRES.map") # clone in metres to allow for slope calculations
DEM = readmap("dem.map")

# Calculate necessary derivations, removing missing values
SlopeDEG = scalar(atan(slope(DEM))) # calculate slope in degrees
aspectmap = aspect(DEM) # calculate directional aspect map
nodir = nodirection(aspectmap) # identify areas of no direction
aspectmap = scalar(aspectmap) # convert directional map to scalar
nodir = scalar(nodir) # convert boolean map to scalar
AspectDEG = ifthenelse (nodir == 1, 0.00000001, aspectmap) # creat aspect map with no mvs

BoolDEM = boolean(DEM) # create boolean DEM

setclone("cloneDD.map") # set clone back to DD for rest of calculations

LatDEG = ycoordinate(BoolDEM) # calculate latitudes
LongDEG = xcoordinate(BoolDEM) # calculate longitudes
time = [600, 700, 800, 900, 1000, 1100, 1200, 1300, 1400, 1500, 1600, 1700, 1800, 1900, 2000, 2100, 2200]


# Convert necessary units from degrees to radians
SlopeRAD = SlopeDEG * (math.pi/180)
LatRAD = LatDEG * (math.pi/180)
LongRAD = LongDEG * (math.pi/180)

# Calculate annual total radiation
DA = []
for dn in range(0,365):
    da = (math.pi * 2) * dn / 365
    DA.append(da) # day angle appended to DA
EmptyMap = 1-(DEM / DEM)
i = 0
for day in DA:
    i = i+1
    print("Day: " + str(i))
```

```
    RunningTotalSR = EmptyMap
    OverallTot = EmptyMap
    for t in time:
        print("Time: " + str(t))
        dec = 0.006918 - 0.399912 * math.cos(day) + 0.070257 * math.sin(day) - 0.006758 * math.cos(2*day) + 0.000907 * math.sin(2*day)
- 0.002697 * math.cos(3*day) + 0.00148 * math.sin(3*day)
        Stime = t + (4 * (0 - LongDEG)) + (0.000075 + 0.001868 * math.cos(day) - 0.032077 * math.sin(day) - 0.014615 * math.cos(2*day)
- 0.04089 * math.sin(2*day)) * (229.18)
        mth = (((1200 - (Stime - 50)) / 100) * 15) * (math.pi / 180)
        eccentric = 1 + 0.033 * math.cos(2 * (math.pi * (float(dn) / 365)))
        ToA = 1367 * eccentric * (math.sin(dec) * sin(LatDEG) + math.cos(dec) * cos(LatDEG) * cos(mth * (180 / math.pi)))
        sfc = 1367 * eccentric * ((sin(LatDEG) * cos(SlopeDEG) - cos(LatDEG) * sin(SlopeDEG) * cos(AspectDEG)) * math.sin(dec) +
(cos(LatDEG) * cos(SlopeDEG) + sin(LatDEG) * sin(SlopeDEG) * cos(AspectDEG)) * math.cos(dec) * cos(mth * (180 / math.pi)) +
math.cos(dec) * sin(SlopeDEG) * sin(AspectDEG) * sin(mth * (180 / math.pi)))
        sfc_noneg = ifthenelse(sfc <= 0, 0, sfc)
        RunningTotalSR = RunningTotalSR + sfc_noneg
    if i == 31 or i == 59  or i == 90 or i == 120 or i == 151 or i == 181 or i == 212 or i == 243 or i == 273 or i == 304 or i == 334
or i == 365:
        report(RunningTotalSR, "SR_" + str(i) + ".map")
        OverallTot = OverallTot + RunningTotalSR
report(OverallTot, "AnnualSR.map")
##########################################################################################################################################
```

Appendix 3

Standard *GDiv* setup

Unless otherwise stated, *GDiv* was run using a kernel of 30 000 m and with an equal weighting of *RES, Sc* and *Tv*. The components were calculated using the variables and datasets set out below.

Variable	*RES*	*Sc*	*Tv*	Dataset
Temperature	Yes	Yes	Yes	WorldClim
Solar Radiation	Yes	Yes	Yes	Calculated
Water Balance	Yes	Yes	Yes	Calculated
Rainfall	Yes	Yes	No	WorldClim
Topographical Wetness	Yes	Yes	No	Calculated
Disturbance	Yes	Yes	No	Calculated
Seasonal Drought	Yes	Yes	No	Calculated
Drought Length	Yes	Yes	No	Calculated
Rivers	No	Yes	No	Calculated
Evapotranspiration*	No	No	No	Calculated
Elevation*	No	No	No	Hydro1k
Cloud cover*	No	No	No	MODIS

* Evapotranspiration was used in the calculation of monthly water-balances, rather than being included as a direct input itself. Similarly, many variables were derived fromthe elevation dataset. Cloud cover was used to correct solar radiation, which was calculated as top of atmosphere.

Appendix 4

Python code to generate artificial DEM as PCRaster map

```
#########################################################################
## ArtDemControl.py
## Also need ArtDEMGenerator.py
## Generates an artificial DEM with altitude varying linearly on the y axis
## and standard deviation of altitude (i.e. ruggedness) varying on x axis.
## Produces an ASCII (csv) file and a .map file for the DEM.
## To run, set rows, columns, minimum and maximum altitude and output files
## Set these variables:
rows = 1200
columns = 1200
cellsize = 1000
max_alt = 6000
min_alt = 300
filter_sizes = [7.5] # in cell lengths
ascii_fname = 'ArtDEM_csv.txt'
map_fname = 'ArtDEM'
#########################################################################
```

```
#########################################################################
## Import functions
from PCRaster import *
from ArtDEMGenerator import *
import os

alt = min_alt

ArtDEM = Matrix(rows,columns)
ArtDEM = pop_matrix(ArtDEM, max_alt, min_alt, rows, columns)
write_ascii(ArtDEM, ascii_fname, rows)
create_clone(rows, columns, cellsize)
write_map(ascii_fname, map_fname)
for filter_size in filter_sizes:
    smooth_map(map_fname, filter_size)
    calc_slope(map_fname, filter_size)
fname = 'clone.map'
os.remove(fname)
fname = ascii_fname
os.remove(fname)
#########################################################################
## ArtDEMGenerator.py
## Defines all functions required for ArtDEMControl.py
#########################################################################
## Following function from http://bytes.com/topic/python/answers/594203-please-how-create-matrix-python
class Matrix(object):
    def __init__(self, cols, rows):
        print("Preparing matrix")
        self.cols = cols
        self.rows = rows
        # initialize matrix and fill with zeroes
        self.matrix = []
        for i in range(rows):
            ea_row = []
            for j in range(cols):
                ea_row.append(0)
            self.matrix.append(ea_row)

    def setitem(self, col, row, v):
        self.matrix[col-1][row-1] = v
```

```
    def getitem(self, col, row):
        return self.matrix[col-1][row-1]

    def __repr__(self):
        outStr = ""
        for i in range(self.rows):
            outStr += '%s\n' % (self.matrix[i])
        return outStr
#############################################################################
def pop_matrix(ArtDEM, max_alt, min_alt, rows, columns):
    import random
    rough = 0
    alt_increment = (max_alt - min_alt) / rows
    alt = max_alt
    for r in range(0, rows):
        alt = alt - alt_increment
        rough_value = rough
        for c in range(0, columns):
            v = random.gauss(alt,rough_value)
            rough_value = rough_value + alt_increment
            ArtDEM.setitem(r+1,c+1,v)
    return(ArtDEM)
#############################################################################
def write_ascii(ArtDEM, ascii_fname, rows):
    print('Writing ASCII file')
    import os
    ArtDEMfile = open(ascii_fname, 'w')
    ArtDEMfile.write(str(ArtDEM).replace('[','').replace(']',''))
    ArtDEMfile.close()
#############################################################################
def create_clone(rows, columns, cellsize):
    print('Creating clone map')
    import os
    command = 'mapattr -s -R%s -C%s -l%s -S clone.map' %(rows, columns, cellsize)
    os.popen(command)
#############################################################################
def write_map(ascii_fname, map_fname):
    print('Writing map')
    import os
    Map_fname = str(map_fname) + '.map'
    command = 'asc2map --clone clone.map -s, %s %s ' %(ascii_fname, Map_fname)
```

```
    os.popen(command)
#########################################################################
def smooth_map(map_fname, filter_size):
    print('Smoothing map')
    from PCRaster import readmap, windowaverage, report
    window = filter_size * 1000
    Map = readmap(str(map_fname) + '.map')
    smoothMap = windowaverage(Map, window)
    report(smoothMap, str(map_fname) + 'smooth' + str(filter_size) + '.map')
#########################################################################
def calc_slope(map_fname, filter_size):
    print('Calculating slope')
    from PCRaster import readmap, slope, scalar, atan, report
    Map = readmap(str(map_fname) + 'smooth' + str(filter_size) + '.map')
    slopeMap = scalar(atan(slope(Map)))
    report(slopeMap, 'slope' + str(map_fname) + 'smooth' + str(filter_size) + '.map')
#########################################################################
def edit_mapattr(map_fname, filter_size):
    print('Setting mapattr')
    import os
    name = (str(map_fname) + 'smooth' + str(filter_size) + '.map')
    command = 'mapattr -s -l 1000 %s' %(name)
    os.popen(command)
#########################################################################
```

Appendix 5.

Phyla included in GBIF analysis.

Acacia
Acokanthera
Acrocarpus
Adansonia
Afrocarpus
Agathis
Alstonia
Anacardium
Aphanamixis
Athertonia
Averrhoa
Banksia
Bauhinia
Bolusanthus
Brachychiton
Brosimum
Brownea
Brugmansia
Brunfelsia
Buckinghamia
Caesalpinia
Calliandra
Callistemon
Callitris
Calodendrum
Calycophyllum
Camellia
Cananga
Canarium
Cassia
Cecropia
Cestrum
Chorisia
Chrysophyllum
Cinnamomum
Cochlospermum
Coffea
Couroupita
Crateva
Dillenia
Dimocarpus
Dombeya
Duabanga
Duranta
Elaeocarpus
Euphorbia
Fernandoa
Ficus
Firmiana
Flacourtia
Fraxinus
Garcinia
Gardenia
Gnetum
Grevillea
Greyia
Gustavia
Gymnostoma
Hamelia
Hevea
Ilex
Ixora
Jacaranda
Juniperus
Khaya
Kigelia
Lagerstroemia
Leucadendron
Litchi
Lonchocarpus
Lophanthera
Lophostemon
Macadamia
Magnolia
Malpighia
Mammea
Mangifera
Markhamia
Mesua
Metrosideros
Michelia
Montezuma
Myroxylon
Napoleonaea
Nauclea
Newbouldia
Nuxia
Nyctanthes
Oncoba
Parinari
Parmentiera
Petrea
Phytolacca
Pinus
Platymiscium
Pleiogynium
Poitea
Portlandia
Posoqueria
Pterocarpus
Punica
Quaribea
Quassia
Radermachera
Santalum
Sarcocephalus
Schizolobium
Schotia
Sesbania
Solanum
Spathodea
Stenocarpus
Stereospermum
Tabernaemontana
Tecoma
Tectona
Tibouchina
Tipuana
Toona
Treculia
Trevesia
Vitex
Wallaceodendron
Warszewiczia
Wrightia
Xanthastemon
Zanthoxylum
Ziziphus

GBIF Citations:

"Ach, du dicke Eiche", Wald an der Oste-Grundschule Heeslingen, http://data.gbif.org/datasets/resource/3003)
"Ahrschleife bei Altenahr", http://data.gbif.org/datasets/resource/3522)
"Laubenheimer Bodenheimer Ried" - von Stromtalwiesen und Flutrasen, http://data.gbif.org/datasets/resource/3501)
"Schlechteberg" Ebersbach/Sa., http://data.gbif.org/datasets/resource/2958)
"Schwarzes Teich" (Waldpark Radebeul), http://data.gbif.org/datasets/resource/3001)
"Schwarzwassertal" bei Pobershau, http://data.gbif.org/datasets/resource/3603)
"Tre Pini" (Montebelluna, Italien), http://data.gbif.org/datasets/resource/2772)
10. GEO - Tag der Artenvielfalt 2008 - LSG "Pfarrhübel" Chemnitz, http://data.gbif.org/datasets/resource/3381)
20 Jahre Naturschutzgebiet Dreienberg, http://data.gbif.org/datasets/resource/2729)
3. Tag der Artenvielfalt Hockenheim, http://data.gbif.org/datasets/resource/2825)
4. GEO-Tag in Eberbach, http://data.gbif.org/datasets/resource/2736)
4. Tag der Artenvielfalt, Naturschutzgebiet Hockenheimer Rheinbogen, http://data.gbif.org/datasets/resource/2847)
AKG-Gelände (Bensheim), http://data.gbif.org/datasets/resource/2639)
ANTARCTIC PLANT DATABASE, http://data.gbif.org/datasets/resource/67)
Aachtobel, http://data.gbif.org/datasets/resource/3514)
Ackerrain Plönhagen, http://data.gbif.org/datasets/resource/3265)
Agentes Bioactivos de Plantas Desérticas de Latinoamérica (ICBG), http://data.gbif.org/datasets/resource/2485)
Aktion der Klasse H2 in Simmelsberg, http://data.gbif.org/datasets/resource/3570)
Altenburg bei Bamberg, http://data.gbif.org/datasets/resource/2844)
Alter Nördlicher Friedhof (München), http://data.gbif.org/datasets/resource/2977)
Am Moosangerweg, http://data.gbif.org/datasets/resource/2634)
Amtsrain Apolda-Zottelstedt, http://data.gbif.org/datasets/resource/3099)
Andes to Amazon Biodiversity Program, http://data.gbif.org/datasets/resource/56)
Angiosperm specimens of Iwate Prefectural Museum, http://data.gbif.org/datasets/resource/1800)
Aranzadi Zientzi Elkartea, http://data.gbif.org/datasets/resource/248)
Arizona State University Vascular Plant Herbarium, http://data.gbif.org/datasets/resource/676)
Artenfülle um das Schalkenmehrener Maar, http://data.gbif.org/datasets/resource/2722)
Arteninventar rund um den Rannahof, http://data.gbif.org/datasets/resource/2860)
Artenvielfalt Kreis Gießen, http://data.gbif.org/datasets/resource/2972)
Artenvielfalt am Schlern, http://data.gbif.org/datasets/resource/8055)
Artenvielfalt auf dem Schulgelände, http://data.gbif.org/datasets/resource/2862)
Artenvielfalt auf der Weide - GEO-Hauptveranstaltung in Crawinkel, http://data.gbif.org/datasets/resource/2697)
Artenvielfalt im Beckerbruch (Dessau), http://data.gbif.org/datasets/resource/3050)
Artenvielfalt im Naturschutzgebiet an der Loreley - Leiselfeld/Spitznack - 2. Jahr, http://data.gbif.org/datasets/resource/3516)
Artenvielfalt in der Stadt: Botanischer Garten Wuppertal und Hardt, http://data.gbif.org/datasets/resource/3385)
Atlas des plantes vasculaires de Lorraine, http://data.gbif.org/datasets/resource/7934)
Auenwiesen und Trockenrasen, http://data.gbif.org/datasets/resource/7888)
Australian National Herbarium (CANB), http://data.gbif.org/datasets/resource/47)
Außenfeuerstelle Königsbol (Hartheim/Meßstetten), http://data.gbif.org/datasets/resource/2755)

BDBCV - II Semana de la Biodiversidad (CastellÃ³n, Spain), 2007,
http://data.gbif.org/datasets/resource/1761)
BDBCV - II Semana de la Biodiversidad (CastellÃ³n, Spain), 2007,
http://data.gbif.org/datasets/resource/9193)
BDBCV - III Semana de la Biodiversidad (Alicante, Spain), 2008,
http://data.gbif.org/datasets/resource/7926)
BDBCV - III Semana de la Biodiversidad (Alicante, Spain), 2008,
http://data.gbif.org/datasets/resource/9194)
BDBCV - IV Semana de la Biodiversidad (Alicante, Spain), 2009,
http://data.gbif.org/datasets/resource/9089)
BDBCV - IV Semana de la Biodiversidad (Alicante, Spain), 2009,
http://data.gbif.org/datasets/resource/9195)
BUND - Dassower See (Lübeck/Dassow), http://data.gbif.org/datasets/resource/2707)
Baekdu Mountain Plant, http://data.gbif.org/datasets/resource/463)
Banco Nacional de Germoplasma Vegetal, México (BANGEV, UACH),
http://data.gbif.org/datasets/resource/1599)
Bannwald Burghauser Forst, http://data.gbif.org/datasets/resource/3379)
Belgian IFBL Flora Checklists (1939-1971), http://data.gbif.org/datasets/resource/10969)
Bergbaufolgelandschaft am Muldestausee, http://data.gbif.org/datasets/resource/2751)
Bergkamen- Bergehalde Großes Holz, http://data.gbif.org/datasets/resource/2797)
Berkel, http://data.gbif.org/datasets/resource/7871)
Bernhardsthal, http://data.gbif.org/datasets/resource/3398)
Besonderer Ort - besondere Natur: Die Mainzer Zitadelle,
http://data.gbif.org/datasets/resource/2985)
Beweidungsprojekt an der Nesse, http://data.gbif.org/datasets/resource/2938)
Binsenwiesen, http://data.gbif.org/datasets/resource/3113)
Biodiversidad de Costa Rica, http://data.gbif.org/datasets/resource/333)
Biological and palaeontological collection and observation data MNHNL,
http://data.gbif.org/datasets/resource/8107)
Biologiezentrum Linz, http://data.gbif.org/datasets/resource/1104)
Biologische Station im Kreis Wesel, http://data.gbif.org/datasets/resource/2703)
Biosphärenpark Wienerwald - Wiener Steinhofgründe,
http://data.gbif.org/datasets/resource/3392)
Biosphärenreservat Münsinger Alb, http://data.gbif.org/datasets/resource/7880)
Biotop "Kohlbeke" (Berlin-Marzahn), http://data.gbif.org/datasets/resource/2954)
Biotop Binsenwiesen und Ernst-Reiter-Wiese (Wehrheim/Taunus),
http://data.gbif.org/datasets/resource/3062)
Birkenloh, http://data.gbif.org/datasets/resource/3120)
Bishop Museum Natural History Specimen Data, http://data.gbif.org/datasets/resource/54)
Bizzenbach-Aue im Bizzenbachtal (Wehrheim/Taunus),
http://data.gbif.org/datasets/resource/2835)
Bizzenbachtal (Wehrheim/Taunus), http://data.gbif.org/datasets/resource/2809)
Blumenrather Heide / Virneburg, http://data.gbif.org/datasets/resource/2694)
BoGART, http://data.gbif.org/datasets/resource/1087)
Bodenseeufer Radolfzell, http://data.gbif.org/datasets/resource/2991)
Bodenteicher Seewiesen, http://data.gbif.org/datasets/resource/3515)
Borstgrasrasen um die Burg Baldenau im Oberen Dhrontal,
http://data.gbif.org/datasets/resource/3107)
Botanic Garden of Finnish Museum of Natural History,
http://data.gbif.org/datasets/resource/2406)
Botanical Collection, http://data.gbif.org/datasets/resource/7932)
Botanical Garden Collection, http://data.gbif.org/datasets/resource/64)

Botanical Museum, Copenhagen. Database of type specimens, http://data.gbif.org/datasets/resource/716)
Botanical Society of the British Isles - Vascular Plants Database, http://data.gbif.org/datasets/resource/839)
Botanical Society of the British Isles - Vascular plant data for Scottish Vice-counties (VCs 80, 84, 103 & 104), http://data.gbif.org/datasets/resource/1887)
Botanical garden, University of Hohenheim, Germany, http://data.gbif.org/datasets/resource/1855)
Botanical specimens database of Mr. Jiro Ito collection, Shizuoka Prefecture Museum of Natural History, http://data.gbif.org/datasets/resource/1811)
Botany (UPS), http://data.gbif.org/datasets/resource/1045)
Botany Vascular Plant Collection, http://data.gbif.org/datasets/resource/7915)
Botany registration database by Danish botanists, http://data.gbif.org/datasets/resource/703)
BotÃ¡nica, Universidad de LeÃ³n: LEB-Brasil, http://data.gbif.org/datasets/resource/8008)
BotÃ¡nica, Universidad de LeÃ³n: LEB-Cormo, http://data.gbif.org/datasets/resource/8003)
Brander Wald (Stolberg), http://data.gbif.org/datasets/resource/3046)
Bundesamt fuer Naturschutz / Netzwerk Phytodiversitaet Deutschland, http://data.gbif.org/datasets/resource/1098)
BÜG, http://data.gbif.org/datasets/resource/2628)
Bäche, Quellen und Teiche im FFH-Gebiet Mühlhauser Halde, http://data.gbif.org/datasets/resource/3160)
CGN-PGR, http://data.gbif.org/datasets/resource/1102)
CIBIO, Alicante:ABH-GBIF, http://data.gbif.org/datasets/resource/251)
CONN GBIF data, http://data.gbif.org/datasets/resource/7857)
CSU Herbarium, http://data.gbif.org/datasets/resource/7892)
California State University, Chico, http://data.gbif.org/datasets/resource/737)
Cameroon National Herbarium, http://data.gbif.org/datasets/resource/1474)
Canadian Museum of Nature Herbarium, http://data.gbif.org/datasets/resource/123)
CartografÃ-a de vegetaciÃ³n a escala de detalle 1:10.000 de la masa forestal de AndalucÃ-a, http://data.gbif.org/datasets/resource/10833)
CeDoc de Biodiversitat Vegetal: BCN-Cormophyta, http://data.gbif.org/datasets/resource/243)
Central African Plants, http://data.gbif.org/datasets/resource/8377)
Colecciones de George Boole Hinton depositadas en el herbario de Kew: Familia Leguminosae, http://data.gbif.org/datasets/resource/2487)
Collection Messelpaläobotanik SMB, http://data.gbif.org/datasets/resource/8322)
Collection Paläobotanik SMB, http://data.gbif.org/datasets/resource/8317)
CommunicA Koblenz - Wildkräuterexkursion - Rheinsteig Bornhofer Höhe, http://data.gbif.org/datasets/resource/3018)
Consortium of California Herbaria, http://data.gbif.org/datasets/resource/9153)
Cuxhavener Küstenheiden, http://data.gbif.org/datasets/resource/2695)
DAO Herbarium Type Specimens, http://data.gbif.org/datasets/resource/527)
DSMZ Collection on Plant Cell Cultures, http://data.gbif.org/datasets/resource/1476)
Dalbekschlucht, http://data.gbif.org/datasets/resource/3122)
Danielsberg (Mölltal, Kärnten), http://data.gbif.org/datasets/resource/2636)
Database Schema for UC Davis [Herbarium Labels], http://data.gbif.org/datasets/resource/734)
Database Schema for UC Davis [TGRC], http://data.gbif.org/datasets/resource/735)
Dellwiger Bach (Dortmund), http://data.gbif.org/datasets/resource/2999)
Departamento de Biolog. Veg. II, Facultad de Farmacia, Universidad Complutense, Madrid: MAF, http://data.gbif.org/datasets/resource/249)
Deponie Klausdorf, http://data.gbif.org/datasets/resource/2976)
Deutsche Schule Budapest, http://data.gbif.org/datasets/resource/2737)

Dierloch, nördlicher Mooswald (Freiburg-Hochdorf),
http://data.gbif.org/datasets/resource/2952)
DirecciÃ³n General de InvestigaciÃ³n, Desarrollo TecnolÃ³gico e InnovaciÃ³n de la Junta de Extremadura(DGIDTI): HSS, http://data.gbif.org/datasets/resource/291)
Dpto de BotÃ¡nica, EcologÃ-a y FisiologÃ-a Vegetal (Historico_cofc). Facultad de Ciencias. Universidad de CÃ³rdoba, http://data.gbif.org/datasets/resource/1520)
Dpto de BotÃ¡nica, EcologÃ-a y FisiologÃ-a Vegetal (herbario_cofc).Facultad de Ciencias.Universidad de CÃ³rdoba, http://data.gbif.org/datasets/resource/292)
Draubiotop Lavamünd, http://data.gbif.org/datasets/resource/3245)
Döchtbühlwald (Bad Waldsee), http://data.gbif.org/datasets/resource/2967)
Dörnberg, http://data.gbif.org/datasets/resource/3222)
Düne am Ulvenberg (Darmstadt), http://data.gbif.org/datasets/resource/3053)
E.C. Smith Herbarium, http://data.gbif.org/datasets/resource/1829)
EDIT - ATBI in Gemer area (Slovakia), http://data.gbif.org/datasets/resource/7950)
EDIT - ATBI in Mercantour/Alpi Marittime (France/Italy),
http://data.gbif.org/datasets/resource/7949)
EKY_Darwincore, http://data.gbif.org/datasets/resource/7894)
ENDEMIC SPECIES RESEARCH INSTITUTE, http://data.gbif.org/datasets/resource/8416)
EUNIS, http://data.gbif.org/datasets/resource/198)
EURISCO, The European Genetic Resources Search Catalogue,
http://data.gbif.org/datasets/resource/1905)
Ehmkendorf, http://data.gbif.org/datasets/resource/2944)
Ejemplares tipo de plantas vasculares del Herbario de la Escuela Nacional de Ciencias Biológicas, México (ENCB, IPN), http://data.gbif.org/datasets/resource/2498)
Entdeckertour am Muldestausee, http://data.gbif.org/datasets/resource/2709)
Environment and Heritage Service - EHS Species Datasets,
http://data.gbif.org/datasets/resource/940)
Eppingen und Umgebung, http://data.gbif.org/datasets/resource/2816)
Erft in Selikum (Neuss), http://data.gbif.org/datasets/resource/3039)
Erlengraben/Lipp-Tal (Östringen), http://data.gbif.org/datasets/resource/2675)
Erzental (Oberotterbach), http://data.gbif.org/datasets/resource/2670)
Escuela TÃ©cnica Superior de Ingenieros de Montes, UPM: EMMA,
http://data.gbif.org/datasets/resource/278)
Estudio Florístico de la Sierra de Pachuca, Hidalgo, México (ENCB, IPN),
http://data.gbif.org/datasets/resource/2499)
Expedition "Schulgelände", http://data.gbif.org/datasets/resource/3391)
Extra-andean Patagonian Herbarrium -CONICET- Argentina,
http://data.gbif.org/datasets/resource/154)
FFH-Gebiet "Calwer Heckengäu", http://data.gbif.org/datasets/resource/3373)
FFH-Gebiet Ahrbachtal, http://data.gbif.org/datasets/resource/2640)
FFH-Gebiet Klosterwasser/Burkau, http://data.gbif.org/datasets/resource/3489)
FND "Weißer Berg" Leißling, http://data.gbif.org/datasets/resource/3294)
FNL e.V., http://data.gbif.org/datasets/resource/2935)
Faberpark (Nürnberg/Stein), http://data.gbif.org/datasets/resource/2779)
Factual Database of Native Flora Seeds in Korea, http://data.gbif.org/datasets/resource/112)
Fairchild Tropical Botanic Garden Virtual Herbarium Darwin Core format,
http://data.gbif.org/datasets/resource/202)
Feldweg Waldkirchen, http://data.gbif.org/datasets/resource/3513)
Fels- und Weinbergsflächen in Hatzenport/Terrassenmosel,
http://data.gbif.org/datasets/resource/2774)
Feriendorf Ober-Seemen, http://data.gbif.org/datasets/resource/2940)
Feriendorf des Kreises Groß-Gerau Ober-Seemen/Gedern,
http://data.gbif.org/datasets/resource/2804)

Feriendorf des Kreises Groß-Gerau/Ober-Seemen,
http://data.gbif.org/datasets/resource/2863)
FloVegSI - Floristical and fitocenological database of ZRC SAZU,
http://data.gbif.org/datasets/resource/2585)
Flora exsiccata Bavarica, http://data.gbif.org/datasets/resource/1092)
Flora of S?owi?ski National Park, Poland, http://data.gbif.org/datasets/resource/2022)
Flora of the Sto?owe Mts., http://data.gbif.org/datasets/resource/8155)
Flora, http://data.gbif.org/datasets/resource/2939)
Floristische Kartierung Österreichs - Mapping the Flora of Austria,
http://data.gbif.org/datasets/resource/1497)
Forster herbarium, Gottingen (GOET), http://data.gbif.org/datasets/resource/1493)
František Nábìlek Herbarium 1909-1910, http://data.gbif.org/datasets/resource/8235)
Frauenholz (Holzmaden), http://data.gbif.org/datasets/resource/2668)
Freiburger Netzwerk Artenvielfalt, http://data.gbif.org/datasets/resource/7866)
Freiburger Tag der Artenvielfalt, http://data.gbif.org/datasets/resource/2669)
Freigelände Naturschutzscheune Reinheimer Teich (Kreis Darmstadt-Dieburg),
http://data.gbif.org/datasets/resource/2845)
Freiheitsring (Frechen), http://data.gbif.org/datasets/resource/2837)
Frohlinder Mühlenbach (Dortmund-Kirchlinde), http://data.gbif.org/datasets/resource/2803)
Fuchsloch (Mohlsdorf/Ostthüringen), http://data.gbif.org/datasets/resource/2960)
Fuldaaue (Stadtgebiet Fulda), http://data.gbif.org/datasets/resource/2790)
FundaciÃ³n Biodiversidad, Real JardÃ-n BotÃ¡nico (CSIC): Anthos. Sistema de InformaciÃ³n de las plantas de EspaÃ±a, http://data.gbif.org/datasets/resource/9090)
Fundación Miguel Lillo Provider, http://data.gbif.org/datasets/resource/2009)
Föhrenried (Fronreute und Baindt), http://data.gbif.org/datasets/resource/2970)
Förderzentrum Schmölln, http://data.gbif.org/datasets/resource/2941)
Fürstenberger Ralley Teil 3, http://data.gbif.org/datasets/resource/3383)
GBIF-PORTUGAL-HerbÃ¡rio JoÃ£o de Carvalho e Vasconcellos, I.S.A./U.T.L.,
http://data.gbif.org/datasets/resource/253)
GEO Biodiversity Day, http://data.gbif.org/datasets/resource/1094)
GEO Hauptveranstaltung Tirol (Innsbruck), http://data.gbif.org/datasets/resource/2662)
GEO-Hauptveranstaltung (Duisburg), http://data.gbif.org/datasets/resource/2705)
GEO-Hauptveranstaltung (Insel Vilm), http://data.gbif.org/datasets/resource/2704)
GEO-Hauptveranstaltung (NLP Harz / Hochharz), http://data.gbif.org/datasets/resource/2643)
GEO-Hauptveranstaltung im Nationalpark Bayerischer Wald,
http://data.gbif.org/datasets/resource/3378)
GEO-Tag der Artenvielfalt auf dem Bausenberg mit den 4. Klassen der Brohltaler Grundschulen,
http://data.gbif.org/datasets/resource/2691)
GEO-Tag mit der NAJU des Landkreises Ahrweiler am Bausenberg,
http://data.gbif.org/datasets/resource/2846)
GNOR-Projekt "Halbwilde Weidehaltung zwischen Kamp-Bornhofen und Kestert" und Umland,
http://data.gbif.org/datasets/resource/2849)
Garten J. Scherrer (Lachen-Speyerdorf), http://data.gbif.org/datasets/resource/3069)
Gelände der Lahntalschule Biedenkopf und Lahnauen,
http://data.gbif.org/datasets/resource/2982)
Gelände des IVL (Zeckern), http://data.gbif.org/datasets/resource/2672)
Gelände des Schulzentrums am Himmelsbarg, http://data.gbif.org/datasets/resource/3136)
Gemeinde Sursee, http://data.gbif.org/datasets/resource/2652)
Gemeindegebiet Weikendorf (Marchfeld), http://data.gbif.org/datasets/resource/2765)
Gemeinschaftsgarten Deluxe (Bernburg), http://data.gbif.org/datasets/resource/2988)
Generalitat Valenciana. Banco de Datos de la Biodiversidad de la Comunitat Valenciana,
http://data.gbif.org/datasets/resource/8004)

Geo-Tag der Artenvielfalt Süßen Hornwiesen-Grundschule,
http://data.gbif.org/datasets/resource/2783)
Geschützter Landschaftsbestandteil - GLB "Troppach",
http://data.gbif.org/datasets/resource/3014)
Gewann Krampf (Heilbronn), http://data.gbif.org/datasets/resource/2653)
Gothenburg Herbarium - General (GBIF:IH:GB:Herbarium),
http://data.gbif.org/datasets/resource/1765)
Gothenburg Herbarium - Types (GBIF:IH:GB:Herbarium),
http://data.gbif.org/datasets/resource/1766)
Gronau - auf der Suche nach dem Neunauge, http://data.gbif.org/datasets/resource/3490)
Gunma Museum of Natural History, Vascular Plant Specimen,
http://data.gbif.org/datasets/resource/8018)
Gurgltal (Tarrenz), http://data.gbif.org/datasets/resource/2727)
Gyeryonsan Natural History Museum Fossil, http://data.gbif.org/datasets/resource/218)
GymnQuerfurt, http://data.gbif.org/datasets/resource/3036)
Gymnicher Mühle, http://data.gbif.org/datasets/resource/7906)
HBGSpermatophyta - Herbarium Hamburgense, http://data.gbif.org/datasets/resource/1604)
Haarbach Höfe, http://data.gbif.org/datasets/resource/3393)
Halberg bei Neumorschen, http://data.gbif.org/datasets/resource/2828)
Halbwilde Weidehaltung zwischen Kamp-Bornhofen und Kestert sowie Umland,
http://data.gbif.org/datasets/resource/7870)
Hamberger Brücke / Würmtal (Pforzheim), http://data.gbif.org/datasets/resource/2644)
Harvard University Herbaria, http://data.gbif.org/datasets/resource/1827)
Hatikka Observation Data Gateway, http://data.gbif.org/datasets/resource/2401)
Heinersdorfer Sumpfwiese, http://data.gbif.org/datasets/resource/2734)
Hemmerder Schelk (Unna), http://data.gbif.org/datasets/resource/2820)
Herbaria of the University and ETH Zürich, http://data.gbif.org/datasets/resource/1903)
Herbario Kew del Real Jardín Botánico (RBGKEW),
http://data.gbif.org/datasets/resource/2486)
Herbario Los Tuxtlas, http://data.gbif.org/datasets/resource/785)
Herbario UNAP, http://data.gbif.org/datasets/resource/223)
Herbario de Universidad de Murcia: MUB, http://data.gbif.org/datasets/resource/8406)
Herbario de la Escuela Nacional de Ciencias Biológicas, México (ENCB, IPN),
http://data.gbif.org/datasets/resource/1601)
Herbario de la Universidad PÃºblica de Navarra, Pamplona: UPNA-H,
http://data.gbif.org/datasets/resource/8007)
Herbario de la Universidad de Almeria, http://data.gbif.org/datasets/resource/244)
Herbario de la Universidad de Arizona, EUA, http://data.gbif.org/datasets/resource/2479)
Herbario de la Universidad de Salamanca: SALA, http://data.gbif.org/datasets/resource/239)
Herbario de la Universidad de Sevilla, SEV, http://data.gbif.org/datasets/resource/283)
Herbario de la Universidad de Sevilla, SEV-Historico,
http://data.gbif.org/datasets/resource/284)
Herbario del Instituto de Ecología, A.C., México (IE-BAJIO),
http://data.gbif.org/datasets/resource/1595)
Herbario del Instituto de Ecología, A.C., México (IE-XAL),
http://data.gbif.org/datasets/resource/1597)
HerbarioHerrerense, http://data.gbif.org/datasets/resource/325)
Herbarium (AMNH), http://data.gbif.org/datasets/resource/232)
Herbarium (ICEL), http://data.gbif.org/datasets/resource/231)
Herbarium (UNA), http://data.gbif.org/datasets/resource/775)
Herbarium BSG Vascular Plants, http://data.gbif.org/datasets/resource/1470)
Herbarium Berolinense, http://data.gbif.org/datasets/resource/1095)
Herbarium GJO, http://data.gbif.org/datasets/resource/1484)

Herbarium GZU, http://data.gbif.org/datasets/resource/1491)
Herbarium Senckenbergianum (FR), http://data.gbif.org/datasets/resource/8311)
Herbarium Specimens of Bonin and Ryukyu Islands,
http://data.gbif.org/datasets/resource/8108)
Herbarium Specimens of Museum of Nature and Human Activities, Hyogo Pref., Japan,
http://data.gbif.org/datasets/resource/589)
Herbarium Specimens of Museum of Nature and Human Activities, Hyogo Prefecture, Japan,
http://data.gbif.org/datasets/resource/1958)
Herbarium Specimens of Tokushima Prefectural Museum, Japan,
http://data.gbif.org/datasets/resource/600)
Herbarium W, http://data.gbif.org/datasets/resource/1479)
Herbarium WRSL, Flora of the Silesia, http://data.gbif.org/datasets/resource/1461)
Herbarium WU, http://data.gbif.org/datasets/resource/1496)
Herbarium Willing, http://data.gbif.org/datasets/resource/1096)
Herbarium collection, http://data.gbif.org/datasets/resource/7943)
Herbarium de Geo. B. Hinton, México, http://data.gbif.org/datasets/resource/1594)
Herbarium des Staatlichen Museums für Naturkunde Görlitz (GLM),
http://data.gbif.org/datasets/resource/1105)
Herbarium of Kitakyushu Museum of Natural History and Human History,
http://data.gbif.org/datasets/resource/606)
Herbarium of Oskarshamn (OHN), http://data.gbif.org/datasets/resource/1024)
Herbarium of The New York Botanical Garden, http://data.gbif.org/datasets/resource/8967)
Herbarium of University of Bia?ystok - Vascular Plants,
http://data.gbif.org/datasets/resource/8164)
Herbarium of the Department of Natural Forests (Forest Research Institute),
http://data.gbif.org/datasets/resource/1486)
Herbarium of the Université Libre de Bruxelles, http://data.gbif.org/datasets/resource/9102)
Herbarium specimen from "BIEL", Germany, http://data.gbif.org/datasets/resource/1857)
Herbarium specimen from "EA", Kenya, http://data.gbif.org/datasets/resource/1854)
Herbarium specimen from the Estacion Scientifica San Francisco, Southern Ecuador,
http://data.gbif.org/datasets/resource/1614)
Herbarium, Biodiversity Research Center, Academia Sinica, Taipei,
http://data.gbif.org/datasets/resource/8300)
Herbarium, http://data.gbif.org/datasets/resource/7984)
Herbier de Strasbourg, http://data.gbif.org/datasets/resource/1849)
Herbier de la Guyane, http://data.gbif.org/datasets/resource/1436)
Herrensee-Gebiet (Fischbachtal im Odenwald), http://data.gbif.org/datasets/resource/3055)
Hintere Halde, http://data.gbif.org/datasets/resource/2830)
Hochschulgelände (Bremen), http://data.gbif.org/datasets/resource/2953)
Hoher Stein Kallenhardt, http://data.gbif.org/datasets/resource/3239)
Hortus Botanicus Sollerensis Herbarium (FBonafÃ¨),
http://data.gbif.org/datasets/resource/300)
IIAPPoa, http://data.gbif.org/datasets/resource/656)
IICT Herbário LISC, http://data.gbif.org/datasets/resource/10840)
IPK Genebank, http://data.gbif.org/datasets/resource/1851)
ISTOTA - Schulgarten in Krakau, Stadtteil Ludwinow,
http://data.gbif.org/datasets/resource/3080)
Ibaraki Nature Museum, Dr.Masatomo Suzuki collection:Vascular Plants (1),
http://data.gbif.org/datasets/resource/1813)
Ibaraki Nature Museum, Vascular Plants collection (1),
http://data.gbif.org/datasets/resource/8030)
Impetus - Herbarium Hamburgense, http://data.gbif.org/datasets/resource/1605)
IndOBIS, Indian Ocean Node of OBIS, http://data.gbif.org/datasets/resource/1471)

Industriegebiet (Kempen), http://data.gbif.org/datasets/resource/2748)
Innenhöfe der Gesamtschule Berger Feld/ Gelsenkirchen,
http://data.gbif.org/datasets/resource/3344)
Innenstadt Göttingen - Natur Zuhause, http://data.gbif.org/datasets/resource/2851)
Insects, http://data.gbif.org/datasets/resource/625)
Insektenvielfalt Ahe/Weichelsee, http://data.gbif.org/datasets/resource/3026)
Institut Botanic de Barcelona, BC, http://data.gbif.org/datasets/resource/299)
Institut Botanic de Barcelona, BC-HistÃ³rico, http://data.gbif.org/datasets/resource/1523)
Institut d'Ecologia Litoral: IEL_Plantae, http://data.gbif.org/datasets/resource/263)
Institut d'Ecologia Litoral: IEL_Seed, http://data.gbif.org/datasets/resource/264)
Institute of Dendrology PAS, Flora of Sudety Mountains,
http://data.gbif.org/datasets/resource/1448)
Institute of Ecology and Evolutionary Biology, National Taiwan University,
http://data.gbif.org/datasets/resource/8089)
Instituto Pirenaico de EcologÃ-a-CSIC: Herbarium JACA,
http://data.gbif.org/datasets/resource/246)
Instituto de Ciencias Naturales, http://data.gbif.org/datasets/resource/2559)
Instituto de Investigación de Recursos Biológicos Alexander von Humboldt,
http://data.gbif.org/datasets/resource/2619)
Inventaire national du Patrimoine naturel (INPN),
http://data.gbif.org/datasets/resource/2620)
Isarufer, http://data.gbif.org/datasets/resource/2947)
Israel Nature and Parks Authority, http://data.gbif.org/datasets/resource/1431)
Jardi Botanic de Valencia: VAL, http://data.gbif.org/datasets/resource/238)
JardÃ-n BotÃ¡nico AtlÃ¡ntico, GijÃ³n: JBAG, http://data.gbif.org/datasets/resource/8083)
JardÃ-n BotÃ¡nico AtlÃ¡ntico, GijÃ³n: JBAG-LaÃ-nz,
http://data.gbif.org/datasets/resource/8082)
JardÃ-n BotÃ¡nico de CÃ³rdoba: Herbarium COA, http://data.gbif.org/datasets/resource/247)
Joint Nature Conservation Committee - Vegetation surveys of coastal shingle in Great Britain,
http://data.gbif.org/datasets/resource/849)
KARSTLANDSCHAFT SÜDHARZ - VOM GIPSABBAU BEDROHT (Grenzstreifen am Röseberg),
http://data.gbif.org/datasets/resource/2726)
KTU Pinophyta, http://data.gbif.org/datasets/resource/8171)
Kabelskebach (Kabelsketal, Saalkreis), http://data.gbif.org/datasets/resource/2993)
Kaisertal, http://data.gbif.org/datasets/resource/3273)
Kaniswall/ Gosener Wiesen an der Spree, http://data.gbif.org/datasets/resource/3390)
Kernberge und Umgebung (Jena), http://data.gbif.org/datasets/resource/2649)
Kiesbagger (Mittelhausen), http://data.gbif.org/datasets/resource/2760)
Kindergarten, http://data.gbif.org/datasets/resource/3033)
Kindervilla Außengelände, http://data.gbif.org/datasets/resource/3599)
Kita-Wäldchen Fuchsturmweg Jena, http://data.gbif.org/datasets/resource/3008)
Klasse 3a, http://data.gbif.org/datasets/resource/2929)
Kloster Eberbach, http://data.gbif.org/datasets/resource/2942)
Klutensee, http://data.gbif.org/datasets/resource/2631)
Knechtweide (Kohlfurth), http://data.gbif.org/datasets/resource/2742)
Kochi Prefectural Makino Botanical Garden, http://data.gbif.org/datasets/resource/1975)
Kohlstattbrunnental, http://data.gbif.org/datasets/resource/7907)
Korean Ethnobotany Database, http://data.gbif.org/datasets/resource/111)
Kremmer Luch, http://data.gbif.org/datasets/resource/2937)
Kurashiki Museum of Natural History, http://data.gbif.org/datasets/resource/599)
Königsdorfer Wald, http://data.gbif.org/datasets/resource/3495)
Königstetten, http://data.gbif.org/datasets/resource/2667)
Küstenschutzwald, http://data.gbif.org/datasets/resource/2934)

LK 11 im Mönchspark, http://data.gbif.org/datasets/resource/3396)
LaBoOb02, http://data.gbif.org/datasets/resource/2629)
Lake Biwa Museum, http://data.gbif.org/datasets/resource/1797)
Landesgartenschau, http://data.gbif.org/datasets/resource/2744)
Landschaftspark St.Leonhard-Deisendorf, http://data.gbif.org/datasets/resource/3161)
Landschaftspflegehof (Berlin), http://data.gbif.org/datasets/resource/2656)
Landschaftsschutzgebiet Buchhorst 3, http://data.gbif.org/datasets/resource/3029)
Landschaftsschutzgebiet Buchhorst 4, http://data.gbif.org/datasets/resource/3334)
Landschaftsschutzgebiet Hexenberg (Erftstadt-Erp),
http://data.gbif.org/datasets/resource/2756)
Langes Tannen (Uetersen), http://data.gbif.org/datasets/resource/2671)
Langes Tannen(LMS), Klasse 5d, http://data.gbif.org/datasets/resource/3491)
Langes Tannen, http://data.gbif.org/datasets/resource/2682)
Laubenheimer Bodenheimer Ried - von Stromtalwiesen und Flutrasen,
http://data.gbif.org/datasets/resource/7875)
Laubwald Dreiländereck (Aachen/Vaals[NL]), http://data.gbif.org/datasets/resource/2975)
Leben im Finkensteiner Moor, http://data.gbif.org/datasets/resource/3154)
Lebensraum Gesamtschule (Langerwehe), http://data.gbif.org/datasets/resource/2767)
Lebensraum Stadt und Park, http://data.gbif.org/datasets/resource/2832)
Lech 2001, http://data.gbif.org/datasets/resource/2946)
Leiner-Herbar Konstanz, http://data.gbif.org/datasets/resource/1473)
Lillachtal mit Kalktuffquelle bei Weißenohe, http://data.gbif.org/datasets/resource/3002)
Limnodata, http://data.gbif.org/datasets/resource/1466)
Lindau im Bodensee, http://data.gbif.org/datasets/resource/2801)
Lothian Wildlife Information Centre - Lothian Wildlife Information Centre Secret Garden
Survey, http://data.gbif.org/datasets/resource/856)
Luch Niederlehme, Schüler der Klasse 7, http://data.gbif.org/datasets/resource/2719)
Lund Botanical Museum (LD), http://data.gbif.org/datasets/resource/1028)
Lund Museum of Zoology - Insect collections (MZLU),
http://data.gbif.org/datasets/resource/1763)
Lustadter Wald ., http://data.gbif.org/datasets/resource/7904)
Lustbach-Umland, http://data.gbif.org/datasets/resource/3494)
Lüner Holz (Lüneburg), http://data.gbif.org/datasets/resource/2798)
ME474, http://data.gbif.org/datasets/resource/2553)
MEXU/Colección Histórica, http://data.gbif.org/datasets/resource/1984)
MEXU/Colección de Plantas Acuáticas, http://data.gbif.org/datasets/resource/8047)
MEXU/Flora de Oaxaca, http://data.gbif.org/datasets/resource/8392)
MEXU/Leguminosae, http://data.gbif.org/datasets/resource/8390)
MEXU/Plantas Vasculares, http://data.gbif.org/datasets/resource/780)
MISS_DC_01MAR2006, http://data.gbif.org/datasets/resource/7895)
Mainfränkischer Trockenrasen und Naturschutzgebiet Höhfeldplatte bei Veitshöchheim,
http://data.gbif.org/datasets/resource/3114)
Mainufer, http://data.gbif.org/datasets/resource/3043)
Malacology specimens, http://data.gbif.org/datasets/resource/1517)
Marine invertabrate(Mollusca) specimen database of Osaka Museum of Natural History,
http://data.gbif.org/datasets/resource/1972)
Mauervegetation,Flechten und anderes, http://data.gbif.org/datasets/resource/3249)
MfN - Fossil plants (Cenophytic), http://data.gbif.org/datasets/resource/9179)
Ministerio de Medio Ambiente, y Medio Rural y Marino. DirecciÃ³n General de Medio Natural
y PolÃ-tica Forestal. Inventario Nacional de Biodiversidad 2007, Flora Vascular Amenazada,
http://data.gbif.org/datasets/resource/3367)
Miscellaneous Vascular Plants, http://data.gbif.org/datasets/resource/10874)
Missouri Botanical Garden, http://data.gbif.org/datasets/resource/621)

Mißmahlsche Anlage, http://data.gbif.org/datasets/resource/2852)
Mokpo Museum of Natural History Plant, http://data.gbif.org/datasets/resource/570)
Mooswald (Freiburg), http://data.gbif.org/datasets/resource/2651)
Motzener Tonsee, http://data.gbif.org/datasets/resource/2978)
Muehlenbach bei Friesheim, http://data.gbif.org/datasets/resource/2793)
Museo Nacional de Ciencias Naturales, ColecciÃ³n de MalacologÃ-a,
http://data.gbif.org/datasets/resource/301)
NABU Naturschutzhof Netttetal (Sassenfeld) e.V.,
http://data.gbif.org/datasets/resource/2759)
NABU VG Weilerbach - NSG Mehlinger Heide, FFH-Gebiet,
http://data.gbif.org/datasets/resource/3088)
NABU-Projekt (Osterode am Harz) Südharzer Gipskarst,
http://data.gbif.org/datasets/resource/2821)
NCSU_Darwincore, http://data.gbif.org/datasets/resource/7898)
NHT_flora, http://data.gbif.org/datasets/resource/8350)
NMNH Botany Collections, http://data.gbif.org/datasets/resource/1874)
NSG Dellwiger Wald, Dortmund, http://data.gbif.org/datasets/resource/7874)
NSG Hülenbuch Hörnle (Tieringen/Meßstetten), http://data.gbif.org/datasets/resource/2679)
NSG Karwendel, http://data.gbif.org/datasets/resource/2678)
NSW herbarium collection, http://data.gbif.org/datasets/resource/968)
Nationaal Herbarium Nederland, http://data.gbif.org/datasets/resource/1211)
Nationaal Herbarium Nederland - Leiden Branch, http://data.gbif.org/datasets/resource/1085)
National Botanic Garden Belgium - Albertian Rift Rubiaceae (ENBI wp13),
http://data.gbif.org/datasets/resource/90)
National Botanic Garden Belgium - Martius, http://data.gbif.org/datasets/resource/89)
National Forest Inventory (SLU), http://data.gbif.org/datasets/resource/8054)
National Museum of Natural Science, http://data.gbif.org/datasets/resource/8090)
National Science Museum of Korea Plant, http://data.gbif.org/datasets/resource/908)
National System of Protected Areas in Poland - Plants,
http://data.gbif.org/datasets/resource/8249)
National Vegetation Data bank, http://data.gbif.org/datasets/resource/2471)
National vegetation diversity inventory and mapping plan,
http://data.gbif.org/datasets/resource/8374)
Natur aus zweiter Hand am Muldestausee, http://data.gbif.org/datasets/resource/2770)
Natur erleben rund um den Seminarbauernhof Gut Hohenberg,
http://data.gbif.org/datasets/resource/3021)
Natur-Erlebnisgebiet der Naturschutz-Akademie Hessen und Umgebung,
http://data.gbif.org/datasets/resource/3388)
Natural History Museum Rotterdam, http://data.gbif.org/datasets/resource/693)
Naturalis National Natural History Museum (NL) – Mollusca fossils,
http://data.gbif.org/datasets/resource/7859)
NatureServe Network Species Occurrence Data, http://data.gbif.org/datasets/resource/607)
Naturgarten Langenholtensen, http://data.gbif.org/datasets/resource/2857)
Naturgrundstück (Eutin), http://data.gbif.org/datasets/resource/2961)
Naturhausgarten, http://data.gbif.org/datasets/resource/3010)
Naturnahes Tal in Siena, http://data.gbif.org/datasets/resource/7909)
Naturparadies in Gräfenhausen am Trifels (bei Annweiler),
http://data.gbif.org/datasets/resource/3093)
Naturpark Drömling, http://data.gbif.org/datasets/resource/7864)
Naturschutzgebiet Bausenberg (Niederzissen), http://data.gbif.org/datasets/resource/2674)
Naturschutzgebiet Bausenberg, http://data.gbif.org/datasets/resource/2657)
Naturschutzgebiet Börstig bei Hallstadt, http://data.gbif.org/datasets/resource/3485)
Naturschutzgebiet Heiliger Hain (Wahrenholz), http://data.gbif.org/datasets/resource/2711)

Naturschutzgebiet Kochertgraben, http://data.gbif.org/datasets/resource/3233)
Naturschutzgebiet Lippeaue (Marl) - Pfadis in Sickingmühle,
http://data.gbif.org/datasets/resource/3087)
Naturschutzgebiet Müchelholz (Mücheln), http://data.gbif.org/datasets/resource/2814)
Naturschutzstation Schmidsfelden, http://data.gbif.org/datasets/resource/2655)
Neckartalsüdhang (Horb), http://data.gbif.org/datasets/resource/2680)
New Mexico Biodiversity Collections Consortium database,
http://data.gbif.org/datasets/resource/7856)
New Zealand Biodiversity Recording Network, http://data.gbif.org/datasets/resource/7910)
New Zealand National Plant Herbarium (CHR), http://data.gbif.org/datasets/resource/474)
New Zealand National Vegetation Survey Databank,
http://data.gbif.org/datasets/resource/473)
Nijmegen Natural History Museum (NL) – Herbarium,
http://data.gbif.org/datasets/resource/9185)
Nordic Genetic Resources, http://data.gbif.org/datasets/resource/1487)
Nottekanal, Klasse 7 - 10, http://data.gbif.org/datasets/resource/2718)
Ober-Olmer Wald, http://data.gbif.org/datasets/resource/3519)
Observational database of Icelandic plants, http://data.gbif.org/datasets/resource/233)
Observations du Conservatoire botanique national du Bassin parisien.,
http://data.gbif.org/datasets/resource/1103)
Obstwiese Osterberg, http://data.gbif.org/datasets/resource/3078)
Oklahoma Vascular Plants Database Provider, http://data.gbif.org/datasets/resource/2558)
Orchideenstandort Nostengraben - Kretzberg (Oßmaritz),
http://data.gbif.org/datasets/resource/2794)
Ortelsbruch - Hangmoor bei Morbach, http://data.gbif.org/datasets/resource/2998)
Oschenberg, NO von Bayreuth-Laineck, http://data.gbif.org/datasets/resource/3083)
Owere Fiddel, http://data.gbif.org/datasets/resource/3497)
Oxford University Herbaria, http://data.gbif.org/datasets/resource/2020)
Paleobiology Database, http://data.gbif.org/datasets/resource/563)
Paul-Gerhardt-Schule Dassel, http://data.gbif.org/datasets/resource/3015)
Peabody Botany DiGIR Service, http://data.gbif.org/datasets/resource/8137)
Peabody Paleobotany DiGIR Service, http://data.gbif.org/datasets/resource/8141)
Peabody Paleoportal DiGIR Service (PB), http://data.gbif.org/datasets/resource/8176)
Perchtoldsdorfer Heide, http://data.gbif.org/datasets/resource/7863)
Pflanzen und Tiere im Burgwald, http://data.gbif.org/datasets/resource/3523)
Phanerogamic Botanical Collections (S), http://data.gbif.org/datasets/resource/8113)
Phanerogamie, http://data.gbif.org/datasets/resource/1506)
Philosophenwald und Wieseckaue in Gießen, http://data.gbif.org/datasets/resource/2690)
Phragma-Thermis/Thessaloniki, http://data.gbif.org/datasets/resource/7882)
Pilstingermoos, http://data.gbif.org/datasets/resource/2721)
Plant Observation Records of Japan, http://data.gbif.org/datasets/resource/2547)
Plant observations from Bia?owie?a National Park,
http://data.gbif.org/datasets/resource/1861)
Plant specimens depodited in Osaka Museum of Natural History, Japan.,
http://data.gbif.org/datasets/resource/1973)
Plant, http://data.gbif.org/datasets/resource/469)
Plantae, TAIF (Taiwan e-Learning and Digital Archives Program, TELDAP),
http://data.gbif.org/datasets/resource/8053)
Plants (GBIF-SE:Artdatabanken), http://data.gbif.org/datasets/resource/1034)
Plants from Costa Rica, illustrations by Teresa Barantes Lobo,
http://data.gbif.org/datasets/resource/1625)
Plants from Costa Rica; Helmut Dalitz, http://data.gbif.org/datasets/resource/1853)
Plants from Costa Rica; Juergen Homeier, http://data.gbif.org/datasets/resource/1612)

Plants from Southern Ecuador; Daniel Piechowski,
http://data.gbif.org/datasets/resource/1638)
Plants from Southern Ecuador; Juergen Homeier, http://data.gbif.org/datasets/resource/1613)
Plants from Southern Ecuador; Ulf Soltau, http://data.gbif.org/datasets/resource/1623)
Plants from the Kakamega Forest, Kenya; Baerbel Bleher,
http://data.gbif.org/datasets/resource/1620)
Plants from the Kakamega Forest, Kenya; Dana Uster,
http://data.gbif.org/datasets/resource/1616)
Plants from the Kakamega Forest, Kenya; Frederike Proewe,
http://data.gbif.org/datasets/resource/1639)
Plants from the Kakamega Forest, Kenya; Helmut Dalitz,
http://data.gbif.org/datasets/resource/1610)
Plants of Papua New Guinea, http://data.gbif.org/datasets/resource/969)
Polish gene bank – passport data of plants accessions which are important in human life,
http://data.gbif.org/datasets/resource/8332)
Polish seed gene bank – historical passport data of accessions,
http://data.gbif.org/datasets/resource/8333)
PonTaurus collection, http://data.gbif.org/datasets/resource/1099)
Pottundkopp, http://data.gbif.org/datasets/resource/2741)
Private collection of Asta Napp-Zinn, http://data.gbif.org/datasets/resource/1637)
Private collection of Eberhard Fischer, http://data.gbif.org/datasets/resource/1852)
Private collection of Helmut Dalitz, http://data.gbif.org/datasets/resource/1635)
Private collection of Juergen Homeier, http://data.gbif.org/datasets/resource/1628)
Private collection of Rainer Bussmann, http://data.gbif.org/datasets/resource/1615)
Programa de repatriación de datos de ejemplares mexicanos,
http://data.gbif.org/datasets/resource/2488)
Promberg1, http://data.gbif.org/datasets/resource/2702)
Pöhlberg bei Annaberg, http://data.gbif.org/datasets/resource/3389)
Quarrendorfer Landschaftsschutzgebiet, http://data.gbif.org/datasets/resource/2778)
RBGE Herbarium (E), http://data.gbif.org/datasets/resource/8402)
RBGE Living Collections, http://data.gbif.org/datasets/resource/9167)
Rapid Assessment Program (RAP) Biodiversity Survey Database,
http://data.gbif.org/datasets/resource/8076)
Real Jardin Botanico (Madrid), Vascular Plant Herbarium (MA),
http://data.gbif.org/datasets/resource/240)
Rechts des Inn Höhe Hofau Rosenheim, http://data.gbif.org/datasets/resource/3584)
Regenrückhaltebecken (Zeulenroda), http://data.gbif.org/datasets/resource/2974)
Registros biológicos en áreas protegidas obtenidos de documentos impresos,
http://data.gbif.org/datasets/resource/10869)
Renaturierung Werse (Innenbereich Beckum), http://data.gbif.org/datasets/resource/2795)
Repatriación de datos del Herbario de Arizona (ARIZ),
http://data.gbif.org/datasets/resource/2480)
Reusaer Wald, http://data.gbif.org/datasets/resource/3583)
Ried und Sand - Artenvielfalt durch Beweidung, http://data.gbif.org/datasets/resource/3023)
Riedensee, http://data.gbif.org/datasets/resource/2724)
Rohrmeistereiplateau und angrenzendes Gebiet, http://data.gbif.org/datasets/resource/3382)
Rotes Steigle (Panzerübungplatz Böblingen), http://data.gbif.org/datasets/resource/3342)
Royal Botanic Gardens, Kew, http://data.gbif.org/datasets/resource/629)
Royal Botanical Gardens Herbarium, http://data.gbif.org/datasets/resource/512)
Royal Museum of Central Africa - Metafro-Infosys - Prelude,
http://data.gbif.org/datasets/resource/96)
Royal Museum of Central Africa - Metafro-Infosys - Xylarium,
http://data.gbif.org/datasets/resource/95)

Ruhrwiesen Arnsberg, Klasse 9 und 10, Fachbereich Biologie,
http://data.gbif.org/datasets/resource/3241)
Ruhrwiesen bei Neheim-Hüsten, http://data.gbif.org/datasets/resource/2854)
Rund um den Eichwald,Schulhof Friedrich Fröbel Gymnasium- Bad Blankenburg,
http://data.gbif.org/datasets/resource/2684)
Rund ums Cani, http://data.gbif.org/datasets/resource/3128)
SABIF Resource, http://data.gbif.org/datasets/resource/8051)
SANT herbarium vascular plants collection, http://data.gbif.org/datasets/resource/222)
SBT-Living, http://data.gbif.org/datasets/resource/7962)
SINGER Coordinator, http://data.gbif.org/datasets/resource/8349)
Schatzinsel Wangerooge, http://data.gbif.org/datasets/resource/3493)
Schlattstaller Tal (Lenningen), http://data.gbif.org/datasets/resource/2813)
Schlern - (Bozen), http://data.gbif.org/datasets/resource/2661)
Schlichemquelle (Tieringen/Meßstetten), http://data.gbif.org/datasets/resource/2650)
Schloß Türnich (Kerpen), http://data.gbif.org/datasets/resource/2776)
Schrebergarten Düsseldorf Oberkassel, http://data.gbif.org/datasets/resource/3218)
Schulbiotop Dr.-Gustav-Schickedanz-Hauptschule (Fürth),
http://data.gbif.org/datasets/resource/2775)
Schule Sulzbach (Oberegg), http://data.gbif.org/datasets/resource/2664)
Schulgarten Hans-Carossa-Oberschule, http://data.gbif.org/datasets/resource/3027)
Schulgarten Huttenheim (Philippsburg/Baden), http://data.gbif.org/datasets/resource/2685)
Schulgarten der Volksschule, http://data.gbif.org/datasets/resource/3511)
Schulgarten mit Klasse 8a (Essen), http://data.gbif.org/datasets/resource/2966)
Schulgelände Gebrüder-Grimm-Schuleund Umgebung (Lingen),
http://data.gbif.org/datasets/resource/2981)
Schulgelände IGS Kaufungen, http://data.gbif.org/datasets/resource/2663)
Schulgelände IGS-Frosch (Thaleischweiler-Fröschen),
http://data.gbif.org/datasets/resource/2687)
Schulgelände SGD/Viersen, http://data.gbif.org/datasets/resource/2864)
Schulgelände Städtisches Gymnasium, http://data.gbif.org/datasets/resource/2855)
Schulgelände des Gymnasiums Nepomucenum (Coesfeld),
http://data.gbif.org/datasets/resource/2984)
Schulhof Goethe-Gymnasium (Emmendingen), http://data.gbif.org/datasets/resource/2758)
Schulhof Gymnasium Hürth Bonnstrasse, http://data.gbif.org/datasets/resource/2757)
Schulhof Liebfrauenschule Oldenburg, http://data.gbif.org/datasets/resource/3215)
Schulhof und Anlagensee in Nellingen, http://data.gbif.org/datasets/resource/2805)
Schulinnenhöfe (Gelsenkirchen), http://data.gbif.org/datasets/resource/3343)
Schulprojekt (Bremen), http://data.gbif.org/datasets/resource/2789)
Schulteich Freie Waldorfschule Darmstadt, http://data.gbif.org/datasets/resource/3335)
Schulteich/Tümpel Thor-Heyerdahl-Gymnasium (Kiel),
http://data.gbif.org/datasets/resource/2732)
Schulwald Marksuhl, http://data.gbif.org/datasets/resource/3402)
Schulzentrum "Parc Hosingen", http://data.gbif.org/datasets/resource/3394)
Schussenaue (Weingarten), http://data.gbif.org/datasets/resource/2833)
Schussenaue bei Berg, http://data.gbif.org/datasets/resource/3020)
Schwanheimer Wald, http://data.gbif.org/datasets/resource/7865)
Schwanner Warte / Kinderhaus St. Elisabeth Waldplatz,
http://data.gbif.org/datasets/resource/3376)
Schwanseepark (87645 Schwangau), http://data.gbif.org/datasets/resource/3058)
Scottish Borders Biological Records Centre - SWT Scottish Borders Local Wildlife Site Survey
data 1996-2000 - species information, http://data.gbif.org/datasets/resource/848)
Seed collection – Dead seeds for evaluation and observation purposes,
http://data.gbif.org/datasets/resource/8334)

Selztal bei Friesenheim, http://data.gbif.org/datasets/resource/3091)
Seodaemun Museum of Natural History Plant, http://data.gbif.org/datasets/resource/673)
Silbertor + Wasserbachtal (Rutesheim / Renningen),
http://data.gbif.org/datasets/resource/2677)
Sistema de InformaciÃ³n de la vegetaciÃ³n IbÃ©rica y MacaronÃ©sica,
http://data.gbif.org/datasets/resource/8143)
Sonnentaugemeinschaft, http://data.gbif.org/datasets/resource/2686)
Specimen Database of Colorado Vascular Plants, http://data.gbif.org/datasets/resource/1832)
Spießwoogtal / Königsbruch (Fischbach), http://data.gbif.org/datasets/resource/3049)
Spreewaldfließe und Feuchtwiese bei Lübbenau, http://data.gbif.org/datasets/resource/3246)
Staatliches Museum für Naturkunde Stuttgart, Herbarium,
http://data.gbif.org/datasets/resource/1100)
Stadt Königs Wusterhausen, http://data.gbif.org/datasets/resource/2799)
Stadtbiotop Ulrichteich, http://data.gbif.org/datasets/resource/2720)
Stadtgebiet (Dannenberg), http://data.gbif.org/datasets/resource/2792)
Stadtpark Herzberg (Elster), http://data.gbif.org/datasets/resource/2979)
Stadtpark Sulzbach-Rosenberg, http://data.gbif.org/datasets/resource/2800)
Stausee (Oberdigisheim/Meßstetten), http://data.gbif.org/datasets/resource/2673)
Steinberg in Heidelberg-Handschuhsheim/Falgen,
http://data.gbif.org/datasets/resource/3191)
Steinbruch Kronungen, http://data.gbif.org/datasets/resource/3518)
Steinbruch Mainz-Weisenau, 2. Jahr, http://data.gbif.org/datasets/resource/3012)
Steinbruch Mainz-Weisenau, 3. Jahr, http://data.gbif.org/datasets/resource/3135)
Steinbruch Pluwig, http://data.gbif.org/datasets/resource/2831)
Sternwiese Mülheim-Broich, http://data.gbif.org/datasets/resource/3200)
Streuobstwiese Haus Zeitz, http://data.gbif.org/datasets/resource/3234)
Streuobstwiese Kugelberg (Ulm), http://data.gbif.org/datasets/resource/2782)
Streuobstwiese/Naturerlebnisraum Koppelsberg (Plön),
http://data.gbif.org/datasets/resource/2768)
Sudeniederung (Amt Neuhaus), Landkreis Lüneburg,
http://data.gbif.org/datasets/resource/2715)
Sudeniederung (Amt Neuhaus), http://data.gbif.org/datasets/resource/3260)
Sukkulentensammlung Zürich, http://data.gbif.org/datasets/resource/8135)
SysTax, http://data.gbif.org/datasets/resource/1875)
Südpark (Bochum-Wattenscheid), http://data.gbif.org/datasets/resource/2987)
Sürther Aue, http://data.gbif.org/datasets/resource/3512)
Tag der Artenvielfalt im Taubental, http://data.gbif.org/datasets/resource/8187)
Tag der Artenvielfalt in Heidelberg, http://data.gbif.org/datasets/resource/3486)
Tag der Artenvielfalt mit SchülerInnen des Leibniz-Gymnasiums in Neustadt a.d.W.,
http://data.gbif.org/datasets/resource/7873)
Tag der Artenvielfalt, http://data.gbif.org/datasets/resource/2861)
Taga Town Museum, Shiga Pref., Japan, http://data.gbif.org/datasets/resource/1964)
Tage der Artenvielfalt rund um die Naturschutzstation Molsberg,
http://data.gbif.org/datasets/resource/7868)
Take a Pride in Fife Environmental Information Centre - Records for Fife from TAPIF EIC,
http://data.gbif.org/datasets/resource/927)
Taxa, http://data.gbif.org/datasets/resource/7903)
Teich Berlin Wuhlheide, http://data.gbif.org/datasets/resource/2853)
The AAU Herbarium Database, http://data.gbif.org/datasets/resource/224)
The Danish Royal Veterinary and Agricultural University's Arboretum,
http://data.gbif.org/datasets/resource/702)
The Flora of County Waterford, http://data.gbif.org/datasets/resource/10797)
The Shimane Nature Museum of Mt. Sanbe, http://data.gbif.org/datasets/resource/1978)

The System-wide Information Network for Genetic Resources (SINGER), http://data.gbif.org/datasets/resource/1430)
Tiere und Pflanzen am Pfannenbach, http://data.gbif.org/datasets/resource/3355)
Tiergarten (Zeitz), http://data.gbif.org/datasets/resource/2769)
Tiergarten Straubing, http://data.gbif.org/datasets/resource/2806)
Tipos de plantas vasculares, http://data.gbif.org/datasets/resource/782)
Tiroler Landesmuseum Ferdinandeum, http://data.gbif.org/datasets/resource/1509)
Tongrube bei Hettstedt, http://data.gbif.org/datasets/resource/3488)
Triebesbach (Zeulenroda-Triebes), http://data.gbif.org/datasets/resource/2996)
Trockenhang Greinhartsberg Edelfingen, http://data.gbif.org/datasets/resource/2642)
Trockenrasen Franzigmark (Halle/Saale), http://data.gbif.org/datasets/resource/3064)
Trockenrasen bei Dörndorf, http://data.gbif.org/datasets/resource/3060)
Trockenrasen und Buchenwald in der Umgebung der Jugendherberge Bad Blankenburg, http://data.gbif.org/datasets/resource/2723)
Truppenübungsplatz Panzerkaserne Böblingen, http://data.gbif.org/datasets/resource/2965)
Type herbarium, Gottingen (GOET), http://data.gbif.org/datasets/resource/1494)
Töpinger Mischwald, http://data.gbif.org/datasets/resource/7881)
UA Herbarium, http://data.gbif.org/datasets/resource/7900)
UAM Botany Specimens, http://data.gbif.org/datasets/resource/975)
UCD BOTANICAL CONSERVATORY, http://data.gbif.org/datasets/resource/739)
USDA PLANTS Database, http://data.gbif.org/datasets/resource/1066)
USU-UTC Specimen Database, http://data.gbif.org/datasets/resource/1508)
Umgebung der Gesamtschule Hamburg-Winterhude, http://data.gbif.org/datasets/resource/2681)
Umgebung der Gesamtschule Winterhude (Hamburg), http://data.gbif.org/datasets/resource/2766)
Umgebung der Grundschule Oderberg, http://data.gbif.org/datasets/resource/3009)
Umgebung des Spalatin Gymnasium Altenburg, http://data.gbif.org/datasets/resource/3085)
United States National Plant Germplasm System Collection, http://data.gbif.org/datasets/resource/1429)
Universidad PolitÃ©cnica de Madrid, Dpto. BiologÃ-a Vegetal, Banco de Germoplasma, http://data.gbif.org/datasets/resource/1521)
Universidad de Extremadura, UNEX, http://data.gbif.org/datasets/resource/255)
Universidad de Granada, Herbario: GDA, http://data.gbif.org/datasets/resource/1741)
Universidad de Granada, Herbario: GDAC, http://data.gbif.org/datasets/resource/1742)
Universidad de MÃ¡laga: MGC-Cormof, http://data.gbif.org/datasets/resource/8105)
Universidad de Oviedo. Departamento de BiologÃ-a de Organismos y Sistemas: FCO, http://data.gbif.org/datasets/resource/245)
Universidad de Oviedo. Departamento de BiologÃ-a de Organismos y Sistemas: FCO-Briof, http://data.gbif.org/datasets/resource/8404)
Universidad del PaÃ-s Vasco/EHU, Bilbao: Herbario BIO, http://data.gbif.org/datasets/resource/242)
Universitat de Girona: HGI-Cormophyta, http://data.gbif.org/datasets/resource/250)
University Museums of Norway (MUSIT), http://data.gbif.org/datasets/resource/1996)
University and Jepson Herbaria DiGIR provider, http://data.gbif.org/datasets/resource/1413)
University of California Botanical Garden DiGIR provider, http://data.gbif.org/datasets/resource/1412)
Unna-Mühlhausen, Wiesen, http://data.gbif.org/datasets/resource/2865)
Unser Schulgelände, http://data.gbif.org/datasets/resource/2714)
Unser Schulhof - eine Apotheke, http://data.gbif.org/datasets/resource/2777)
Unser Schulhof, http://data.gbif.org/datasets/resource/2780)
Unser kleines Rasenstück/ Dürer-Gymnasium Nürnberg, http://data.gbif.org/datasets/resource/2810)

Unterbrucker Weiher, http://data.gbif.org/datasets/resource/2824)
Urwald 1 (Bad Waldsee), http://data.gbif.org/datasets/resource/2788)
Urwald 3 (Bad Waldsee), http://data.gbif.org/datasets/resource/3063)
Utah Valley State College Herbarium, http://data.gbif.org/datasets/resource/1013)
VFD-BW, Dinkelberg: Pferdeweiden Oberminseln,
http://data.gbif.org/datasets/resource/8058)
VFD-BW, Linzgau: Pferdeweiden Neuweiler Hof, http://data.gbif.org/datasets/resource/8061)
VFD-BW, Oberrhein/Schwarzwaldrand: Pferdeweiden Liel,
http://data.gbif.org/datasets/resource/8059)
VFD-BW, Schwäbische Alb: Pferdeweiden Zainingen,
http://data.gbif.org/datasets/resource/8060)
VFD-H: Heidenrod: Beckers Weide mit Wald, http://data.gbif.org/datasets/resource/3509)
VFD-H: Heidenrod: Pferdeweide Mürth, http://data.gbif.org/datasets/resource/3137)
VFD-H: Heidenrod: Weide am Ortsrand, http://data.gbif.org/datasets/resource/3521)
VFD-RP: Eifel: Orchideenweide Ankly, http://data.gbif.org/datasets/resource/3400)
VFD-RP: Hunsrück: Pferdeweide Kucher, http://data.gbif.org/datasets/resource/3503)
VSN-Wiese, http://data.gbif.org/datasets/resource/2858)
Vascular Plant Collection - University of Washington Herbarium (WTU),
http://data.gbif.org/datasets/resource/126)
Vascular Plant Collection, http://data.gbif.org/datasets/resource/622)
Vascular Plant Herbarium, Oslo (O), http://data.gbif.org/datasets/resource/1078)
Vascular Plant Herbarium, Trondheim (TRH), http://data.gbif.org/datasets/resource/7978)
Vascular Plant Specimen Database of Kanagawa Prefectural Museum of Natural History,
http://data.gbif.org/datasets/resource/8011)
Vascular Plants Collection of National Museum of Nature and Science,
http://data.gbif.org/datasets/resource/596)
Vascular Plants Collection of Sagamihara City Museum,
http://data.gbif.org/datasets/resource/1809)
Vascular Plants, Field notes, Agder naturmuseum (KMN),
http://data.gbif.org/datasets/resource/7966)
Vascular Plants, Field notes, Oslo (O), http://data.gbif.org/datasets/resource/1079)
Vascular Plants, Field notes, Trondheim (TRH), http://data.gbif.org/datasets/resource/8064)
Vascular plant collection of Jyvaskyla University Museum,
http://data.gbif.org/datasets/resource/462)
Vascular plant herbarium, Agder naturmuseum og botaniske hage,
http://data.gbif.org/datasets/resource/7965)
Vascular plants collection of Hiratsuka City Museum,
http://data.gbif.org/datasets/resource/8034)
Vascular plants of south-central China, http://data.gbif.org/datasets/resource/1828)
VegetWeb: zentrale Datenbank der Arbeitsgemeinschaft Vegetationsdatenbanken; Teil des
Netzwerks für Phytodiversität Deutschland (NetPhyD),
http://data.gbif.org/datasets/resource/1081)
Verwilderter Hausgarten mit angrenzendem Gelände (Laufenburg-Hochsal),
http://data.gbif.org/datasets/resource/2986)
Vom Gipfel ins Moor, Transekt im NSG Allgäuer Hochalpen,
http://data.gbif.org/datasets/resource/8056)
Von A(horn) bis Z(ecke) des WWP Chemnitz, http://data.gbif.org/datasets/resource/2956)
Wahner Heide LK 12 Biologie, http://data.gbif.org/datasets/resource/3569)
Wald am Schloss Wittgenstein Bad Laasphe, http://data.gbif.org/datasets/resource/2747)
Wald und Wiese am Buchwald, http://data.gbif.org/datasets/resource/2676)
Waldfläche im Natur-Erlebnis-Pfad Pfinztal, http://data.gbif.org/datasets/resource/3380)
Waldi-Weiher, http://data.gbif.org/datasets/resource/3346)

Waldränder der Frankenhöhe (Rothenburg ob der Tauber),
http://data.gbif.org/datasets/resource/2647)
Waldstück Bremerhagen LK Bio Kl. 12, http://data.gbif.org/datasets/resource/3126)
Waldstück am Schullandheim Bad Bederkesa, http://data.gbif.org/datasets/resource/7886)
Waldwiese, http://data.gbif.org/datasets/resource/3525)
Walldorf-Wiesloch: "Natur über den Gleisen", http://data.gbif.org/datasets/resource/2850)
Wanderweg am Windebyer Noor (bei Eckernförde),
http://data.gbif.org/datasets/resource/2706)
Wangerooge, http://data.gbif.org/datasets/resource/3007)
Wassermann, http://data.gbif.org/datasets/resource/3034)
Weide am Ostufer des Zotzensees, Müritz-Nationalpark,
http://data.gbif.org/datasets/resource/3111)
Weidenhüttendorf an der Würm (München), http://data.gbif.org/datasets/resource/2822)
Weidewirtschaft, http://data.gbif.org/datasets/resource/3119)
Weinberg Reichersdorf, http://data.gbif.org/datasets/resource/3401)
Weinberge und angrenzende Felsflächen (Drieschen) in Hatzenport/Terrassenmosel,
http://data.gbif.org/datasets/resource/2752)
Westerwälder Umwelt- und Naturschutztag Limesgemeinde Hillscheid,
http://data.gbif.org/datasets/resource/3017)
Wetland Inventory (NV), http://data.gbif.org/datasets/resource/7961)
Wiese am Waldrand (Gurtweil), http://data.gbif.org/datasets/resource/2784)
Wildes Bremer Leben im Park, http://data.gbif.org/datasets/resource/2708)
Wildkräuter, http://data.gbif.org/datasets/resource/2745)
Wirbach, http://data.gbif.org/datasets/resource/3013)
Wirbach-Taubental (Bad Blankenburg), http://data.gbif.org/datasets/resource/3059)
Wupperaue bei Kemna (Wuppertal), http://data.gbif.org/datasets/resource/2834)
Wälder im Hainbachtal, http://data.gbif.org/datasets/resource/3517)
Zielbach (Töll), http://data.gbif.org/datasets/resource/2983)
Zitadelle Berlin-Spandau (7b), http://data.gbif.org/datasets/resource/2992)
Zukünftiges NSG Höftland/Bockholmwik, http://data.gbif.org/datasets/resource/2665)
Zwei Flüsse - eine Stadt (Villingen-Schwenningen),
http://data.gbif.org/datasets/resource/2829)
herbario, http://data.gbif.org/datasets/resource/566)
herbier de Wallis et Futuna, http://data.gbif.org/datasets/resource/2602)
herbier de nouvelle-caledonie, http://data.gbif.org/datasets/resource/1990)
inatura - Erlebnis Naturschau Dornbirn ://data.gbif.org/datasets/resource/1866)
katzenbuckel, http://data.gbif.org/datasets/resource/2701)
nazza, http://data.gbif.org/datasets/resource/2699)
privater Garten, http://data.gbif.org/datasets/resource/3016)
renaturierter Main (Kemmern bei Bamberg), http://data.gbif.org/datasets/resource/2823)
schulgarten, http://data.gbif.org/datasets/resource/2738)
vegoek, http://data.gbif.org/datasets/resource/3130)
verschiedene Kleingewässer um Oldenburg/Holstein,
http://data.gbif.org/datasets/resource/3000)
Árboles de la Península de Yucatán, Flora del Distrito de Tehuantepec, Oaxaca y Familia
Asteraceae en México (IBUNAM), http://data.gbif.org/datasets/resource/2491)
Árboles y Arbustos Nativos para la Restauración Ecológica y Reforestación de México (IE-
DF,UNAM), http://data.gbif.org/datasets/resource/2484)
Ökologischer Weinberg (Guntersblum), http://data.gbif.org/datasets/resource/3056)
Ökostation (Freiburg), http://data.gbif.org/datasets/resource/2750)